

GEOLOGICA ULTRAIECTINA

Mededelingen van de  
Faculteit Geowetenschappen  
Universiteit Utrecht

No. 228

**Reactivity of Organic Matter and other  
Reductants in Aquifer Sediments**

NIELS HARTOG



# **Reactivity of Organic Matter and other Reductants in Aquifer Sediments**

## **Reactiviteit van Organisch Materiaal en andere Reductoren in Aquifersedimenten**

(met een samenvatting in het Nederlands)

### PROEFSCHRIFT

ter verkrijging van de graad van doctor aan de Universiteit Utrecht op gezag van de Rector Magnificus, Prof. Dr. W.H. Gispen, ingevolge het besluit van het College voor Promoties in het openbaar te verdedigen op woensdag 1 oktober 2003 des morgens te 10:30 uur

door

Niels Hartog  
geboren op 14 april 1974  
te Zaandam

Promotores: Prof. C.H. Van der Weijden  
Department of Geochemistry  
Faculty of Earth Sciences  
Utrecht University

Prof. J.W. de Leeuw  
Department of Geochemistry  
Faculty of Earth Sciences  
Utrecht University

Co-promotores: Dr. J. Griffioen  
Groundwater  
Netherlands Institute of Applied Geosciences–TNO  
Utrecht

Dr. P.F. Van Bergen  
Flow Assurance (OGUA)  
Shell Global Solutions International  
Amsterdam

Under the auspices of the Interfaculty Centre for Hydrology Utrecht (ICHU), this research was conducted at the Department of Geochemistry, Faculty of Earth Sciences, Utrecht University, The Netherlands. The Netherlands Institute of Applied Geosciences (NITG–TNO) provided financial support for this study.

Printing: Grafisch bedrijf Ponsen & Looijen, Wageningen, The Netherlands

ISBN 90-5744-087-3

## **Voor Tjok**

Looking forward,  
All that I can see,  
Is good things happening  
to you and to me.

I'm not waiting,  
For times to change.  
I'm going to live,  
Like a free-roamin' soul,  
On the highway of our love.

*(Neil Young—Looking Forward)*



# Table of Contents

<b>Dankwoord–Acknowledgements .....</b>	<b>9</b>
<b>General Introduction .....</b>	<b>13</b>
1.1 Reduction Capacity of Aquifers .....	15
1.2 Composition of Sedimentary Organic Matter .....	17
1.3 Reactivity of SOM in Groundwater Systems .....	19
1.4 Scope of this Study .....	21
1.5 Outline of this Thesis.....	23
<b>Fluidized-Bed Reactor to Study Physico-Chemical Kinetics in Heterogeneous Soils and Sediments .....</b>	<b>31</b>
2.1 Introduction.....	31
2.2 Theoretical Background.....	33
2.3 Material and Methods.....	36
2.4 Results and Discussion .....	37
2.5 Conclusions.....	41
<b>Distribution and Reactivity of O<sub>2</sub>-reducing Components in Sediments from a Layered Aquifer .....</b>	<b>43</b>
3.1 Introduction.....	43
3.2 Materials and Methods .....	44
3.3 Results and Discussion .....	48
3.4 Implications for Field Studies.....	61
<b>Nitrate Reduction Potential of Aquifer Sediments: Role of Microbial Adaptation .....</b>	<b>69</b>
4.1 Introduction.....	69
4.2 Material and Methods.....	70
4.3 Results.....	75
4.4 Discussion.....	82
4.5 Conclusions.....	87

**Reactivity of Organic Matter in Aquifer Sediments: Geological and Geochemical Controls .....93**

5.1	Introduction.....	93
5.2	Geological setting .....	94
5.3	Materials and methods .....	95
5.4	Results.....	100
5.5	Discussion.....	112
5.6	Conclusions.....	119

**Hydrogeological Controls on the Reactivity of Organic Matter and other Reductants in Aquifer Sediments .....127**

6.1	Introduction.....	127
6.2	Site Description .....	129
6.3	Materials and Methods .....	132
6.4	Results.....	135
6.5	Discussion.....	142
6.6	Conclusions.....	151

**Synthesis .....159**

7.1	Introduction.....	159
7.2	Reactivity of Sedimentary Reductants .....	160
7.3	Molecular Composition and Reactivity of SOM.....	162

**Samenvatting .....167**

	Introductie .....	167
	Reactiviteit van Sedimentaire Reductoren .....	168
	Moleculaire Samenstelling en Reactiviteit van SOM .....	171

**Curriculum vitae .....173**



## Dankwoord–Acknowledgements

Mijn proefschrift, één naam op de voorkant. Dit promotieonderzoek had ik echter niet in m'n eentje kunnen volbrengen. In dit ongetwijfeld meest gelezen onderdeel van m'n proefschrift wil ik daarom hen bedanken die op de bühne en achter de schermen hebben bijgedragen aan de totstandkoming van dit proefschrift.

- Allereerst mijn promotoren Kees van der Weijden en Jan de Leeuw die mij de mogelijkheid gaven vernieuwend onderzoek te doen op het grensvlak van chemische hydrogeologie en organische geochemie. Jan was een grote inspiratiebron voor nieuwe ideeën, terwijl Kees ervoor zorgde dat ik oog bleef houden voor details. Bedankt voor jullie vertrouwen over de manier waarop ik het onderzoek naar eigen inzicht invulde. In roerige tijden bleven jullie aansturen op het hoofddoel: “proefschrift af”.
- De levendige discussies met Jasper Griffioen en Pim van Bergen waren de drijvende kracht achter het analyseren, interpreteren en opschrijven van de resultaten. Ik hoop dat ik iets van hun manier van wetenschappelijk werken heb kunnen overnemen. Jasper's kritische houding kwam goed van pas bij het ziften van al te wilde ideeën, hierdoor kon het proefschrift afkomen. Als *newby* in de organische geochemie kon ik niet zonder het geduld van Pim. Jouw aanstekelijke enthousiasme wetenschappelijke doelgerichtheid maakten dat het onderzoek leuk bleef.
- *For critically reading and judging the final draft of this thesis I am grateful to the members of the thesis committee: Dieke Postma, Michael Barcelona, Peter Burrough, Philippe Van Cappellen and Stefan Schouten.*
- Ik dank Herco van Liere en Hugo van Buijsen van TNO-MEP die het mogelijk daar mijn oxymax experimenten uit te voeren.
- Michiel Kienhuis en Elda Panoto hebben mij op voortreffelijke wijze geholpen bij de pyrolse GC/MS metingen. Dankzij hen, en de anderen op de afdeling Mariene Biochemie en Toxicologie van het NIOZ, heb ik me daar drie keer een week thuis gevoeld.

- *I am grateful to Polish MSc student Artur Kawicki for working hard and accurate on the determination of the relationship between mineral surface area and organic carbon content. Thanks again for bringing those bottles of Zubrowka.*
- Dank aan Marjan Reith en Paul Anten van het Sedimentologisch Lab voor het verrichten van korrelgrootte analyses. Ook de analytische inzet van Arnold van Dijk, Dineke van de Meent, Erik van Vilsteren en Helen de Waard van het Geochemisch Lab hebben gegevens gegenereerd die cruciaal waren voor dit proefschrift. Het enthousiasme en de praktische *know-how* van Pieter Kleingeld waren onmisbaar bij ontwikkelen van de *fluidized-bed* reactoren.
- Boris van Breukelen en Kay Beets van de Vrije Universiteit in Amsterdam werkten mee aan een nieuwe techniek om gehalten aan ijzerhoudende carbonaten vast te stellen. Ik hoop dat we daar in de toekomst nog verder aan kunnen werken.
- *Georg Houben for interesting discussions on the reactivity of aquifer sediments and for offering assistance in quantifying ferrous iron bearing carbonates.*
- Geen onderzoek zonder monsters. Hartelijk dank dus aan Harry Timmer van waterleiding bedrijf Zuid-Holland Oost (Langerak) en aan Kees van Beek van het KIWA ('t Klooster) voor het beschikbaar stellen van aquifer materiaal.
- Hans Huisman en Gerard Klaver wekten mijn enthousiasme voor wetenschappelijk onderzoek tijdens mijn afstudeerstage bij de toenmalige RGD (1996). Ook tijdens mijn promotieonderzoek kon ik bij hen en andere medewerkers van TNO-NITG terecht, waarvoor hartelijk dank.
- Ik denk met veel plezier terug aan gezellige momenten beleefd met de collega's van de projectgroep Geochemie. Deze presenteerde zich vooral tijdens pauzes in de koffiehoek, maar ook door het gezamenlijk gaan klimmen (Diana, Yvonne en Pierre). Vooral met Gernot kon ik het over onderzoek, aio-frustraties en van alles en nog wat hebben. Verder heb ik het getroffen met m'n kamergenoten met wie het vanaf de eerste dag klikte, allereerst met Gerben (*Counseling Sessions*), daarna met Mariëtte, Anja (Dames, bedankt voor de vele koppen thee) en *petit* Laurent.
- Niet aan je onderzoek denken is soms moeilijk. Daarom bedank ik alle vrienden, de leden van Iets Blauws en huisgenoten voor de broodnodige lol en afleiding.

- Mijn ouders en mijn zus: jullie niet aflatende belangstelling en het rotsvaste vertrouwen in alles wat ik doe zijn een enorme steun in de rug is geweest.
- Tjok.



# General Introduction

Groundwater is a major source for our drinking, industrial, and agricultural water needs worldwide. However, contamination of aquifers with organic and inorganic compounds threatens the long-term value and exploitation of groundwater resources. Detailed knowledge of factors that control the fate of groundwater contaminants is therefore of great importance. The strong influence of groundwater oxidation state on the fate of contaminants is well known. For example, chromium and uranium are soluble (mobile) under oxidizing conditions (Blowes, 2002; Senko *et al.*, 2002). In contrast, reducing conditions keep iron and manganese in solution by preventing the precipitation of their insoluble hydroxides at neutral pHs (Appelo and Postma, 1993). The fate of organic contaminants in groundwater is particularly dependent on the oxidation state of groundwater, since carbon occurs in a wide range of oxidation numbers (IV to -IV). For example, chlorinated solvents are more degradable under reducing conditions, while aromatic compounds (*e.g.* BTEX) are more degradable in oxic groundwaters (Bradley *et al.*, 1998; Nielsen *et al.*, 1995; Schreiber and Bahr, 1999; Skubal *et al.*, 2001). Aim of this thesis is to contribute to the knowledge of how reactive components in aquifer sediments affect the oxidation state of groundwater. The oxidation state of groundwater is controlled by thermodynamic imbalances that drive reduction–oxidation (redox) reactions during which electrons are transferred from a reductant (electron donor) to an oxidant (electron acceptor).

Chromate ( $\text{CrO}_4^-$ ) and chlorinated hydrocarbons (*e.g.* TCE) are examples of contaminants with oxidizing properties (Fig. 1.1). Oxygen, nitrate and sulfate are the major oxidants in pristine groundwater. Besides these dissolved oxidants, solid iron and manganese oxides are important sediment-associated oxidants (Fig. 1.1). Reductants present in the aquifer consume these oxidants sequentially along a groundwater flow path in an order that mainly depends on their relative oxidation potential (Fig. 1.1). Consequently, dissolved oxygen initially present in shallow groundwater is removed at depth by naturally occurring biogeochemical processes,

leading to aquifers that are free of oxygen (anoxic). Only under sufficiently depleted oxygen concentrations, the reductive transformation of nitrate ( $\text{NO}_3$ ) to dinitrogen ( $\text{N}_2$ ) gas occurs (Hiscock *et al.*, 1991; Korom, 1992; Tiedje, 1988). This process, known as denitrification, involves a multitude of intermediate electron transfer steps (Fig. 1.2). Commonly, denitrification in groundwater is coupled to the oxidation of sediment-associated reductants, such as pyrite (Böhlke and Denver, 1995; Kelly, 1997; Postma *et al.*, 1991) and organic matter (Bengtsson and Bergwall, 1995; Obenhuber and Lowrance, 1991; Smith *et al.*, 1991; Trudell *et al.*, 1986).

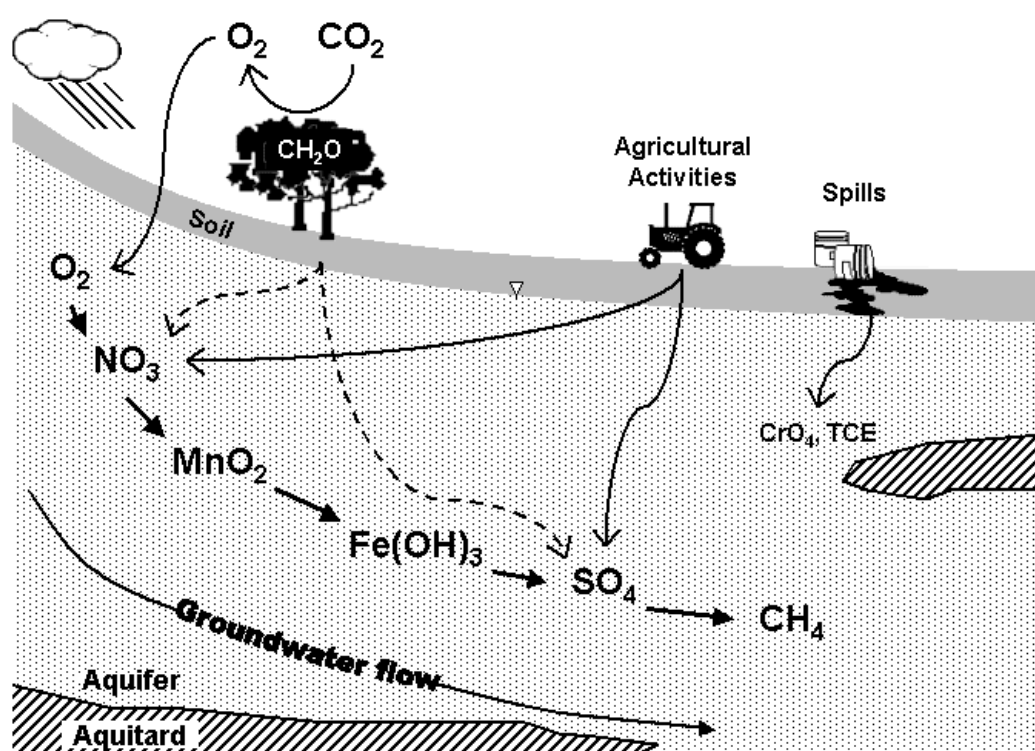


**Figure 1.1** Oxidant sources and sequence of reduction reactions in groundwater: aerobic respiration,  $\text{NO}_3^-$ -reduction, Mn-reduction, Fe-reduction,  $\text{SO}_4$ -reduction and  $\text{CO}_2$ -reduction (methanogenesis). Solid lines represent predominant sources. Dashed lines indicate additional sources.

Redox processes are generally mediated by microbes that derive energy from the transfer of electrons. The amount of dissolved organic matter in most pristine groundwaters ( $<1$  mg C/l) is too small and recalcitrant to create oxidant-depleted conditions (Aiken, 1985; Frimmel, 1998; Pettersson *et al.*, 1994; Thurman, 1985). Only when easily degradable organic compounds are excessively present (*e.g.* landfill

leachate, petroleum spills), oxidant-limited conditions may occur. Otherwise, microbial metabolism is inherently limited by the availability of organic substrate or other potential reductants (Chapelle, 2000). Thus, while the *sequence* of oxidant consumption depends largely on their relative oxidative strength, the reactivity of reductants dominantly controls the *rate* of oxidant consumption. Therefore, to understand and predict the direction and magnitude of redox-related changes in the chemistry of both contaminated and pristine groundwater systems, detailed knowledge on the factors that control the reduction capacity of aquifers is essential.

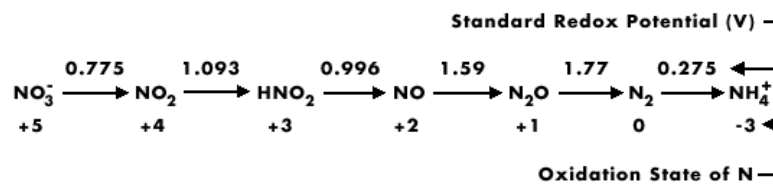


**Figure 1.2** The range in oxidation states of nitrogen. Denitrification involves the transfer of electrons during the reductive transformation of nitrate-N (V) to harmless dinitrogen (0) gas. Ammonium-N (-III) is the most reduced form of nitrogen and is the end product of dissimilatory nitrate reduction (Tiedje, 1988).

## 1.1 REDUCTION CAPACITY OF AQUIFERS

The reduction capacity of aquifer sediments determines the extent to which natural attenuation of contaminating oxidants such as chromate or nitrate occurs (Fig. 1.1). In addition, it negatively affects the efficiency during the remediation of reducing contaminants (*e.g.* petroleum), since sedimentary reductants will compete for injected oxidants (Baker *et al.*, 2000; Barcelona and Holm, 1991; Broholm *et al.*, 2000; Heron and Christensen, 1995; Nelson *et al.*, 2001; Schäfer and Kinzelbach, 1996; Schreiber and Bahr, 1999).

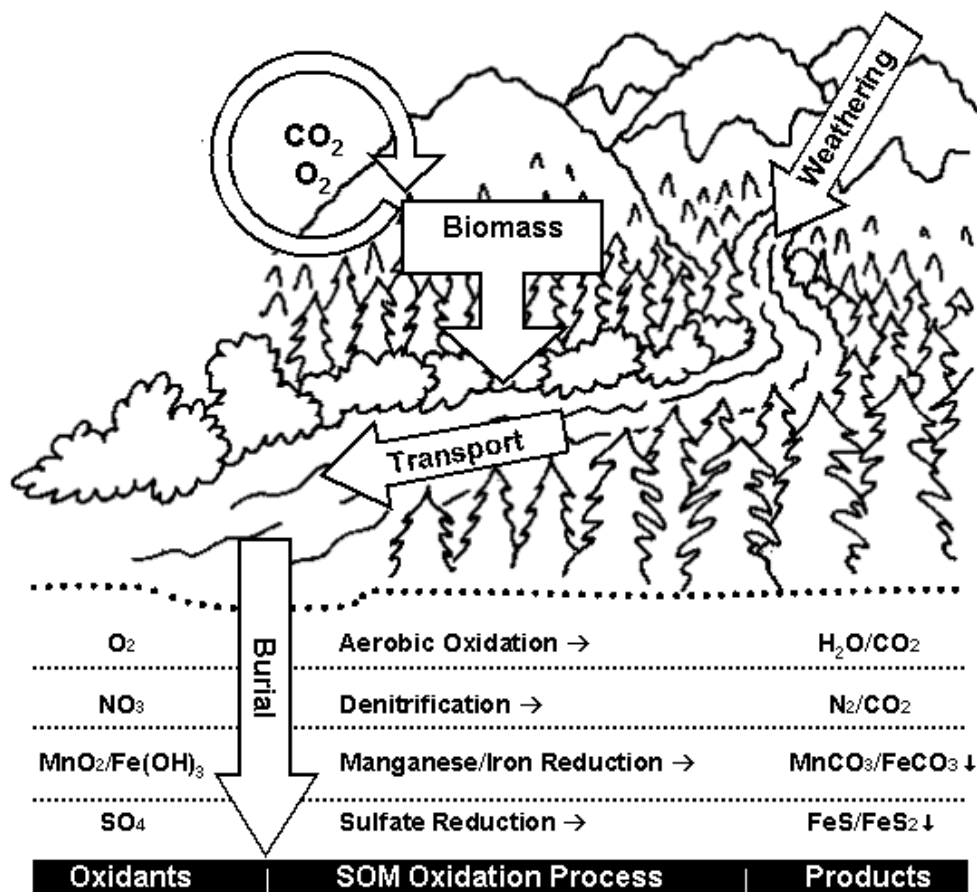


**Figure 1.3** The incorporation of sedimentary organic matter (SOM) during sediment deposition and subsequent diagenetic SOM oxidation processes. Aerobic oxidation and denitrification results in a loss of sediment reduction capacity. During manganese and iron reduction, the precipitation ( $\downarrow$ ) of mineral reductants retains sedimentary reduction capacity derived from SOM. Based on an illustration by Karen Hart.

To understand the reduction capacity of aquifer sediments, knowledge of the amount, type and reactivity of sedimentary reductants present is crucial. Sedimentary organic matter (SOM) and a range of minerals that contain reduced sulfur, iron or manganese are potentially reactive in aquifers. For example, the anaerobic degradation of labile SOM during early sediment diagenesis components may drive the precipitation of pyrite ( $FeS_2$ ), siderite ( $FeCO_3$ ) or other mineral reductants (Berner, 1971). Therefore, the occurrence of these diagenetic processes affects the nature of the reduction capacity of aquifer sediments (Fig. 1.3). These secondary reductants are generated at the expense of labile SOM components (Berner, 1971; Sagemann *et al.*,



1999). The composition of SOM is thus a critical control in determining the nature of the reduction capacity of sedimentary aquifers, as it 1) influences the reactivity of SOM as a reductant and 2) controls the importance of mineral reductants that were formed during early diagenesis.

## 1.2 COMPOSITION OF SEDIMENTARY ORGANIC MATTER

The importance of SOM as a reductant in the redox chemistry of groundwater systems is long known (Freeze and Cherry, 1979; Johns, 1968; Plummer, 1977; Thornstenson and Fisher, 1979), but its molecular composition is still largely unexplored. Consequently, SOM in aquifers is generally referred to in ill-defined terms such as refractory, humic, amorphous or kerogen, without molecular verification of its nature. To date, research on the composition and degradation of organic matter has primarily focused on soils and marine surface sediments, environments that are significantly richer in organic matter than sandy aquifers (Fig. 1.4). As a result, numerous comprehensive books and thorough reviews on the nature of organic matter are available, mainly in the context of soil fertility, climate reconstruction and hydrocarbon source rock potential (*e.g.* Hedges and Oades, 1997; Stevenson, 1994; Tissot and Welte, 1984; Tyson, 1995).

The predominant source of SOM is the burial of primary biomass with accumulating sediment (Tyson, 1995). Plant and microbial biomass consist of complex organic mixtures and the relative abundances of organic compounds vary with biomass type (Kogel-Knabner, 2002). Therefore, the compositional variation of SOM reflects to some extent differences in the composition of the biomass source. Marine phytoplankton is a considerable source for amino acids and short-chain lipids (Camacho-Ibar *et al.*, 2003; Grossi *et al.*, 2001; Sun *et al.*, 2002), while land plants are predominantly composed of the carbohydrate-based macromolecules. In addition, higher plants contain lignin compounds that provide strength to support tree trunks and branches and comprise 5–30 % of dry biomass. These heterogeneous polyphenolic macromolecules are specific for higher land plants and thus act as biomarkers for a terrigenous SOM origin (Hedges and Oades, 1997; Tyson, 1995).

Although the initial composition of SOM strongly reflects the composition of the biomass source, oxidation reactions alter the composition of SOM during and after burial (Fig. 1.3). Most of buried SOM (63–98%) does not survive beyond early diagenesis (Tyson, 1995). In particular, the mineralization of labile compounds such as plankton-derived amino acids is faster than of macromolecular compounds such as lignin (Cowie and Hedges, 1992; Cowie *et al.*, 1992; Henrichs, 1993; Tegelaar *et al.*, 1995). Consequently, SOM degradation rates in soils and marine sediments range in orders of magnitude, depending on the reactivity of the compounds present (Henrichs, 1993; Kogel-Knabner, 2002).

The mineralization rate of organic matter partly depends on oxidant type. Studies have indicated that the rates for aerobic and anaerobic degradation of labile organic compounds are similar (Henrichs and Reeburgh, 1987; Lee, 1992). However, recalcitrant organic components such as lignin or macromolecular aliphatics degrade much faster under aerobic than under anaerobic conditions (Canfield, 1994; Hulthe *et al.*, 1998; Kristensen and Holmer, 2001). The chief explanation for these observations is that during aerobic degradation, oxygen not only functions as an oxidant, it also serves as a co-substrate for enzymes (oxygenases) that aid the oxidation of recalcitrant aromatic and aliphatic compounds. As a result of the lack of these oxygenases, anaerobic degradation proceeds through less efficient pathways, such as benzoyl-CoA metabolism (Harwood *et al.*, 1999).

For an assessment of the overall potential reactivity of SOM, its bulk composition must be characterized. While several analytical techniques are available (Kögel-Knabner, 2000), common elemental analysis is not sufficiently specific to cover the wide range of organic compounds present. In addition, the abundance of macromolecular compounds in biomass (Kogel-Knabner, 2002) makes SOM unavailable to any direct analytical approach (Saiz-Jimenez, 1994).  $^{13}\text{C}$  NMR spectroscopy and other spectroscopic techniques are now widely used for the chemical characterization of SOM (Kögel-Knabner, 2000). These techniques provide information about the nature of carbon environments such as functional groups or aromaticity, and the non-destructiveness and the lack of major pretreatment

requirements are big advantages for samples. However, the low organic matter contents and the presence of Fe-bearing paramagnetic compounds limit their applicability of SOM in aquifer sediments. Furthermore, these techniques do not provide information on the molecular associations of SOM. Pyrolysis is a powerful thermal degradation technique that allows the characterization of the building blocks of complex macromolecular organic matter when coupled to gas chromatograph and mass spectrometer (Py-GC/MS). It is frequently used to characterize the bulk composition of organic matter in both soils and sediments (Chiavari *et al.*, 1994; Kögel-Knabner, 2000; Levy, 1966; Saiz-Jimenez, 1994; Saiz-Jimenez and De Leeuw, 1986). Although several pitfalls exist, it is currently the main technique available for the molecular bulk characterization of complex SOM (Chiavari *et al.*, 1994).

### **1.3 REACTIVITY OF SOM IN GROUNDWATER SYSTEMS**

Rates of SOM oxidation in aquifer sediments are several orders of magnitude lower than observed in environments that recurrently receive fresh organic matter, such as marine surface sediments (Chapelle and Lovley, 1990; Jakobsen and Postma, 1994). In groundwater systems with an ample, continuous supply of fresh labile organic matter (*e.g.* land-fill leachate), the availability of oxidants commonly limits organic matter degradation rates (Chapelle, 2000). In addition, environmental conditions, such as nutrient level, temperature or acidity potentially control microbial activity (Atlas and Bartha, 1998).

A number of studies have shown that not the addition of nitrate but the addition of a labile carbon source, such as glucose, significantly increased denitrification rates in groundwater systems (Bengtsson and Bergwall, 1995; Bradley *et al.*, 1992; Hill *et al.*, 2000; Obenhuber and Lowrance, 1991; Smith and Duff, 1988; Starr and Gillham, 1993). This indicates that neither microbial activity nor the amount of oxidants is rate limiting and supports the general idea that the availability of SOM controls the rate of its degradation in aquifer sediments.

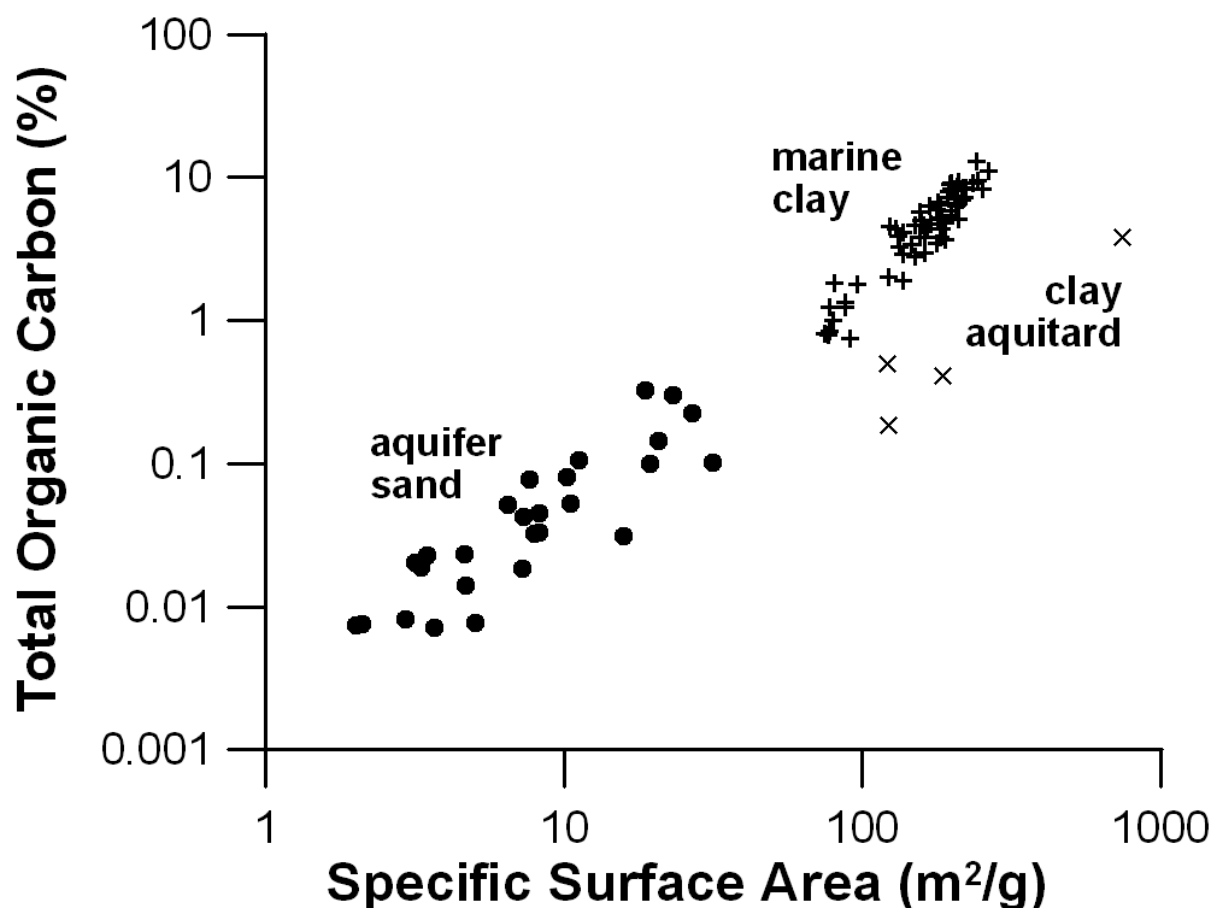


**Figure 1.4** Cross plot of total organic carbon versus specific surface area of the mineral phase. A preliminary study (unpublished results) at the 't Klooster site (Fig. 1.5) provided the data for the aquifer sands. Data for marine clay is taken from a study on black shale (Kennedy *et al.*, 2002). Clay aquitard data are taken from a study on four different aquitards (Allen-King *et al.*, 1995). All specific surface areas (SSA) were determined by sorption of ethyl-glycol monoethyl (Churchman *et al.*, 1991).

Both its accessibility (physical) and degradability (chemical) potentially control the availability of SOM in aquifer sediments. Physical limitations on its reactivity occur at a grain scale when particle–organic compound interactions protects a part of the organic matter against microbial degradation. Studies have indicated a relationship between SOM availability and sorption to mineral surfaces in both marine clay sediments (Keil *et al.*, 1994; Mayer, 1994a; Mayer, 1994b; Mayer, 1999) and soils (Chorover and Amistadi, 2001; Salmon *et al.*, 2000; Sollins *et al.*, 1996). In groundwater systems, it has been shown that microbes in clay aquitards are unable to mineralize the SOM present due to pore size restrictions (Chapelle and Bradley, 1996; Chapelle and Lovley, 1990; McMahon and Chapelle, 1991). In a preliminary study, a positive relationship was found between the specific surface area and total organic

carbon contents of aquifer sands (Fig. 1.4, unpublished results). While considerable scatter in the data exists, the general trend compares favorably with data for clayey sediments (Allen-King *et al.*, 1995; Kennedy *et al.*, 2002). Therefore, the interaction of SOM with mineral surfaces may decrease its availability in aquifer sediments.

Alternatively, SOM may be chemically refractory towards oxidation. From studies on organic matter in soils and marine sediments, it is generally recognized that its reactivity decreases with continuing degradation. More precisely, the most labile compounds are consumed at a higher rate, resulting in an overall decrease of SOM reactivity with time. Built on this notion, several descriptive models have incorporated SOM fractions with different reactivities to account for the decreasing reactivity of SOM with time (Berner, 1980; Middelburg, 1989). However, these fractions are arbitrary and no tools exist to assess the size and reactivity of these different kinetic pools (Almendros and Dorado, 1999; Gleixner *et al.*, 2002).

## 1.4 SCOPE OF THIS STUDY

This thesis focuses on the role of SOM as a reductant in aquifer sediments. Using pyrolysis-GC/MS, the molecular composition of SOM is characterized and the controls on its reactivity are assessed.

As stated earlier, SOM generally co-occurs and is frequently even closely associated with other sedimentary reductants in aquifer sediments. Therefore, the relative contribution of SOM to oxidant consumption during sediment oxidation depends on the reactivity of other reductants present. The amounts of these reductants present depend on the diagenetic history and provenance of the sediment. For example, pyrite and Fe(II)-bearing glauconite are commonly formed in marine depositional environments, while siderite is predominantly formed in terrestrial settings (Berner, 1971; Postma, 1982). While the reactivity of SOM in aquifers is either chemically or physically controlled, the oxidation of these reductants under pH-neutral conditions is mainly determined by surface oxidation kinetics. Therefore, the precipitation of metal hydroxide on mineral surfaces is an impediment that controls their reactivity (Nicholson *et al.*, 1990; Postma, 1983; Postma, 1990). The co-

occurrence of several potentially reactive sedimentary reductants in aquifer sediments complicates the isolated study of SOM reactivity upon exposure to oxidants. Therefore, the separation of and the controls on the contributions of various reductants to the reduction capacity of aquifer sediments is another aim of this study.

Aquifer sediments from two drinking water production sites were studied (Fig. 1.5). The Langerak site is located in the central part of the Netherlands. Here, a confined sedimentary aquifer is recharged with water from the River Lek. Proposed future induced riverbank infiltration will increase the oxidant loadings of  $\text{NO}_3$  and  $\text{O}_2$ . The site 't Klooster is located in the eastern part of the Netherlands. Here, knowledge on the reactivity of aquifer sediments is particularly important as the excessive use of agricultural fertilizers on sandy soils cause elevated nitrate concentrations in shallow groundwater (Fraters *et al.*, 1998; Hefting and de Klein, 1998; Pomper, 1989; Reijnders *et al.*, 1998; van Beek *et al.*, 1994; van Beek and Vogelaar, 1998).

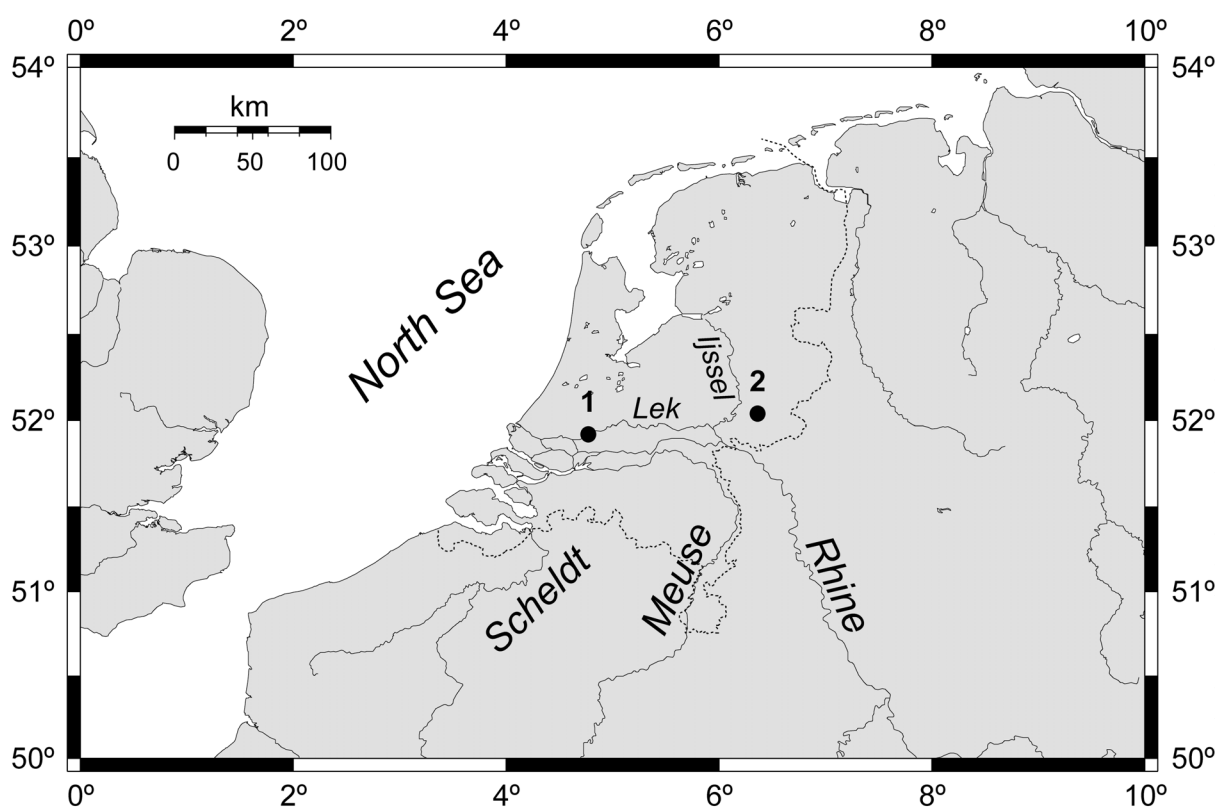


**Figure 1.5** Location of the Langerak (1) and 't Klooster (2) aquifers in the Rhine–Meuse delta. The Langerak site is located along the River Lek. The 't Klooster site is located in between the River Rhine and River Ijssel. Dotted line represents the Dutch national boundary.

## 1.5 OUTLINE OF THIS THESIS

This chapter serves as an introduction for the following research chapters. *Chapter 2* describes the design and development of a fluidized-bed reactor for anaerobic biogeochemical sediment incubations; the developed fluidized-bed reactor was tested during denitrification experiments described in *Chapter 4*. In *Chapter 3*, sediments from the Langerak aquifer were characterized for the presence and reactivity of potential reductants. The reactivity towards oxygen was determined during sediment incubations. A method is developed to discriminate between contributions from SOM, pyrite and siderite oxidation based on CO<sub>2</sub>/O<sub>2</sub> ratios and sulfate production. This method is also applied for the sediment incubations describe in *Chapters 5 and 6*. In *Chapter 4*, the nitrate reduction potential of anaerobic sediments from the Langerak aquifer is assessed using fluidized-bed (*Chapter 2*) and batch reactor experiments. The geochemical and microbial controls on denitrification are discussed.

*Chapter 5* describes the molecular composition of SOM in aquifer sediments selected from a marine and fluvio-glacial formation at the Klooster site. Molecular indications on the degradation status of SOM are linked with the reactivity of SOM as observed during aerobic incubation experiments. *Chapter 6* discusses the molecular composition of SOM in different geological formations at the Klooster site. The controls on SOM preservation as well as the presence of pyrite and ferroan carbonates in aquifer sediments at this site are assessed. The controls on the reduction capacity and on the contributions of various reductants are discussed using aerobic sediment oxidation experiments. Lastly, *Chapter 7* provides a synthesis of the thesis, in which the main findings are summarized and discussed, and where implications and future research directions are considered.

## References

Aiken G. (1985) Humic Substances in Soil, Sediment, and Water; Geochemistry, Isolation, and Characterization, pp. 692 pp.

- Allen-King R. M., Groenevelt H., Waren C. J., and Mackay D. M. (1995) Non-linear chlorinated-solvent sorption in four aquitards. *Journal of Contaminant Hydrology* **22**, 203-221.
- Almendros G. and Dorado J. (1999) Molecular characteristics related to the biodegradability of humic acid preparations. *European Journal of Soil Science* **50**, 227-236.
- Appelo C. A. J. and Postma D. (1993) *Geochemistry, Groundwater and Pollution*. Balkema.
- Atlas R. M. and Bartha R. (1998) *Microbial Ecology: Fundamentals and Applications*. Benjamin/Cummings Science Publishing.
- Baker R. J., Baehr A. L., and Lahvis M. A. (2000) Estimation of hydrocarbon biodegradation rates in gasoline-contaminated sediment from measured respiration rates. *Journal of Contaminant Hydrology* **41**, 175-192.
- Barcelona M. J. and Holm R. T. (1991) Oxidation-reduction capacities of aquifer solids. *Environmental Science and Technology* **25**, 1565-1572.
- Bengtsson G. and Bergwall C. (1995) Heterotrophic denitrification potential as an adaptive response in groundwater bacteria. *FEMS Microbiology Ecology* **16**, 307-318.
- Berner R. A. (1971) *Principles of Chemical Sedimentology*. McGraw-Hill.
- Berner R. A. (1980) A rate model for organic matter decomposition during bacterial sulfate reduction in marine sediments. In *Biogéochimie de la matière organique à l'interface eau-sédiment marin*, Vol. 293 (ed. C. I. d. C.N.R.S.), pp. 35-44.
- Blowes D. (2002) Environmental chemistry - Tracking hexavalent Cr in groundwater. *Science* **295**(5562), 2024-2025.
- Böhlke J. K. and Denver J. M. (1995) Combined use of groundwater dating, chemical, and isotopic analyses to resolve the history and fate of nitrate contamination in two agricultural watersheds, Atlantic coastal plain, Maryland. *Water Resources Research* **31**(9), 2319-2339.
- Bradley P. M., Chapelle F. H., and Wilson J. T. (1998) Field and laboratory evidence for intrinsic biodegradation of vinyl chloride contamination in a Fe(III)-reducing aquifer. *Journal of Contaminant Hydrology* **31**, 111-127.
- Bradley P. M., Fernandez Jr M., and Chapelle F. H. (1992) Carbon limitation of denitrification rates in an anaerobic groundwater system. *Environmental Science and Technology* **28**(12), 2377-2381.
- Broholm M. M., Crouzet C., Arvin E., and Mouvet C. (2000) Concurrent nitrate and Fe(III) reduction during anaerobic biodegradation of phenols in a sandstone aquifer. *Journal of Contaminant Hydrology* **44**, 275-300.
- Camacho-Ibar V. F., Aveytua-Alcazar L., and Carriquiry J. D. (2003) Fatty acid reactivities in sediment cores from the northern Gulf of California. *Organic Geochemistry* **34**(3), 425-439.
- Canfield D. E. (1994) Factors influencing organic carbon preservation in marine sediments. *Chemical Geology* **114**, 315-329.
- Chapelle F. H. (2000) The significance of microbial processes in hydrogeology and geochemistry. *Hydrogeology Journal* **8**(1), 41-46.



- Chapelle F. H. and Bradley P. M. (1996) Microbial acetogenesis as a source of organic acids in ancient Atlantic Coastal Plain sediments. *Geology* **24**(10), 925-928.
- Chapelle F. H. and Lovley D. R. (1990) Rates of microbial metabolism in deep coastal plain aquifers. *Applied and Environmental Microbiology* **56**(6), 1865-74.
- Chiavari G., Torsi G., Fabbri D., and Galletti G. C. (1994) Comparative study of humic substances in soil using pyrolytic techniques and other conventional chromatographic methods. *Analyst* **119**, 1141-1150.
- Chorover J. and Amistadi M. K. (2001) Reaction of forest floor organic matter at goethite, birnessite and smectite surfaces. *Geochimica et Cosmochimica Acta* **65**(1), 95-109.
- Churchman G. J., Burke C. M., and Parfitt R. L. (1991) Comparison of various methods for the determination of specific surfaces of subsoils. *Journal of Soil Science* **42**, 449-461.
- Cowie G. L. and Hedges J. I. (1992) Sources and reactivities of amino-acids in a coastal marine environment. *Limnology and Oceanography* **37**(4), 703-724.
- Cowie G. L., Hedges J. I., and Calvert S. E. (1992) Sources and relative reactivities of amino acids, neutral sugars, and lignin in an intermittently anoxic marine environment. *Geochimica et Cosmochimica Acta* **56**, 1963-1978.
- Fraters D., Boumans L. J. M., van Drecht G., de Haan T., and de Hoop W. D. (1998) Nitrogen monitoring in groundwater in the sandy regions of the Netherlands. *Environmental Pollution* **102**, 479-485.
- Freeze R. A. and Cherry J. A. (1979) *Groundwater*. Prentice-Hall, Inc.
- Frimmel F. H. (1998) Characterization of natural organic matter as major constituents in aquatic systems. *Journal of Contaminant Hydrology* **35**(1-3), 201-216.
- Gleixner G., Poirier N., Bol R., and Balesdent J. (2002) Molecular dynamics of organic matter in a cultivated soil. *Organic Geochemistry* **33**(3), 357-366.
- Grossi V., Blokker P., and Damste J. S. S. (2001) Anaerobic biodegradation of lipids of the marine microalga *Nannochloropsis salina*. *Organic Geochemistry* **32**(6), 795-808.
- Harwood C. S., Bruchhardt G., Herrmann H., and Fuchs G. (1999) Anaerobic metabolism of aromatic compounds via the benzoyl-CoA pathway. *FEMS Microbiology Reviews* **22**, 439-458.
- Hedges J. I. and Oades J. M. (1997) Comparative organic geochemistries for soils and marine sediments. *Organic Geochemistry* **27**(7/8), 319-363.
- Hefting M. M. and de Klein J. J. M. (1998) Nitrogen removal in buffer strips along a lowland stream in the Netherlands: a pilot study. *Environmental Pollution* **102**(1), 521-526.
- Henrichs S. M. (1993) Early diagenesis of organic matter: the dynamics (rates) of cycling of organic compounds. In *Organic Geochemistry* (ed. M. H. Engel and S. A. Macko), pp. 101-117. Plenum Press.
- Henrichs S. M. and Reeburgh W. S. (1987) Anaerobic mineralization of marine sediment organic matter: rates and the role of anaerobic processes in the oceanic carbon economy. *Geomicrobiology Journal* **5**(3-4), 191-237.

- Heron G. and Christensen T. H. (1995) Impact of Sediment-Bound Iron on Redox Buffering in a Landfill Leachate Polluted Aquifer (Vejen, Denmark). *Environmental Science & Technology* **29**(1), 187-192.
- Hill A. R., Devito K. J., Campagnolo S., and Sanmugadas K. (2000) Subsurface denitrification in a forest riparian zone: Interactions between hydrology and supplies of nitrate and organic carbon. *Biogeochemistry* **51**, 193-223.
- Hiscock K. M., Lloyd J. W., and Lerner D. N. (1991) Review of natural and artificial denitrification of groundwater. *Water Research* **25**(8), 1099-1111.
- Hulthe G., Hulth S., and Hall P. O. J. (1998) Effect of oxygen on degradation rate of refractory and labile organic matter in continental margin sediments. *Geochimica et Cosmochimica Acta* **62**(8), 1319-1328.
- Jakobsen R. and Postma D. (1994) In situ rates of sulfate reduction in an aquifer (Rømø, Denmark) and implications for the reactivity of organic matter. *Geology* **22**, 1103-1106.
- Johns M. W. (1968) Geochemistry of groundwater from Upper Cretaceous-Lower Tertiary sand aquifers in South-Western Victoria, Australia. *Journal of Hydrology* **6**(4), 337-357.
- Keil R. G., Tsamakis E., Fuh C. B., Giddings J. C., and Hedges J. I. (1994) Mineralogical and textural controls on the organic composition of coastal marine sediments: hydrodynamic separation using SPLITT-fractionation. *Geochimica et Cosmochimica Acta* **58**(2), 879-893.
- Kelly W. R. (1997) Heterogeneties in ground-water geochemistry in a sand aquifer beneath an irrigated field. *Journal of Hydrology* **198**, 154-176.
- Kennedy M. J., Pevear D. R., and Hill R. J. (2002) Mineral surface control of organic carbon in black shale. *Science* **295**, 657-660.
- Kogel-Knabner I. (2002) The macromolecular organic composition of plant and microbial residues as inputs to soil organic matter. *Soil Biology and Biochemistry* **34**(2), 139-162.
- Kögel-Knabner I. (2000) Analytical approaches for characterizing soil organic matter. *Organic Geochemistry* **31**, 609-625.
- Korom S. F. (1992) Natural denitrification in the saturated zone: A review. *Water Resources Research* **28**(6), 1657-1668.
- Kristensen E. and Holmer M. (2001) Decomposition of plant materials in marine sediment exposed to different electron acceptors (O<sub>2</sub>, NO<sub>3</sub><sup>-</sup> and SO<sub>4</sub><sup>2-</sup>), with emphasis on substrate origin, degradation kinetics, and the role of bioturbation. *Geochimica et Cosmochimica Acta* **65**(3), 419-433.
- Lee C. (1992) Controls on organic carbon preservation: The use of stratified water bodies to compare intrinsic rates of decomposition in oxic and anoxic systems. *Geochimica et Cosmochimica Acta* **56**, 3323-3335.
- Levy R. L. (1966) Pyrolysis gas chromatography : A review of the technique. *Chromatographic Reviews* **8**, 48-89.
- Mayer L. M. (1994a) Relationships between mineral surfaces and organic carbon concentrations in soils and sediments. *Chemical Geology* **114**, 347-363.

- Mayer L. M. (1994b) Surface area control of organic carbon accumulation in continental shelf sediments. *Geochimica et Cosmochimica Acta* **58**(4), 1271-1284.
- Mayer L. M. (1999) Extent of coverages of mineral surfaces by organic matter in marine sediments. *Geochimica et Cosmochimica Acta* **63**(2), 207-215.
- McMahon P. B. and Chapelle F. H. (1991) Microbial production of organic acids in aquitard sediments and its role in aquifer geochemistry. *Nature* **349**, 233-235.
- Middelburg J. J. (1989) A simple rate model for organic matter decomposition in marine sediments. *Geochimica et Cosmochimica Acta* **53**, 1577-1581.
- Nelson M. D., Parker B. L., Al T. A., Cherry J. A., and Loomer D. (2001) Geochemical reactions resulting from in situ oxidation of PCE- DNAPL by KMnO<sub>4</sub> in a sandy aquifer. *Environmental Science & Technology* **35**(6), 1266-1275.
- Nicholson R. V., Gillham R. W., and Reardon E. J. (1990) Pyrite oxidation in carbonate-buffered solution: 2. Rate control by oxide coatings. *Geochimica et Cosmochimica Acta* **54**, 395-402.
- Nielsen P. H., Bjarnadóttir H., Winter P. L., and Christensen T. H. (1995) In situ and laboratory studies on the fate of specific organic compounds in an anaerobic landfill leachate plume, 2. Fate of aromatic and chlorinated aliphatic compounds. *Journal of Contaminant Hydrology* **20**, 51-66.
- Obenhuber D. C. and Lowrance R. (1991) Reduction of nitrate in aquifer microcosms by carbon additions. *Journal of Environmental Quality* **20**(1), 255-8.
- Pettersson C., Ephraim J., and Allard B. (1994) On the composition and properties of humic substances isolated from deep groundwater and surface waters. *Organic Geochemistry* **21**(5), 443-451.
- Plummer L. N. (1977) Defining reactions and mass transfer in part of the Floridan Aquifer. *Water Resources Research* **15**(5), 801-812.
- Pomper A. B. (1989) Human influences on groundwater quality in a sandy region with multiple land use. *Chemical Geology* **76**(3-4), 371-383.
- Postma D. (1982) Pyrite and siderite formation in brackish and freshwater swamp sediments. *American Journal of Science* **282**, 1151-1183.
- Postma D. (1983) Pyrite and siderite oxidation in swamp sediments. *Journal of Soil Science* **34**, 163-182.
- Postma D. (1990) Kinetics of nitrate reduction by detrital Fe(II)-silicates. *Geochimica et Cosmochimica Acta* **54**(3), 903-908.
- Postma D., Boesen C., Kristiansen H., and Larsen F. (1991) Nitrate reduction in an unconfined sandy aquifer: Water chemistry, reduction processes, and geochemical modeling. *Water Resources Research* **27**(8), 2027-2045.
- Reijnders H. F. R., van Drecht G., Prins H. F., and Boumans L. J. M. (1998) The quality of the groundwater in the Netherlands. *Journal of Hydrology* **207**, 179-188.

- Sagemann J., Bale S. J., Briggs D. E. G., and Parkes R. J. (1999) Controls on the formation of authigenic minerals in association with decaying organic matter: An experimental approach. *Geochimica et Cosmochimica Acta* **63**(7/8), 1083-1095.
- Saiz-Jimenez C. (1994) Analytical pyrolysis of humic substances: pitfalls, limitations and possible solutions. *Environmental Science and Technology* **28**(11), 1773-1780.
- Saiz-Jimenez C. and De Leeuw J. W. (1986) Chemical characterization of soil organic matter fractions by analytical pyrolysis-gas chromatography-mass spectrometry. *Journal of Analytical and Applied Pyrolysis* **9**(2), 99-119.
- Salmon V., Derenne S., Lallier-Vergès, Largeau C., and Beaudoin B. (2000) Protection of organic matter by mineral matrix in a Cenomanian black shale. *Organic Geochemistry* **31**, 463-474.
- Schäfer W. and Kinzelbach W. (1996) Numerical modelling of in situ aquifer remediation with a biological component - three case studies. *European Water Pollution Control* **6**(5), 19-35.
- Schreiber M. E. and Bahr J. M. (1999) Spatial Electron Acceptor Variability: Implications for Assessing Bioremediation Potential. *Bioremediation Journal* **3**(4), 363-378.
- Senko J. M., Istok J. D., Suflita J. M., and Krumholz L. R. (2002) *In-situ* evidence for uranium immobilization and remobilization. *Environmental Science & Technology* **36**(7), 1491-1496.
- Skubal K. L., Barcelona M. J., and Adriaens P. (2001) An assessment of natural biotransformation of petroleum hydrocarbons and chlorinated solvents at an aquifer plume transect. *Journal of Contaminant Hydrology* **49**, 151-169.
- Smith R. L. and Duff J. H. (1988) Denitrification in a sand and gravel aquifer. *Applied and Environmental Microbiology* **54**(5), 1071-1078.
- Smith R. L., Howes B. L., and Duff J. H. (1991) Denitrification in nitrate-contaminated groundwater: occurrence in steep vertical geochemical gradients. *Geochimica et Cosmochimica Acta* **55**(1815-1825).
- Sollins P., Homann P., and Caldwell B. A. (1996) Stabilization and destabilization of soil organic matter: mechanisms and controls. *Geoderma* **74**(1-2), 65-105.
- Starr R. C. and Gillham R. W. (1993) Denitrification and organic carbon availability in two aquifers. *Ground Water* **31**(6), 935-947.
- Stevenson F. J. (1994) *Humus Chemistry. Genesis, Compositions, Reactions*. Wiley.
- Sun M. Y., Cai W. J., Joye S. B., Ding H. B., Dai J. H., and Hollibaugh J. T. (2002) Degradation of algal lipids in microcosm sediments with different mixing regimes. *Organic Geochemistry* **33**(4), 445-459.
- Tegelaar E. W., Hollman G., van der Vegt P., de Leeuw J. W., and Holloway P. J. (1995) Chemical characterization of the periderm tissue of some angiosperm species: recognition of an insoluble, non-hydrolyzable, aliphatic biomacromolecule (Suberan). *Organic Geochemistry* **23**(3), 239-251.

- Thornstenson D. C. and Fisher D. W. (1979) The geochemistry of the Fox Hills-Basal Hell Creek aquifer in Southwestern North Dakota and Northwestern South Dakota. *Water Resources Research* **15**(6), 1479-1498.
- Thurman E. M. (1985) *Organic Geochemistry of Natural Waters*, pp. 512 pp.
- Tiedje J. M. (1988) Ecology of denitrification and dissimilatory nitrate reduction to ammonium. In *Biology of anaerobic microorganisms* (ed. A. J. B. Zehnder), pp. 179-244. John Wiley and Sons.
- Tissot B. P. and Welte D. H. (1984) *Petroleum Formation and Occurrence*. Springer-Verlag.
- Trudell M. R., Gillham R. W., and Cherry J. A. (1986) An *in-situ* study of the occurrence and rate of denitrification in a shallow unconfined sand aquifer. *Journal of Hydrology (Amsterdam, Netherlands)* **83**(3-4), 251-268.
- Tyson R. V. (1995) *Sedimentary Organic Matter*. Chapman & Hall.
- van Beek C. G. E. M., Laeven M. P., and Vogelaar A. J. (1994) Modelling denitrificatie in grondwater onder invloed van organisch materiaal. *H<sub>2</sub>O* **27**(7), 180-184.
- van Beek C. G. E. M. and Vogelaar A. J. (1998) Pompstation Hengelo 't Klooster—*Geohydrologische, geochemische en hydrochemische beschrijving*, pp. 84. KIWA N.V.



# **Fluidized-Bed Reactor to Study Physico-Chemical Kinetics in Heterogeneous Soils and Sediments**

## **2.1 INTRODUCTION**

Chemical reactivity assessments of unconsolidated geosolids as sediments or soils (hereafter sediments) are typically performed by batch or column experiments. Within well-mixed batch reactors fluid and solids interact in a homogeneous suspension, while within column reactors the packed solid matrix interacts with the passing fluid. The main disadvantage of the batch reactor type is the build-up of reaction products and depletion of reactants. This transient state of chemical conditions complicates the assessment of kinetic controls (Chou and Wollast, 1984). Column experiments come closest to simulating hydrogeochemical processes under natural flow conditions. However, chemical gradients across the column and physically controlled kinetics, such as inter-aggregate and film diffusion, complicate the assessment of chemical reaction kinetics during column experiments.

Fluidized-bed reactors are a hybrid of column and batch reactors, in that aqueous chemical conditions can be kept constant while maintaining a well-mixed system and minimizing physical control on reaction kinetics. Unlike batch reactors, however, used, fluidized-bed reactors have been used rarely for sediment reactivity experiments. Some applied the fluidized-bed technique in weathering studies using particles with narrow grain size ranges (Chou and Wollast, 1984; Postma, 1990; van Hees *et al.*, 2002), while (Griffioen, 1999) performed fluidized-bed experiments on aquifer sediments to study the biodegradation of organic contaminants.

Here, fluidization is defined as the suspension of grains by a sufficiently fast upward flow through a granular bed (*e.g.* Leeder, 1982; Viessman and Hammer, 1998) and occurs when the upward flow velocity in the reactor overcomes the gravitational force on the solid grain particles (Fig. 2.1). Fluidized-bed reactors are widely used in chemical and biological engineering for chemical and physical production or treatment processes. In these reactors, the carrier or sorbent particles used are typically of uniform size and density. Therefore, the wide range of particle sizes and densities in natural sediments is an important difference with most industrial applications of fluidization.

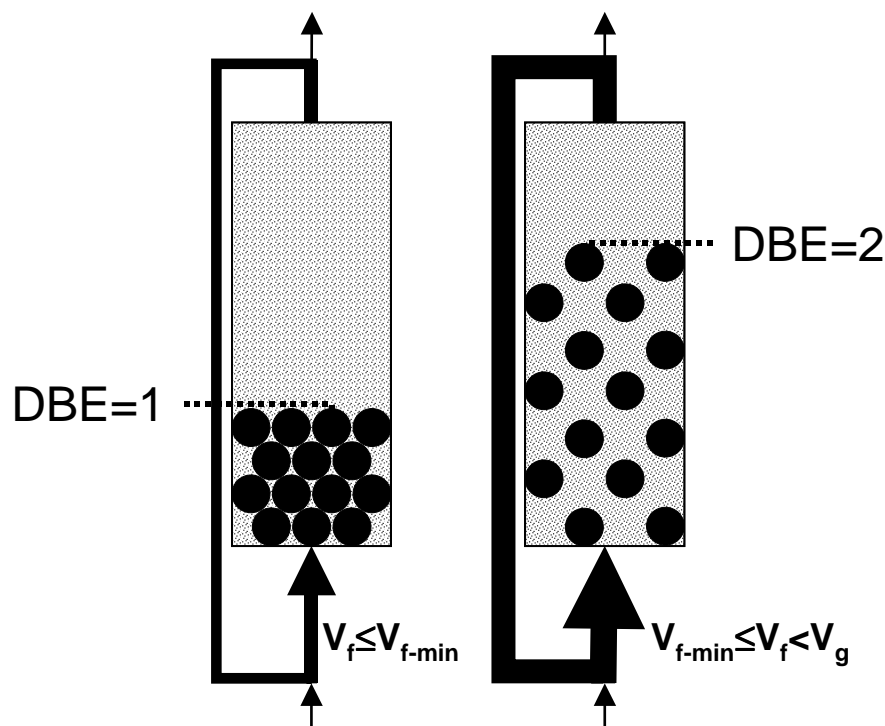


**Figure 2.1** Conceptual Fluidized-Bed Reactor containing uniform particles. Degree of Bed Expansion (DBE) as related to upward flow velocity ( $V_f$ ).

Not only do sediment particles exhibit a variety of particle sizes and densities, they also differ in physico-chemical reactivity. While in batch experiments all particles are retained within the reactor, fluidization can result in the loss of particles from the reactor. Minimization of particle loss due to elutriation is therefore important



to prevent bias of experimental results. Additionally, reduction of particle elutriation may prevent technical problems due to clogging of tubing or filters.

Here, the hydrodynamical behavior of sandy sediments is studied during fluidization to determine how fluidized-bed reactors can be used in biogeochemical kinetic experiments. An experimental fluidized-bed reactor is designed and built considering specifically both the wide range in hydrodynamic behavior of sediment particles and experimental requirements.

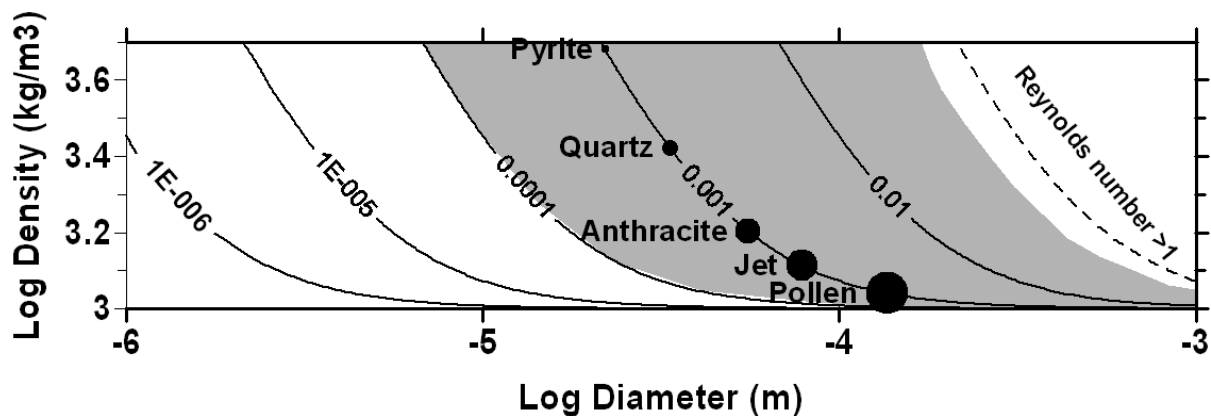


**Figure 2.2** Nomograph of settling velocities (m/s) as a function of particle size and density according to Stokes' law (Eq. 2.1). Lines represent equal settling velocities according to Equation 2.2. Reynolds' number  $<1$  correspond roughly to settling velocities below 0.01 m/s. As an example, common sedimentary particles with various densities and sizes (Table 2.1) are plotted for an equal settling velocity of 0.001 m/s. Symbol size represents relative linear diameter. Shaded area represents an example range of the particles that can be fluidized by the reactor designed.

## 2.2 THEORETICAL BACKGROUND

Settling velocity is the main particle characteristic that determines its behavior during fluidization. Sediment particles exhibit a variety of particle sizes and densities, resulting in a wide range of settling velocities (Fig. 2.2). Stokes' law describes the dependency of unhindered terminal particle settling velocities ( $V_g$ ) on the basis of their diameters ( $d_p$  in m) and densities ( $\rho_p$  in  $\text{kg/m}^3$ ) under laminar flow conditions:

$$V_g = \frac{gd_p^2(\rho_p - \rho_w)}{18\mu} \quad \text{Equation 2.1}$$

where  $\rho_w$  is the density of water,  $\mu$  is the dynamic viscosity of water (1 mPa.s) and  $g$  the gravitational acceleration (9.81 m/s<sup>2</sup>).

**Table 2.1** According to Stokes' law, these examples of quartz and potentially redox-reactive sedimentary particles have a settling velocity of 1 mm/s and illustrates the interaction between density and particle size, as shown in Figure 2.4. Density data obtained from (Tyson, 1995).

Species	Density (Kg/m <sup>3</sup> )	Particle Diameter ( $\mu$ m)	Settling Velocity (mm/s)
Pollen	1100	135	1
Jet	1300	78	1
Anthracite	1600	55	1
Quartz	2650	33	1
Pyrite	4800	22	1

On the basis of Stokes' law, particles of different densities and size have identical settling velocities (Fig. 2.2) when:

$$\frac{\rho_1 - \rho_w}{\rho_2 - \rho_w} = \left( \frac{d_2}{d_1} \right)^2 \quad \text{Equation 2.2}$$

where subscript 1 and subscript 2 refer to particle type 1 and 2, respectively.

When the Reynolds number ( $V_g \rho_w d_p / \mu$ ) increases above 1, the error in the absolute value of calculated settling velocities increases, owing to turbulent effects. Additionally, Stokes' law does not account for effects of shape and roughness. Nevertheless, Stokes' law-like behavior has been observed for settling porous sediment aggregates with a Reynolds number up to 11 (Van der Lee, 2000; Wu and Lee, 1998).

Under laminar flow conditions, Stokes' law is used directly to describe either settling or fluidization behavior of a sufficiently isolated particle. However, the physical interaction of neighboring particles in a fluidized-bed results in a loss of kinetic energy. Moreover, the particle concentration in the bed affects the space for the upward fluid to flow through and thus influences the effective flow velocity. Therefore, the minimum flow velocity ( $V_{f-\min}$ ) required to fluidize a certain set of particles depends on porosity ( $\epsilon$ ) as follows;

$$V_{f-\min} = \epsilon^n V_g \quad \text{Equation 2.3}$$

where  $n$  is a function of particle characteristics and flow regime as described in engineering textbooks or specialized publications (e.g. Godard and Richardson, 1969;

Richardson and da S. Jeronimo, 1979; Viessman and Hammer, 1998). For the practical purpose of this study we assume Stokes' law and porosity only (i.e.  $n=1$ , Eq. 2.3).

### **2.2.1 Geo-scientific Applications of Fluidized-bed Reactors**

Resuspension of sediment and intense mixing within the water column occurs in deltaic and continental systems. These natural dynamic conditions resemble those of fluidized-bed reactors and result in the efficient mineralization of sedimentary organic matter (Aller, 1998; Aller *et al.*, 1996). Therefore, fluidization is not only a valuable experimental technique. It has also the potential to simulate the specific physico-chemical conditions during intense reworking, re-suspension and liquefaction of sediments.

Fluidized-bed reactors have been applied for various environmental and geochemical research purposes. Most studies have used such reactors mainly in the context of wastewater engineering because the high degree of mixing of the water and solid phase minimizes physical limitations and favors microbial growth processes. For example, a fluidized-bed reactor allows high substrate loadings to enrich slow growing solid-phase-associated biomass on sparingly soluble polyaromatic hydrocarbons (Rockne and Strand, 1998). Furthermore, during the bioremediation of contaminated water the recirculation of the water phase may dilute the influent contaminant concentration below a toxic level that allows its degradation (Langwaldt and Puhakka, 2000). Abiotic studies used fluidized bed reactors to study mineral dissolution to enable the maintenance of a constant undersaturation in the aqueous phase with respect to the mineral under study (Chou and Wollast, 1984). The control of pH on dissolution kinetics was tested by the possibility of instantly changing the acidity of the influent without disturbing the solid phase. Clearly, the use of a fluidized-bed reactor enables to evaluate the effect of various chemical conditions on the (bio)geochemical process of interest, by an instant change of the influent composition without manipulation of the solid phase.

An alternative application of sediment fluidization is hydrodynamic separation. Hydrodynamic separation of fine sediments fractions has been achieved using

SPLITT-fractionation (Contado *et al.*, 1997; Keil *et al.*, 1994). Unfortunately, this technique is not applicable for coarser ( $> 100\mu\text{m}$ ) size fractions due to technical limitations. Hydrodynamic separation of coarser grained particles can be achieved by a sequence of widening elutriation columns (Nicholas and Walling, 1996; Walling and Woodward, 1993). Alternatively, fluidization is used for hydrodynamic separation as shown for binary particle mixtures (Rasul *et al.*, 2000) and offers the advantage that flow velocity is a continuous variable.

## 2.3 Material and Methods

Grain size fractions of crushed silicate rock, taken from a previous study on the dissolution kinetics of olivine (Jonckbloedt, 1998), were obtained by wet-sieving 2 kg of sand for 20 min, using 20 cm diameter sieves and a sieve machine (Retsch Vibro). The sieved fractions were subsequently ultrasonically treated to remove adhering fines. Grain size distributions of the particle fractions and sediments were determined with a Laser Particle Sizer (Malvern Series 2600).

Fluidization experiments were performed with different size fractions of silicate sand (Table 2.1). The particles had a packed porosity of 0.39 and a density of  $2.9 \text{ kg}\cdot\text{m}^{-3}$  as determined using standard techniques (Goudie, 1990). Experiments were performed in graded glass columns of 30 cm height (internal  $\varnothing$  5.7 cm) with a bottom glass filter to evenly distribute the upward water flow from a water faucet. Velocity measurements were determined using a stopwatch.

Elutriation experiments were performed using the graded glass columns described above. After each experiment, elutriates and residues were collected after which their particle size distributions were determined. A 1:1 weight mixture of the 63–150 and the 150–500  $\mu\text{m}$  sieve fractions served as starting material. This mixture was exposed to the upward flow velocity (1.6 cm/s) that was required to totally elutriate the 63–150  $\mu\text{m}$  sieve fraction. The collected elutriate of this mixture at this flow velocity was exposed to a halved upward flow velocity of 8 mm/s. In addition, a sample taken from a sandy soil in the eastern part of the Netherlands was exposed to this upward flow velocity.

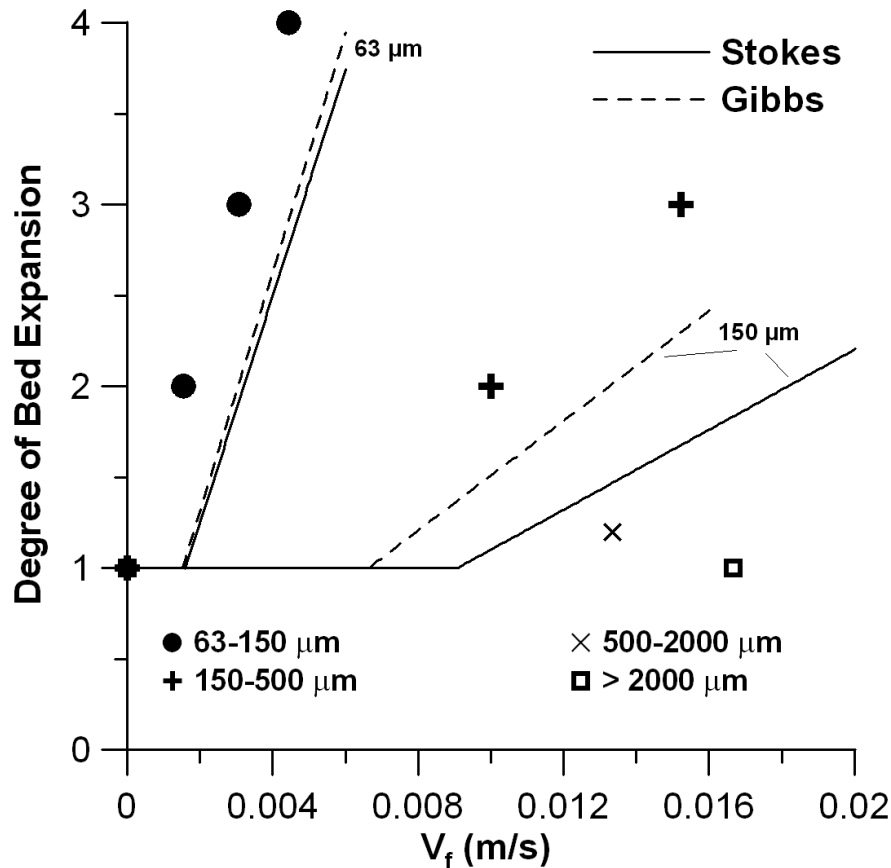


**Figure 2.3** Behavior of the particle size fractions 63–150  $\mu\text{m}$ , 150–500  $\mu\text{m}$ , 500–2000  $\mu\text{m}$  and >2000  $\mu\text{m}$  during fluidization experiments. Solid lines represent the predicted behavior using Stokes' law (Eq. 2.1). Dashed lines represent the predicted behavior using the empirical model developed by (Gibbs *et al.*, 1971). Both predictions were corrected for porosity using Equation 2.3. Porosity of 0.39 at DBE=1, density 2900  $\text{kg}/\text{m}^3$ .

## 2.4 RESULTS AND DISCUSSION

Sieve fractions of crushed silicate rock were used to study the hydrodynamic behavior of sediments during fluidization. Firstly, the relation between upward flow velocity ( $V_f$ ) and the degree of bed expansion (DBE, Fig. 2.1) is discussed. Secondly, the relation between upward flow velocity and the elutriation of particles is assessed. Finally, the design of the fluidized-bed reactor is presented.

### 2.4.1 Fluidization Behavior of Sieved Particle Size Fractions

The increase of upward flow velocities resulted in a smooth progressive expansion of the bed for the two finest fractions (Fig. 2.3). This indicated homogeneous fluidized-bed conditions during the fluidization experiments. The

minimum upward effective flow velocities through the bed needed for fluidization of the 63–150  $\mu\text{m}$  fraction is similar to the settling velocity of their finest end member as predicted by Stokes' law (Eq. 2.1). With increasing flow velocities, the Reynolds number increases and Stokes' law is no longer valid. Therefore, the fluidization velocity of the 150–500  $\mu\text{m}$  particle sieve fractions is better described by an empirical relationship derived for silicate-density particles by (Gibbs *et al.*, 1971). Fluidization of the two coarsest fractions required very turbulent flow conditions and these fractions could not be stably fluidized under the experimental conditions.

The elutriation experiments performed on the silicate sand fraction and a natural soil sample showed that, at a certain upward flow velocity, the finest particles are flushed out of the column while keeping a range of larger sized particle fluidized (Fig. 2.4). At an upward flow velocity of 16 mm/s, the sieve fraction 63–150  $\mu\text{m}$  was completely flushed out of the column. When exposing the 63–500  $\mu\text{m}$  mixture (Fig. 2.4a) to the same upward flow velocity the particle size distributions of the resulting elutriated and residual fractions were very similar to that of the original 63–150  $\mu\text{m}$  and 150–500  $\mu\text{m}$  sieve fractions (Fig. 2.4b).

When the particle fraction elutriated at 16 mm/s and the bulk soil was exposed to an upward flow velocity of 8 mm/s, particles with an average size of 100  $\mu\text{m}$  were flushed out in both samples (Fig 4c). The particle size distribution of the elutriated material was very similar in both samples, considering the differences in material composition. The particle size distributions of both residue fractions were dissimilar. This is mainly due to the presence of coarser particles in the original soil sample.

The elutriation experiments show that the technical challenge of fluidizing a complete sediment sample is to keep the heavier and larger particles fluidized while preventing the lighter and smaller particles to escape the fluidized-bed column. A practical solution to this problem is to decrease the upward flow velocity in the upper part of the column by increasing the cross-sectional area of the column. For example, doubling the internal diameter of the reactor produces a four-fold increase in its cross-sectional area and a similar reduction in upward flow velocity.

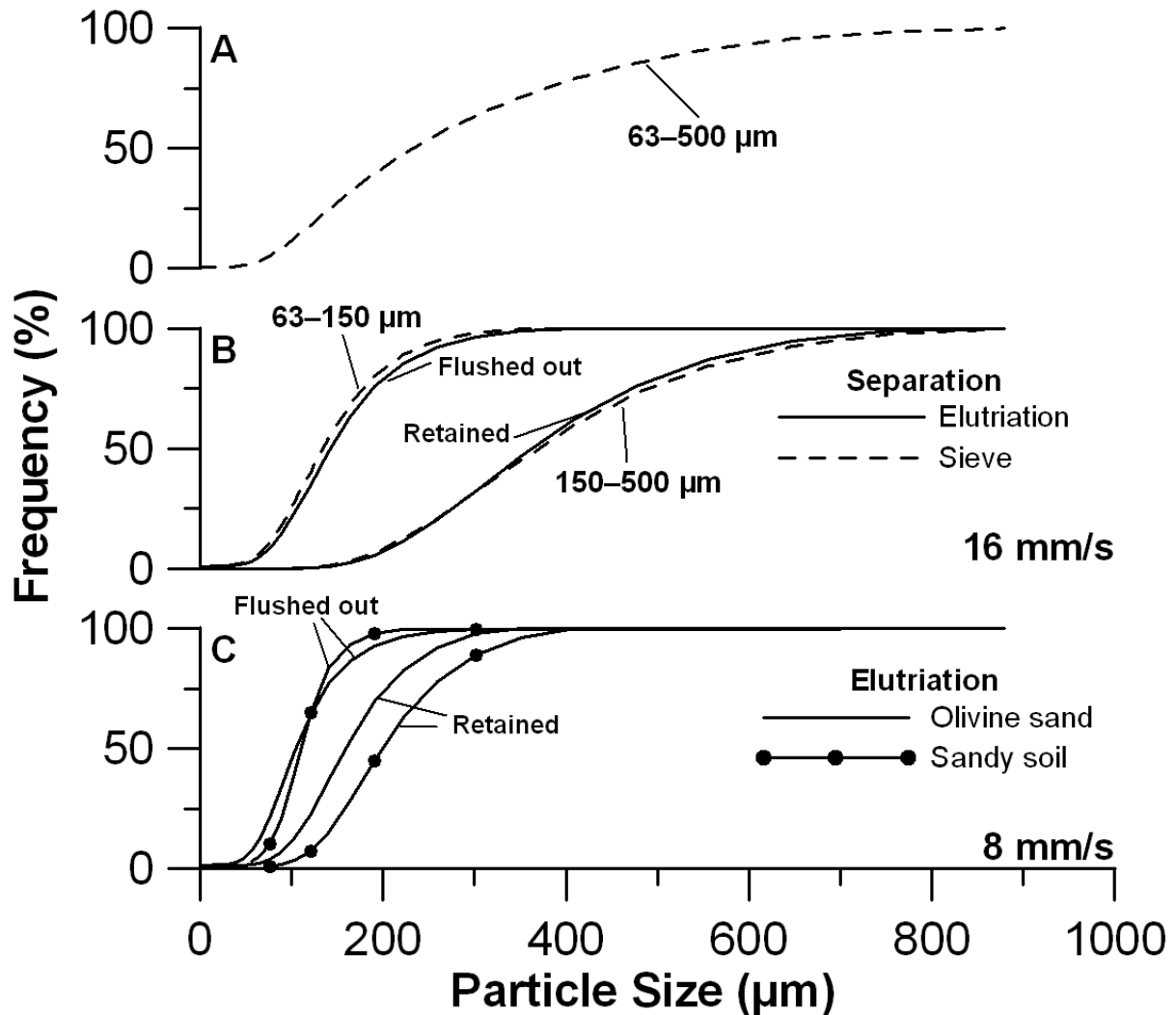
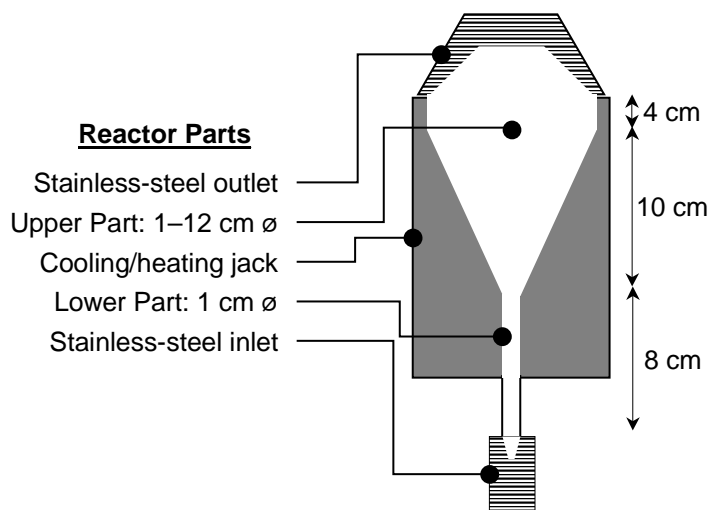


Figure 2.4 Cumulative frequency curve of sieved and elutriated particle size fractions

## 2.4.2 Design of Fluidized-bed Reactor

A fluidized-bed reactor was designed and built for the specific purpose of kinetic sediment experiments (Fig. 2.5). The reactor has a volume of 1 liter with a diameter of 1 cm in the lower part of the reactor and a diameter of 12 cm in the upper part. The small reactor volume enables both high liquid mixing and refresh rates. Moreover, the 12-fold increase in cross-sectional diameter from the bottom to the top of the column results in a large retainment capacity of sedimentary particles, since the decrease in upward flow velocity allows for a 144-fold range in particle settling velocities. Additionally, the minimum flow velocity to fluidize the particle in the lower part of the reactor depends on the porosity of the fluidized-bed (Eq. 3). Assuming a porosity of 0.25 ( $DBE=1$ ) in the lower part of the fluidized-bed, even a

maximum range in settling velocities of 576-fold is achieved. For example, sediment particles with a settling velocity of 5.76 cm/s (~200  $\mu\text{m}$  quartz grains) can be fluidized, while retaining sediment particles with a settling velocity of 0.1 mm/s, which corresponds roughly to quartz grains of 10  $\mu\text{m}$  (Fig. 2.2).



**Figure 2.5 Fluidized-bed reactor design**

Characteristic upward velocities needed to fluidize sediments range from 0.001 to 0.01 m/s (Fig. 2.2). This requires a combined flux from the influent and recirculation pumps of about 5–50 ml/min. Despite the strong radius increase in the upper part of the fluidized-bed reactor, the relatively small total reactor volume of one liter allows for fast response with hydraulic retention times smaller than one day and recirculation rates of several times per hour. Moreover, the steep internal angle ( $61^\circ$ ) of the glass column prevents significant deposition of fine particles on the reactor walls.

In addition to these experimental requirements regarding sediment particle characteristics and flow conditions, reactors may be used to study biogeochemical processes that require anoxia. Therefore, the fluidized-bed reactor consists of glass and the main tubing consists of stainless steel with gastight connections (Serto). Peristaltic pumps instead of piston pumps were used to add and recirculate the aqueous solution, since they allow the transfer of unfiltered solutions. To minimize the potential for oxygen diffusion into the system, Tygon tubing (Tygon LFL,



Masterflex) was used in the peristaltic pumps because of its low gas permeability of  $0.79 \times 10^{-10} \text{ m}^2 \cdot \text{s}^{-1}$  (Kjeldsen, 1993).

## 2.5 CONCLUSIONS

Sediments contain potentially reactive particles that cover a wide range in size and density. To be able to retain this variety of representative particles, a fluidized-bed reactor for sediments was developed on the basis of observed hydrodynamical behavior during fluidization. This fluidized-bed reactor is suitable for sediment studies on biogeochemical kinetics under minimized physical kinetic limitations. The reactor is suitable for both oxic and anoxic experimental conditions.

## References

- Aller R. C. (1998) Mobile deltaic and continental shelf muds as suboxic, fluidized bed reactors. *Marine Chemistry* **61**, 143-155.
- Aller R. C., Blair N. E., Xia Q., and Rude P. D. (1996) Remineralization rates, recycling, and storage of carbon in Amazon shelf sediments. *Continental Shelf Research* **16**(5-6), 753-786.
- Chou L. and Wollast R. (1984) Study of the weathering of albite at room temperature and pressure with a fluidized bed reactor. *Geochimica et Cosmochimica Acta* **48**, 2205-2217.
- Contado C., Dondi F., Beckett R., and Giddings J. C. (1997) Separation of particulate environmental samples by SPLITT fractionation using different operating modes. *Analytica Chimica Acta* **345**(1-3), 99-110.
- Gibbs R. J., Matthews M. D., and Link D. A. (1971) The relationship between sphere size and settling velocity. *Journal of Sedimentary Petrology* **41**(1), 7-18.
- Godard K. and Richardson J. F. (1969) Correlation of data for minimum fluidising velocity and bed expansion in particulate fluidised systems. *Chemical Engineering Science* **24**(2), 363-367.
- Goudie A. (1990) *Geomorphological Techniques*, pp. 570. Unvwin Hyman Ltd.
- Griffioen J. V. d. G., Bas; Buijs, Alice; Hartog, Niels. (1999) Oxygen consumption of natural reductants in aquifer sediment related to in situ bioremediation. *Int. In Situ On-Site Biorem. Symp., 5th*, 463-468.
- Jonckbloedt R. C. L. (1998) Olivine dissolution in sulphuric acid at elevated temperatures-- implications for the olivine process, an alternative waste acid neutralizing process. *Journal of Geochemical Exploration* **62**(1-3), 337-346.

- Keil R. G., Tsamakis E., Fuh C. B., Giddings J. C., and Hedges J. I. (1994) Mineralogical and textural controls on the organic composition of coastal marine sediments: hydrodynamic separation using SPLITT-fractionation. *Geochimica et Cosmochimica Acta* **58**(2), 879-893.
- Kjeldsen P. (1993) Evaluation of Gas-Diffusion through Plastic Materials Used in Experimental and Sampling Equipment. *Water Research* **27**(1), 121-131.
- Langwaldt J. H. and Puhakka J. A. (2000) On-site biological remediation of contaminated groundwater: a review. *Environmental Pollution* **107**, 187-197.
- Leeder M. R. (1982) *Sedimentology, Process and Product*. George Allen & Unwin Ltd.
- Nicholas A. P. and Walling D. E. (1996) The significance of particle aggregation in the overbank deposition of suspended sediment on river floodplains. *Journal of Hydrology* **186**(1-4), 275-293.
- Postma D. (1990) Kinetics of nitrate reduction by detrital Fe(II)-silicates. *Geochimica et Cosmochimica Acta* **54**(3), 903-908.
- Rasul M. G., Rudolph V., and Wang F. Y. (2000) Particles separation using fluidization techniques. *International Journal of Mineral Processing* **60**, 163-179.
- Richardson J. F. and da S. Jeronimo M. A. (1979) Velocity-voidage relations for sedimentation and fluidisation. *Chemical Engineering Science* **34**(12), 1419-1422.
- Rockne K. J. and Strand S. E. (1998) Biodegradation of bicyclic and polycyclic aromatic hydrocarbons in anaerobic enrichments. *Environmental Science & Technology* **32**(24), 3962-3967.
- Tyson R. V. (1995) *Sedimentary Organic Matter*. Chapman & Hall.
- Van der Lee W. T. B. (2000) Temporal variation of floc size and settling velocity in the Dollard estuary. *Continental Shelf Research* **20**(12-13), 1495-1511.
- van Hees P. A. W., Lundstrom U. S., and Morth C.-M. (2002) Dissolution of microcline and labradorite in a forest O horizon extract: the effect of naturally occurring organic acids. *Chemical Geology* **189**(3-4), 199-211.
- Viessman J., W. and Hammer J. (1998) *Water supply and pollution control*. Addison Wesley Longman, Inc.
- Walling D. E. and Woodward J. C. (1993) Use of a Field-Based Water Elutriation System for Monitoring the *in-Situ* Particle-Size Characteristics of Fluvial Suspended Sediment. *Water Research* **27**(9), 1413-1421.
- Wu R. M. and Lee D. J. (1998) Hydrodynamic drag force exerted on a moving floc and its implication to free-settling tests. *Water Research* **32**(3), 760-768.

# Distribution and Reactivity of O<sub>2</sub>-reducing Components in Sediments from a Layered Aquifer

## 3.1 INTRODUCTION

The natural potential of aquifer sediments to reduce oxidants is of general interest in groundwater chemistry. For instance, due to excessive fertilization and manuring extensive leaching of nitrate from agricultural fields occurs (Fraters *et al.*, 1998; Goodrich *et al.*, 1991; Lin *et al.*, 2001; Spalding and Exner, 1993) and the fate of this nitrate is controlled by the reactivity of the reductants present in the subsurface (Bradley *et al.*, 1992; Moncaster *et al.*, 2000; Pauwels *et al.*, 2000; Pauwels *et al.*, 1998; Postma *et al.*, 1991; Robertson *et al.*, 1996; Smith and Duff, 1988). Degradation of organic contaminants is also controlled by the redox status of the contaminated groundwater (Nielsen *et al.*, 1995a; Nielsen *et al.*, 1995b; Nielsen and Christensen, 1994a; Nielsen and Christensen, 1994b). The anaerobic degradation of benzene is of prime interest (Coates *et al.*, 2001; Lovely, 2000), as is the reductive dechlorination of chlorinated hydrocarbons by reactive reductants (Bradley *et al.*, 1998; Skubal *et al.*, 2001). The injection of oxidants such as oxygen, nitrate or sulfate may enhance the breakdown of mono-aromatics (Coates *et al.*, 2001; Cunningham *et al.*, 2000; Lovely, 2000), but an important drawback for stimulated *in-situ* bioremediation in contaminated aquifers, is the competition of natural reductants for injected oxidants (Baker *et al.*, 2000; Barcelona and Holm, 1991b).

Understanding the reactivity of reductants present in aquifer sediments thus deserves attention. Common reductants in aquifer sediments are sedimentary organic

---

Published as: N. Hartog, J. Griffioen, and C.H. Van Der Weijden (2002) *Environmental Science and Technology*, 36(11), 2436-2442

matter (SOM) and pyrite ( $\text{FeS}_2$ ), but ferrous iron in silicates, siderite ( $\text{FeCO}_3$ ) and vivianite as well as exchangeable ferrous iron are potentially reactive reductants too (Appelo and Postma, 1993). Pyrite and siderite are commonly found in close association with organic matter due to redox processes occurring during or after deposition (Berner, 1971). Therefore, a relationship between the reduction capacity and the diagenetic history of sediment can be expected. Furthermore, fine-grained sediments are generally richer in organic material and associated reduced mineral phases (McMahon and Chapelle, 1991; Robertson *et al.*, 1996) and higher total reduction capacities for aquifer sediments with a larger fine fraction has been suggested (Pedersen *et al.*, 1991). Recently, Christensen *et al.* (2000) discussed studies on the reduction capacity of aquifer sediments. The TRC of sediments can be calculated if all relevant reduced components are recognized and their quantification is sufficiently accurate. However, this approach yields a maximum potential, since it does not account for the reactivities of these components.

In this study, we focus on the reduction reactivity of pristine aquifer sediments by measuring the  $\text{O}_2$  consumption during incubations. Together with the overall change in aqueous composition, we use the stoichiometry between the  $\text{O}_2$  consumption and  $\text{CO}_2$  production to identify the ongoing oxidation reactions. Our objectives were 1. to determine the relative contribution of the identified reductants to the reduction activity, 2. to assess the difference in the reduction capacity of different grain size fractions, and 3. to evaluate the impact of geological stratification on the reduction activity within a layered single aquifer unit that consists of three geological units.

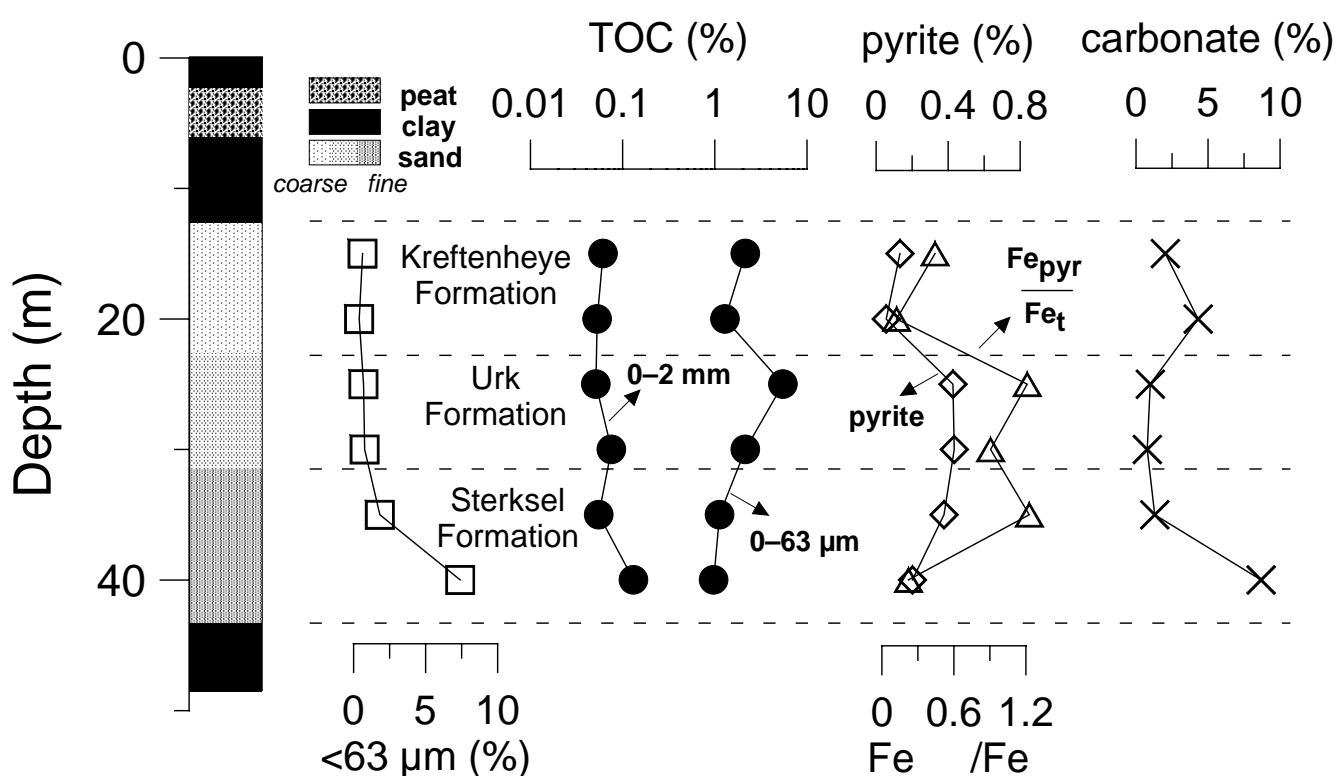
## **3.2 MATERIALS AND METHODS**

### **3.2.1 Sample Collection and Processing**

Six core samples were taken from a borehole in a sandy aquifer at the drinking water production site 'De Steeg' near Langerak, The Netherlands. This aquifer was

---

selected since it contains three distinct geological formations, covering a range from coarse to fine sands (Fig. 3.1). Furthermore, this location is proposed as a site for recharge through riverbank infiltration, which would result in a gradual oxidation of this aquifer that is currently under iron(III)-reducing conditions. Sediment cores were collected anaerobically at depth using Akkerman sampling tubes. The tubes were stored under a nitrogen atmosphere at 8°C directly after field collection. The tubes were opened in a N<sub>2</sub>-filled glovebox in which sediment samples were prepared for further study. By wet sieving, three particle size fractions were separated: 0–2000 µm



(total fraction), 0–63 µm (fine fraction) and 63–2000 µm (coarse fraction). The remaining fraction containing particles larger than 2 mm was not further analyzed.

**Figure 3.1** Geological description of the sediments and geochemical characteristics of the total fractions (0–2 mm) used. Depth is referenced in meters below surface level. A log scale was used for the TOC (%) to show also the data for the fine fraction (< 63 µm).

### 3.2.2 Geology

Holocene clays and peat confine the top of the aquifer; Early Pleistocene clays confine its bottom. The Kreftenheye Formation contains coarse fluvio-glacial sands,

deposited during the Late Pleistocene. The Urk Formation consists of medium sized Middle Pleistocene fluvial sands, deposited in a perimarine environment. The Sterksel Formation consists of fine fluvial sands from the Early Pleistocene (Fig. 3.1).

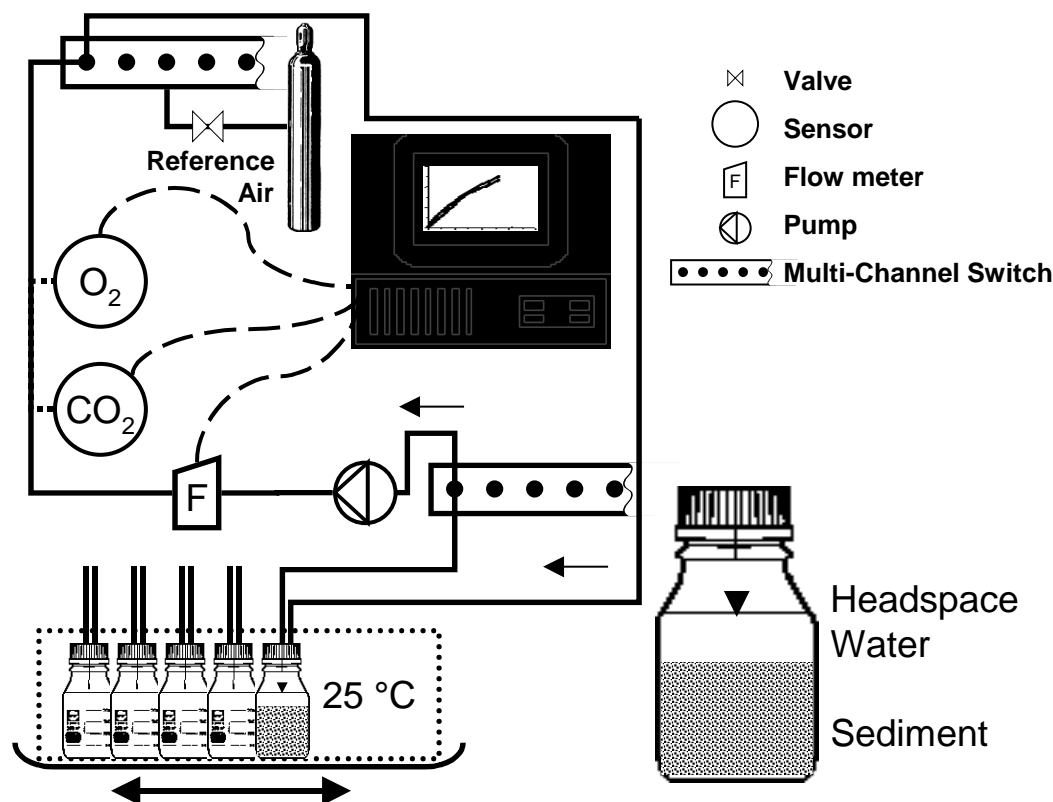


Figure 3.2 Schematic representation of the experimental set-up used (Micro-Oxymax, Columbus Instruments, OH).

### 3.2.3 Sediment Incubations

Samples were incubated under dark conditions. Twenty-five ml of vitamin and trace element solution were added in order to prevent inhibition due to nutrient limitation. Sample weight ranged from a few grams for the fine fraction to 100 g for the total fraction. The reaction chambers (100-ml bottle, Duran) were connected to the closed circuit of a respirometer (Fig. 3.2, Micro-Oxymax, Columbus Instruments). Water-saturated gasses were used to prevent evaporation in the reaction chambers. Oxygen ( $p_{\text{O}_2} = 10^{-0.69 \pm 0.004}$  atm) and carbon dioxide ( $p_{\text{CO}_2} = 10^{-3.3 \pm 0.11}$  atm) levels in the headspaces were kept at atmospheric conditions at 25°C ( $\pm 1^\circ\text{C}$ ). The O<sub>2</sub> consumption and CO<sub>2</sub> production were measured every 3 hours for 54 days, using an infrared sensor and an oxygen battery (fuel cell), respectively. The reaction chambers were

shaken (100 rpm) to ensure a well-mixed chemical system and prevent oxygen transfer limitations.

### **3.2.4 Analytical Procedures**

Directly after incubation pH was measured with a standard pH meter (Orion) and alkalinity was determined by acid titration. Dissolved cations and sulfate were analyzed using ICP-AES (Perkin-Elmer ICP-optima 3000). X-ray fluorescence (XARL8410) was used to determine total iron (Fe<sub>t</sub>) and total sulfur (S<sub>t</sub>) contents of the sediments. Total organic carbon (TOC) was measured on freeze-dried sediments using a method adapted from Jakobsen and Postma (1999), in which we used 2.6 M HCl to remove inorganic carbon. TOC was determined as the sum of two fractions: acid dissolvable organic carbon (ADOC), and the residual organic carbon (NADOC). ADOC content was measured as dissolved organic carbon in the acid solution (TOC-500, Shimadzu), while NADOC content was determined in the remaining solid sample by oxidation (NA1500 NCS, Carlo Erba). Pyrite contents were determined by HNO<sub>3</sub> extraction and total carbonate contents were determined as weight loss after acid digestion. Thermogravimetry is often used to assess the amounts of carbonates, but no good method yet exists to quantify low siderite concentrations in aquifer sediments (Christensen *et al.*, 2000). We tested a combination of thermogravimetry (TGA) and differential thermal analysis (TG-DTA92, Setaram).

### **3.2.5 Total Reduction Capacity**

The TRC was expressed in mmol O<sub>2</sub>/g.sed to enable direct comparison with the experimental data and was calculated using analyzed contents of total organic carbon [TOC], pyrite [FeS<sub>2</sub>] according to Equation 3.1.

$$TRC = 3\frac{3}{4} [FeS_2] + 1 [TOC] \text{ (mmol O}_2\text{/g.sed)} \quad \text{Equation 3.1}$$

Here, 3<sup>3</sup>/<sub>4</sub> and 1 refer to the stoichiometric coefficients of pyrite and SOM oxidation, respectively (Table 3.1). When present, siderite contributes to the TRC as well, but was left out of the calculation, because of its qualitative determination (see results and discussion section).

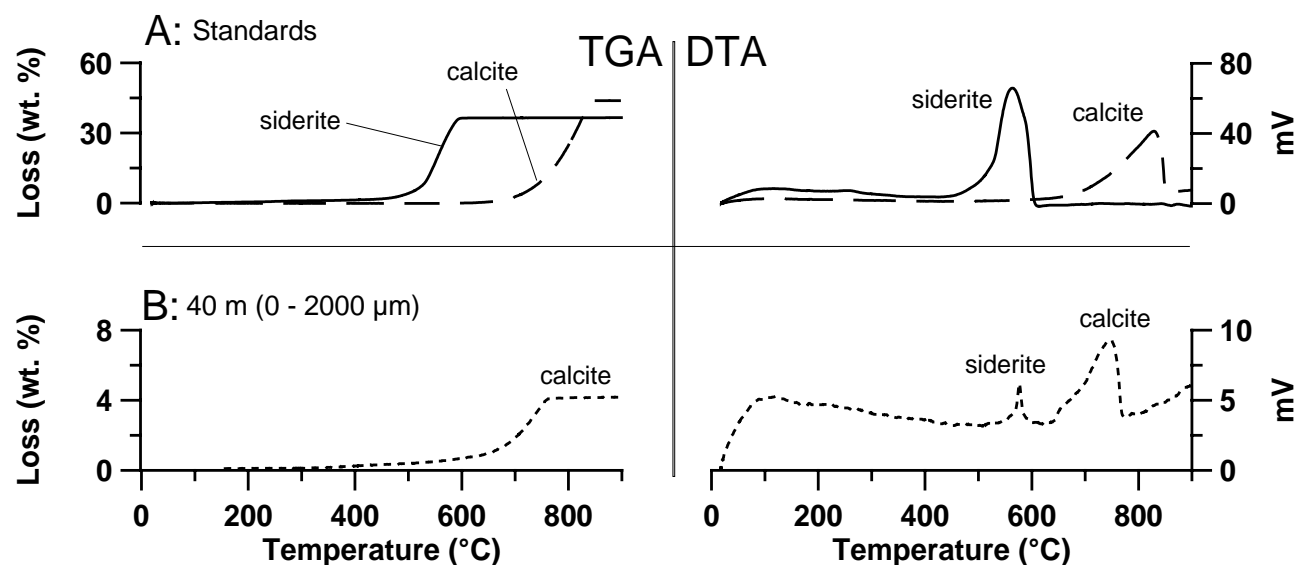


**Figure 3.3** A: TGA-DTA measurements ( $N_2$ -atmosphere/ $5^\circ C \cdot min^{-1}$  to  $900^\circ C$  on a Setaram TG-DTA92) A: TGA of ( $FeCO_3$ ) and calcite ( $CaCO_3$ ) standards and 0-2 mm fraction from 40 meters deep. B: DTA of ( $FeCO_3$ ) and calcite ( $CaCO_3$ ) standards and 0-2 mm fraction from 40 meters deep.

### 3.2.6 Geochemical Modeling

PHREEQC-2 (Parkhurst and Appelo, 1999) was used to model the chemical evolution in the batch chambers, using the  $O_2$  consumption over time as an input and the  $CO_2$  production as an output constraint. PHREEQC-2 was also used to determine saturation indices (SI), where SI is equal to the logarithmic value of the ratio between the ion activity product (IAP) and the solubility product ( $K_s$ ) for the mineral phases considered.

## 3.3 RESULTS AND DISCUSSION

### 3.3.1 Reductants present in the Aquifer Sediments

Significant amounts of pyrite and organic matter were present in all sediment samples (Fig. 3.1). In the Urk Formation, where the highest pyrite contents (up to 4350 ppm) were found, pyritic iron ( $Fe_{pyr}$ ) accounted for most of the total iron ( $Fe_t$ , Fig. 3.1) Furthermore, the molar ratio between  $Fe_t$  and total sulfur contents ( $Fe_t/S_t$ ) was close to 0.5. This indicates that other iron containing minerals were insignificant.



High Fe<sub>t</sub> and low S<sub>t</sub> concentrations were present in the deepest sediment taken from the Sterksel Formation. With 22% of Fe<sub>t</sub> present in pyrite, an additional source of iron, such as iron hydroxides, detrital phyllosilicates or siderite must be present. The weight loss during heating (TGA) confirmed the presence of calcite, but not of siderite. However, using differential thermal analysis (DTA), two distinct endothermic peaks between 500–600°C and 700–850°C were observed (Fig. 3.3) that are in agreement with both the disintegration temperatures of siderite and calcite from literature data (Borrego *et al.*, 2000; Gotor *et al.*, 2000; Vassilev and Vassileva, 1996) and the standards used. These results point to a siderite content of less than 1% in this carbonate-rich sediment. Thus, organic matter, pyrite and siderite are the main potentially reactive reductants present in the aquifer sediments studied. However, predicting which reductant is most prone to oxidation is difficult because these species have comparable energy yields for their oxidation (Pankow, 1991), while their oxidation mechanisms are distinctly different (Table 3.1).

**Table 3.1** Oxidation reactions of considered reduced components with molecular oxygen

				CO <sub>2</sub> /O <sub>2</sub>	ΔG <sub>r</sub> <sup>0 a</sup>
a	FeCO <sub>3</sub> + ¼ O <sub>2</sub> + 1½ H <sub>2</sub> O	→	Fe(OH) <sub>3</sub> + CO <sub>2</sub>	4	-468
b	C <sub>9</sub> H <sub>10</sub> O <sub>5</sub> <sup>b</sup> + 9 O <sub>2</sub>	→	9 CO <sub>2</sub> + 5 H <sub>2</sub> O	1	-433 <sup>c</sup>
c	FeS <sub>2</sub> + 3¾ O <sub>2</sub> + 1½ H <sub>2</sub> O + 2 CaCO <sub>3</sub>	→	Fe(OH) <sub>3</sub> + 2 Ca <sup>2+</sup> + 2 SO <sub>4</sub> <sup>2-</sup> + 2 CO <sub>2</sub>	8/15	-507
d	FeS <sub>2</sub> + 3¾ O <sub>2</sub> + 3½ H <sub>2</sub> O	→	Fe(OH) <sub>3</sub> + 2 SO <sub>4</sub> <sup>2-</sup> + 4 H <sup>+</sup>	0	-477
And with ferrous iron on exchange site X <sub>2</sub>					
e	Fe-X <sub>2</sub> + ¼ O <sub>2</sub> + CaCO <sub>3</sub> + 1½ H <sub>2</sub> O	→	Ca-X <sub>2</sub> + Fe(OH) <sub>3</sub> + CO <sub>2</sub>	4	

<sup>a</sup>ΔG<sub>r</sub><sup>0</sup> values calculated from Pankow (1991). <sup>b</sup>Syringate (C<sub>9</sub>H<sub>10</sub>O<sub>5</sub>) is used as a model compound for SOM (Chapelle and Bradley, 1996). <sup>c</sup>value for acetic acid.

### 3.3.2 Identification of important Oxidation Reactions: Theoretical CO<sub>2</sub>/O<sub>2</sub> Ratios

The ratio of CO<sub>2</sub> production to O<sub>2</sub> consumption is commonly used as respiratory quotient for the organic substrate. The molar CO<sub>2</sub>/O<sub>2</sub> ratio for the complete oxidation of organic matter varies with chemical composition from 1.0 for the oxidation of carbohydrates (C<sub>n</sub>H<sub>2n</sub>O<sub>n</sub>) to 0.8 for the oxidation of a more reduced organic compound as benzene (C<sub>6</sub>H<sub>6</sub>). The composition of SOM in the sediments studied, as derived from pyrolysis-GC-MS analyses, shows a predominantly aromatic signature derived lignin. Syringate (C<sub>9</sub>H<sub>10</sub>O<sub>5</sub>) has a chemical structure similar to methoxylated aromatic compounds that make up lignin (Chapelle and Bradley, 1996). Therefore we use syringate as a model compound for SOM, as shown in reaction (b) (Table 3.1).

While CO<sub>2</sub> production is inherent to the oxidation of organic matter, CO<sub>2</sub> production during pyrite or Fe(II) oxidation depends on the presence of reactive carbonates. Under carbonate equilibrium conditions, the theoretical molar CO<sub>2</sub>/O<sub>2</sub> ratio is distinctly different during pyrite oxidation, as shown in reaction (c), than during the sole oxidation of ferrous iron, as shown in reaction (a). In the absence of reactive carbonates, pyrite oxidation will not result in CO<sub>2</sub> production and the CO<sub>2</sub>/O<sub>2</sub> ratio will therefore be zero, shown in reaction (d). Pyrite, SOM and siderite are commonly found in other sedimentary aquifers, but reactive reductants, such as MnCO<sub>3</sub> (CO<sub>2</sub>/O<sub>2</sub>=2) or FeS (CO<sub>2</sub>/O<sub>2</sub>=0.44), can be assessed using the same approach. Since the resulting CO<sub>2</sub>/O<sub>2</sub> ratio of co-oxidizing reductants is not unique, constraints are needed to calculate their relative contributions. Here, sulfate is used to constrain the importance of pyrite oxidation

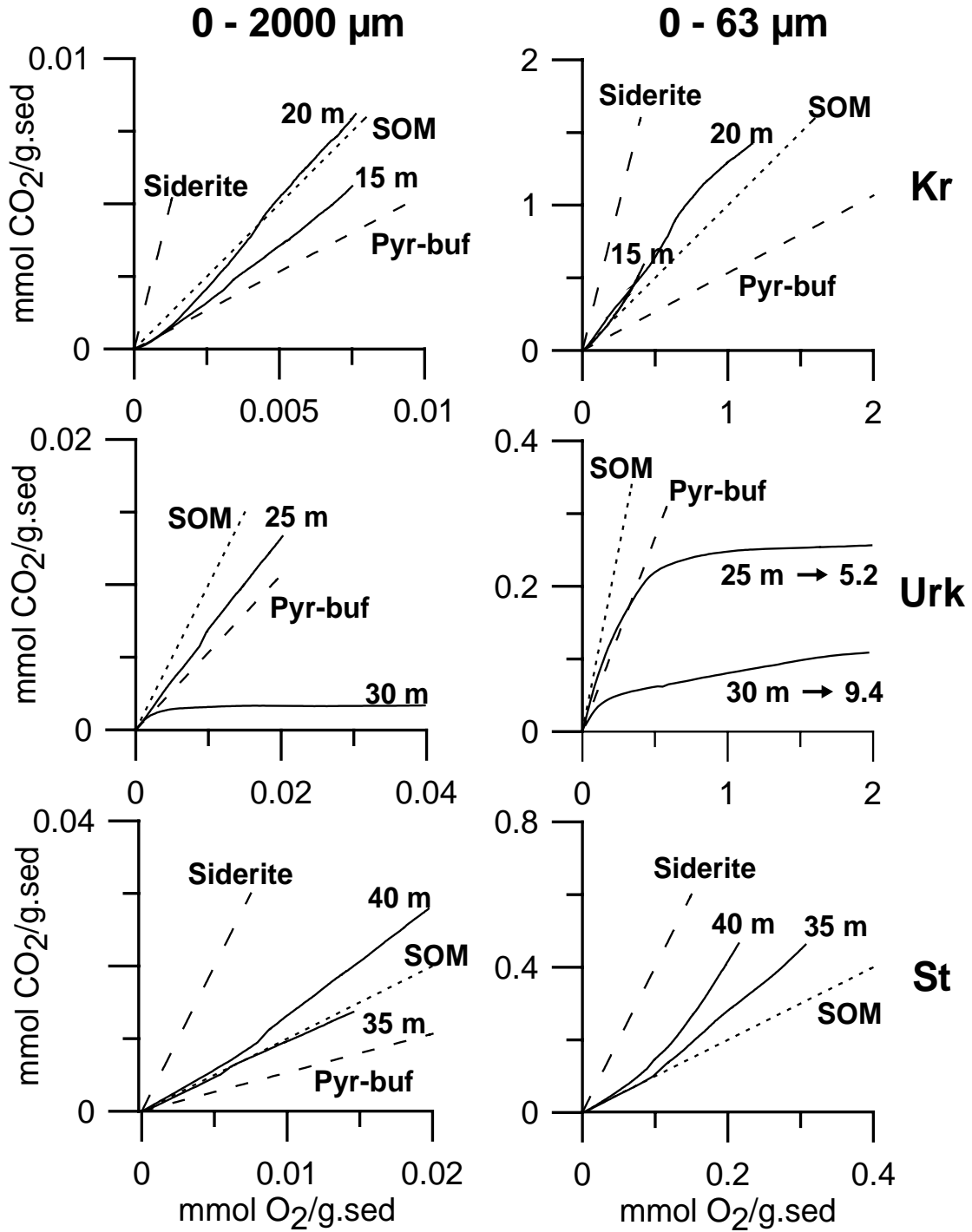


**Figure 3.3** Cumulative O<sub>2</sub> consumption and CO<sub>2</sub> production during the total and fine sediment fraction incubations (54 days) are represented by solid lines. Kr, Urk and St denote Kreftenheye, Urk and Sterksel Formation, respectively. The fine fractions of the Urk Formation were plotted up to 2 mmol O<sub>2</sub>/g.sed (total consumption indicated with arrow). Stoichiometric lines (dashed) are shown for siderite, SOM and pyrite oxidation under carbonate buffered conditions. Note the different scales for the axes.

### 3.3.3 Calculating the Relative Importance of Reductants

The relative contribution of pyrite ( $f_{pyr - buf}$ ) to the total oxygen consumption under carbonate buffered and unbuffered ( $f_{pyr - unbuf}$ ) conditions can be calculated from the total sulfate production (Eq. 3.3). Then, the relative contribution of siderite ( $f_{sid}$ ), SOM ( $f_{SOM}$ ) to the total  $O_2$  consumption can be calculated using the cumulative  $CO_2/O_2$  ratios (Eq. 3.4).

$$f_{pyr} + f_{SOM} + f_{sid} = 1 \quad \text{Equation 3.2}$$

$$f_{pyr} = f_{pyr - buf} + f_{pyr - unbuf} = \frac{3^{3/4} \sum SO_4}{2 \sum O_2} \quad \text{Equation 3.3}$$

$$\frac{\sum CO_2}{\sum O_2} = 4 f_{sid} + f_{SOM} + \frac{2}{3^{3/4}} f_{pyr - buf} \quad \text{Equation 3.4}$$

Here,  $\sum O_2$ ,  $\sum CO_2$  and  $\sum SO_4$  are the total amounts of  $O_2$  consumed,  $CO_2$  produced and sulfate produced, respectively. Equation 3.4 is valid if carbonate equilibrium and undersaturation for gypsum ( $CaSO_4 \cdot 2H_2O$ ) are maintained during the incubation.

When pyrite oxidation proceeds unbuffered by carbonate dissolution,  $f_{pyr - unbuf}$  is calculated using Equation 3.5, where  $\sum O_2^*$  is the total amount of oxygen consumption that was unaccompanied by  $CO_2$  release.

$$f_{pyr - unbuf} = \frac{\sum O_2^*}{\sum O_2} \quad \text{Equation 3.5}$$

### 3.3.4 Observed Processes during Sediment Incubations

The ratios between total  $CO_2$  produced and total  $O_2$  consumed during the incubation experiments ranged between 0.05 and 2.7 (Fig. 3.4). These are within the range of  $CO_2/O_2$  stoichiometries for the oxidation of pyrite, organic matter and siderite (Table 3.1), but do not correspond to the stoichiometric oxidation of one of

these main reductants. Therefore the observed CO<sub>2</sub>/O<sub>2</sub> ratios must be the result of their combined oxidation (Eq. 3.2).

### **3.3.5 Processes during Incubation**

#### *3.3.5.1 Total Fraction Incubations*

As shown in Figure 3.4, SOM oxidation is predominant in the Kreftenheye Formation, as based on the theoretical oxidation stoichiometry (Table 3.1). Pyrite oxidation is the foremost process in the Urk Formation. Initially, the 30-meter incubation shows CO<sub>2</sub> production and O<sub>2</sub> consumption according to the stoichiometric oxidation of pyrite oxidation under carbonate buffered conditions and subsequently O<sub>2</sub> consumption without CO<sub>2</sub> production. This indicates that the buffering capacity is limited and that the oxidation of organic matter or siderite is insignificant during the acidification, caused by unbuffered pyrite oxidation. Sediment incubations of the Sterksel Formation (35 and 40 m) show the oxidation of pyrite, SOM and siderite. Especially, the deepest sediment shows elevated (>1) CO<sub>2</sub>/O<sub>2</sub> ratios and thus the largest contribution by siderite oxidation. This is in line with the detection of siderite in this sediment. The CO<sub>2</sub>/O<sub>2</sub> ratios changed little during the total fraction incubations that were carbonate buffered, indicating that the reductants were oxidized concurrently.

#### *3.3.5.2 Fine Fraction Incubations*

The oxidation of SOM is most pronounced in the fine fraction incubations of the Kreftenheye Formation (Fig. 3.4), indicating that diagenetically formed reductants were absent or less reactive. The fine fractions of the Sterksel Formation show elevated CO<sub>2</sub>/O<sub>2</sub> ratios towards the end of the incubations (Fig. 3.4), indicating an increasing importance of siderite oxidation. Although the oxidation of exchangeable ferrous iron, as shown in reaction (e), would result in an identical CO<sub>2</sub>/O<sub>2</sub> ratio, the estimated release of ferrous iron from cation-exchange sites in these fine fractions was insignificant compared with the total observed O<sub>2</sub> consumption. Moreover, it would be expected to proceed early in the experiments, since desorption (Koretsky, 2000;

Sposito, 1989) and oxidation of aqueous ferrous iron at circumneutral pH (Stumm and Morgan, 1970) are both almost instantaneous. The  $\text{CO}_2/\text{O}_2$  ratios of the fine fraction incubations of the Urk Formation (Fig. 3.4) initially show buffered pyrite oxidation followed within a week by pyrite oxidation unbuffered by carbonate dissolution. Even though the fine fractions of the Urk and Sterksel Formation are relatively enriched in TOC (Fig. 3.1), the diagenetically formed reductants in the fine fractions are more reactive than SOM.

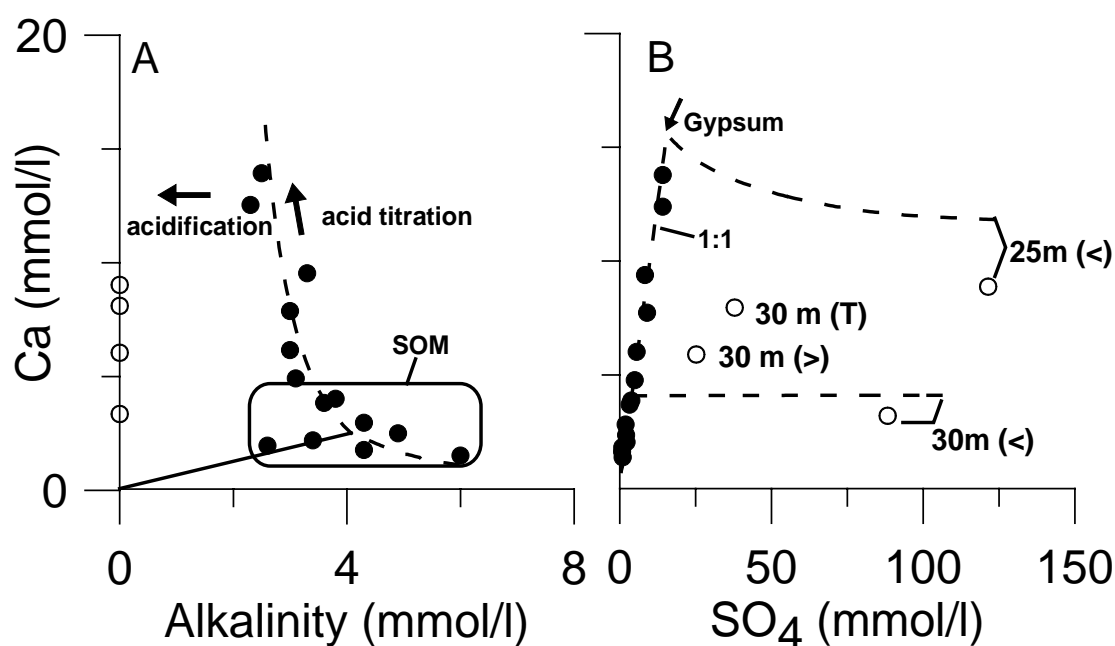


**Figure 3.4** Final concentrations in the supernatants of (A) calcium and alkalinity and (B) calcium and sulfate. Filled and open circles represent buffered and acidified samples, respectively. The solid line in (A) represents calcite equilibrium for increasing  $\text{CO}_2$ -pressure, the rectangle encompasses samples that show over 70% SOM oxidation and that are therefore less influenced by acid titration. The arrow in (B) indicates the onset of gypsum saturation and the dashed lines describe the modeling results. Depth (m) is shown for the acidified total (T), coarse (>) and fine (<) fractions.

### 3.3.5.3 Coarse Fraction Incubations

The coarse fractions were less reactive (55–86%) compared with the total fractions. The carbonate buffered coarse fractions show a greater contribution (52–86%) by SOM oxidation compared with the corresponding total and fine fractions. However, SOM oxidation was insignificant during the incubation of the coarse

fraction from 30 meters depth, which acidified due to the pyrite oxidation that proceeded largely (75%) unbuffered by carbonates.

### **3.3.6 Chemical Evolution of Supernatants during Incubation**

Final pHs, alkalinities and calcium concentrations of the supernatants were all in agreement with carbonate equilibrium, except for the incubations that showed unbuffered pyrite oxidation, which acidified to pH values of 1.6 to 2.5 (Table 3.2, Fig. 3.5a). The relatively high CO<sub>2</sub> production rates in combination with the low equilibrium concentration of CO<sub>2</sub> (10<sup>-3.5</sup> atm) caused a build-up of CO<sub>2</sub> (10<sup>-1.7</sup> atm) in the supernatants. However, this was less than 1% of the total CO<sub>2</sub> production in all incubations. Therefore, overall CO<sub>2</sub>/O<sub>2</sub> ratios were not significantly affected.

The interpretations based on CO<sub>2</sub>/O<sub>2</sub> ratios are in keeping with the chemical composition of the supernatants after incubation. Incubations that dominantly showed buffered pyrite oxidation have higher calcium concentrations (up to 15 mmol/l) and lower alkalinities compared with those expected from calcite dissolution in equilibrium with the CO<sub>2</sub> pressure in the headspaces. Especially, final calcium and sulfate concentrations in the supernatant of the carbonate buffered incubations were highly correlated along the theoretical stoichiometry for pyrite oxidation, but were still undersaturated with respect to gypsum (Fig. 3.5b). This indicates that H<sup>+</sup> production during pyrite oxidation was the main drive for the dissolution of sedimentary calcite. Total sulfate production was highest for samples that showed a pyrite oxidation CO<sub>2</sub>/O<sub>2</sub> stoichiometry (Urk Formation). In these samples the total sulfate production was also related to the total O<sub>2</sub> consumption along the pyrite oxidation stoichiometry (Fig. 3.6). The incubated fractions of the Kreftenheye Formation from 20 meters depth show CO<sub>2</sub>/O<sub>2</sub> ratios that are closest to SOM oxidation. If sulfate in these experiments is the product of SOM oxidation only, then the degree of sulfurization (S/C) of the oxidized SOM (0.03) is high compared with those of organic matter (0.006–0.03) in freshwater lake sediments (Urban *et al.*, 1999). Although it is not possible to distinguish between an organic or pyritic source of the sulfate, it is clear that pyrite oxidation contributes very little to the observed total O<sub>2</sub> consumption in these incubations.

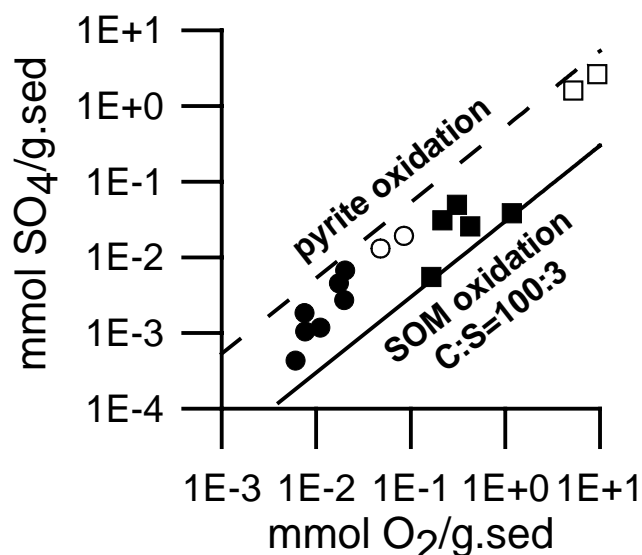


**Figure 3.5** O<sub>2</sub> consumption and total sulfate production for total and coarse (both circles) and fine (squares) fractions. Carbonate buffered and acidified incubations are represented by filled and open symbols, respectively. Lines refer to stoichiometric oxidation of pyrite and SOM. Note the logarithmic scales.

In the four samples where pyrite oxidation resulted in acidic supernatants, final sulfate concentrations could only account for half of the total O<sub>2</sub> consumption. Since CO<sub>2</sub> production ceased in these incubations (Fig. 3.4), the additional oxidation of SOM or siderite oxidation cannot account for this discrepancy. Therefore, the precipitation of sulfate-containing solids controlled the final sulfate concentrations in these samples. This hypothesis was tested by modeling the pyrite oxidation in the two fine fractions of the Urk Formation with PHREEQC-2 (Parkhurst and Appelo, 1999). We used the total amount of O<sub>2</sub> consumption and CO<sub>2</sub> production as a constraint for the total amount of pyrite oxidation and the total amount of reactive carbonate buffer, respectively. A model containing only calcite and pyrite and K-feldspar (as a source of potassium) was used. Results (Fig. 3.5b) indicated the likely precipitation of K-jarosite (KAl<sub>3</sub>(OH)<sub>6</sub>(SO<sub>4</sub>)<sub>2</sub>) as well as gypsum during the incubation of the fine fraction from 30 meters and 25 meters depth, respectively. Considering the limited number of input constraints, the modeled pH and final calcium and sulfate concentrations agree very well with the measured values in the supernatants.



### 3.3.7 Reactivity of Reduced Components

Our results show that pyrite, SOM and siderite were oxidized simultaneously during our sediment incubations (Table 3.2). To assess their separate reactivities, we will next consider experiments in which one reductant was dominantly important.

#### 3.3.7.1 *Sedimentary Organic Matter*

In the fine (Fig. 3.7a) and coarse (Fig. 3.7b) fraction from 20 meters depth, SOM accounted for 85% and 86% of the total O<sub>2</sub> consumption. Both incubations show continuously decreasing O<sub>2</sub> consumption rates. Decreasing respiration rates are often observed (*e.g.* Kristensen *et al.*, 1995) and are attributed to an increasing stability of the residual organic compounds (Cowie and Hedges, 1994; Hulthe *et al.*, 1998). In comparison with the coarse fractions, the importance of SOM oxidation was less important in the fine fractions than the oxidation of pyrite and siderite. This can be due to a decreased reactivity of SOM in the fine fractions as a result of physical protection through sorption and complexation of SOM by clay minerals (Mayer, 1994) or to a higher degree of mineralization of the original SOM during to the formation of reduced secondary minerals, like pyrite and siderite, during diagenesis (Cowie and Hedges, 1994). Even though the acid hydrolysis of SOM during unbuffered pyrite oxidation resulted in final DOC concentrations up to 87 mg/l, SOM oxidation was not observed. This is probably due to the inhibition of microbial respiration under acid conditions (Atlas and Bartha, 1998).

#### 3.3.7.2 *Pyrite*

Buffered pyrite oxidation is the dominant (86%) oxygen-consuming process in the coarse fraction from 25 meters (Fig. 3.7a). Here, the O<sub>2</sub> consumption rates decreased continuously. Pyrite oxidation will result in the formation of iron hydroxides provided that the proton production is buffered by carbonate dissolution to keep the pH circumneutral. These iron hydroxides may precipitate on the pyrite surfaces and act as a diffusive resistance, slowing its oxidation (Nicholson *et al.*, 1990; Andersen *et al.*, 2001).

After the carbonate buffer had been consumed within one week of incubation, unbuffered pyrite oxidation started in the coarse (30 m, 75%) and fine (25 m, 77%) fractions (Figs. 3.7a and 3.7b). During the acidification O<sub>2</sub> consumption rates started to increase up to a maximum, after which the rates dropped until the end of the experiments when the samples had acidified to a pH < 2. Since only the samples that showed unbuffered pyrite oxidation exhibit this typical sequence, we interpret this maximum in the O<sub>2</sub> consumption rate to be a pH effect. The pH-dependent dissolution of an inhibiting iron hydroxide coating, formed during buffered pyrite oxidation, and the subsequent production of ferric iron at acid pH, which is a rate-controlling intermediate in the oxidation of pyrite by O<sub>2</sub> (Moses and Herman, 1991), are probable causes for the increased rates compared with buffered pyrite oxidation. Furthermore, the modeled pH values of 2–4 during the maximum O<sub>2</sub> consumption rates approximate the reported optimal pH conditions for microbial ferrous iron oxidation (Roychoudhury *et al.*, 1998). This suggests that bacteria, capable to facilitate acid pyrite oxidation, were already present in this initially reduced sediment. The final decrease in pyrite oxidation rates is probably due to the slow, rate-controlling, abiotic oxidation of ferrous iron at a pH < 2 (Stumm and Morgan, 1970).

### 3.3.7.3 *Siderite*

Although the quantification of low contents of siderite remains difficult, our CO<sub>2</sub>/O<sub>2</sub> ratios indicate the importance of siderite as a reactive species in subsurface sediments. The fine fraction from 40 meters depth showed the highest (43%) contribution by siderite oxidation (Table 3.2) and continuously decreasing O<sub>2</sub> consumption rates (Fig. 3.7b). It also has the lowest total oxygen consumption of all incubated fine fractions, while the corresponding total fraction is relatively much more reactive. This suggests that the oxidation of siderite is a slower process, compared with the oxidation of pyrite or SOM. The chemical stability and weathering of siderite to form iron hydroxides in geological environments is well documented but rather little is known about the nature of siderite weathering itself (McMillan and Schwertmann, 1998; Postma, 1983; Weber *et al.*, 2001). Similar to the inhibition

during buffered pyrite oxidation, the iron oxyhydroxides coatings formed during siderite oxidation can potentially slow down its oxidation.

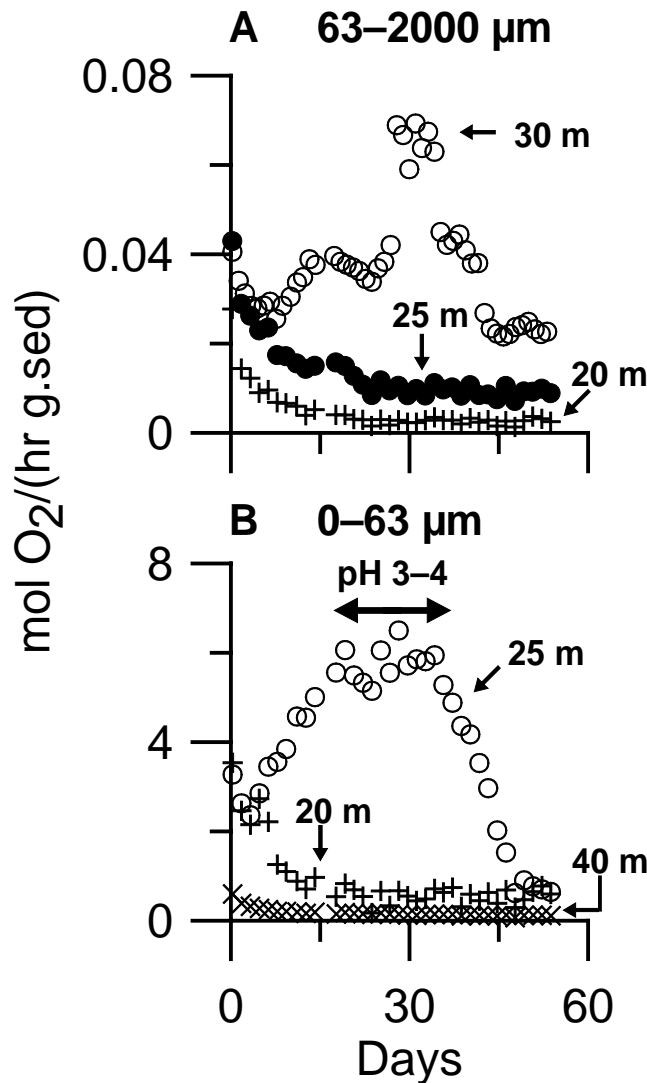


**Figure 3.6** O<sub>2</sub> consumption rates during the incubation of coarse (A) and fine (B) fractions that dominantly showed unbuffered pyrite oxidation (open circles, buffered pyrite oxidation (filled circles), SOM oxidation (pluses) or siderite oxidation (crosses). The rate maxima in O<sub>2</sub> consumption during unbuffered pyrite oxidation correspond with a modeled pH range of 3–4.

### 3.3.8 Measured Reduction Capacity

Oxygen consumption of the sediment fractions slowed down considerably during incubation, but had not ended at the end of the incubations. Therefore, the total amount of O<sub>2</sub> consumption on a dry weight basis will be referred to as measured reduction capacity (mRC). The mRC of the total fractions (Table 3.2) was related to their geology and ranged from 8 μmol O<sub>2</sub>/g in Kreftenheye Formation, to 20–84 μmol

$O_2/g$  in the Urk Formation. The mRCs of the sediments from the Sterksel Formation were intermediate (15–20  $\mu\text{mol } O_2/g$ ). This relative trend for the different formations is also reflected in the mRCs of the coarse (6–47  $\mu\text{mol } O_2/g$ ) and fine fractions (Table 3.2). This suggests that the reducing capacity of these sediments is related to their geological histories.

**Table 3.2** TRC values of the total fractions, as calculated from SOM and pyrite contents and final mRC values for the total and fine fractions. Final pHs and total produced sulfate in the supernatants. Cumulative molar  $CO_2/O_2$  ratios and sulfate production were used to calculate the relative contribution to the total  $O_2$  consumption of the oxidation reactions (a-d, Table 3.1).

Depth (m)	TRC ( $\mu\text{mol } O_2/g$ )	mRC ( $\mu\text{mol } O_2/g$ )	pH	$SO_4$ ( $\mu\text{mol/g}$ )	$CO_2/O_2$ (molar)	Oxidation reactions (%)			
						(a)	(b)	(c)	(d)
<b>Total Fractions (0–2 mm)</b>									
15	93	8	7.2	1.8	0.75		54	46	
20	62	8	7.5	1.0	1.06	6	68	26	
25	176	20	6.3	6.7	0.66		38	62	
30	199	84	2.1	19.1	0.02			9	91
35	164	15	6.8		0.94		87	13	
40	172	20	7.1	2.7	1.41	18	56	26	
<b>Fine Fractions (&lt; 63 <math>\mu\text{m}</math>)</b>									
15		422	7.2	25.5	1.40	15	74	11	
20		1169	6.6	38.3	1.22	8	86	6	
25		5217	1.6	1598	0.06			23	77
30		9357	1.6	2628	0.02			8	92
35		307	7.1	49.4	1.51	22	48	30	
40		215	7.2	30.7	2.17	43	30	27	

The mRCs of the fine fractions (Table 3.2) were around two orders of magnitude higher than those of the corresponding total fractions, due to the higher content of TOC (Fig. 3.1) and associated diagenetic reductants in the fine fractions. However, the greater importance of the fine fraction in the Sterksel sediments (Fig. 3.1) is not reflected by the intermediate mRCs of their total fractions. Moreover, the mRCs of the fine Sterksel fractions are lowest of all fine fractions. Probably, the differences in grain size distribution between the studied aquifer sands are too minor for the higher reduction capacity of the fine fraction to have profound effect on the reduction capacity of the total fractions. This is due to the fact that the significance of the fine fraction is relatively small in the total grain size distribution. Consequently, the coarse fraction mainly diluted the reduction activity of the fine fraction with its

lowest overall mRC. This conclusion is in line with the lack of correlation found between the clay content and TRC of a sandy aquifer material (Pedersen *et al.*, 1991).

### **3.3.9 Kinetic Controls on the Available Reduction Capacity**

The mRCs after 54 days of incubation were around 10% of the TRC calculated from pyrite and TOC contents of the carbonate buffered total fractions (Table 3.2). Thus, only a small fraction of the TRC present reacted during these incubations. As an exception, the mRC of the total fraction from 30 meters depth was 42% of the calculated TRC. While SOM oxidation was suppressed at these low pHs, these results indicate that pH is an important factor controlling the oxidation rates of different reductants.

Previous studies on aquifer sediments used the standard method of acid dichromate oxidation (Christensen *et al.*, 2000; Pedersen *et al.*, 1991) to measure reduction capacities. Using this method, Barcelona and Holm, (1991a) and Barcelona and Holm (1991b) found the mRCs to be around 50% of the TRCs calculated from the total amounts of reduced solid species. While this indicates that still only a part of the TRC present in aquifer sediments is reactive at experimental time scales, this higher recovery is likely caused by the use of this abiotic method with a stronger oxidant under acid conditions that would promote pyrite oxidation. Furthermore, Pedersen *et al.* (1991) found around 40% of the mRC remaining after having been exposed to oxygen and nitrate for about 2 years, in a study on an oxidation–reduction front in a shallow sandy aquifer using the same method.

## **3.4 IMPLICATIONS FOR FIELD STUDIES**

Clearly, the reactivity of the subsurface reductants depends on the physicochemical conditions (oxidant type, temperature, pH) as well as on the intrinsic characteristics of the reductants that make up the TRC. For instance, the degradability of SOM is determined by its chemical composition and the strength of the degrading oxidant (Kristensen *et al.*, 1995), while the occurrence of iron sulfide oxidation depends strongly on oxidant type and pH (Schippers and Jørgensen, 2002). Therefore,

the mRC of subsurface sediments depends on the strength of the oxidant used and the applied conditions as well as on exposure time. Thus, while the use of the acid dichromate oxidation method may be appropriate in the context of an *in-situ* contaminant oxidation using Fenton's reagents, it is prone to overestimate the reduction capacity of aquifer sediments under milder conditions, since most redox reactions occurring in aquifers involve oxidation by weaker oxidants, such as oxygen, nitrate, ferric iron, sulfate or tetrachloroethylene and are microbially mediated (Jakobsen and Postma, 1994; Murphy *et al.*, 1992).

So far, studies did not address the contributions of various reductants (Barcelona and Holm, 1991a; Barcelona and Holm, 1991b; Christensen *et al.*, 2000; Pedersen *et al.*, 1991). However, the secondary effects on groundwater quality may be quite different for the oxidation of SOM versus that of pyrite. For example the release of increased mobility of trace metals during pyrite oxidation (Larsen and Postma, 1997; Nickson *et al.*, 2000) or the eutrophication by  $\text{NH}_4^+$  or  $\text{PO}_4^{2-}$  during SOM oxidation (Nolan and Stoner, 2000).

The reactivity of natural reductants is an important environmental issue, either during the natural attenuation of percolating nitrate or in competition with contaminants for injected oxidants. Our oxidation experiments with  $\text{O}_2$ , showed the simultaneous oxidation of reductants. Their relative contribution depends both on their relative amounts and their relative reactivity towards  $\text{O}_2$ . However, there is still limited knowledge about the controls on reactivity of characteristics such as the specific surface area of and coatings on pyrite (Andersen *et al.*, 2001) and the association and composition of SOM (Christensen *et al.*, 2000) on their reactivity of within aquifer sediments. Moreover, the reactivities of reductants present are affected by the conditions of the system to which they are exposed.

Incubations, which resulted in acidification, bear more resemblance to pyrite oxidation in leached topsoil. However, incubations under permanent carbonate buffering are relevant for many natural aquifer settings. Our buffered batch incubations show considerably lowered but still continuous oxygen consumption rates. Extrapolation of these rates, using an exponential decrease model, suggests that

20–40% of the TRC present in the sediments would remain after 2 years. While this estimate is in agreement with previous data (Pedersen *et al.*, 1991), this is a crude estimate, since the calculated TRC does not account for contributions by reductants other than pyrite and SOM and assumes constant conditions.

In the field of reactive transport modeling, major uncertainties exist about the availability and reactivity of the solid redox-sensitive phases. Results of this study indicate that several reductants can be oxidized simultaneously and that their reactivities depend on both geological and environmental factors. These factors should be taken into account in order to describe and predict the development of groundwater chemistry. Moreover, considering the vertical heterogeneity in reduction activity in the studied aquifer, a reactive transport model would not only require model layering in its physical properties but in its geochemical reactivity as well (Islam *et al.*, 2001).

## **References**

- Andersen M. S., Larsen F., and Postma D. (2001) Pyrite oxidation in unsaturated aquifer sediments. Reaction stoichiometry and rate of oxidation. *Environmental Science and Technology* **35**, 4074-4079.
- Appelo C. A. J. and Postma D. (1993) *Geochemistry, Groundwater and Pollution*. Balkema.
- Atlas R. M. and Bartha R. (1998) *Microbial Ecology: Fundamentals and Applications*. Benjamin/Cummings Science Publishing.
- Baker R. J., Baehr A. L., and Lahvis M. A. (2000) Estimation of hydrocarbon biodegradation rates in gasoline-contaminated sediment from measured respiration rates. *Journal of Contaminant Hydrology* **41**, 175-192.
- Barcelona M. J. and Holm R. T. (1991a) Additions and Corrections: Oxidation-reduction capacities of aquifer solids. *Environmental Science and Technology* **26**(12), 2540.
- Barcelona M. J. and Holm R. T. (1991b) Oxidation-reduction capacities of aquifer solids. *Environmental Science and Technology* **25**, 1565-1572.
- Berner R. A. (1971) *Principles of Chemical Sedimentology*. McGraw-Hill.
- Borrego A. G., Prado J. G., Fuente E., Guillén M. D., and Blanco C. G. (2000) Pyrolytic behaviour of Spanish oil shales and their kerogens. *Journal of Analytical and Applied Pyrolysis* **56**, 1-21.
- Bradley P. M., Chapelle F. H., and Wilson J. T. (1998) Field and laboratory evidence for intrinsic biodegradation of vinyl chloride contamination in a Fe(III)-reducing aquifer. *Journal of Contaminant Hydrology* **31**, 111-127.

- Bradley P. M., Fernandez Jr M., and Chapelle F. H. (1992) Carbon limitation of denitrification rates in an anaerobic groundwater system. *Environmental Science and Technology* **28**(12), 2377-2381.
- Chapelle F. H. and Bradley P. M. (1996) Microbial acetogenesis as a source of organic acids in ancient Atlantic Coastal Plain sediments. *Geology* **24**(10), 925-928.
- Christensen T. H., Bjerg P. L., Banwart S. A., Jakobsen R., Heron G., and Albrechtsen H.-J. (2000) Characterization of redox conditions in groundwater contaminant plumes. *Journal of Contaminant Hydrology* **45**, 165-241.
- Coates J. D., Chakraborty R., Lack J. G., O'Connor S. M., Cole K. A., Bender K. S., and Achenbach L. A. (2001) Anaerobic benzene oxidation coupled to nitrate reduction in pure culture by two strains of *Dechloromonas*. *Nature* **411**, 1039-1043.
- Cowie G. L. and Hedges J. I. (1994) Biochemical indicators of diagenetic alteration in natural organic matter mixtures. *Nature* **369**, 304-307.
- Cunningham J. A., Hopkins G. D., Lebron C. A., and Reinhard M. (2000) Enhanced anaerobic bioremediation of groundwater contaminated by fuel hydrocarbons at Seal Beach, California. *Biodegradation* **11**, 159-170.
- Fraters D., Boumans L. J. M., van Drecht G., de Haan T., and de Hoop W. D. (1998) Nitrogen monitoring in groundwater in the sandy regions of the Netherlands. *Environmental Pollution* **102**, 479-485.
- Goodrich J. A., Lykins J., B.W., and Clarck R. M. (1991) Drinking water from agriculturally contaminated groundwater. *Journal of Environmental Quality* **20**(4), 707-717.
- Gotor F. J., Macías M., Ortega A., and Criado J. M. (2000) Comparative study of the kinetics of the thermal decomposition of synthetic and natural siderite samples. *Physics and Chemistry of Minerals* **27**, 495-503.
- Hulthe G., Hulth S., and Hall P. O. J. (1998) Effect of oxygen on degradation rate of refractory and labile organic matter in continental margin sediments. *Geochimica et Cosmochimica Acta* **62**(8), 1319-1328.
- Islam J., Singhal N., and O'Sullivan M. (2001) Modeling biogeochemical processes in leachate-contaminated soils: a review. *Transport in Porous Media* **43**, 407-440.
- Jakobsen R. and Postma D. (1994) In situ rates of sulfate reduction in an aquifer (Rømø, Denmark) and implications for the reactivity of organic matter. *Geology* **22**, 1103-1106.
- Jakobsen R. and Postma D. (1999) Redox zoning, rates of sulfate reduction and interactions with Fe-reduction and methanogenesis in a shallow sandy aquifer, Rømø, Denmark. *Geochimica et Cosmochimica Acta* **63**(1), 137-151.
- Koretsky C. (2000) The significance of surface complexation reactions in hydrologic systems: a geochemist's perspective. *Journal of Hydrology* **230**, 127-171.
- Kristensen E., Ahmed S. I., and Devol A. H. (1995) Aerobic and anaerobic decomposition of organic matter in marine sediments: Which is fastest. *Limnology and Oceanography* **40**(8), 1430-1437.



- Larsen F. and Postma D. (1997) Nickel mobilization in a groundwater well field: Release by pyrite oxidation and desorption from manganese oxides. *Environmental Science and Technology* **31**, 2589-2595.
- Lin B.-L., Sakoda A., Shibasaki R., and Suzuki M. (2001) A modelling approach to global nitrate leaching caused by anthropogenic fertilisation. *Water Research* **35**(8), 1961-1968.
- Lovely D. R. (2000) Anaerobic benzene degradation. *Biodegradation* **11**, 107-116.
- Mayer L. M. (1994) Relationships between mineral surfaces and organic carbon concentrations in soils and sediments. *Chemical Geology* **114**, 347-363.
- McMahon P. B. and Chapelle F. H. (1991) Microbial production of organic acids in aquitard sediments and its role in aquifer geochemistry. *Nature* **349**, 233-235.
- McMillan S. G. and Schwertmann U. (1998) Morphological and genetic relations between siderite, calcite and goethite in a Low Moor Peat from southern Germany. *European Journal of Soil Science* **49**, 283-293.
- Moncaster S. J., Botrell S. H., Tellam J. H., Lloyd J. W., and Konhauser K. O. (2000) Migration and attenuation of agrochemical pollutants: insights from isotopic analysis of groundwater sulphate. *Journal of Contaminant Hydrology* **43**, 147-163.
- Moses C. O. and Herman J. S. (1991) Pyrite oxidation at circumneutral pH. *Geochimica et Cosmochimica Acta* **55**, 471-482.
- Murphy E. M., Schramke J. A., Fredrickson J. K., Bledsoe H. W., Francis A. J., Sklarew D. S., and Linehan J. C. (1992) The influence of microbial activity and sedimentary organic carbon on the isotope geochemistry of the Middendorf aquifer. *Water Resources Research* **28**(3), 723-740.
- Nicholson R. V., Gillham R. W., and Reardon E. J. (1990) Pyrite oxidation in carbonate-buffered solution: 2. Rate control by oxide coatings. *Geochimica et Cosmochimica Acta* **54**, 395-402.
- Nickson R. T., McArthur J. M., Ravenscroft P., Burgess W. G., and Ahmed K. M. (2000) Mechanism of arsenic release to groundwater, Bangladesh and West Bengal. *Applied Geochemistry* **15**, 403-413.
- Nielsen P. H., Albrechtsen H.-J., Heron G., and Christensen T. H. (1995a) In situ and laboratory studies on the fate of specific organic compounds in an anaerobic landfill leachate plume, 1. Experimental conditions and fate of phenolic compounds. *Journal of Contaminant Hydrology* **20**, 27-50.
- Nielsen P. H., Bjarnadóttir H., Winter P. L., and Christensen T. H. (1995b) In situ and laboratory studies on the fate of specific organic compounds in an anaerobic landfill leachate plume, 2. Fate of aromatic and chlorinated aliphatic compounds. *Journal of Contaminant Hydrology* **20**, 51-66.
- Nielsen P. H. and Christensen T. H. (1994a) Variability of biological degradation of aromatic-hydrocarbons in an aerobic aquifer determined by laboratory batch experiments. *Journal of Contaminant Hydrology* **15**(4), 305-320.

- Nielsen P. H. and Christensen T. H. (1994b) Variability of biological degradation of phenolic hydrocarbons in an aerobic aquifer determined by laboratory batch experiments. *Journal of Contaminant Hydrology* **17**(1), 55-67.
- Nolan B. T. and Stoner J. D. (2000) Nutrients in groundwaters of the conterminous United States 1992-1995. *Environmental Science & Technology* **34**(7), 1156-1165.
- Pankow J. F. (1991) *Aquatic Chemistry Concepts*. Lewis Publishers.
- Parkhurst D. L. and Appelo C. A. J. (1999) User's guide to PHREEQC (Version 2). U.S. Geological Survey.
- Pauwels H., Foucher J.-C., and Kloppmann W. (2000) Denitrification and mixing in a schist aquifer: influence on water chemistry and isotopes. *Chemical Geology* **168**, 307-324.
- Pauwels H., Kloppmann W., Foucher J.-C., Martelat A., and Fritsche V. (1998) Field tracer test for denitrification in a pyrite-bearing schist aquifer. *Applied Geochemistry* **13**(6), 767-778.
- Pedersen J. K., Bjerg P. L., and Christensen T. H. (1991) Correlation of nitrate profiles with groundwater and sediment characteristics in a shallow sandy aquifer. *Journal of Hydrology* **124**, 263-277.
- Postma D. (1983) Pyrite and siderite oxidation in swamp sediments. *Journal of Soil Science* **34**, 163-182.
- Postma D., Boesen C., Kristiansen H., and Larsen F. (1991) Nitrate reduction in an unconfined sandy aquifer: Water chemistry, reduction processes, and geochemical modeling. *Water Resources Research* **27**(8), 2027-2045.
- Robertson W. D., Russell B. M., and Cherry J. A. (1996) Attenuation of nitrate in aquitard sediments of southern Ontario. *Journal of Hydrology* **180**, 267-281.
- Roychoudhury A. N., Viollier E., and Van Cappellen P. (1998) A plug flow-through reactor for studying biogeochemical reactions in undisturbed aquatic sediments. *Applied Geochemistry* **13**, 269-280.
- Schippers A. and Jørgensen B. B. (2002) Biogeochemistry of pyrite and iron sulfide oxidation in marine sediments. *Geochimica et Cosmochimica Acta* **66**(1), 85-92.
- Skubal K. L., Barcelona M. J., and Adriaens P. (2001) An assessment of natural biotransformation of petroleum hydrocarbons and chlorinated solvents at an aquifer plume transect. *Journal of Contaminant Hydrology* **49**, 151-169.
- Smith R. L. and Duff J. H. (1988) Denitrification in a sand and gravel aquifer. *Applied and Environmental Microbiology* **54**(5), 1071-1078.
- Spalding R. F. and Exner M. E. (1993) Occurrence of nitrate in groundwater-A review. *Journal of Environmental Quality* **22**, 392-402.
- Sposito G. (1989) *The Chemistry of Soils*. Oxford University Press.
- Stumm W. and Morgan J. J. (1970) *Aquatic Chemistry*. Wiley-Interscience.
- Urban N. R., Ernst K., and Bernasconi S. (1999) Addition of sulfur to organic matter during early diagenesis of lake sediments. *Geochimica et Cosmochimica Acta* **63**(6), 837-853.

Vassilev S. V. and Vassileva C. G. (1996) Occurrence, abundance and origin of minerals in coals and coal ashes. *Fuel Processing Technology* **48**, 85-106.

Weber K. A., Picardal F. W., and Roden E. E. (2001) Microbially catalyzed nitrate-dependant oxidation of biogenic solid-phase Fe(II) compounds. *Environmental Science and Technology* **35**, 1644-1650.



# **Nitrate Reduction Potential of Aquifer Sediments: Role of Microbial Adaptation**

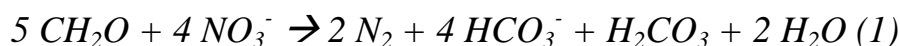
## **4.1 INTRODUCTION**

Nitrate is a common contaminant of shallow freshwater aquifers in many rural regions of the world, mainly due to its extensive leaching from manured and fertilized agricultural soils (Fraters *et al.*, 1998; Goodrich *et al.*, 1991; Lin *et al.*, 2001; Spalding and Exner, 1993). The removal of nitrate from abstracted groundwater is difficult because of its high solubility and low potential for co-precipitation or adsorption (Kapoor and Viraraghavan, 1997; Shrimali and Singh, 2001). Therefore, the natural capacity of many groundwater systems to remove nitrate is of great significance.

Nitrate becomes the thermodynamically favorable terminal electron acceptor after dissolved oxygen concentrations have been sufficiently depleted. Denitrification refers to the reduction of nitrate to gaseous nitrogen compounds. Under the commonly carbon-limited conditions of pristine groundwater systems, this is the main mechanism of nitrate removal (Freeze and Cherry, 1979; Korom, 1992; Smith and Duff, 1988; Smith *et al.*, 1991). The transfer of electrons during the transformation of nitrate to harmless dinitrogen (N<sub>2</sub>) gas proceeds through a series of four reduction steps (NO<sub>3</sub><sup>-</sup> → NO<sub>2</sub><sup>-</sup> → NO → N<sub>2</sub>O → N<sub>2</sub>) that are microbially mediated (Atlas and Bartha, 1998).

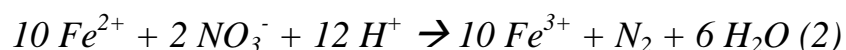
The attenuation of nitrate in groundwater is generally controlled by the reactivity of the reductants present in the subsurface (Bradley *et al.*, 1992; Postma *et al.*, 1991; Richards and Webster, 1999; Smith *et al.*, 1991). Aquifer sediments contain various electron donors that can potentially drive the reduction of nitrate. Sedimentary

organic matter (SOM) is a common reductant that facilitates heterotrophic denitrification (Bates and Spaldin, 1998; Clay *et al.*, 1996; Grischek *et al.*, 1998; Smith *et al.*, 1991; Starr *et al.*, 1996) as follows:

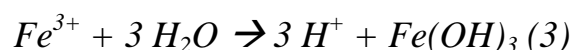


Here, CH<sub>2</sub>O is used as a simplified representation of SOM.

Alternatively, denitrification can be driven autotrophically by inorganic electron donors such as ferrous iron in silicates, siderite (FeCO<sub>3</sub>), pyrite (FeS<sub>2</sub>) or exchangeable ferrous iron (Ottley *et al.*, 1997; Postma, 1990; Postma *et al.*, 1991; Sorensen and Thorling, 1991; Weber *et al.*, 2001). For example, ferrous iron oxidation coupled to complete nitrate reduction is described as:



Under carbonate-buffered conditions, this reaction is rapidly followed by:



In *Chapter 3*, the reactivity of sediments from a sandy aquifer towards molecular oxygen was described. Sedimentary organic matter, pyrite and siderite were identified as the major reactive reductants. In this study, the biogeochemical controls on the potential denitrification activity of two of these sediments were investigated using fluidized-bed reactor and batch reactor experiments. The objectives were to: 1) determine which reductants are reactive during nitrate reduction, 2) compare the nitrate and oxygen reduction potentials of sediments studied, and 3) assess the role of microbial mediation during nitrate reduction.

## 4.2 MATERIAL AND METHODS

### 4.2.1 Sample Collection and Processing

Core samples were selected from a borehole in a sandy aquifer at the drinking water production site 'De Steeg' near Langerak, The Netherlands. The aquifer is currently under iron-reducing conditions. The sediment core was collected anoxically

at depth using Akkerman sampling tubes. The tubes were stored under a nitrogen atmosphere at 8°C directly after collection in the field. The tubes were opened in a N<sub>2</sub>-filled glove box in which sediment samples were prepared for further study. Two sediment samples (Table 4.1) from different sandy geological formations were selected for the experiments of this study: LA4 (Middle Pleistocene, Urk Formation) and LA6 (Early Pleistocene, Sterksel Formation). The geological origin of the samples has been described in more detail in *Chapter 3*. The 0–2000 µm particle size fraction was isolated by wet sieving. This fraction was used for the experiments; the remaining fraction (> 2 mm) was discarded.

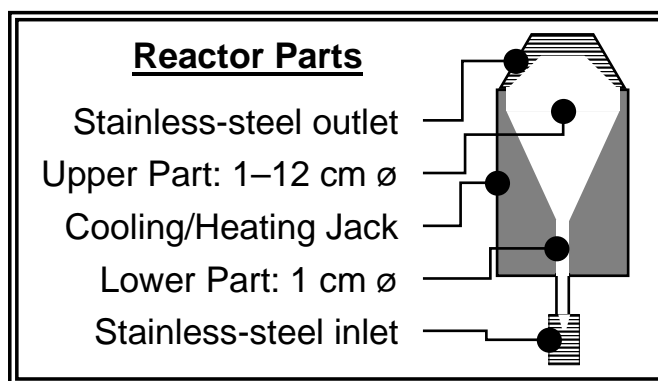
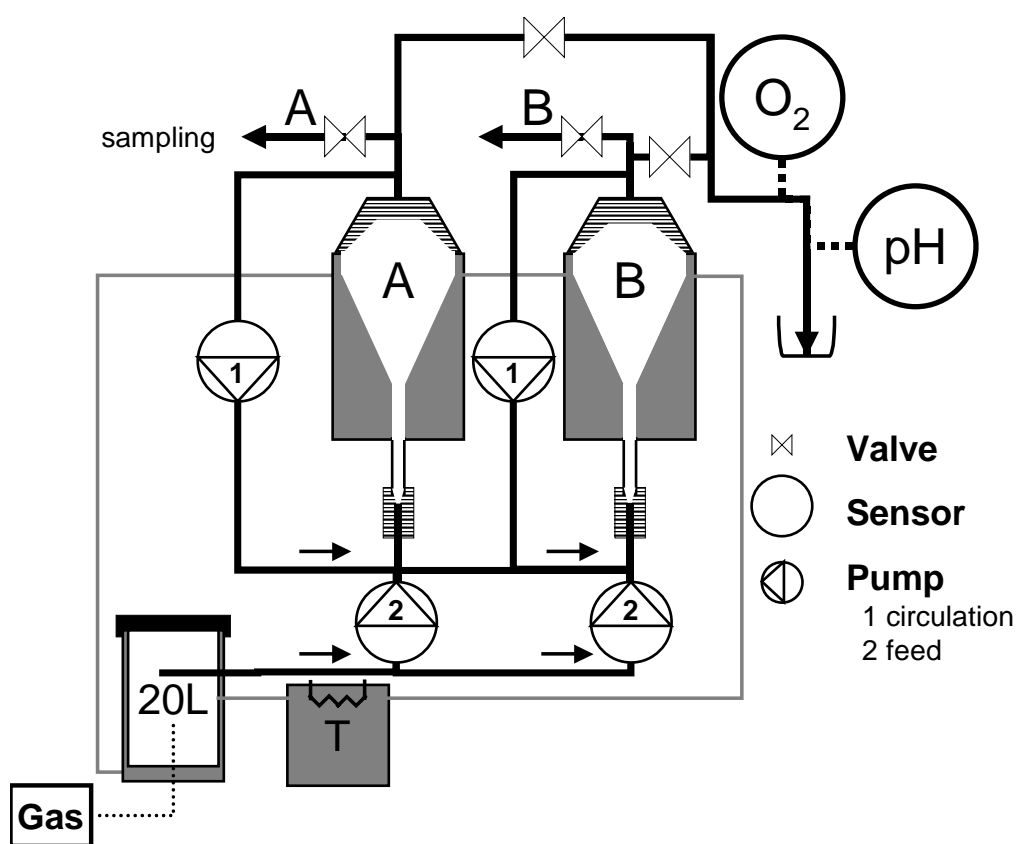


**Figure 4.1 Schematic representation of the fluidized-bed reactor.****Table 4.1 Bulk composition of the sediment samples (0–2 mm) studied. Depth in meters below surface level (m-bsl).**

Sample	Depth (m-bsl) <sup>a</sup>	SiO <sub>2</sub> (wt.%)	Al <sub>2</sub> O <sub>3</sub> (wt.%)	Fe (wt.%)	S (wt.%)	Pyrite (wt.%)	TOC <sup>b</sup> (wt.%)	TIC <sup>c</sup> (wt.%)
LA-4	30	92.19	3.76	0.22	0.15	0.43	0.08	0.79
LA-6	40	82.06	5.55	0.42	0.06	0.2	0.13	8.68

(a) Meters below surface level

(b) Total organic carbon

(c) Total inorganic carbon

## 4.2.2 Fluidized-bed Experiments

Nitrate reduction experiments were conducted in a funnel-shaped glass fluidized-bed reactor (~1 l) for 49 days in the dark (Fig. 4.1). The temperature of the reactor was controlled at 10° (day 1–13) or 25°C (day 13–49) with a cooling jacket connected to a thermostated ( $\pm 1^\circ\text{C}$ ) water bath. One variable-speed peristaltic pump (Cole Parmer, Masterflex console drive, 1–100 rpm, with Easy Load Pump Head) operating at a rate of 2 ml/min, supplied the influent to the fluidized-bed reactor. At day 19 the influent flow rates were decreased to 1 ml/min to increase the experimental resolution. Another peristaltic pump (Cole Parmer, Masterflex console drive, 6–600 rpm console drive, 1–100 rpm, with Easy Load Pump Head) recirculated the solution. The funnel shape of the reactor enables the fluidization of the coarser sediment particles in the lower upper part of the reactor with a liquid velocity of 0.01–0.02 m/s, while retaining the finer sediment particles in the upper part. Sediment loss from the column was less than 0.1 wt.%. Flow conditions resulted in a hydraulic retention time of 8–19 hours and a mixing rate of 2.8–3.6/hour. Tubing with low gas permeability (Tygon LFL, Masterflex) was used in the peristaltic pumps and remaining tubing and connectors consisted of stainless steel (Serto) to prevent oxygen diffusion.

Influent with a concentration of 1.3 mM nitrate was prepared by adding CaNO<sub>3</sub>·4H<sub>2</sub>O (Merck) to tap water in a 20-l PVC tank (Table 3.2). Calcite pieces were added to the tank to sustain pH-buffering of the influent. During the first 37 days of the experiment, the influent was kept oxygen-free by flushing either with N<sub>2</sub>/CO<sub>2</sub> (99%/1%) or N<sub>2</sub> (100%) gas, to control the pH of the influent at 7.2 and 8.4,



respectively. The influent was oxygenated during the last 12 days of the experiment by flushing with air. After the experiments, the sediment samples were removed from the reactors and stored under N<sub>2</sub> at 8°C until transfer to the acetylene-block experiments.

**Table 4.2** Chemical composition of influent used for the fluidized-bed experiments.

Species	Concentration (mmol/l)
Ca	1.7
NO <sub>3</sub>	1.3
Cl	0.4
SO <sub>4</sub>	0.2
NO <sub>2</sub>	0.0

### 4.2.3 Acetylene-block Batch Experiments

The potential for denitrification was measured using acetylene (C<sub>2</sub>H<sub>2</sub>) to block the microbial reduction step of N<sub>2</sub>O → N<sub>2</sub> (Yoshinari *et al.*, 1977), during parallel batch incubations of eight sediment slurries in 50 ml-glass bottles (Table 4.4). Besides the two samples from the preceding fluidized-bed experiments (LA4-FB and LA6-FB), two samples of untreated sediment (LA4-1/2 and LA6-1/2) were incubated in duplicate. In addition, two abiotic controls (LA4-X and LA6-X) of untreated sediment received mercury chloride (HgCl<sub>2</sub>) in a resulting concentration of 100 mg/l. One ml of 1 M KNO<sub>3</sub>-solution was added to all samples to obtain an excess concentration of 30 mM of NO<sub>3</sub>. The bottles were stoppered, crimped, and flushed for 15 minutes with oxygen-free helium after which 10 % of the headspace volume was replaced by acetylene. Slurry incubations were performed in the dark and shaken at room temperature. Five ml of gas was withdrawn daily from the headspace of each bottle using a gas-tight syringe and was replaced by an equal volume of helium to maintain constant pressure. Acetylene concentrations in the headspaces remained constant except for the abiotic controls. Here, the presence of HgCl<sub>2</sub> resulted in the oxidation of acetylene to CO<sub>2</sub>, as suggested by the high CO<sub>2</sub> production and acetylene consumption in the controls. Therefore, the acetylene concentrations in the controls were maintained by extra additions. The total amount of gases in the bottles was calculated from the partial pressures in the headspace plus the amount dissolved in the aqueous phase, using Henry's Law constant of 34.1\*10<sup>-3</sup> (M/atm at 25 °C) for CO<sub>2</sub>

(D'Angelo and Reddy, 1999) and using a Bunsen absorption coefficient of 0.544 for N<sub>2</sub>O (Tiedje, 1982).

## 4.2.4 Analytical Procedures

### 4.2.4.1 Sediment Analysis

X-ray fluorescence (XARL8410) was used to determine total aluminum, silicon, iron and sulfur contents of the sediments. Pyrite contents were determined by HNO<sub>3</sub> extraction. Total organic carbon (TOC) was measured on freeze-dried sediments using a method adapted from (Jakobsen and Postma, 1999), in which 2.6 M HCl was used to remove inorganic carbon. TOC was determined as the sum of two fractions: acid dissolvable organic carbon (ADOC), and the residual organic carbon (NADOC). The ADOC content was measured as dissolved organic carbon in the acid solution (TOC-500, Shimadzu), while the NADOC content was determined in the remaining solid sample by oxidation (NA1500 NCS, Carlo Erba). Total inorganic carbon (TIC) content was determined as weight loss after the acid digestion.

### 4.2.4.2 Gas and Wet Analysis

During the fluidized-bed experiments, the oxygen concentration in the effluent was measured within a flow cell using a dissolved-oxygen electrode (WTW Cellox-325) connected to an oxymeter (WTW Oxi-538). Effluent and influent water samples were taken periodically and filtered through a 0.45 µm membrane filter (Whatmann, no. 5). Samples for sulfate, nitrate and nitrite concentrations were frozen (-20°C) until analysis using an ion-chromatograph (Dionex DX-120). Samples for dissolved cations and total sulfur were acidified (< pH 1) with 1 M HCl and stored at 8°C until analysis using ICP-AES (Perkin-Elmer ICP-optima 3000). The strong 1 to 1 correlation ( $R^2=0.92$ ) between dissolved total sulfur and sulfate (SO<sub>4</sub>) indicates that SO<sub>4</sub> was the dominant dissolved sulfur species.

Headspace gas samples from the acetylene-block experiments were injected into a sample loop of a gas chromatograph (Trace GC-Thermoquest) and assayed for N<sub>2</sub>O, CO<sub>2</sub> and C<sub>2</sub>H<sub>2</sub>. Gas samples were separated on a 25-m capillary plot-fused silica

column (Poraplot Q, film thickness 10 $\mu$ m, i.d. 0.32 mm, Chrompack) with He as the carrier gas (flow rate 4.2 ml min<sup>-1</sup>). A Valco valve with a split-ratio of 1:10, split the GC eluent to either the electron capture detector (ECD) for N<sub>2</sub>O analysis or to the thermal conductivity detector (TCD) for CO<sub>2</sub> and C<sub>2</sub>H<sub>2</sub> analyses. The oven temperature was 40°C and the inlet temperature was 90°C. The temperatures of the ECD and TCD were 280 °C and 180 °C, respectively.

## **4.3 RESULTS**

### **4.3.1 Nitrate Reduction during Fluidized-bed Experiments**

The conditions during the fluidized-bed experiments can be split into three redox phases. The initial phase was aerobic and lasted for 5 days. Following the removal of oxygen, the second phase was anaerobic and lasted for a month. The last phase represents the return of aerobic conditions upon re-oxygenation.

During the first 5 days of the fluidized-bed experiments, oxygen concentrations in the effluent gradually decreased to below 2  $\mu$ M in both sediment incubations. During the LA4-FB experiment (Fig. 4.2), sulfate concentrations decreased parallel to the oxygen decrease and the pH increased from 6.6 to 7.1–7.2, which is the value for calcite equilibrium at the  $p_{\text{CO}_2}$  of 10<sup>-2</sup> atm (Figs. 4.2 and 4.3).

At the onset of the second phase, sulfate concentrations returned to input concentrations and nitrate concentrations decreased with a simultaneous increase of nitrite concentrations during both sediment incubations (Figs. 4.2 and 4.3). Lowering influent flow rates at day 19 resulted in doubling of the nitrite concentrations, after which nitrite production rates gradually decreased again, while nitrate reduction rates decreased more slowly.

Stoichiometric evaluation indicated that 10–100% of the observed nitrate loss is accounted for by its reduction to nitrite (Fig. 4.4). Net nitrite production rates, as calculated from concentrations and flow rate, were highest at day 15 (LA4-FB) and day 10 (LA6-FB). However, during the anoxic phase, the ratios of nitrite production to nitrate reduction declined, indicating that nitrite reduction was progressively more

important. Towards the end of the anoxic second phase, nitrite production accounted for 60% of the observed nitrate loss for the LA4-FB sample and down to 15% for the LA6-FB sample. The average nitrate to nitrite conversion ratio was higher for the LA4-FB sediment sample (0.72) than for the LA6-FB sediment sample (0.45; Table 4.3). Increase of the experimental temperature from 10 to 25°C (day 13) or pH from 7.2 to 8.7 (day 12–15) had no observable effect on the nitrate reduction rates.

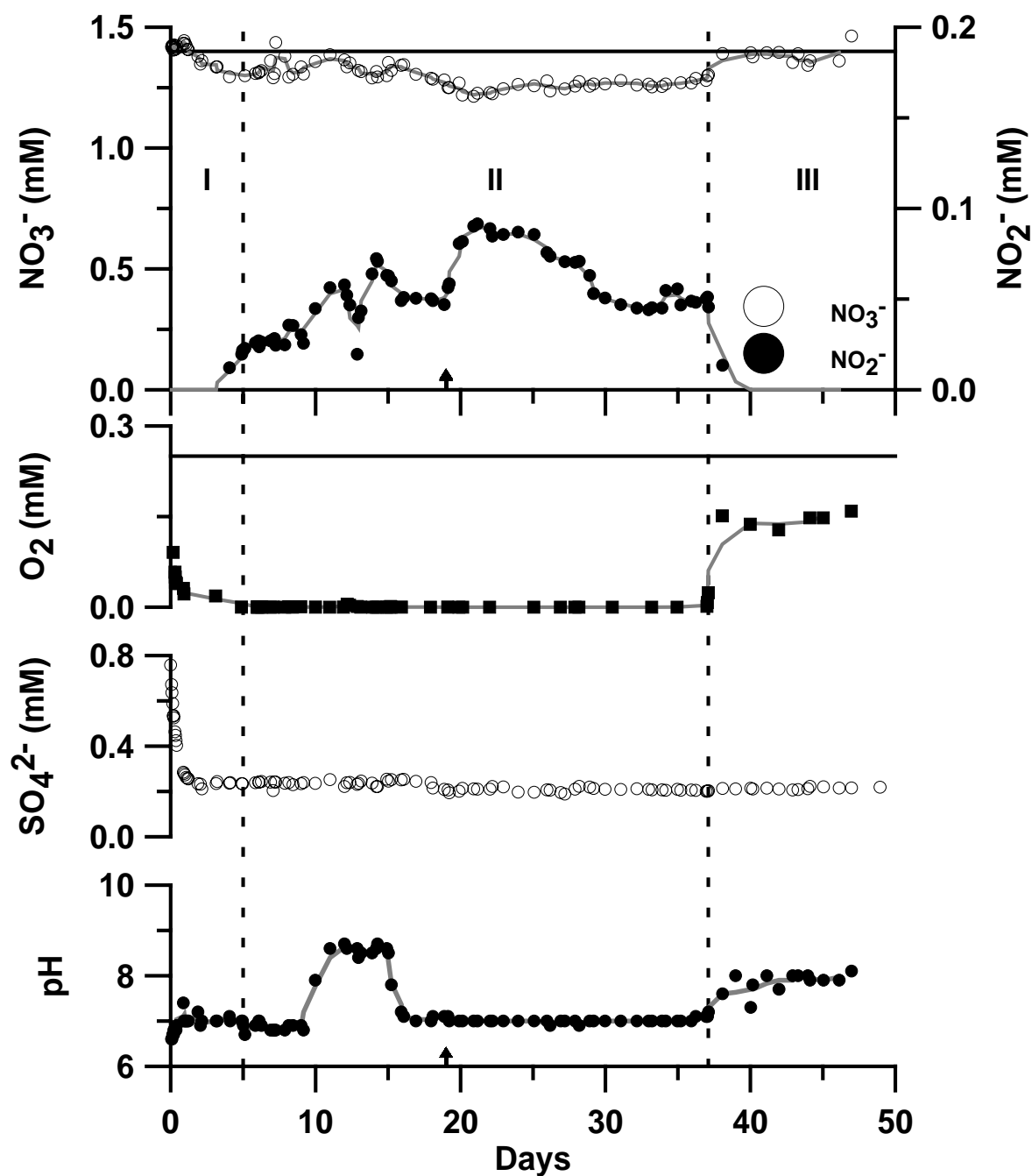


Figure 4.2 Chemical evolution during the fluidized-bed experiments with sediment sample LA4-FB. Arrow at day 19 indicates the decrease of influent flow rates. Roman numerals I, II and III represent the first suboxic phase, the anoxic phase and

**final oxic phase, respectively. Horizontal lines represent average influent concentrations for sulfate and nitrate, and atmospheric equilibrium concentration for oxygen**

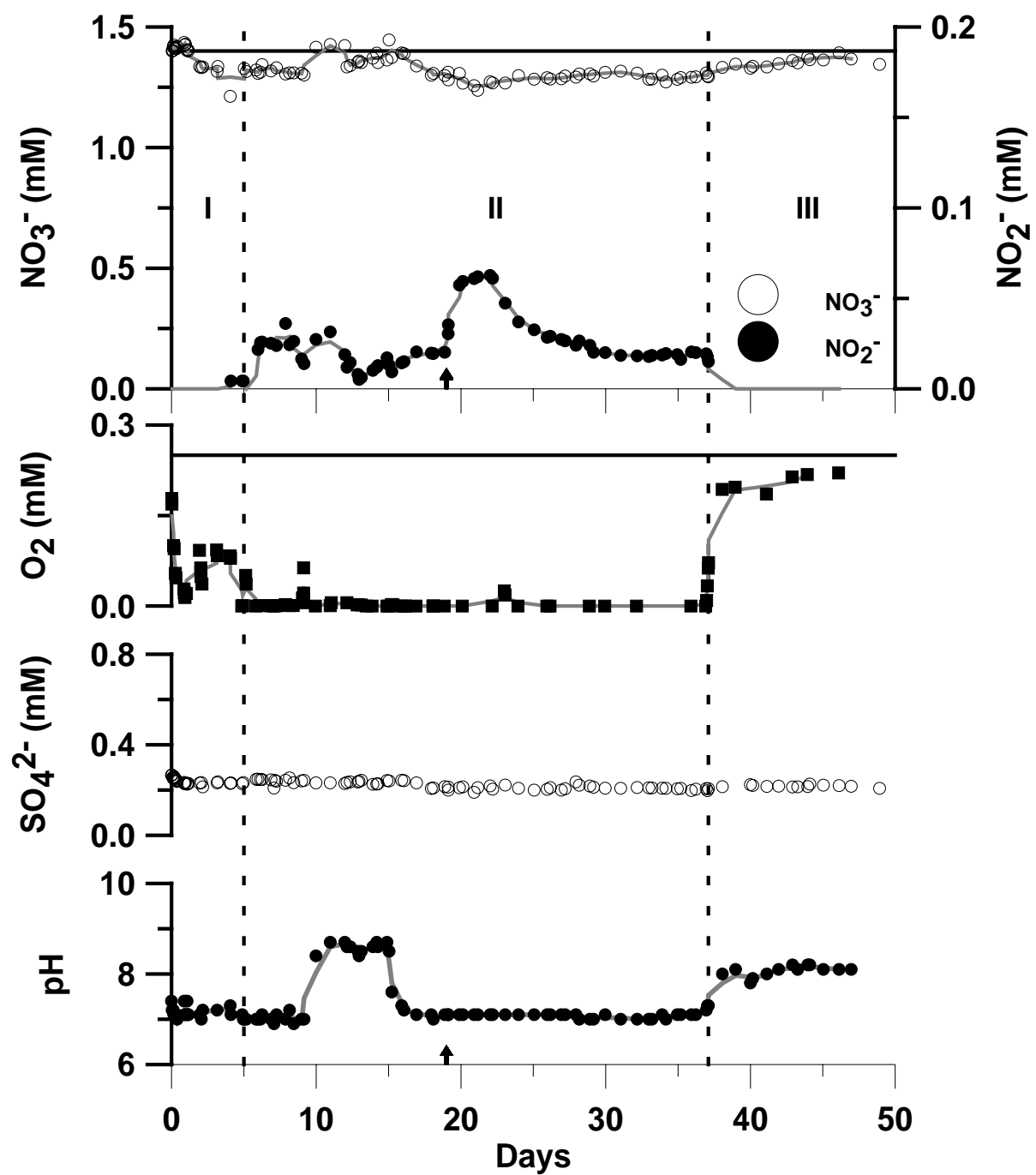


Figure 4.3 Chemical evolution during the fluidized-bed experiments with sediment sample LA6-FB. Details as for Figure 4.2.

**Table 4.3** Results of the fluidized-bed experiments. Total nitrate reduction, nitrite production, nitrite production to nitrate reduction ratio and aerobic respiration rates. Nitrate reduction and nitrite production rates are averaged over phase II. For oxygen, reduction rates are averaged over phase III.

Sample Code	Sample Weight (g)	$\Delta\text{NO}_3^-$ ( $\mu\text{mol/g}$ )	$\Delta\text{NO}_2^-$ ( $\mu\text{mol/g}$ )	$\frac{\Delta\text{NO}_2^-}{\Delta\text{NO}_3^-}$	$\text{NO}_2^-$ ( $\mu\text{mol/g.day}$ )	$\text{NO}_3^- \rightarrow \text{NO}_2^-$ <sup>a</sup> ( $\mu\text{eq e}^-/\text{g.day}$ )	$\text{O}_2$ ( $\mu\text{mol/g.day}$ )	$\text{O}_2$ <sup>a</sup> ( $\mu\text{eq e}^-/\text{g.day}$ )
LA4-FB	16.5	143	104	0.72	3.24	6.48	3.9	15.6
LA6-FB	18.39	190	86	0.45	2.70	5.40	3.0	12.0

(a) Reduction rates normalized to electron ( $e^-$ ) transfer.

**Table 4.4** Cumulative results of the cetylene-block sediment incubations. Ratios for  $\text{N}_2\text{O}$  production to  $\text{CO}_2$  production and rates for  $\text{N}_2\text{O}$  production and  $\text{NO}_3^-$  reduction are averaged over the total duration of the experiments.

Sample Code	Sample Weight (g)	final pH	$\text{CO}_2$ ( $\mu\text{mol/g}$ )	$\text{N}_2\text{O}$ ( $\mu\text{mol/g}$ )	$\frac{\text{N}_2\text{O}}{\text{CO}_2}$	$\text{N}_2\text{O}$ ( $\mu\text{mol/g.day}$ )	$\text{NO}_3^- \rightarrow \text{N}_2\text{O}$ <sup>a</sup> ( $\mu\text{eq e}^-/\text{g.day}$ )
LA4-1	16.5	3.28	0.14	ND	0	ND	ND
LA4-2	20.05	3.46	0.09	ND	0	ND	ND
LA4-X	15.48	2.17	1.00	0.01	0.01	0.002	0.007
LA4-FB	12.95	6.72	1.41	0.29	0.20	0.042	0.167
LA6-1	18.39	7.20	0.39	0.04	0.10	0.006	0.022
LA6-2	17.68	7.10	0.60	0.06	0.10	0.009	0.035
LA6-X	20.46	6.09	11.66	ND	0	ND	ND
LA6-FB	8.57	7.15	1.24	0.43	0.35	0.063	0.250

(a) Reduction rates normalized to electron ( $e^-$ ) transfer.

ND Not detected

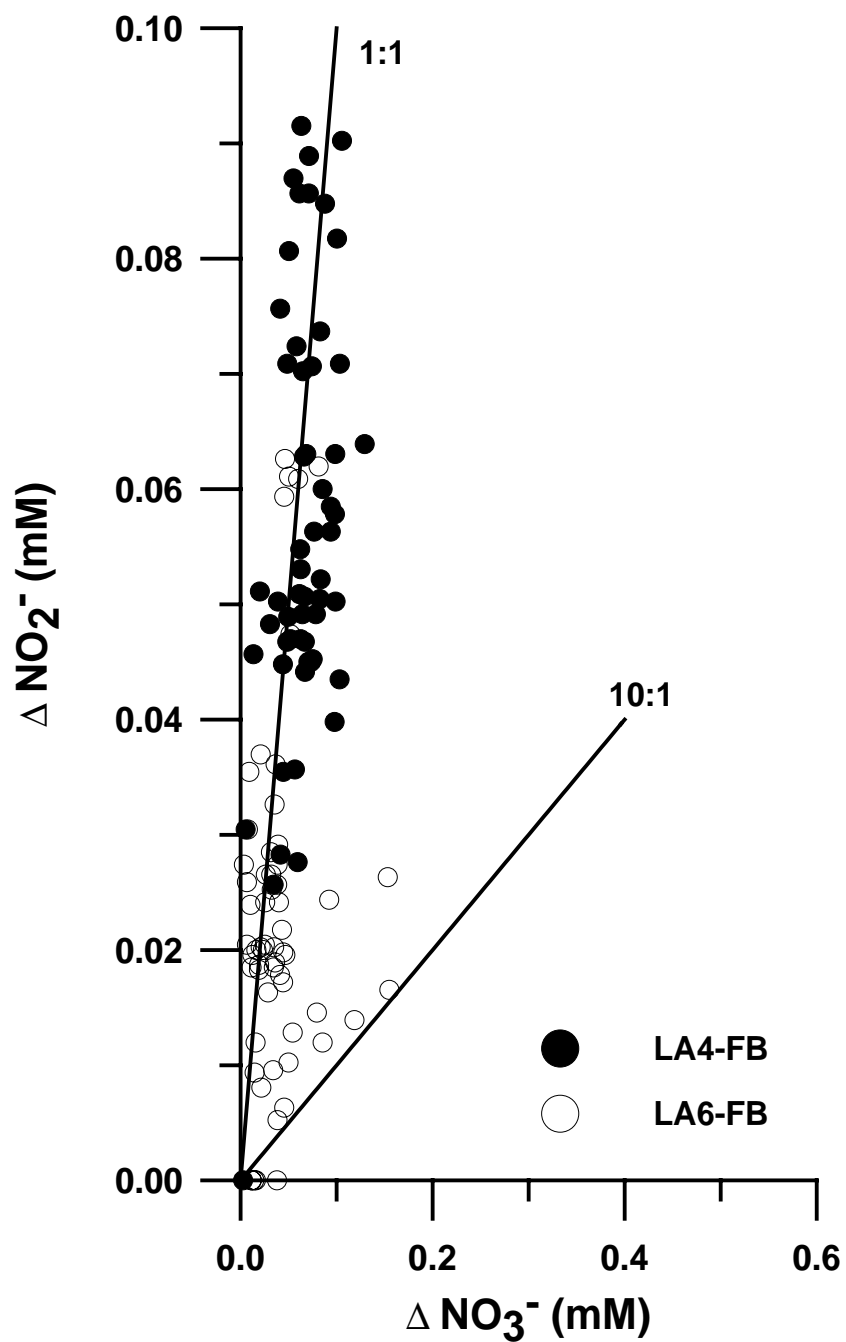


**Figure 4.1** Amount of nitrate reduced ( $\Delta \text{NO}_3^-$ ) versus the amount of nitrite produced ( $\text{NO}_2^-$ ). The 1 to 1 line represents the situation where nitrite production accounts for 100% of the observed nitrate reduction. The other line represents the situation where nitrite production accounts for only 10% of the observed nitrate reduction.

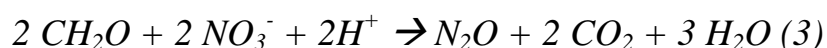


Directly after the re-oxygenation of the influent, nitrite concentrations dropped and nitrate concentrations returned to influent values. Oxygen concentrations increased sharply to 0.16 mmol/l (LA4-FB) and 0.22 mmol/l (LA6-FB), but remained below atmospheric equilibrium values (0.25 mmol/l). The calculated average oxygen consumption rates are 3.9 (LA4-FB) and 3.0 (LA6-FB)  $\mu\text{mol/day}$  (Table 4.3). Sulfate concentrations did not evidently change in response to re-oxygenation.

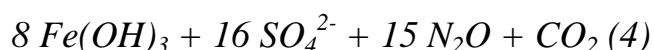
### 4.3.2 Nitrate Reduction during Batch Experiments

The fluidized-bed experiments were followed by acetylene-block experiments to assess the potential of the sediment samples to denitrify nitrate to gaseous nitrogen products. Production of  $\text{N}_2\text{O}$  and  $\text{CO}_2$  were measured during batch incubations lasting 7 days (Table 4.4). The pH values at the end of the incubations were circumneutral except for the incubated LA4-1/2 and LA4-X samples ( $\text{pH} < 4$ ). These, as well the control samples (LA4/6-X), did not reveal significant  $\text{N}_2\text{O}$  production, demonstrating the absence of denitrification.

The sediments pre-exposed to nitrate (and oxygen) during the fluidized-bed experiments (LA4-FB and LA6-FB) showed the highest  $\text{N}_2\text{O}$  production rates ( $> 0.03 \mu\text{mol/g.day}$ ) during the subsequent batch incubations. After day 1 (LA6-FB) and day 3 (LA4-FB), these sediment samples produced  $\text{N}_2\text{O}$  and  $\text{CO}_2$  according to the characteristic 1:2 stoichiometry of  $\text{NO}_3^-$  reduction to  $\text{N}_2\text{O}$  (Fig. 4.5):



In contrast, denitrification coupled to pyrite oxidation would yield a  $\text{N}_2\text{O}/\text{CO}_2$  ratio of 15 following:



The incubated LA6-1/2 sediment samples exhibited lower  $\text{N}_2\text{O}$  to  $\text{CO}_2$  ratios, reflecting incomplete denitrification.

## 4.4 DISCUSSION

### 4.4.1 pH-Control on Pyrite Oxidation

Increased sulfate concentrations and acidity during the first phase of the fluidized-bed experiments reflect the aerobic oxidation of sulfides, such as pyrite (Table 4.1). These chemical changes are especially pronounced during the LA4-FB incubation (Fig. 4.2) and are in agreement with the dominance of pyrite oxidation as observed for this sample during oxic incubations (*Chapter 3*). Moreover, the final pH of 2–4 of the LA4-1/2 samples in the acetylene-block incubations (Table 4.4) points to untimely aerobic oxidation of some of the reactive pyrite during transfer of these samples causing an inhibition of microbial denitrification.

The integrated amount of sulfate released during the first phase was one (LA4-FB) to two (LA6-FB) orders of magnitude smaller than the sulfur contents initially present as sulfide in pyrite (Table 4.1). Thus, only a small fraction of the initial pyrite amount was oxidized during the fluidized-bed experiment and pyrite was still present during the following phases of the experiments. While in the aerobic first phase pyrite was readily oxidized by oxygen, no sulfate was released during the second, anoxic phase. Since sulfate production was also absent during the aerobic final phase, this suggests that the surface oxidation of pyrite was inhibited by the precipitation of iron hydroxides, as observed for the oxidation of pyrite under carbonate-buffered conditions (Nicholson *et al.*, 1990). Alternatively, the low solubility of pyrite under slightly alkaline pHs limits its role as a reductant of nitrate in carbonate-buffered marine sediments (Schippers and Jørgensen, 2002). Therefore, the observed nitrate reduction during the suboxic phase was unlikely to be coupled to the oxidation of iron sulfides. Rather, a coupling with SOM or ferrous iron oxidation is expected since these were identified as reactive reductants during previous aerobic experiments (*Chapter 3*), in addition to pyrite.

### 4.4.2 SOM Oxidation coupled to Nitrate Reduction

Denitrification coupled to the oxidation of SOM or to the oxidation of ferrous iron can be separated on the basis of the opposite effects on alkalinity. While SOM

oxidation (reaction 1) results in the production of bicarbonate, ferrous iron oxidation leads to the net production of protons when reaction 2 is followed by reaction 3. Unfortunately however, the high  $p_{\text{CO}_2}$  ( $10^{-2}$  atm) of the influent solution obscured any alkalinity effects during the fluidized-bed experiments. Still, the  $\text{N}_2\text{O}$  to  $\text{CO}_2$  stoichiometries during the acetylene-block incubations of the LA4-FB and LA6-FB samples point to SOM oxidation as the dominant pathway of denitrification (Table 4.4). Thus, while pyrite was the reactive phase during oxygen reduction, nitrate reduction is dominated by SOM oxidation. This selective preference for SOM oxidation under denitrifying conditions is in agreement with the mass balance observations during aquifer recharge experiments (Stuyfzand, 1998).

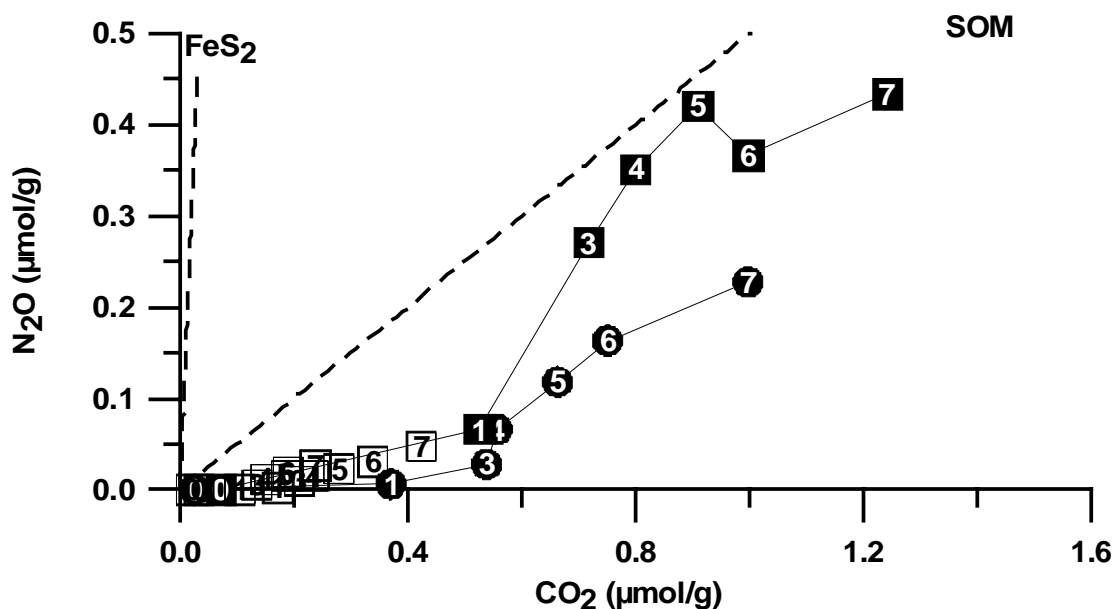


**Figure 4.2** Cross plot of  $\text{CO}_2$  and  $\text{N}_2\text{O}$  production during the sediment incubations with final circumneutral pH values. Closed symbols represent the sediment samples pre-exposed to nitrate (FB). Open symbols represent the unexposed sediment samples (1/2). Squares represent LA6-FB sediment samples, while circles represent LA4-FB sediment samples. Numbers in symbols represent days. Lines representing oxidation stoichiometries of SOM and pyrite under carbonate-buffered conditions are also shown.

The undersaturated oxygen concentrations of the effluent during the third phase of the fluidized-bed experiments demonstrate the instant recovery of aerobic respiration upon re-oxygenation. Based on electron transfer, the oxygen reduction rates during this phase are about two times faster than the average nitrate reduction

rates observed in the preceding phase (Table 4.3). In addition, these nitrate reduction rates are similarly slower than those measured for the same sediments during oxic batch incubations of 54 days (*Chapter 3*). This difference is in agreement with the observation of slower anaerobic as compared to aerobic oxidation rates (D'Angelo and Reddy, 1999; Jacobsen and Bossi, 1997; Kristensen *et al.*, 1995; Rockne and Strand, 1998).

#### **4.4.3 Role of Microbial Adaptation**

The very low N<sub>2</sub>O production for the poisoned controls (Table 4.4) confirmed that nitrate reduction in the sediments was microbially mediated. Nitrite accumulation has frequently been observed during the initial stages of denitrification, both under laboratory (Broholm *et al.*, 1999; Burland and Edwards, 1999; Devlin *et al.*, 2000; Oh and Silverstein, 1999; Spence *et al.*, 2001) and *in situ* conditions (Bates *et al.*, 1998; Smith *et al.*, 2001; Spence *et al.*, 2001). The temporary build-up of nitrite has been interpreted as either slow microbial generation of nitrite reductase (Shi *et al.*, 1999; Smith *et al.*, 2001) or as the effect of carbon-limited conditions (Kelso *et al.*, 1999; Oh and Silverstein, 1999; Spence *et al.*, 2001; Stief, 2001). But while the reactivity of the organic substrate being oxidized presumably decreased, nitrite accumulation rates diminished during the fluidized-bed experiments in this study. Therefore, the initial nitrite accumulation observed was probably related to the slow microbial adaptation to the instant nitrate availability. The aquifer, from which the sediment samples were collected, contains no nitrate and is presently under iron-reducing conditions. Therefore, the delay in the microbial ability to reduce nitrite is fully explained by an adaptive response in reductase production of the bacterial population upon nitrate exposure (Bengtsson and Bergwall, 1995; Shi *et al.*, 1999).

The slow N<sub>2</sub>O production rates of the unexposed sediments during the acetylene-block incubations (Table 4.4) compare favorably with the rates obtained from other deep aquifer sediments (Morris *et al.*, 1988). While, this indicates that little denitrifying potential was initially present, the decrease in the ratios of nitrite production to nitrate reduction during the fluidized-bed experiments (Figs. 4.2 and 4.3) brings forward a growing significance of denitrification as compared to the partial

reduction of nitrate to nitrite. This is confirmed by the higher N<sub>2</sub>O production of the sediment pre-exposed to nitrate (LA6-FB) as compared with the unexposed sediments (LA6-1/2) during the acetylene-block experiments. Thus, pre-exposure to nitrate allowed microbial adaptation to facilitate denitrification.

The bacterial population in the sediments studied needed over a month to fully develop the ability to denitrify. These adaptation times are long in comparison with those in the order of days found for studies using sediments pre-exposed to nitrate *in situ* (Bengtsson and Bergwall, 1995; Obenhuber and Lowrance, 1991). Moreover, response times for denitrification using more labile organic substrates (*e.g.* acetic acid) were similarly faster (Constantin and Fick, 1997; Gómez *et al.*, 2000; Kelso *et al.*, 1999; Roy and Greer, 2000). In contrast, the biodegradation of recalcitrant aromatic hydrocarbons resulted in an accumulation of nitrite that lasted for over one month (Hutchins *et al.*, 1991). Therefore, the absence of denitrification *in situ* as well as the refractory nature of SOM are likely responsible for the observation of long microbial adaptation times and initial build-up of nitrite.

Since SOM oxidation was the dominant nitrate reduction process during all experiments, a decreased SOM reactivity is expected for the samples that were transferred from the fluidized-bed to the batch reactors (LA4-FB, LA6-FB). Therefore, a higher degree of degradation of SOM may explain why the N<sub>2</sub>O production rates of the these samples were two orders of magnitude lower than the average NO<sub>3</sub> reduction rates during the fluidized-bed experiments (Table 4.2). However, the absence of physical limitations in the fluidized-bed reactors or the build up of reaction products in the batch experiments probably contributes as well.

#### **4.4.4 Experimental Results in View of Field Observations**

Nitrite is not commonly observed during natural attenuation of nitrate (Appelo and Postma, 1993). Whereas the nitrite accumulation observed during the fluidized-bed experiments was substantial, natural groundwater flow rates are slow enough to enable the bacterial population to develop a full denitrifying potential as nitrate percolates (Puckett and Cowdery, 2002) and thus minimizing the zone where temporary nitrite build-up occurs. Moreover, unconfined aquifers are subject to low

natural background concentrations of nitrate at shallow depths. This facilitates a more rapid response to an increased nitrate supply than sediments that have been unexposed to nitrate at a geological time scale, such as the sediments studied here (Bengtsson and Bergwall, 1995).

Results of this study point to several complications for the assessment of denitrification potentials of sediments. While  $N_2O$  production in acetylene block experiments is a good measure of total microbial denitrification potential of sediments that are adapted to an abundant nitrate supply,  $N_2O$  production results in an underestimation of this potential when microbial ability to facilitate complete denitrification is underdeveloped. Conversely, sole dependence on decreases in nitrate concentrations results in an overestimation of denitrification potential when the reduction of nitrate is incomplete, i.e. when part of the reduced nitrate accumulates as intermediates. Therefore, nitrite is an intermediate that should be measured in denitrification studies, especially when microbial adaptation time is potentially longer than the experiment duration.

Numerous field studies have ascribed the disappearance of nitrate in groundwater at least partly to pyrite oxidation (Cravotta, 1998; Houben *et al.*, 2001; Kelly, 1997; Molenat *et al.*, 2002; Pauwels *et al.*, 2000; Pauwels *et al.*, 1998; Pauwels *et al.*, 2001; Pinault *et al.*, 2001; Postma *et al.*, 1991; Tesoriero *et al.*, 2000). In addition, the oxidation of dissolved dihydrogen sulfide by nitrate, as mediated by *Thiobacillus denitrificans*, is a well-known process (*e.g.* Hole *et al.*, 2002). To date however, laboratory experiments to confirm the role of pyrite during nitrate reduction in field studies were unsuccessful (Devlin *et al.*, 2000; Houben *et al.*, 2001). Moreover, observations of nitrate reduction coupled to pyrite oxidation are largely confined to mildly acidic (pH 5–7) groundwater systems (Cravotta, 1998; Houben *et al.*, 2001; Kelly, 1997; Molenat *et al.*, 2002; Pauwels *et al.*, 2000; Pauwels *et al.*, 1998; Pauwels *et al.*, 2001; Pinault *et al.*, 2001; Postma *et al.*, 1991; Tesoriero *et al.*, 2000). Therefore, nitrate reduction by pyrite seems limited to environments free of reactive carbonates. This is demonstrated by the localization of denitrification coupled to pyrite oxidation within weathered, acidic iron oxyhydroxide crusts in a limestone

aquifer (Moncaster *et al.*, 2000). Alternatively, denitrification in these studies may be coupled to the oxidation of ferrous iron, as derived from incomplete aerobic pyrite oxidation (Postma *et al.*, 1991). Overall, there is a clear need for experimental results that define the biogeochemical controls on nitrate reduction by pyrite in groundwater systems.

## **4.5 CONCLUSIONS**

The potential for denitrification of the anaerobic aquifer sediments studied is primarily controlled by microbial adaptation and secondarily by the recalcitrant nature of SOM. In the absence of oxygen, reduction of nitrate to nitrite occurs readily upon nitrate exposure. However, nitrite accumulated until slow microbial adaptation enabled complete denitrification.

Sedimentary organic matter was the principal electron donor during denitrification under the carbonate-buffered experimental conditions. Nitrate reduction coupled to pyrite oxidation is probably limited by either its low solubility at circumneutral to slightly alkaline pH or by an inhibition due to the precipitation of iron oxyhydroxides on its surface. The experimental results differ from those obtained for oxygen reduction, where pyrite oxidation was an important process. Overall, the rates obtained for nitrate reduction are two times slower than those obtained for oxygen reduction.

## **References**

- Appelo C. A. J. and Postma D. (1993) *Geochemistry, Groundwater and Pollution*. Balkema.
- Atlas R. M. and Bartha R. (1998) *Microbial Ecology: Fundamentals and Applications*. Benjamin/Cummings Science Publishing.
- Bates H. K., Martin G. E., and Spalding R. F. (1998) Kinetic isotope effects in production of nitrite-nitrogen and dinitrogen gas during in situ denitrification. *Journal of Environmental Quality* **27**, 183-191.
- Bates H. K. and Spalding R. F. (1998) Aquifer denitrification as interpreted from in situ microcosm experiments. *Journal of Environmental Quality* **27**, 174-182.

- Bengtsson G. and Bergwall C. (1995) Heterotrophic denitrification potential as an adaptive response in groundwater bacteria. *FEMS Microbiology Ecology* **16**, 307-318.
- Bradley P. M., Fernandez Jr M., and Chapelle F. H. (1992) Carbon limitation of denitrification rates in an anaerobic groundwater system. *Environmental Science and Technology* **28**(12), 2377-2381.
- Broholm K., Hansen A. B., Jorgensen P. R., Arvin E., and Hansen M. (1999) Transport and biodegradation of creosote compounds in a large, intact, fractured clayey till column. *Journal of Contaminant Hydrology* **39**(3-4), 331-348.
- Burland S. M. and Edwards E. A. (1999) Anaerobic benzene biodegradation linked to nitrate reduction. *Applied and Environmental Microbiology* **65**(2), 529-533.
- Clay D. E., Clay S. A., Moorman T. B., Brix-Davis K., Scholes K. A., and Bender A. R. (1996) Temporal Variability of organic C and nitrate in a shallow aquifer. *Water Res.* **30**(3), 559-568.
- Constantin H. and Fick M. (1997) Influence of C-sources on the denitrification rate of a high-nitrate concentrated industrial wastewater. *Water Research* **31**(3), 583-589.
- Cravotta C. A. (1998) Effect of sewage sludge on formation of acidic ground water at a reclaimed coal mine. *Ground Water* **36**(1), 9-19.
- D'Angelo E. M. and Reddy K. R. (1999) Regulators of heterotrophic microbial potentials in wetland soils. *Soil Biology & Biochemistry* **31**(6), 815-830.
- Devlin J. F., Eedy R., and Butler B. J. (2000) The effects of electron donor and granular iron on nitrate transformation rates in sediments from a municipal water supply aquifer. *Journal of Contaminant Hydrology* **46**, 81-97.
- Fraters D., Boumans L. J. M., van Drecht G., de Haan T., and de Hoop W. D. (1998) Nitrogen monitoring in groundwater in the sandy regions of the Netherlands. *Environmental Pollution* **102**, 479-485.
- Freeze R. A. and Cherry J. A. (1979) *Groundwater*. Prentice-Hall, Inc.
- Gómez M. A., González-López J., and Hontaria-García E. (2000) Influence of carbon source on nitrate removal of contaminated groundwater in a denitrifying submerged filter. *Journal of Hazardous Materials* **B80**, 69-80.
- Goodrich J. A., Lykins J., B.W., and Clarck R. M. (1991) Drinking water from agriculturally contaminated groundwater. *Journal of Environmental Quality* **20**(4), 707-717.
- Grischek T., Hiscock K. M., Metschies T., Dennis P. F., and Nestler W. (1998) Factors affecting denitrification during infiltration of river water into a sand and gravel aquifer in Saxony, Germany. *Water Resources* **32**(2), 450-460.
- Hole U. H., Vollack K. U., Zumft W. G., Eisenmann E., Siddiqui R. A., B. F., and P.M.H. K. (2002) Characterization of the membranous denitrification enzymes nitrite reductase (cytochrome cd(1)) and copper-containing nitrous oxide reductase from *Thiobacillus denitrificans*. *Archives of Microbiology* **165**, 55-61.
- Houben G. J., Martiny A., Bäßler N., Langguth H.-R., and Plüger W. L. (2001) Assessing the reactive transport of inorganic pollutants in groundwater of the Bourtanger Moor area (NW Germany). *Environmental Geology* **41**, 480-488.



- Hutchins S. R., Sewell G. W., Kovacs D. A., and Smith G. A. (1991) Biodegradation of aromatic hydrocarbons by aquifer microorganisms under denitrifying conditions. *Environmental Science and Technology* **25**(1), 68-76.
- Jacobsen O. S. and Bossi R. (1997) Degradation of ethylenethiourea (ETU) in oxic and anoxic sandy aquifers. *FEMS Microbiology Reviews* **20**, 539-544.
- Jakobsen R. and Postma D. (1999) Redox zoning, rates of sulfate reduction and interactions with Fe-reduction and methanogenesis in a shallow sandy aquifer, Rømø, Denmark. *Geochimica et Cosmochimica Acta* **63**(1), 137-151.
- Kapoor A. and Viraraghavan T. (1997) Nitrate removal from drinking water - Review. *Journal of Environmental Engineering-Asce* **123**(4), 371-380.
- Kelly W. R. (1997) Heterogeneties in ground-water geochemistry in a sand aquifer beneath an irrigated field. *Journal of Hydrology* **198**, 154-176.
- Kelso B. H. L., Smith R. V., and Laughlin R. J. (1999) Effects of carbon substrates on nitrite accumulation in freshwater sediments. *Applied and Environmental Microbiology* **65**(1), 61-66.
- Korom S. F. (1992) Natural denitrification in the saturated zone: A review. *Water Resources Research* **28**(6), 1657-1668.
- Kristensen E., Ahmed S. I., and Devol A. H. (1995) Aerobic and anaerobic decomposition of organic matter in marine sediments: Which is fastest. *Limnology and Oceaonography* **40**(8), 1430-1437.
- Lin B.-L., Sakoda A., Shibasaki R., and Suzuki M. (2001) A modelling approach to global nitrate leaching caused by anthropogenic fertilisation. *Water Research* **35**(8), 1961-1968.
- Molenat J., Durand P., Gascuel-Oudoux C., Davy P., and Gruau G. (2002) Mechanisms of nitrate transfer from soil to stream in an agricultural watershed of French Brittany. *Water Air and Soil Pollution* **133**(1-4), 161-183.
- Moncaster S. J., Botrell S. H., Tellam J. H., Lloyd J. W., and Konhauser K. O. (2000) Migration and attenuation of agrochemical pollutants: insights from isotopic analysis of groundwater sulphate. *Journal of Contaminant Hydrology* **43**, 147-163.
- Morris J. T., Whiting G. J., and Chapelle F. H. (1988) Potential denitrification rates in deep sediments from the southeastern coastal plain. *Environmental Science and Technology* **22**(7), 832-836.
- Nicholson R. V., Gillham R. W., and Reardon E. J. (1990) Pyrite oxidation in carbonate-buffered solution: 2. Rate control by oxide coatings. *Geochimica et Cosmochimica Acta* **54**, 395-402.
- Obenhuber D. C. and Lowrance R. (1991) Reduction of nitrate in aquifer microcosms by carbon additions. *Journal of Environmental Quality* **20**(1), 255-258.
- Oh J. and Silverstein J. (1999) Acetate limitation and nitrite accumulation during denitrification. *Journal of Environmental Engineering-Asce* **125**(3), 234-242.
- Ottley C. J., Davison W., and Edmunds W. M. (1997) Chemical catalysis of nitrate reduction by iron(II). *Geochimica Et Cosmochimica Acta* **61**(9), 1819-1828.

- Pauwels H., Foucher J.-C., and Kloppmann W. (2000) Denitrification and mixing in a schist aquifer: influence on water chemistry and isotopes. *Chemical Geology* **168**, 307-324.
- Pauwels H., Kloppmann W., Foucher J.-C., Martelat A., and Fritsche V. (1998) Field tracer test for denitrification in a pyrite-bearing schist aquifer. *Applied Geochemistry* **13**(6), 767-778.
- Pauwels H., Lachassagne P., Bordenave P., Foucher J. C., and Martelat A. (2001) Temporal variability of nitrate concentrations in a schist aquifer and transfer to surface waters. *Applied Geochemistry* **16**, 583-596.
- Pinault J. L., Pauwels H., and Cann C. (2001) Inverse modeling of the hydrological and the hydrochemical behavior of hydrosystems: Application to nitrate transport and denitrification. *Water Resources Research* **37**(8), 2179-2190.
- Postma D. (1990) Kinetics of Nitrate Reduction by Detrital Fe(II)-Silicates. *Geochimica Et Cosmochimica Acta* **54**(3), 903-908.
- Postma D., Boesen C., Kristiansen H., and Larsen F. (1991) Nitrate reduction in an unconfined sandy aquifer: Water chemistry, reduction processes, and geochemical modeling. *Water Resources Research* **27**(8), 2027-2045.
- Puckett L. J. and Cowdery T. K. (2002) Transport and fate of nitrate in a glacial outwash aquifer in relation to ground water age, land use practices, and redox processes. *Journal of Environmental Quality* **31**(3), 782-796.
- Richards J. E. and Webster C. P. (1999) Denitrification in the subsoil of the Broadbalk Continuous Wheat Experiment. *Soil Biology and Biochemistry* **31**, 747-755.
- Rockne K. J. and Strand S. E. (1998) Biodegradation of bicyclic and polycyclic aromatic hydrocarbons in anaerobic enrichments. *Environmental Science & Technology* **32**(24), 3962-3967.
- Roy R. and Greer C. W. (2000) Hexadecane mineralization and denitrification in two diesel fuel-contaminated soils. *Fems Microbiology Ecology* **32**(1), 17-23.
- Schippers A. and Jørgensen B. B. (2002) Biogeochemistry of pyrite and iron sulfide oxidation in marine sediments. *Geochimica et Cosmochimica Acta* **66**(1), 85-92.
- Shi Y., Zwolinski M. D., Schreiber M. E., Bahr J. M., Sewell G. W., and Hickey W. J. (1999) Molecular analysis of microbial community structures in pristine and contaminated aquifers: Field and laboratory microcosm experiments. *Applied and Environmental Microbiology* **65**(5), 2143-2150.
- Shrimali M. and Singh K. P. (2001) New methods of nitrate removal from water. *Environmental Pollution* **112**(3), 351-359.
- Smith R. L. and Duff J. H. (1988) Denitrification in a sand and gravel aquifer. *Applied and Environmental Microbiology* **54**(5), 1071-1078.
- Smith R. L., Howes B. L., and Duff J. H. (1991) Denitrification in nitrate-contaminated groundwater: occurrence in steep vertical geochemical gradients. *Geochimica et Cosmochimica Acta* **55**(1815-1825).

- Smith R. L., Miller D. N., Brooks M. H., Widdowson M. A., and Killingstad M. W. (2001) In situ stimulation of groundwater denitrification with formate to remediate nitrate contamination. *Environmental Science & Technology* **35**(1), 196-203.
- Sorensen J. and Thorling L. (1991) Stimulation by Lepidocrocite (Gamma-Fe<sub>3</sub>O<sub>4</sub>) of Fe(II)-Dependent Nitrite Reduction. *Geochimica Et Cosmochimica Acta* **55**(5), 1289-1294.
- Spalding R. F. and Exner M. E. (1993) Occurrence of nitrate in groundwater-A review. *Journal of Environmental Quality* **22**, 392-402.
- Spence M. J., Bottrell S. H., Higgs J. J., Harrison I., and Fallick A. E. (2001) Denitrification and phenol degradation in a contaminated aquifer. *Journal of Contaminant Hydrology* **53**(3-4), 305-318.
- Starr J. L., Sadeghi A. M., and Parkin T. B. (1996) A tracer test to determine the fate of nitrate in shallow groundwater. *Journal of environmental quality* **25**, 917-923.
- Stief P. (2001) Influence of sediment and pore-water composition on nitrite accumulation in a nitrate-perfused freshwater sediment. *Water Research* **35**(12), 2811-2818.
- Stuyfzand P. J. (1998) Quality changes upon injection into anoxic aquifers in the Netherlands: Evaluation of 11 experiments. *Artificial Recharge of Groundwater*, 283-291.
- Tesoriero A. J., Liebscher H., and Cox S. E. (2000) Mechanism and rate of denitrification in an agricultural watershed: Electron and mass balance along groundwater flow paths. *Water Resources Research* **36**(6), 1545-1559.
- Tiedje J. M. (1982) Denitrification. In *Methods of Soil Analysis. Part 2: Chemical and Microbiological Properties* (ed. A. L. Page, R. H. Miller, and D. R. Keeney), pp. 1011-1026. Amer. Soc. Agron.,.
- Weber K. A., Picardal F. W., and Roden E. E. (2001) Microbially catalyzed nitrate-dependant oxidation of biogenic solid-phase Fe(II) compounds. *Environmental Science and Technology* **35**, 1644-1650.
- Yoshinari T., Hynes R., and Knowles R. (1977) Acetylene inhibition of nitrous oxide reduction and measurement of denitrification and nitrogen fixation in soil. *Soil Biology and Biochemistry* **9**(3), 177-183.



# **Reactivity of Organic Matter in Aquifer Sediments: Geological and Geochemical Controls**

## **5.1 INTRODUCTION**

The natural reduction capacity of aquifer sediments is of general importance to the redox processes within groundwater, but has only received increased attention over recent years. This is mainly related to the natural attenuation of nitrate in groundwater percolating from agricultural fields (Bradley *et al.*, 1992; Moncaster *et al.*, 2000; Pauwels *et al.*, 2000; Pauwels *et al.*, 1998; Postma *et al.*, 1991; Robertson *et al.*, 1996; Smith and Duff, 1988) and to the background consumption of oxidants injected during organic contaminant remediation (Barcelona and Holm, 1991; Schreiber and Bahr, 1999).

The reactivity of sedimentary organic matter (SOM) towards oxidants plays a prominent role in controlling the redox status of groundwater systems, since its oxidation can drive the formation of secondary solid reductants such as pyrite ( $\text{FeS}_2$ ) or siderite ( $\text{FeCO}_3$ ). These minerals are formed during sediment diagenesis and are often found in close association with organic matter (Anderson *et al.*, 1997; Grimes *et al.*, 2001).

Several factors are known to affect the reactivity of SOM towards oxidants, including environmental conditions, such as pH, temperature and oxidant concentrations (Tyson, 1995; van Bergen *et al.*, 1998), physical protection mechanisms as sorption to mineral surfaces (Collins *et al.*, 1995; Keil *et al.*, 1994;

Mayer, 1994) and the chemical composition (i.e., quality) of SOM (Canuel, 1996; Henrichs, 1993; Kristensen and Holmer, 2001).

Over the last decades, research has focused on the degradability of SOM in surface soils and marine sediments (Hedges and Oades, 1997 and references therein). In aquifers, SOM is ubiquitously present but generally in low contents (0.01–0.2 wt.%). Field studies have shown that SOM oxidation rates in aquifers are generally carbon limited (Bradley *et al.*, 1992; Hansen *et al.*, 2001; Postma *et al.*, 1991; Starr *et al.*, 1996). These findings suggest that the composition of SOM is a rate-controlling factor. To date however, little is known about the molecular composition and reactivity of SOM in aquifer sediments. Hence, the aim of this study was 1) to assess the controls on the molecular composition of SOM present in two distinct aquifer-forming geological formations and 2) to verify a relationship between the molecular composition of SOM in these sediments and its reactivity towards molecular oxygen.

## 5.2 GEOLOGICAL SETTING

The study site is located in the eastern part of The Netherlands near groundwater pumping location 't Klooster (Fig. 5.1a). Here, thick sedimentary deposits of near-shore marine and fluvial origin (van den Berg *et al.*, 2000) form interconnected aquifers (van Beek and Vogelaar, 1998). Regional groundwater levels are shallow (2–6 m-bs). The hydrogeological base at over 120 m below surface (m-bs) is formed by unconsolidated Miocene marine deposits of silty clay, loam and very fine sand of the Breda Formation (Fig. 5.1b). These are overlain by Pliocene deposits composed of calcareous silty and medium fine sands. At the location of core 34C-104 these deposits have been eroded. The erosion valley is filled with Upper Pliocene fluvial coarse sands and covered with Middle Pleistocene fluvio-glacial calcareous very fine sand and clay deposited during the Saalian. The upper 30 meters of the deposits consist of Upper Pleistocene fluvial and fluvio-glacial sediments, including a 5 m thick top layer of Weichselian non-calcareous sands and loam, which are of fluvial and aeolian origin. Holocene aeolian deposits of the Holocene Kootwijk Formation (*e.g.*, 't Zand) form the local topography (van den Berg *et al.*, 2000).

Largest part of the sedimentary sequence is presently under anoxic conditions. Groundwater chemistry reveals an approximately stratified redox zonation. Oxygen is consumed within the first 10 m below surface. The NO<sub>3</sub>/Fe redoxcline lies between 6 and 12 m below surface, while sulfate disappears in the depth interval between 30 and 55 m below surface (Griffioen, 2001; van Beek and Vogelaar, 1998).

## 5.3 MATERIALS AND METHODS

### 5.3.1 Sediment Selection

Sediment cores were obtained in 40 cm long stainless steel tubing with a 90 mm inner diameter, using a hollow stem auger with a Nordmeyer drilling rig. Pristine sediment samples were taken at two stratigraphic depths from the Pleistocene fluvio-glacial Drente Formation (DR-1 and DR-2— core 34C-104) and from the Pliocene shallow marine Oosterhout Formation (OO-1 and OO-2—core 34C-105). At these depths, iron-reducing conditions currently prevail (van Beek and Vogelaar, 1998). These sediment samples (Table 5.1, Fig. 5.1b) were selected because their geological formations 1) form important aquifer units in the local hydrogeology, 2) have a similar provenance (river Rhine) and 3) were deposited in contrasting environments (van den Berg *et al.*, 2000).

**Table 5.1 Bulk characteristics of the total (0-2000 µm) and fine (0-63 µm) sediment fractions studied**

Core	Sample	Depth (m-bs)	TOC (wt.%)	TIC (wt.%)	SiO <sub>2</sub> (wt.%)	Al <sub>2</sub> O <sub>3</sub> (wt.%)	Fe (wt.%)	S (wt.%)	TOC (wt.%)	TIC (wt.%)
					0-2000 µm			0-63 µm		
34C-104	DR-1	26.7	0.10	1.14	86.3	7.8	1.55	0.53	0.33	0.76
34C-104	DR-2	32.7	0.11	1.32	85.4	8.2	1.41	0.47	0.42	0.6
34C-105	OO-1	34.0	0.14	1.59	84.5	7.1	4.15	0.68	1.08	0.69
34C-105	OO-2	54.0	0.12	1.73	83.9	6.0	4.14	0.69	0.89	0.27

TOC: Total Organic Carbon

TIC: Total Inorganic Carbon

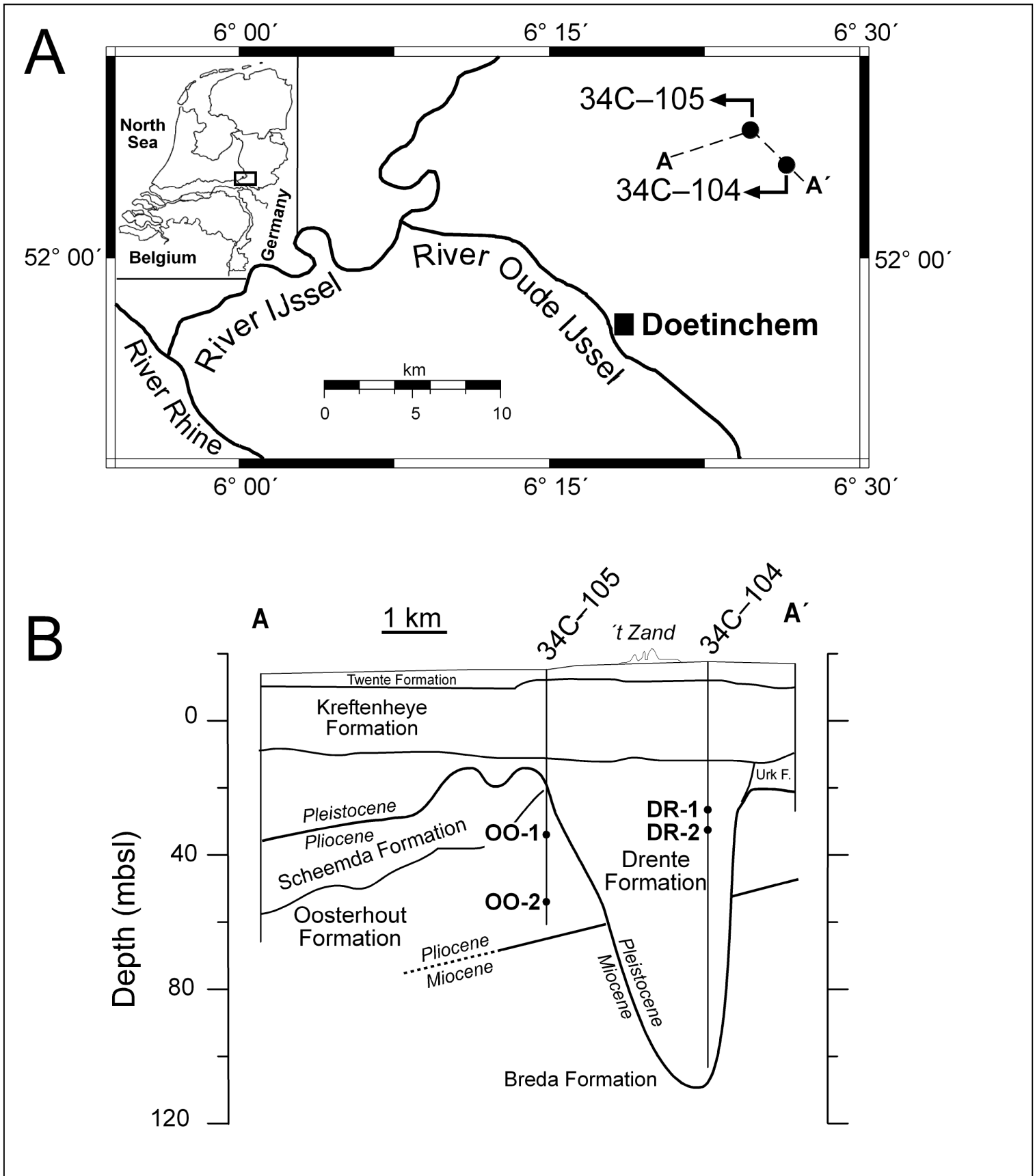


**Figure 5.1** (a) Location of the study area near Doetinchem, The Netherlands, showing the location of the geological cross-section along A–A' and the cores used; (b) Geological cross-section along A–A and location of the selected samples. Adapted from Van Beek and Vogelaar (1998) and Van den Berg *et al.* (2000)

5.3.2



## **Sample Processing**

Sediment samples collected were stored in glass bottles at 8°C until they were wet sieved into four particle size fractions: 0–63 µm (fine fraction), 63–2000 µm (coarse fraction), a separate 0–2000 µm (total fraction) and >2000µm. The latter (<5 wt.%) was discarded. Fractions were freeze-dried (-40°C) and stored in glass jars under N<sub>2</sub> at 8°C in the dark until subsamples were taken for bulk sediment chemistry, organic matter isolation and batch incubation experiments.

### **5.3.3 Bulk Sediment Chemistry**

Total Al, Si, Fe and S contents of the total fraction samples were determined by X-ray fluorescence spectroscopy, using a XARL8410 spectrometer. Total inorganic carbonate (TIC) contents were determined by weight loss after acid digestion with 2.6 M HCl. Subsequently, total organic carbon (TOC) contents were measured in duplicate on decarbonated freeze-dried sediment fractions by combustion in an elemental analyzer (NA1500 NCS, Carlo Erba) with an analytical precision (1σ) better than 5%.

### **5.3.4 Organic Matter Isolation**

Samples were treated with excess 10% HCl to remove carbonates and settled overnight, after which the samples were centrifuged at 2200 rpm for 7 minutes and the supernatant was decanted. Samples were then treated with excess 38% HF to dissolve the silicate mineral matrix, shaken at 250 rpm for two hours, after which the samples were centrifuged at 2200 rpm for 7 minutes and the supernatant was decanted. Subsequently, the samples were washed three times with distilled water by centrifugation and decantation as described above. Then, the HCl/HF procedure as described above was repeated. Finally, samples were treated with 30% HCl to remove any potential fluoride gels and were washed as described above until the samples were diluted to an aqueous pH of 7. Samples were freeze-dried and weighed. The dried isolates were stored in glass at 8°C in the dark until analysis by pyrolysis-gas chromatography/mass spectrometry (Py-GC/MS).

### 5.3.5 Curie-point Pyrolysis-Gas Chromatography/Mass Spectrometry

The organic matter isolates were pressed onto a ferromagnetic wire with a Curie temperature of 610°C. Py-GC/MS analyses were carried out on a Hewlett-Packard 5890 gas chromatograph (GC) equipped with a FOM-3LX unit for pyrolysis. The GC was interfaced to a VG Autospec Ultima mass spectrometer operated at 70eV with a mass range of  $m/z$  50-800 and a cycle time of 1.7 s (resolution 1000). The gas chromatograph, equipped with a cryogenic unit, was programmed from 0°C (5 min) to 300°C (10 min) at a rate of 3°C/min. Separation was achieved using a fused silica capillary column (25 m × 0.32 mm) coated with CP Sil-5CB (film thickness 0.4 µm). Helium was used as a carrier gas.

### 5.3.6 Sediment Fraction Incubations

A few grams of the fine fractions or 20 grams of the total fractions were added to individual reactions chambers (100 ml bottle, Duran). Fifty milliliters of solution containing vitamins, trace elements and  $K_2HPO_4/KH_2PO_4$  were added (Table 5.2). The phosphate buffer serves as an additional pH buffer to the carbonate buffer present in the sediment and impedes potential pyrite oxidation (Elstnow *et al.*, 2001). One additional set of total fraction samples received glucose amendments with half of the amounts of vitamins and trace elements (Table 5.2) to check for nutrient or substrate limitations. The reaction chambers were connected to the closed circuit of a 30-channel computerized respirometer (Columbus Instruments Micro-Oxymax). The respirometer was used to simultaneously measure  $O_2$  uptake and  $CO_2$  production every 4 hours as an indication for the respiration activities of the microorganisms in the sediment samples. Carbon dioxide ( $p_{CO_2} = 10^{-3.35 \pm 0.34}$  atm) and oxygen ( $p_{O_2} = 10^{0.68 \pm 0.001}$  atm) levels in the headspaces of the reaction chambers were kept constant throughout the experiments. The evaporation of water in the reaction chambers enlarges the headspace volumes causing reduced oxygen concentrations. Therefore, a reaction chamber with 50 ml of the added solution was simultaneously run as a blank. Reported oxygen consumptions were corrected for this background 'consumption'. The effect of evaporation on the  $CO_2$  production was negligible, because of the low

atmospheric concentrations of CO<sub>2</sub> in the headspace atmosphere. The sediment slurries were incubated for 106 days in the dark at 25°C (± 1°C), while shaken gently at 100 rpm to ensure sufficient mixing of the solid and water phase and to enhance exchange with the gas phase in the reaction chambers.

**Table 5.2 Medium composition of the unamended and glucose-amended incubations**

Component	Unamended	Glucose-amended
<b>pH Buffer (g/l)</b>		
KH <sub>2</sub> PO <sub>4</sub>	4	4
K <sub>2</sub> HPO <sub>4</sub>	4	4
<b>Basic media (mg/l)</b>		
CaCl <sub>2</sub> ·2H <sub>2</sub> O	13.25	6.63
NaCl	10	5
NH <sub>4</sub> Cl	1.7	0.85
<b>Amendment (g/l)</b>		
Glucose	-	0.4
<b>Trace metals (µg/l)</b>		
FeCl <sub>3</sub>	120	60
H <sub>3</sub> BO <sub>3</sub>	50	25
CuSO <sub>4</sub> ·5 H <sub>2</sub> O	10	5
KI	10	5
MnSO <sub>4</sub> ·H <sub>2</sub> O	45	22.5
Na <sub>2</sub> MoO <sub>4</sub>	20	10
ZnSO <sub>4</sub> ·7 H <sub>2</sub> O	75	37.5
CoCl <sub>2</sub> ·6 H <sub>2</sub> O	50	25
Alk(SO <sub>4</sub> )·12 H <sub>2</sub> O	20	10
<b>Vitamins (µg/l)</b>		
Nicotinic acid	100	50
Ca-pantothenate	200	100
Cyanocobalamin	25	12.5
Inositol	100	50
P-aminobenzoate	20	10
Thiamine.HCl	50	25
Pyridoxine.HCl	25	12.5
Biotine	10	5
Riboflavine	10	5
Folic acid	10	5
Thiotic acid	10	5

## 5.4 RESULTS

### 5.4.1 Physical and Bulk Geochemical Characteristics

The bulk mineral composition of the total fraction samples consists of quartz as indicated by the dominance (>80 wt.%) of SiO<sub>2</sub> (Table 5.1). The particles in both the Drente and Oosterhout total fraction samples are predominantly (> 90 wt.%) larger than 63µm. Total organic carbon contents are low in all total fractions (0.1–0.14 wt.%). Highest TOC contents are observed in the fine fractions (0.3–1.0 wt.%). Total sulfur contents and especially total iron contents are higher in the Oosterhout total fraction samples relative to those of the Drente samples.

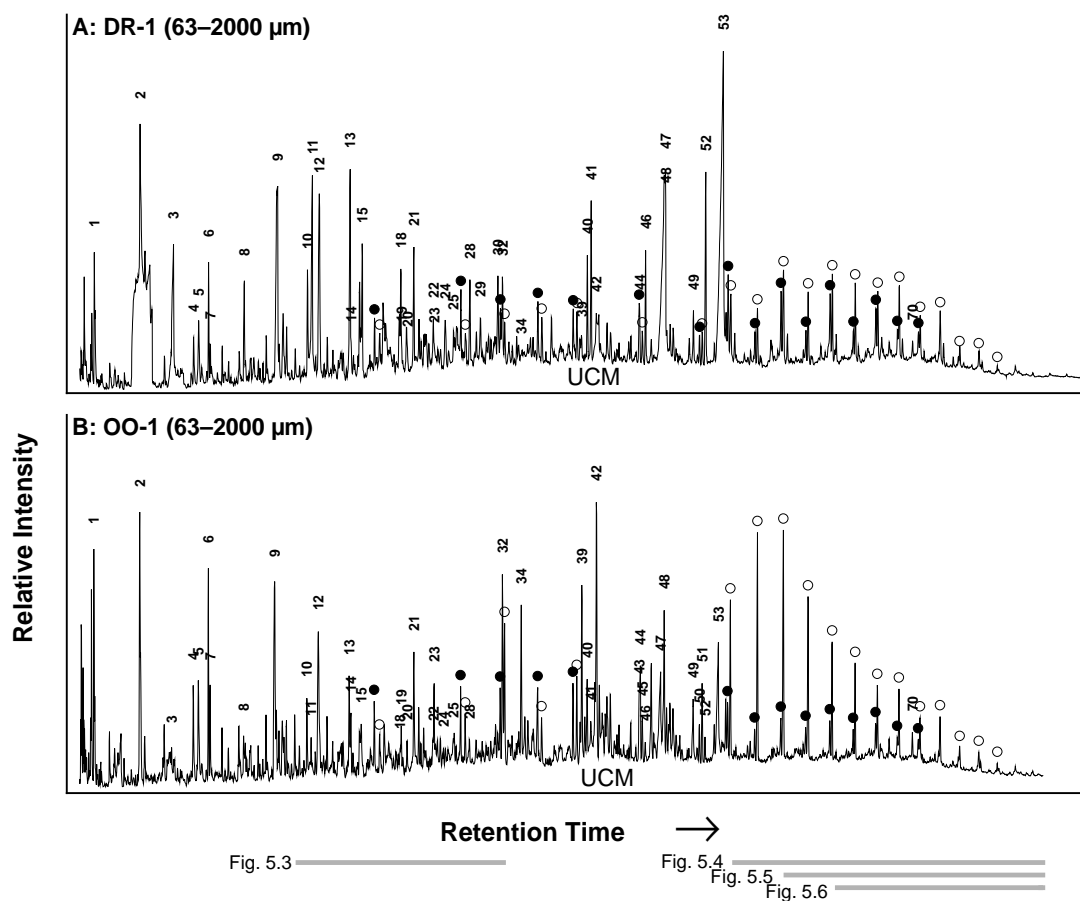


**Figure 5.2** Representative gas chromatograms of the evaporate/pyrolysate mixtures of (a) the Drente samples and (b) the Oosterhout samples. Peak numbers refer to the compounds listed in Table 5.4. ○ = alkane, ● = alkene. Gray bars indicate the trace position in Figures 5.3–5.6.

## 5.4.2 Pyrolysis-Gas Chromatography/Mass Spectrometry

Curie point pyrolysis-GC/MS was used as a qualitative method to characterize the chemical composition of SOM in the selected aquifer sediments. The flash heating results in an evaporate/pyrolysate mixture due to the evaporation of “free” low-molecular-weight (LMW) compounds and the pyrolysis of macromolecular compounds (Faure and Landais, 2001). Due to the presence of an unresolved complex mixture (UCM) in all evaporate/pyrolysate mixtures (Fig. 5.2), the organic composition of the isolates does not fully represent the chemical composition of SOM present in the incubated sediment samples. Also acid hydrolysis of organic compounds during HF/HCl isolation inevitably results in the loss of some compounds, studies have indicated that HF/HCl treatment does not significantly affect the bulk composition of the organic matter isolated (Sanchez-Monedero *et al.*, 2002; Schmidt *et al.*, 1997).

### 5.4.2.1 Bulk Chemical Composition of SOM

Overall, the obtained organic matter compositions of the samples are remarkably similar for the fractions analyzed. The evaporate/pyrolysate mixtures are dominated by aromatic compounds and homologous series of alk-1-enes and alkanes, with contributions from alkylthiophenes, fatty acids and branched hydrocarbons. However, the gas chromatogram of the fine fraction of the DR-1 sample was dominated by C<sub>16</sub> and C<sub>18</sub> nitrils and fatty acids, and showed a homologous series of alkenes. Because of the paucity of other identifiable compounds, this fraction will not be further discussed. The amount of isolate obtained from the coarse fraction of the OO-2 sample was insufficient to be analyzed. The total ion current traces of the Drente and Oosterhout evaporates/pyrolysates show a significant contribution of unidentified compounds present as UCM. The main compounds identified (Table 5.4) can be grouped into four classes of compounds and are discussed accordingly: lignin-derived compounds (LG), long-chain aliphatics (ALK), fatty acids (FA), and hopanoids (HOP).

**Table 5.3** Compounds identified in the evaporate/pyrolysate mixtures

Peak <sup>a</sup>	Compound Name	Characteristic Fragments ( <i>m/z</i> )	M+ ( <i>m/z</i> )	Compound Class <sup>b</sup>
1	benzene	78	78	
2	toluene	91, 92	92	
3	2-furaldehyde	95, 96	96	
4	C <sub>2</sub> -alkylbenzene	91, 106	106	
5	C <sub>2</sub> -alkylbenzene	91, 106	106	
6	styrene	104	104	
7	C <sub>2</sub> -alkylbenzene	91, 106	106	
8	5-methyl-2-furaldehyde	53, 109, 110	110	
9	phenol	94	94	
10	2-Methylphenol	107, 108	108	
11	2-methoxyphenol (guaiacol)	81, 109, 124	124	LG
12	3-methyl- and 4-methylphenol	107, 108	108	
13	C <sub>4</sub> -alkylbenzene	133, 134	134	
14	Naphthalene	128	128	
15	4-methyl-2-methoxyphenol	123+138	138	LG
16	Dodecene	55+69	168	ALK
17	Dodecane	57, 71	170	ALK
18	ethyl-2-methoxyphenol	137, 152	152	LG
19	C <sub>1</sub> -naphthalene	127, 162	162	
20	C <sub>1</sub> -naphthalene	127, 162	162	
21	4-vinyl-2-methoxyphenol	135, 150	150	LG
22	4-(2-propenyl)-2-methoxyphenol	164	164	LG
23	1-chloronaphthalene	127, 162	162	
24	4-formyl-2-methoxyphenol	151, 152	152	LG
25	<i>cis</i> -4-(1-propenyl)-2-methoxyphenol	164	164	LG
26	butadecene (C <sub>14:1</sub> )	55, 69	196	ALK
27	butadecane (C <sub>14</sub> )	57, 71	198	ALK
28	<i>trans</i> -4-(1-propenyl)-2-methoxyphenol	164	164	LG
29	4-acetyl-2-methoxyphenol	151	166	LG
30	4-(propane-2-one)-2-methoxyphenol	137, 180	180	LG
31	pentadecene (C <sub>15:1</sub> )	55, 69	210	ALK

32	3,5-di-(tert-butyl)-phenol	191, 206	206	CONT
33	pentadecane (C <sub>15</sub> )	57, 71	212	ALK
34	C <sub>18</sub> -alkane (branched)	57, 71	254	ALK
35	hexadecene (C <sub>16:1</sub> )	55, 69	224	ALK
36	hexadecane (C <sub>16</sub> )	57, 71	226	ALK
37	heptadecene (C <sub>17:1</sub> )	55, 69	238	ALK
38	heptadecane (C <sub>17</sub> )	57, 71	240	ALK
39	C <sub>18</sub> -alkane (branched)	57, 71	254	ALK
40	prist-1-ene (C <sub>19:1</sub> )	69, 126, 266	266	ALK
41	prist-2-ene (C <sub>19:1</sub> )	69, 126, 266	266	ALK
42	C <sub>20</sub> -alkane (branched)	57, 71	282	ALK
43	nonadecene (C <sub>19:1</sub> )	55, 69	266	ALK
44	octasulfur (S <sub>8</sub> )	64, 256	256	
45	nonadecane (C <sub>19</sub> )	57, 71	268	ALK
46	methylhexadecanoate	74, 270	270	
47	hexadecanoic acid (C <sub>16</sub> )	73, 256	256	FA
48	C <sub>24</sub> -alkane (branched)	57, 71	338	ALK
49	octadecanenitrile (C <sub>18</sub> )	57, 97	265	
50	hencosene (C <sub>21:1</sub> )	55, 69	294	ALK
51	hencosane (C <sub>21</sub> )	57, 71	296	ALK
52	methyloctadecanoate (C <sub>18</sub> )	74, 298	298	
53	octadecanoic acid (C <sub>18</sub> )	73, 284	284	FA
54	docosene (C <sub>22:1</sub> )	55, 69	308	ALK
55	docosane (C <sub>22</sub> )	57, 71	310	ALK
56	tricosene (C <sub>23:1</sub> )	55, 69	322	ALK
57	tricosane (C <sub>23</sub> )	57, 71	324	ALK
58	tetracosene (C <sub>24:1</sub> )	55, 69	336	ALK
59	tetracosane (C <sub>24</sub> )	57, 71	338	ALK
60	pentacosene (C <sub>25:1</sub> )	55, 69	350	ALK
61	pentacosane (C <sub>25</sub> )	57, 71	352	ALK
62	hexacosene (C <sub>26:1</sub> )	55, 69	364	ALK
63	hexacosane (C <sub>26</sub> )	57, 71	366	ALK
64	heptacosene (C <sub>27:1</sub> )	55, 69	378	ALK
65	heptacosane (C <sub>27</sub> )	57, 71	380	ALK
66	octacosene (C <sub>28:1</sub> )	55, 69	392	ALK

67	octacosane (C <sub>28</sub> )	57, 71	394	ALK
68	nonacosene (C <sub>29:1</sub> )	55, 69	406	ALK
69	nonacosane (C <sub>29</sub> )	57, 71	408	ALK
70	nor-17(21)-hopene	191, 231, 367	396	HOP
71	triacontene (C <sub>30:1</sub> )	55, 69	420	ALK
72	triacontane (C <sub>30</sub> )	57, 71	422	ALK
73	hentriacontane (C <sub>31</sub> )	57, 71	434	ALK
74	dotriacontane (C <sub>32</sub> )	57, 71	448	ALK
75	tritriacontane (C <sub>33</sub> )	57, 71	462	ALK
76	pentatriacontane (C <sub>34</sub> )	57, 71	476	ALK

<sup>a</sup> Peak numbers refer to Figure 5.2

<sup>b</sup> lignin-derived compounds (LG), long-chain aliphatics (ALK), fatty acids (FA), and hopanoids (HOP), contaminants (CONT)

The types of compounds detected in the evaporate/pyrolysate mixtures are similar for the Drente and Oosterhout fractions. However, lignin-derived markers dominate the Drente samples, whereas the Oosterhout samples show an equal contribution from aliphatics and lignin-derived compounds (Fig. 5.2, Table 5.4).

#### 5.4.2.2 Lignin-derived Pyrolysis Products

Lignin-derived 2-methoxyphenol (guaiacol) pyrolysis products are relatively abundant in all samples. A small amount of 2,6-dimethoxyphenol (syringol) was detected only in the evaporate/pyrolysate mixture of the OO-2 fine fraction.

As indicated by the summed mass chromatograms *m/z* 124+138+150+152+164+166 (Fig. 5.3), 2-methoxyphenol (**I**; see Fig. 5.3 for structures), 4-methyl-2-methoxyphenol (**II**) and 4-ethyl-2-methoxyphenol (**III**) are the dominant guaiacyl-lignin derivatives in the Drente samples. In the Oosterhout samples, 4-vinyl-2-methoxyphenol (**IV**) is the most important guaiacyl-lignin derivative. In addition, 2-methoxy-4-(2-propenyl)-phenol (**V**) and the 2-methoxy-4-(1-propenyl)-phenol isomers (**VII** and **VIII**) are as important as 2-methoxyphenol (**I**) and 4-methyl-2-methoxyphenol (**II**). The oxidized lignin derivatives 4-formyl-2-methoxy-phenol (**VI**), 4-acetyl-2-methoxyphenol (**IX**) and 4-(propan-2-one)-2-methoxyphenol (not shown) were most pronounced in the Drente samples.



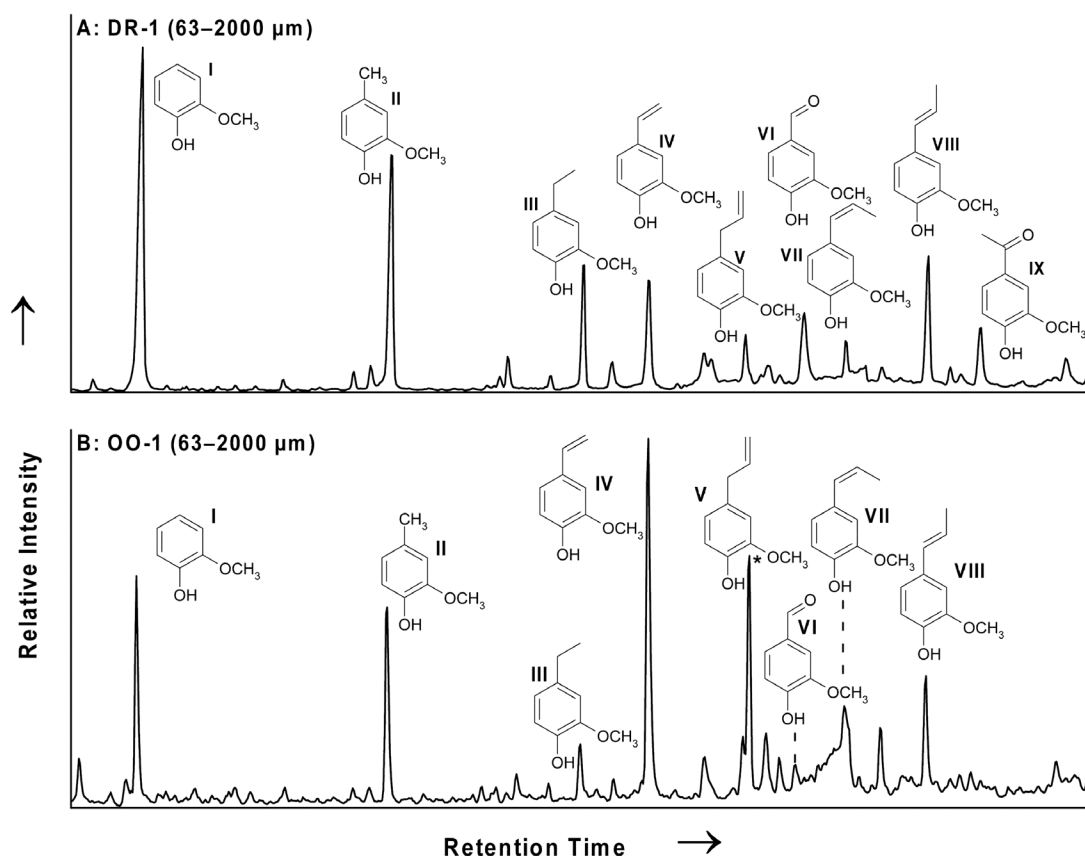


**Figure 5.3** Representative partial mass chromatograms for guaiacyl derivatives ( $m/z$  124+138+150+152+164+166) of the evaporate/pyrolysate mixtures of (a) the Drente samples (b) the Oosterhout samples. \*Co-elution of 1-chloronaphthalene ( $M^+=164$ ) with 2-methoxy-4-(2-propenyl)-phenol (V). Roman numbers in bold refer to compounds, as discussed in section 5.4.2.2 of the text.

#### 5.4.2.3 Alkanes and Alkenes

In both the Oosterhout and Drente samples, the alkane distribution is dominated by long chain ( $C_{23}$ - $C_{31}$ ) alkanes with a maximum in the  $C_{23}$ - $C_{25}$ -range, as illustrated by the mass chromatograms  $m/z$  55+57 in Figure 5.4. The relative amounts decrease from the  $C_{24}$ -alkane towards the longer alkanes. In the distributions of  $C_{27}$ - $C_{31}$  alkanes, the odd-carbon-numbered alkanes are relatively more pronounced in the Oosterhout samples, while alkene counterparts accompany the alkanes less prominently as compared with the Drente samples (Table 5.3).

In the Oosterhout samples, several branched alkanes ( $C_{18}$ ,  $C_{20}$  and  $C_{24}$ ) are clearly present (Table 5.4, Fig. 5.2). While the overall hydrocarbon content of the Drente samples is lower than that of the Oosterhout samples, the relative amounts of

prist-1-ene (2,6,10,14-tetramethyl-1-pentadecene) and prist-2-ene (2,6,10,14-tetramethyl-2-pentadecene) are more pronounced in the Drente samples (Table 5.4, Fig. 5.2).

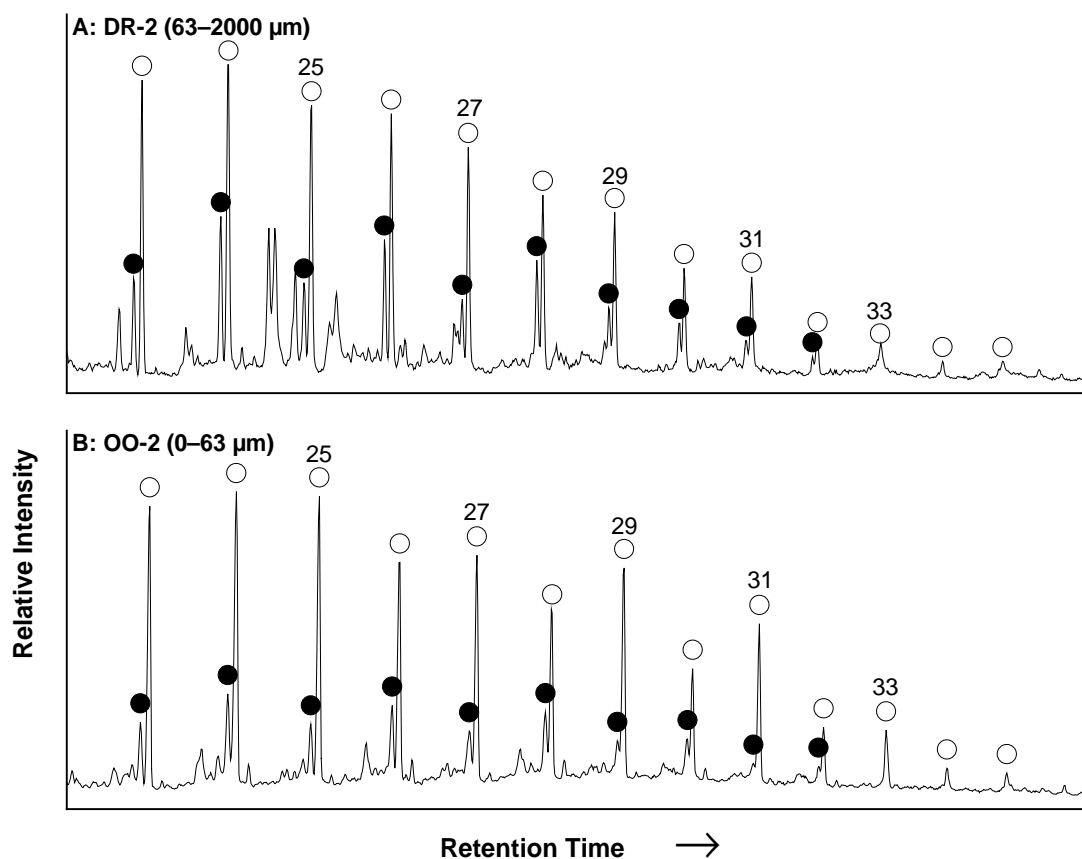


**Figure 5.4** Representative partial mass chromatograms for alkenes and alkanes ( $m/z$  55+57) of the evaporate/pyrolysate mixtures of (a) the Drente samples (b) the Oosterhout samples ○ = alkane, ● = alkene. Numbers above peaks indicate number of carbon atoms.

#### 5.4.2.4 2-Alkanones

The 2-alkanone distributions, as indicated by the mass chromatograms  $m/z$  59 (Fig. 5.5) are dominated by the  $C_{23}$  to  $C_{31}$  2-alkanones with a maximum at  $C_{29}$  for the Drente samples, while in the Oosterhout samples the 2-alkanones are more evenly distributed. In the  $C_{25}$ - to  $C_{31}$ -2-alkanone distributions, the 2-alkanones with an odd carbon number are relatively most pronounced in the Drente samples as compared with the Oosterhout samples. The odd-over-even predominance can be expressed using a carbon preference index (CPI). The following equation was used for the CPI calculation (Table 5.3):

$$CPI = \frac{2C_{29}}{(C_{28} + C_{30})}$$

Calculated CPI's for the 2-alkanones in the Drente samples (3.2–4.0) were higher than in the Oosterhout samples (2.3–2.8).

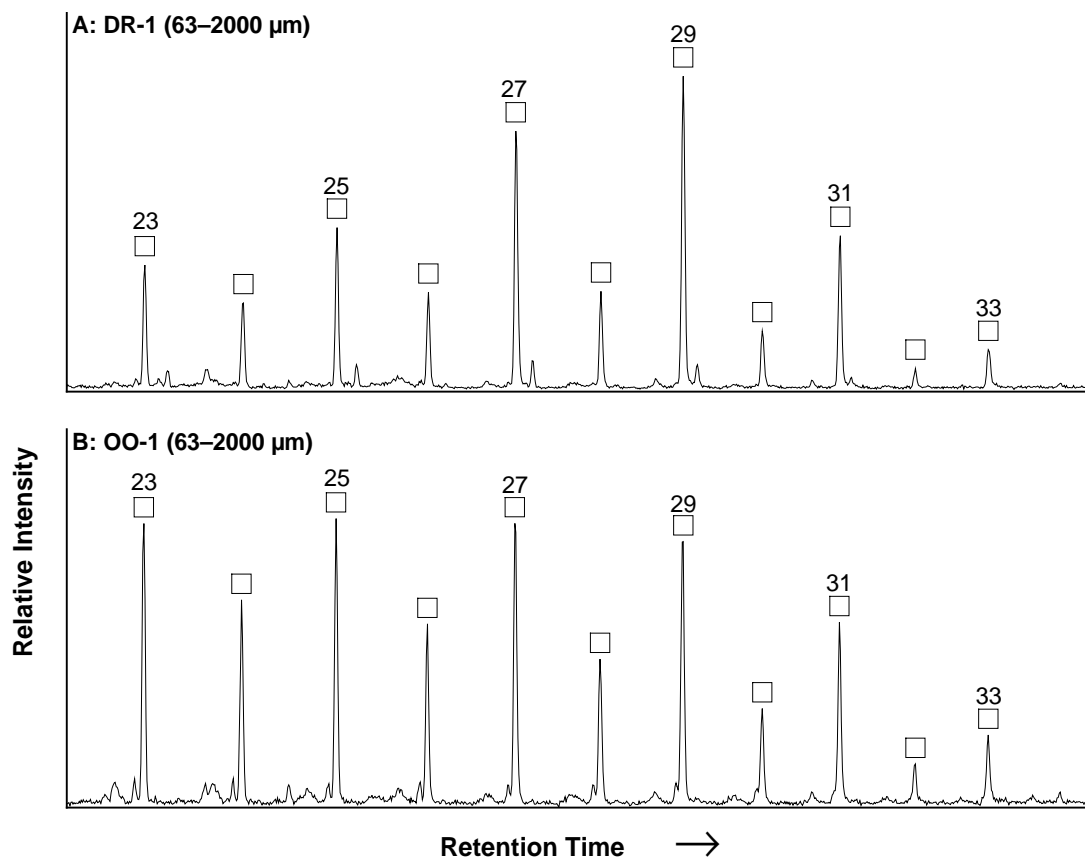


**Figure 5.5** Representative partial mass chromatograms for 2-alkanones ( $m/z$  59) of the evaporate/pyrolysate mixtures of (a) the Drente samples (b) the Oosterhout samples. Numbers above peaks indicate number of carbon atoms

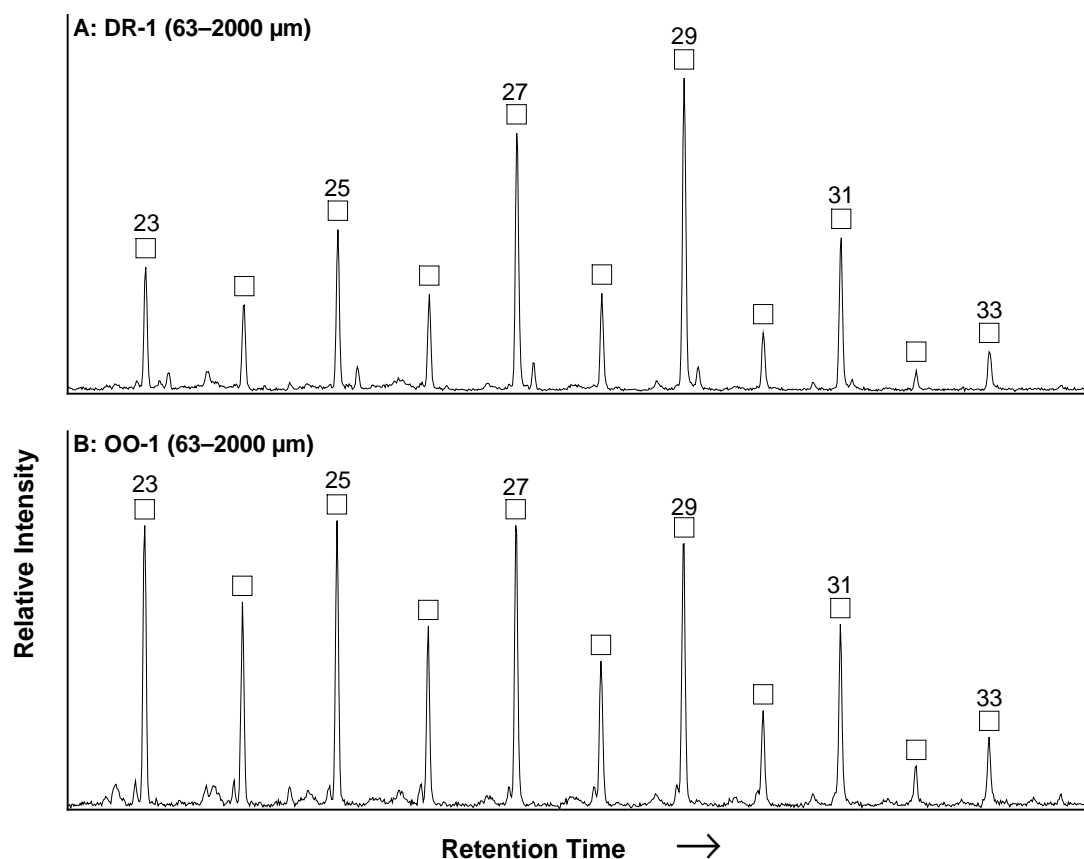


**Figure 5.6** Representative partial mass chromatograms for 2-alkanones ( $m/z$  59) of the evaporate/pyrolysate mixtures of (a) the Drente samples (b) the Oosterhout samples. Numbers above peaks indicate number of carbon atoms

**Table 5.4** Organic geochemical results for the incubated fine and coarse fractions of the Drente (DR) and Oosterhout (OO) sediments

Sample	Fraction	Initial Sample (g)	Removal <sup>a</sup> (%)	$\frac{\text{alkane}}{\text{alkene}}$ <sup>b</sup>	CPI <sup>c</sup> alkanones
DR-1	Fine	0.13	95.7	n.d <sup>d</sup>	n.d.
DR-1	Coarse	14.47	98.8	2.19	4.04
DR-2	Fine	0.87	98.8	1.22	3.24
DR-2	Coarse	14.39	98.2	1.75	3.78
OO-1	Fine	1.42	94.0	3.28	2.55
OO-1	Coarse	16.29	99.3	5.93	2.31
OO-2	Fine	13.44	92.9	2.49	2.79

(a) Matrix removal efficiency of the HF/HCl treatment.

(b) Calculated average for  $C_{23}$ – $C_{31}$

(c) Calculated as  $CPI = \frac{2C_{29}}{(C_{28} + C_{30})}$

(d) Not determined

### 5.4.2.5 Fatty Acids

Fatty acids, as indicated by the mass chromatograms  $m/z$  60+73 (not shown), display a strong even-over-odd predominance and range from  $C_{12}$  to  $C_{26}$ . The  $C_{16}$  and  $C_{18}$  fatty acids predominate the mixtures. In all Drente samples, the  $C_{16}$  fatty acid is relatively less important than the  $C_{18}$  fatty acid, whereas they are equally important in the samples from the Oosterhout Formation. Small relative amounts of *iso*- and *anteiso*- $C_{15}$  and  $C_{17}$  fatty acids were detected in the Oosterhout samples. Only minor amounts of *iso*- and *anteiso*- $C_{15}$  were observed in the Drente samples.

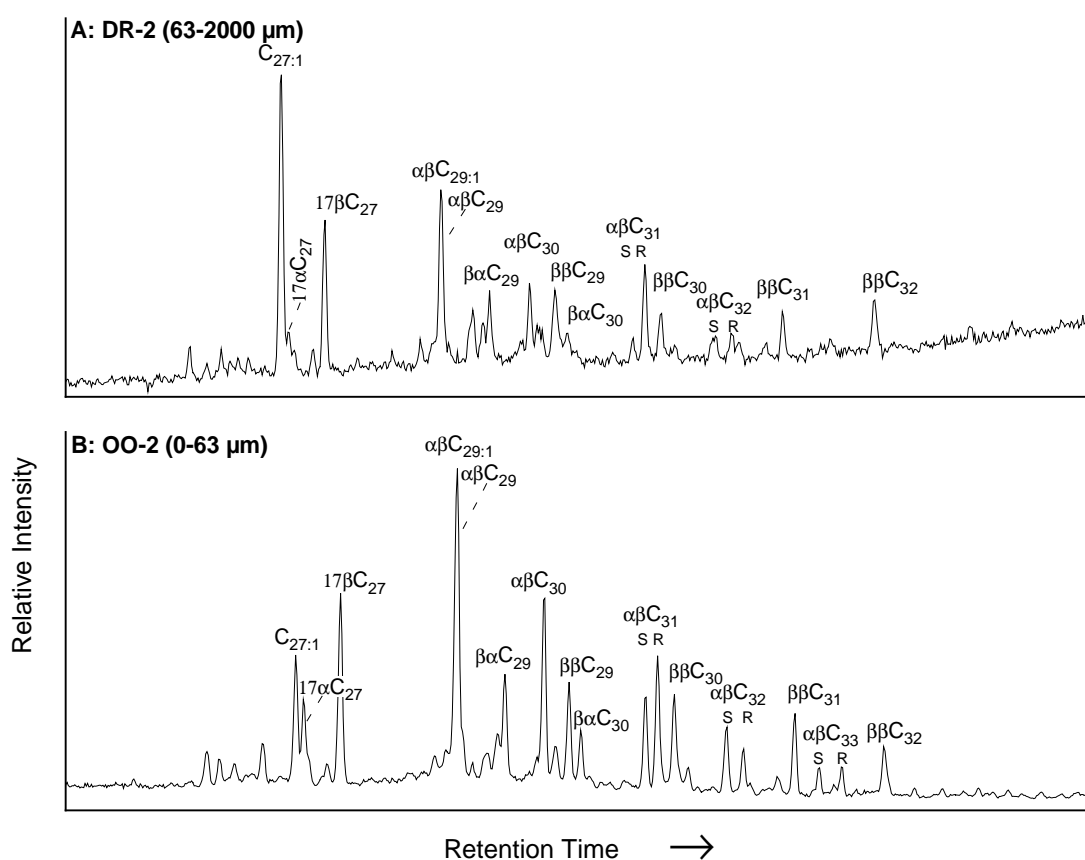


**Figure 5.7** Representative partial mass chromatograms for hopanoids ( $m/z$  191) of the evaporate/pyrolysate mixtures of (a) the Drente samples (b) the Oosterhout samples.

### 5.4.2.6 Hopanoids

A number of triterpenoidal hydrocarbons of hopanoid origin were identified in all samples. Hopanoid distributions ranged from  $C_{27}$  to  $C_{33}$  (Fig. 5.6). Maxima in the hopanoid distributions are at  $C_{27}$  in the Drente samples and at  $C_{29}$  in the Oosterhout

samples. The hopanes are present in both the 17 $\alpha$ (H),21 $\beta$ (H) (i.e.,  $\alpha\beta$ ) as well as the less stable natural  $\beta\beta$  configuration. The relative amounts of the more stable 22S and the natural 22R isomers are variable for the C<sub>31</sub>- to C<sub>33</sub>-hopanes. Trisnor-17(21)-hopene (C<sub>27</sub>) and nor-17(21)-hopene (C<sub>27</sub>) prominently accompany C<sub>27</sub>- and C<sub>29</sub>-hopane counterparts.

### 5.4.3 Incubation Experiments

#### 5.4.3.1 Oxygen Consumption of the Unamended Sediment Fractions

Sediment fractions were incubated for 106 days under constant atmospheric conditions to assess their reactivity towards oxygen. Oxygen consumption rates decreased continuously during all unamended incubations. However, two major differences in reactivity were observed. Firstly, the fine and total fractions of the Oosterhout samples consumed up to 14 times more O<sub>2</sub>/g than the corresponding fractions of the Drente samples. Secondly, the weight-based oxygen uptake of the fine fractions was 1.2 to 4.9 times higher than that of the corresponding total fractions (Table 5.5).

**Table 5.5** Cumulative results for the incubations of the unamended fine and total fractions, and the glucose-amended total fractions

Fraction	Sample code	Total O <sub>2</sub> consumption (μmol/g.sed)	CO <sub>2</sub> /O <sub>2</sub> (molar)	TOC (wt. %)	TOC-oxidized <sup>a</sup> (% initial)
< 63 μm	DR-1	6.1	0.96	0.33	2
	DR-2	6.4	0.71	0.42	2
	OO-1	83.4	0.59	1.08	9 <sup>b</sup>
	OO-2	47.3	0.76	0.89	6
0-2000 μm	DR-1	5.3	0.99	0.10	6
	DR-2	1.9	1.19	0.11	2
	OO-1	16.9	0.64	0.14	14 <sup>b</sup>
	OO-2	11.1	1.17	0.12	11
0-2000 μm + Glucose	DR-1	25.9	1.11	0.04 <sup>c</sup>	62 <sup>c</sup>
	DR-2	25.5	1.15	0.04 <sup>c</sup>	71 <sup>c</sup>
	OO-1	34.3	0.86	0.04 <sup>c</sup>	52 <sup>c</sup>
	OO-2	31.1	1.09	0.04 <sup>c</sup>	60 <sup>c</sup>

(a) The initial TOC contents and total oxygen consumptions (RQ=1) were used to calculate the amount of organic carbon oxidized.

(b) Maximum estimate due to the possible contribution of pyrite oxidation.

(c) Represents the glucose-C added as a calculated sediment weight percentage.

### 5.4.3.2 Oxygen Consumption of the Glucose-amended Sediment Fractions

In the glucose-amended incubations, oxygen consumption rates were elevated during the first 20 days as compared with the unamended incubations (Fig. 5.7). This resulted in a 17–24  $\mu\text{mol O}_2/\text{g}$  higher total oxygen consumption, indicating the mineralization of 52–71 % of the glucose added (Table 5.5). Oxygen consumption rates of the amended samples equaled those of the unamended incubations towards the end of the incubations (Fig. 5.7) and the absolute differences in total  $\text{O}_2/\text{g}$  uptake between the glucose-amended incubations were similar to the differences between the corresponding unamended total fractions (Table 5.5).

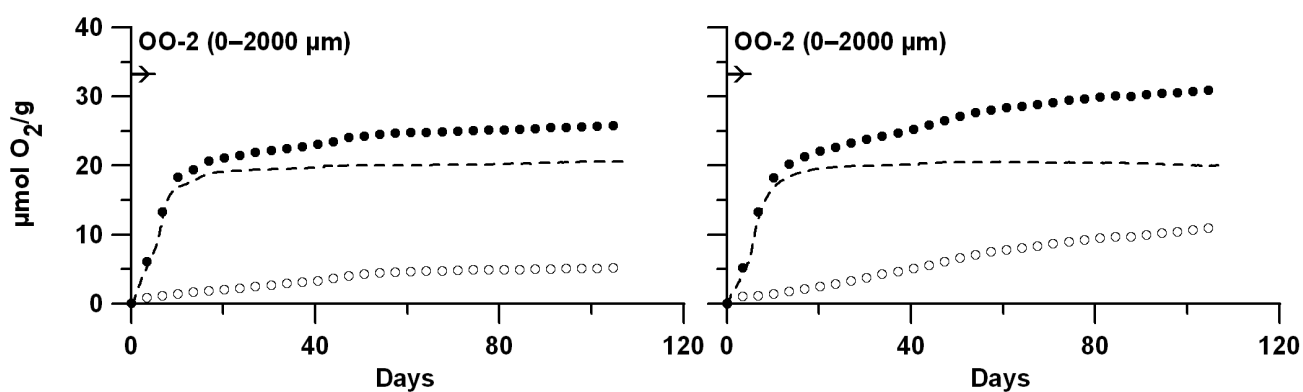


**Figure 5.8** Cumulative oxidation consumption during the incubation of the glucose-amended (●) and unamended (○) total fraction of the DR-1 and OO-2 sediment samples. Dashed lines represent the glucose-attributed difference between the amended and unamended fractions. Arrow on Y-axes indicates the amount of glucose added to the amended fractions.

### 5.4.3.3 Respiration Quotients of the Incubations

Molar respiratory quotients (RQ) of  $\text{CO}_2$  production and  $\text{O}_2$  consumption of the unamended incubations were near unity, ranging between 0.59 and 1.19 (Table 5.5). The lowest RQ's were observed for the incubations of the OO-1 sediment samples. The RQ's of the glucose-amended total fraction incubations were closer to unity than the unamended samples.

## 5.5 DISCUSSION

In this study we have characterized SOM in aquifer sediments from two distinct geological formations, assessed its origin and degradation status and measured its reactivity towards molecular oxygen.

### 5.5.1 “Free” and Macromolecular SOM

During flash heating of SOM, “free“ LMW compounds evaporate, while compounds bound within a macromolecular structure are revealed as degraded products upon pyrolysis (Faure and Landais, 2001). The significant presence of alkenes relative to their alkane counterparts (Fig. 5.4, Table 5.3) indicates that a substantial part of the straight chain hydrocarbons are pyrolysis products released from macromolecular structures (Derenne *et al.*, 1991; Lichtfouse *et al.*, 1998a). Moreover, the importance of hopenes relative to their hopane counterparts (Fig. 5.6) and unsaturated isoprenoids (Table 5.4) indicates that, during early diagenesis, a significant fraction of SOM has been incorporated within macromolecular structures in both the Drente and Oosterhout samples (Ambles *et al.*, 1996; Lichtfouse *et al.*, 1998b; Qu *et al.*, 1996; Reiss *et al.*, 1997).

Since unsaturated counterparts did not accompany the fatty acids and 2-alkanones, these compounds occur as such in both the Oosterhout and Drente samples and therefore simply evaporate. Summarizing, SOM is thus present as macromolecules and “free” LMW compounds in both the Drente and Oosterhout samples. However, the higher ratio of alkane to alkene counterparts (Table 5.3) as well as the dominance of hopane over hopene counterparts (Fig. 5.6) indicates “free” LMW compounds are relatively more important in the SOM of the Oosterhout samples than in the SOM of the Drente samples.

### 5.5.2 Origin of Sedimentary Organic Matter

The bulk inorganic composition of the Oosterhout sediments is in line with a shallow marine depositional environment as opposed to the sediments from the Drente formation. The elevated total sulfur and total iron contents in the Oosterhout sediments (Table 5.2) is attributed to the presence of iron sulfides, formed under



sulfate-reducing conditions. Glauconite (a Fe(II),Fe(III)-silicate mineral) can be an additional source of iron. Glauconite is indicative for diagenesis in shallow marine environments (Berner, 1971) and is frequently observed in the Oosterhout Formation (Griffioen, 2001; van den Berg *et al.*, 2000). Thus, the inorganic geochemical composition of the Oosterhout samples is consistent with the near coastal origin of the formation. Therefore, an input of marine-derived organic matter to SOM would be expected during the deposition of the Oosterhout sediments.

Despite the coastal depositional environment of the Oosterhout Formation, no compounds of an unequivocal marine origin were observed in the Oosterhout samples. Instead, the abundance of long chain (C<sub>23</sub>–C<sub>33</sub>) alkanes (Fig. 5.4) and 2-alkanones (Fig. 5.5) with an odd-over-even predominance of the C<sub>27</sub> to C<sub>33</sub>-alkanes (Fig. 5.4) is characteristic for aliphatics derived from the cuticular waxes of higher plants (Eglinton and Hamilton, 1967). Finally, the importance of guaiacyl lignin-derived markers in the total ion current traces (Fig. 5.2) reflects the input of angiosperm wood components (Saiz-Jimenez and De Leeuw, 1986). Thus, the SOM in both the Drente and Oosterhout sediments is dominantly of a terrestrial, higher plant origin.

Besides a higher plant-derived origin, a small input of bacterial biomass to SOM is observed. This is indicated by the presence of C<sub>27</sub>–C<sub>33</sub>-hopanoids (Fig. 5.6), which are derived from C<sub>35</sub>-bacterial hopanoids and related bacterial lipids (Dorsselaer *et al.*, 1974; Kannenberg and Poralla, 1999; Otto and Simoneit, 2001; Rullkötter, 1983), as well as by small amounts of *iso*- and *anteiso*-C<sub>15</sub> and C<sub>17</sub> fatty acids in the Oosterhout samples (Leo and Parker, 1966; Schmitter *et al.*, 1978). Although living biomass is undoubtedly present, hopanoids with functional groups attached to their hopanoid skeleton were not observed. Therefore, dead bacterial biomass is probably the main source of the microbial-derived SOM with an insignificant contribution of active bacterial biomass.

### 5.5.3 Diagenetic Effect on the Composition of Sedimentary Organic Matter

Signs of diagenetic SOM oxidation are found in both the Drente and Oosterhout samples, but results indicate that SOM degradation in the Drente samples has been more intense. Firstly, side chains of the lignin derivatives are shorter in the

Drente samples and lignin derivatives with an oxidized propyl side chain (**VI** and **IX**, Fig. 5.3) are more abundant in the Drente samples (Fig. 5.3), as compared with the Oosterhout samples. These features are typical for aerobic lignin degradation (Dittmar and Lara, 2001), and thus indicate a more extensive aerobic oxidation of the propyl side chain on guaiacyl-lignin derivatives (Dijkstra *et al.*, 1998; Kuder and Krüge, 1998) in the Drente samples. Secondly, a higher degree of side chain oxidation of the hopanoids is indicated for the Drente samples, where C<sub>27</sub>-hopanoids are dominant, while the longer hopanoids (> C<sub>29</sub>) are more prominent in the Oosterhout samples (Fig. 5.6). The oxidation of linear side chains is thus more pronounced in the Drente samples than in the Oosterhout samples.

The higher degree of side chain oxidation is in line with the aforementioned relative importance of macromolecular SOM in the Drente samples. The presence of 2-alkanones with a high odd-over-even predominance (Fig. 5.4, Table 5.3) indicates the partial oxidation of corresponding plant wax-derived alkanes (Ambles *et al.*, 1993). Since odd-over-even predominance is typical for plant wax-derived alkanes, the more pronounced odd-over-even predominance of these 2-alkanones (Fig. 5.4) as compared with the long-chain alkanes (Fig. 5.3) indicates that these alkanes are preferentially oxidized over macromolecular alkyl moieties. Therefore, the higher CPI's for the 2-alkanones in the Drente samples (Table 5.3) as compared with the Oosterhout samples imply that the plant wax derived lipid fraction in the Drente samples is more degraded than in the Oosterhout samples. Since macromolecular SOM is in general more resistant to oxidation than "free" LMW compounds (*e.g.*, (Jenisch-Anton *et al.*, 2000)), the greater importance of macromolecular SOM in the Drente samples can be explained by a more extensive oxidation of SOM as compared with the Oosterhout samples.

#### **5.5.4 Geochemical Controls on the Reactivity of SOM**

The less degraded status of SOM in the Oosterhout samples is in agreement with their high affinities towards molecular oxygen during incubation, as compared with the Drente samples. However, verification that mineralization of SOM was the most important oxidation reaction during the incubations is needed, because of the

potential oxidation of other reduced components such as pyrite or glauconite-Fe(II). The observed RQ's are near unity in the unamended and amended (as expected for glucose oxidation) incubations and thus point to the respiration of organic matter as dominant oxygen consuming process during the sediment incubations (Table 5.5). The lowest RQ's (0.6) are observed for the unamended OO-1 incubations hint towards the oxidation of pyrite as an additional oxygen consuming process (*Chapter 3*) and would suggest that the phosphate present could not fully impede pyrite oxidation. However, RQ's lower than unity can also reflect the oxidation of substrates as aliphatic compounds or fatty acids (*e.g.*, (Dilly, 2001).

Calculations for the unamended incubations indicate that total SOM oxidation after 106 days ranged from 2% in the Drente to at most 14% in the Oosterhout total fraction samples (Table 5.5), corresponding to first-order degradation constants of  $1.91 \cdot 10^{-4}$ /day and  $1.42 \cdot 10^{-4}$ /day, respectively. In contrast, initial oxygen consumption was much faster during the amended incubations. However, rates became similar to the corresponding unamended samples after 20 days (Fig. 5.7). An estimated 52% to 71% of the added glucose was respired after 20 days, which is similar to the mineralization observed during glucose-amended soil experiments (Sollins *et al.*, 1996; Tsai *et al.*, 1997; Witter and Dahlin, 1995). The high initial oxidation rates during the glucose-amended incubations indicate that microbial activity could be stimulated, despite the reduced nutrient concentrations (Table 5.2). Since a fraction of the unrespired glucose was likely transferred into biomass (Tsai *et al.*, 1997), the similar final respiration rates of the amended and unamended incubations indicate that a more active microbial population did not stimulate the respiration of SOM. Therefore, we conclude that the oxidation of SOM towards molecular oxygen was not controlled by nutrient, oxidant or microbial limitations, but was instead limited by its reactivity (*i.e.*, substrate limited) during the incubations.

The aerobic degradation rates of SOM observed in the Drente and Oosterhout samples are substantially slower than that of fresh organic matter in soils and marine sediments (Hedges and Oades, 1997; Henrichs, 1993; Sollins *et al.*, 1996). For example, 37 to 47% of the organic matter of fresh plant residues was lost during 85

days of incubation (Franchini *et al.*, 2002). This indicates that the organic matter present in aquifer sediments studied is already substantially degraded, as was confirmed by the absence of readily degradable compounds such as sugars or cellulose in the aquifer sediments studied here. Moreover, the significantly lower oxygen consumptions during the incubations of the Drente samples and the more degraded status of their SOM point to the chemical composition of SOM being a main control on its reactivity, as was previously shown for soil humic material (Almendros and Dorado, 1999).

Besides the chemical composition as a control on the degradability of SOM, results suggest a small particle size effect. The similar chemical composition of the SOM present in the fine and coarse fractions, the significantly higher amounts of SOM in the fine fractions (Table 5.1) and the smaller average extent of SOM degradation (Table 5.5) in the fine fractions (4.8%) compared with that in the corresponding total fractions (8.3%) suggests that the degradation of SOM is hampered in the fine fraction samples (Anderson *et al.*, 1981; Christensen and Sørensen, 1985). However, this particle size effect is less apparent than that of chemical composition.

### **5.5.5 Geological Controls on the Degradation Status of SOM**

A general decrease in SOM reactivity with increasing sediment age would be expected at first sight, since reactive organic compounds are degraded preferentially. In contrast, our results show that absolute age is not controlling the degradation status of SOM since the reactivity of SOM is significantly higher in the samples from the Oosterhout Formation than in those from the Drente Formation, despite the age difference of over 3 My. Thus, although a generally lower reactivity in older aquifer sediments is expected (Jakobsen and Postma, 1994), differences in conditions during or after burial must have overridden the effect of age with respect to SOM reactivity in the sediments studied.

As indicated by the oxidized lignin-derivatives (Fig 3.) and 2-ketones (Fig. 5.5), a more severe aerobic degradation of SOM is responsible for the less preserved status of SOM in the Drente samples, as compared with the Oosterhout samples. The

importance of oxygen availability in microbial SOM degradation is related to the enzymatic ability of most aerobic microorganisms to perform a total mineralization of complex organic substrates like lignin (Benner *et al.*, 1984; Miki *et al.*, 1987; Odier and Monties, 1983) and recent studies have pointed to the oxygen exposure time (OET) of sediments as the dominant control on the degradation status of SOM (Gélinas *et al.*, 2001; Hartnett *et al.*, 1998; Hulthe *et al.*, 1998). A significantly higher OET of the Drente sediments can therefore explain its more degraded and less reactive SOM, as compared with the Oosterhout sediments. This would suggest that the OET of the Oosterhout sediments during and after deposition was sufficiently shorter to preserve reactive organic matter. The different depositional environments for the Drente and Oosterhout Formation are a likely cause for different OET's. Higher sediment deposition rates and less reworking of the sediments in the shallow marine Oosterhout Formation as compared with the fluvio-glacial Drente sediments can have resulted in shorter sediment OET's (Betts and Holland, 1991; Gélinas *et al.*, 2001; Hartnett *et al.*, 1998). In line with this interpretation, Routh *et al.* (1999) observed more intensive degradation of SOM in terrestrially deposited regressive sediments as compared with offshore-deposited transgressive sediments.

Moreover, marine-derived organic matter is more prone to oxidation, since recalcitrant biomacromolecules (as lignin) are less abundant in organic matter derived from marine microorganisms (Aller, 1998; Colombo *et al.*, 1996). Therefore, the input of marine-derived organic matter may have enhanced relative preservation of terrestrial SOM, additional to the effect of shorter exposure of oxygen to the shallow marine Oosterhout sediments.

In addition to aerobic oxidation during deposition or early diagenesis, re-exposure to oxygen following a period of anoxia will affect the degradation status of SOM (Hulthe *et al.*, 1998). Various changes in hydrogeological conditions, from intensified drainage to tectonic uplift, can cause a return to oxic conditions. Specific examples for the area studied are the development of push-moraines (van den Berg *et al.*, 2000) during the Saalian glaciation, which strongly affected regional groundwater

pressures and velocities (van Weert *et al.*, 1997) and the fluvio-glacial incisions (Fig. 5.1b) that may have increased oxygen exposure of adjoining sediments.

After primary deposition and diagenesis, SOM can be eroded and redeposited. Especially fluvio-glacial deposits, such as the Drente Formation, frequently include sediments that are reworked by glacial erosion. Expectedly, the reworking of sediments increases OET (Binger *et al.*, 1999), and thus affects the reactivity of SOM. Reworked SOM has been found to be the dominant form of SOM in several fluvio-glacial sediments (Allen-King *et al.*, 1997; Binger *et al.*, 1999; Buckau *et al.*, 2000; Keller and Bacon, 1998; Postma *et al.*, 1991). For example, SOM in Pleistocene aquifer sediments contained organic components that were reworked from Miocene deposits within a braided river system (Postma *et al.*, 1991). Also in the Drente sediments, the presence of reworked organic matter is likely, since reworked fluvial sediments from the Pleistocene Urk Formation (Fig. 5.1b) contributed to the Pleistocene Drente sediments (van Beek and Vogelaar, 1998; van den Berg *et al.*, 2000). Thus, sediment re-exposure to oxic conditions during sediment reworking likely resulted in further degradation of SOM in the Drente sediments as compared with the Pliocene Oosterhout sediments.

The sediments studied were taken from stratigraphic depths that are under iron reducing conditions (van Beek and Vogelaar, 1998). Therefore, these sediments are presumably under anoxic conditions for the greatest part of their burial history as the groundwater system studied is largely anoxic (Griffioen, 2001; van Beek and Vogelaar, 1998). However, if anaerobic degradation would have a predominant effect on the preservation status of SOM, age would be expected to negatively relate with SOM reactivity. In contrast, since aerobic SOM degradation is orders of magnitude faster than anaerobic degradation of SOM (Canfield, 1994; Kristensen and Holmer, 2001), the exposure of SOM in aquifer sediments to oxic groundwater significantly diminishes its reactivity during anaerobic degradation by, for instance, nitrate, iron (III) or sulfate reducers.

### 5.5.6 Sedimentary Organic Matter as a Reactive Component in Aquifers

Several studies on SOM in aquifer sediments have focused on its role as the principal sorbent of organic contaminants (Murphy and Zachara, 1995; Pignatello, 1998) and have shown that its bulk chemical composition controls its sorption capacity (Karapanagioti and Sabatini, 2000; Kleineidam *et al.*, 1999; Weber Jr. *et al.*, 1998). Few studies have characterized organic matter present in groundwater systems on a molecular level. Routh *et al.* (2001) characterized the molecular composition of solvent-extractable OM in transgressive and regressive sediments within an aquitard/aquifer system, while others have used the chemical composition of dissolved organic matter (DOM) in groundwater as an indication of the composition of SOM in its source aquifer (Grøn *et al.*, 1996; Sukhija *et al.*, 1996; Wassenaar *et al.*, 1990).

In addition to the sorption capacity of SOM, its reactivity towards oxidants is controlled by the molecular composition of SOM as shown in this study. To date, the reactivity of SOM in aquifer sediments is generally considered 'low' (Christensen *et al.*, 2000). However, SOM degradation rates range in several orders of magnitude (Jakobsen and Postma, 1994; Korom, 1992). Our results bring forward that this range in SOM reactivity may reflect the compositional variety of SOM in aquifer sediments due to both its origin and OET. Overall, the chemical composition is an important property of aquifer sediments and more research is needed to better define the control of SOM composition on its reactivity.

## 5.6 CONCLUSIONS

Organic compounds with a terrestrial, higher plant origin dominate the composition of SOM in the aquifer sediments from the fluvio-glacial Drente and near coastal Oosterhout Formation. No indications for an input of marine-derived organic matter in SOM were found. While SOM is present both as high- and low-molecular-weight components, the macromolecular fraction of SOM is more important in the Drente samples. The dominance of resistant macromolecular compounds is in line with the more degraded status of the SOM in the Drente samples as indicated by its more degraded hopanoid and lignin side chains and the more extensive oxidation of

its long chain alkanes. These oxidation features point to the effect of aerobic degradation on the diagenetic status of SOM in aquifers. In the Pliocene Oosterhout sediments SOM is up to an order of magnitude more reactive towards oxygen than in the Pleistocene Drente formation, despite the age difference of over 3 My. Hence, syn- and post-depositional conditions are more important than absolute age in controlling the degradation status of SOM. Especially the oxygen exposure time during and after sediment deposition is considered a controlling factor.

## References

- Allen-King R. M., McKay L. D., and Trudell M. R. (1997) Organic carbon dominated trichloroethene sorption in a clay-rich glacial deposit. *Ground Water* **35**(1), 124-130.
- Aller R. C. (1998) Mobile deltaic and continental shelf muds as suboxic, fluidized bed reactors. *Marine Chemistry* **61**, 143-155.
- Almendros G. and Dorado J. (1999) Molecular characteristics related to the biodegradability of humic acid preparations. *European Journal of Soil Science* **50**, 227-236.
- Ambles A., Grasset L., Dupas G., and Jacquesy J. C. (1996) Ester- and ether bond cleavage in immature kerogens. *Organic Geochemistry* **24**(6-7), 681-690.
- Ambles A., Jambu P., Jacquesy J. C., Parlanti E., and Secouet B. (1993) Changes in the Ketone Portion of Lipidic Components During the Decomposition of Plant Debris in a Hydromorphic Forest-Podzol. *Soil Science* **156**(1), 49-56.
- Anderson D. W., Saggar S., Bettany J. R., and Stewart J. W. B. (1981) Particle size fractions and their use in studies of soil organic matter: I The nature and distribution of forms of carbon, nitrogen, and sulfur. *Soil Sci. Soc. Am. j.* **45**, 767-772.
- Anderson L. I., Dunlop J. A., Horrocks C. A., Winkelmann H. M., and Eagar R. M. C. (1997) Exceptionally preserved fossils from Bickershaw, Lancashire UK (Upper Carboniferous, Westphalian A (Langsettian)). *Geological Journal* **32**, 197-210.
- Barcelona M. J. and Holm R. T. (1991) Oxidation-reduction capacities of aquifer solids. *Environmental Science and Technology* **25**, 1565-1572.
- Benner R., Maccubbin A. E., and Hodson R. E. (1984) Anaerobic biodegradation of the lignin and polysaccharide components of lignocellulose and synthetic lignin by sediment microflora. *Applied and environmental microbiology* **47**(5), 998-1004.
- Berner R. A. (1971) *Principles of Chemical Sedimentology*. McGraw-Hill.
- Betts J. N. and Holland H. D. (1991) The oxygen content of ocean bottom waters, the burial efficiency of organic carbon, and the regulation of atmospheric oxygen. *Global and Planetary Change* **97**, 5-18.



- Binger C. A., Martin J. P., Allen-King R. M., and Fowler M. (1999) Variability of chlorinated-solvent sorption associated with oxidative weathering of kerogen. *Journal of Contaminant Hydrology* **40**, 137-138.
- Bradley P. M., Fernandez Jr M., and Chapelle F. H. (1992) Carbon limitation of denitrification rates in an anaerobic groundwater system. *Environmental Science and Technology* **28**(12), 2377-2381.
- Buckau G., Artinger R., Fritz P., Geyer S., Kim J. I., and Wolf M. (2000) Origin and mobility of humic colloids in the Gorleben aquifer system. *Applied Geochemistry* **15**, 171-179.
- Canfield D. E. (1994) Factors influencing organic carbon preservation in marine sediments. *Chemical Geology* **114**, 315-329.
- Canuel E. A. (1996) Reactivity of recently deposited organic matter: Degradation of lipid compounds near the sediment-water interface. *Geochimica et Cosmochimica Acta* **60**(10), 1793-1806.
- Christensen B. T. and Sørensen L. H. (1985) The distribution of native and labelled carbon between soil particle size fractions isolated from long-term incubation experiments. *Journal of Soil Science* **36**, 219-229.
- Christensen T. H., Bjerg P. L., Banwart S. A., Jakobsen R., Heron G., and Albrechtsen H.-J. (2000) Characterization of redox conditions in groundwater contaminant plumes. *Journal of Contaminant Hydrology* **45**, 165-241.
- Collins M. J., Bishop A. N., and Farrimond P. (1995) Sorption by mineral surfaces: Rebirth of the classical condensation pathway for kerogen formation? *Geochimica et Cosmochimica Acta* **59**(11), 2387-2391.
- Colombo J. C., Silverberg N., and Gearing J. N. (1996) Biogeochemistry of organic matter in the Laurentian Trough, II. Bulk composition of the sediments and relative reactivity of major components during early diagenesis. *Marine Chemistry* **51**(4), 295-314.
- Derenne S., Largeau C., Casadevall E., Berkaloff C., and Rousseau B. (1991) Chemical Evidence of Kerogen Formation in Source Rocks and Oil Shales Via Selective Preservation of Thin Resistant Outer Walls of Microalgae - Origin of Ultralaminae. *Geochimica Et Cosmochimica Acta* **55**(4), 1041-1050.
- Dijkstra E. F., Boon J. J., and van Mourik J. M. (1998) Analytical pyrolysis of a soil profile under Scots pine. *European Journal of Soil Science* **49**, 295-304.
- Dilly O. (2001) Microbial respiratory quotient during basal metabolism and after glucose amendment in soils and litter. *Soil Biology and Biochemistry* **33**, 117-127.
- Dittmar T. and Lara R. J. (2001) Molecular evidence for lignin degradation in sulfate-reducing mangrove sediments (Amazônia, Brazil). *Geochimica et Cosmochimica Acta* **65**(9), 1417-1428.
- Dorsselaer A. V., Ensminger A., Spyckerelle C., Dastillung M., Sieskind O., Arpino P., Albrecht P., Ourisson G., Brooks P. W., Gaskell S. J., Kimble B. J., and Philp R. P. (1974) Degraded and extended hopane derivatives (C27 to C35) as ubiquitous geochemical markers. *Tetrahedron Letters* **15**(14), 1349-1352.

- Eglinton G. and Hamilton R. J. (1967) Leaf epicuticular waxes. *Science* **156**(780), 1322-1335.
- Elstino A. R., Schoonen M. A. A., and Strongin D. R. (2001) Aqueous geochemical and surface science investigation of the effect of phosphate on pyrite oxidation. *Environmental Science and Technology* **35**(11), 2252-2257.
- Faure P. and Landais P. (2001) Rapid contamination screening of river sediments by flash pyrolysis-gas chromatography-mass spectrometry (PyGC-MS) and thermodesorption GCMS (TdGC-MS). *Journal of Analytical and Applied Pyrolysis* **57**(2), 187-202.
- Franchini J. C., González-Vila F. J., and Rodriguez J. (2002) Decomposition of plant residues used in no-tillage systems as revealed by flash pyrolysis. *Journal of Analytical and Applied Pyrolysis* **62**, 35-43.
- Gélinas Y., Baldock J. A., and Hedges J. I. (2001) Organic carbon composition of marine sediments: Effect of oxygen exposure time on oil generation potential. *Science* **294**, 145-148.
- Griffioen J. (2001) Potassium adsorption ratios as an indicator for the fate of agricultural potassium in groundwater. *Journal of Hydrology* **254**(1-4), 244-254.
- Grimes S. T., Brock F., Rickard D., Davies K. L., Edwards D., Briggs D. E. G., and Parkes R. J. (2001) Understanding fossilization: Experimental pyritization of plants. *Geology* **29**(2), 123-126.
- Grøn C., Wassenaar L., and Krog M. (1996) Origin and structures of groundwater humic substances from three danish aquifers. *Environment International* **22**(5), 519-534.
- Hansen L. K., Jakobsen R., and Postma D. (2001) Methanogenesis in a shallow sandy aquifer, Rømø, Denmark. *Geochimica et Cosmochimica Acta* **65**(17), 2925-2935.
- Hartnett H. E., Keil R. G., Hedges J. I., and Devol A. H. (1998) Influence of oxygen exposure time on organic carbon preservation in continental margin sediments. *Nature* **391**, 572-574.
- Hedges J. I. and Oades J. M. (1997) Comparative organic geochemistries for soils and marine sediments. *Organic Geochemistry* **27**(7/8), 319-363.
- Henrichs S. M. (1993) Early diagenesis of organic matter: the dynamics (rates) of cycling of organic compounds. In *Organic Geochemistry* (ed. M. H. Engel and S. A. Macko), pp. 101-117. Plenum Press.
- Hulthe G., Hulth S., and Hall P. O. J. (1998) Effect of oxygen on degradation rate of refractory and labile organic matter in continental margin sediments. *Geochimica et Cosmochimica Acta* **62**(8), 1319-1328.
- Jakobsen R. and Postma D. (1994) In situ rates of sulfate reduction in an aquifer (Rømø, Denmark) and implications for the reactivity of organic matter. *Geology* **22**, 1103-1106.
- Jenisch-Anton A., Adam P., Michaelis W., Connan J., Herrmann D., Rohmer M., and Albrecht P. (2000) Molecular evidence for biodegradation of geomacromolecules. *Geochimica et Cosmochimica Acta* **64**(20), 3525-3537.
- Kannenber E. L. and Poralla K. (1999) Hopanoid biosynthesis and function in bacteria. *Naturwissenschaften* **86**, 168-176.

- Karapanagioti H. K. and Sabatini D. A. (2000) Impacts of heterogeneous organic matter on phenanthrene sorption: different aquifer depths. *Environmental Science and Technology* **34**, 2453-2460.
- Keil R. G., Tsamakis E., Fuh C. B., Giddings J. C., and Hedges J. I. (1994) Mineralogical and textural controls on the organic composition of coastal marine sediments: hydrodynamic separation using SPLITF-fractionation. *Geochimica et Cosmochimica Acta* **58**(2), 879-893.
- Keller C. K. and Bacon D. H. (1998) Soil respiration and georespiration distinguished by transport analyses of vadose CO<sub>2</sub>, (CO<sub>2</sub>)-C-13, and (CO<sub>2</sub>)-C-14. *Global Biogeochemical Cycles* **12**(2), 361-372.
- Kleineidam S., Rügner H., Ligouis B., and Grathwohl P. (1999) Organic matter facies and equilibrium sorption of phenanthrene. *Environmental Science and Technology* **33**, 1637-1644.
- Korom S. F. (1992) Natural denitrification in the saturated zone: A review. *Water Resources Research* **28**(6), 1657-1668.
- Kristensen E. and Holmer M. (2001) Decomposition of plant materials in marine sediment exposed to different electron acceptors (O<sub>2</sub>, NO<sub>3</sub><sup>-</sup> and SO<sub>4</sub><sup>2-</sup>), with emphasis on substrate origin, degradation kinetics, and the role of bioturbation. *Geochimica et Cosmochimica Acta* **65**(3), 419-433.
- Kuder T. and Krüge M. A. (1998) Preservation of biomolecules in sub-fossil plants from raised peat bogs — a potential paleoenvironmental proxy. *Organic Geochemistry* **29**(5-7), 1355-1368.
- Leo R. F. and Parker P. L. (1966) Branched-chain fatty acids in sediments. *Science* **152**, 649-650.
- Lichtfouse E., Chenu C., Baudin F., LeBlond C., Da Silva M., Behar F., Derenne S., Largeaou C., Wherung P., and Albrecht P. (1998a) A novel pathway of soil organic matter formation by selective preservation of resistant straight-chain biopolymers: chemical and isotope evidence. *Organic Geochemistry* **28**(6), 411-415.
- Lichtfouse E., Leblond C., Da Silva M., and Behar F. (1998b) Occurrence of biomarkers and straight-chain biopolymers in humin: Implication for the origin of soil organic matter. *Naturwissenschaften* **85**(10), 497-501.
- Mayer L. M. (1994) Surface area control of organic carbon accumulation in continental shelf sediments. *Geochimica et Cosmochimica Acta* **58**(4), 1271-1284.
- Miki K., Renganathan V., Mayfield M. B., and Gold M. H. (1987) Aromatic ring cleavage of a [beta]-biphenyl ether dimer catalyzed by lignin peroxidase of *Phanerochaete chrysosporium*. *FEBS Letters* **210**(2), 199-203.
- Moncaster S. J., Botrell S. H., Tellam J. H., Lloyd J. W., and Konhauser K. O. (2000) Migration and attenuation of agrochemical pollutants: insights from isotopic analysis of groundwater sulphate. *Journal of Contaminant Hydrology* **43**, 147-163.
- Murphy E. M. and Zachara J. M. (1995) The role of sorbed humic substances on the distribution of organic and inorganic contaminants in groundwater. *Geoderma* **67**(1-2), 103-124.

- Odiar E. and Monties B. (1983) Absence of microbial mineralization of lignin in anaerobic enrichment cultures. *Applied and Environmental Microbiology* **46**(3), 661-665.
- Otto A. and Simoneit B. R. T. (2001) Chemosystematics and diagenesis of terpenoids in fossil conifer species and sediment from the Eocene Zeitz formation, Saxony, Germany. *Geochimica et Cosmochimica Acta* **65**(20), 3505-3527.
- Pauwels H., Foucher J.-C., and Kloppmann W. (2000) Denitrification and mixing in a schist aquifer: influence on water chemistry and isotopes. *Chemical Geology* **168**, 307-324.
- Pauwels H., Kloppmann W., Foucher J.-C., Martelat A., and Fritsche V. (1998) Field tracer test for denitrification in a pyrite-bearing schist aquifer. *Applied Geochemistry* **13**(6), 767-778.
- Pignatello J. J. (1998) Soil organic matter as a nanoporous sorbent of organic pollutants. *Advances in Colloid and Interface Science* **76-77**, 445-467.
- Postma D., Boesen C., Kristiansen H., and Larsen F. (1991) Nitrate reduction in an unconfined sandy aquifer: Water chemistry, reduction processes, and geochemical modeling. *Water Resources Research* **27**(8), 2027-2045.
- Qu D. G., Shi J. Y., and Xiang M. J. (1996) Novel extended side-chain-unsaturated hopenes released from the kerogen macromolecules under artificial conditions. *Organic Geochemistry* **24**(8-9), 815-823.
- Reiss C., Blanc P., Trendel J. M., and Albrecht P. (1997) Novel Hopanoid Derivatives Released by Oxidation of Messel Shale Kerogen. *Tetrahedron* **53**(16), 5767-5774.
- Robertson W. D., Russell B. M., and Cherry J. A. (1996) Attenuation of nitrate in aquitard sediments of southern Ontario. *Journal of Hydrology* **180**, 267-281.
- Routh J., Grossman E. L., Murphy E. M., and Benner R. (2001) Characterization and origin of dissolved organic carbon in Yegua ground water in Brazos County, Texas. *Ground Water* **39**(5), 760-767.
- Routh J., McDonald T. J., and Grossman E. L. (1999) Sedimentary organic matter sources and depositional environment in the Yegua formation (Brazos County, Texas). *Organic Geochemistry* **30**(11), 1437-1453.
- Rullkötter J. (1983) Gas chromatography/mass spectrometry of degraded triterpanes in fossil organic matter - a record of microbial action. *International Journal of Mass Spectrometry and Ion Physics* **48**, 39-42.
- Saiz-Jimenez C. and De Leeuw J. W. (1986) Chemical characterization of soil organic matter fractions by analytical pyrolysis-gas chromatography-mass spectrometry. *Journal of Analytical and Applied Pyrolysis* **9**(2), 99-119.
- Sanchez-Monedero M. A., Roig A., Cegarra J., Bernal M. P., and Paredes C. (2002) Effects of HCl-HF purification treatment on chemical composition and structure of humic acids. *European Journal of Soil Science* **53**(3), 375-381.
- Schmidt M. W. I., Knicker H., Hatcher P. G., and KogelKnabner I. (1997) Improvement of C-13 and N-15 CPMAS NMR spectra of bulk soils, particle size fractions and organic material by treatment with 10% hydrofluoric acid. *European Journal of Soil Science* **48**(2), 319-328.

- Schmitter J. M., Arpino P., and Guiochon G. (1978) Investigation of high-molecular-weight carboxylic acids in petroleum by different combinations of chromatography (gas and liquid) and mass spectrometry (electron impact and chemical ionization). *Journal of Chromatography A* **167**(1), 149-158.
- Schreiber M. E. and Bahr J. M. (1999) Spatial Electron Acceptor Variability: Implications for Assessing Bioremediation Potential. *Bioremediation Journal* **3**(4), 363-378.
- Smith R. L. and Duff J. H. (1988) Denitrification in a sand and gravel aquifer. *Applied and Environmental Microbiology* **54**(5), 1071-1078.
- Sollins P., Homann P., and Caldwell B. A. (1996) Stabilization and destabilization of soil organic matter: mechanisms and controls. *Geoderma* **74**(1-2), 65-105.
- Starr J. L., Sadeghi A. M., and Parkin T. B. (1996) A tracer test to determine the fate of nitrate in shallow groundwater. *Journal of environmental quality* **25**, 917-923.
- Sukhija B. S., Varma V. N., Nagabhushanam P., and Reddy D. V. (1996) Differentiation of palaeomarine and modern seawater intruded salinities in coastal groundwaters (of Karaikal and Tanjavur, India) based on inorganic chemistry, organic biomarker fingerprints and radiocarbon dating. *Journal of Hydrology* **174**(1-2), 173-201.
- Tsai C.-S., Killham K., and Cresser M. S. (1997) Dynamic response of microbial biomass, respiration rate and ATP to glucose additions. *Soil Biology and Biochemistry* **29**(8), 1249-1256.
- Tyson R. V. (1995) *Sedimentary Organic Matter*. Chapman & Hall.
- van Beek C. G. E. M. and Vogelaar A. J. (1998) Pompstation Hengelo 't Klooster—*Geohydrologische, geochemische en hydrochemische beschrijving*, pp. 84. KIWA N.V.
- van Bergen P. F., Nott C. J., Bull I. D., Poulton P. R., and Evershed R. P. (1998) Organic geochemical studies of soils from the Rothamsted Classical Experiments--IV. Preliminary results from a study of the effect of soil pH on organic matter decay. *Organic Geochemistry* **29**(5-7), 1779-1795.
- van den Berg M. W., van Houten C. J., and den Otter C. (2000) Geologische Kaart van Nederland
- Blad Enschede West (34W) en Enschede Oost/Glanerbrug (34O/35). Nederlands Instituut voor Toegepaste Geowetenschappen TNO.
- van Weert F. H. A., van Gijssel K., Leijnse A., and Boulton G. S. (1997) The effects of Pleistocene glaciations on the geohydrological system of Northwest Europe. *Journal of Hydrology* **195**(1-4), 137-159.
- Wassenaar L., Aravena R., Fritz P., and Barker J. (1990) Isotopic Composition (C-13, C-14, H-2) and Geochemistry of Aquatic Humic Substances from Groundwater. *Organic Geochemistry* **15**(4), 383-396.
- Weber Jr. W. J., Huang W., and Yu H. (1998) Hysteresis in the sorption and desorption of hydrophobic organic contaminants by soils and sediments; 2. Effects of soil organic matter heterogeneity. *Journal of Contaminant Hydrology* **31**(1-2), 149-165.

Witter E. and Dahlin S. (1995) Microbial utilization of [U-14C]-labelled straw and [U-13C]-labelled glucose in soils of contrasting pH and metal status. *Soil Biology and Biochemistry* **27**(12), 1507-1516.

# **Hydrogeological Controls on the Reactivity of Organic Matter and other Reductants in Aquifer Sediments**

## **6.1 INTRODUCTION**

A number of common groundwater contaminants, such as nitrate, chromate or chlorinated hydrocarbons, are susceptible to reductive transformations that may affect their solubility or toxicity (Blowes, 2002; Bradley *et al.*, 1998; Postma *et al.*, 1991; Smith and Duff, 1988). Sedimentary reductants represent the predominant pool of reduction capacity as compared to dissolved reduced species for most aquifers (Amirbahman *et al.*, 1998; Barcelona and Holm, 1991; Heron and Christensen, 1995; Pedersen *et al.*, 1991), thus their reactivity largely controls the fate of these contaminants in groundwater systems.

Sedimentary organic matter (SOM) is an ubiquitous reductant in aquifers and numerous groundwater field studies have identified the coupling of SOM oxidation with the reduction of oxygen, nitrate, iron(III) and sulfate (Jakobsen and Postma, 1994; Lovley *et al.*, 1990; Morris *et al.*, 1988; Puckett and Cowdery, 2002; Smith and Duff, 1988). Furthermore, it has been demonstrated that the degradability of SOM controls these reduction rates (*Chapter 5*, Bradley *et al.*, 1995; Desimone and Howes, 1996; Hill *et al.*, 2000; Jakobsen and Postma, 1994; Pfenning and McMahon, 1996; Starr *et al.*, 1996). Sedimentary organic matter is made up by a wide variety of organic compounds and its reactivity towards oxygen can be related to its molecular composition (*Chapter 5*).

Clearly, SOM plays a central role in the redox chemistry of groundwater systems. While SOM may act as a reactive reductant itself, the anaerobic degradation of SOM drives the diagenetic formation of reactive iron(II)-, manganese(II)- or sulfide-bearing minerals in aquifers (Jakobsen and Postma, 1999; Magaritz and Luzier, 1985). These secondary reductants, such as pyrite ( $\text{FeS}_2$ ) or siderite ( $\text{FeCO}_3$ ), may also react with introduced oxidants. Pyrite oxidation coupled to oxygen and nitrate reduction is frequently reported in field studies (Kelly, 1997; Molenat *et al.*, 2002; Pauwels *et al.*, 2001; Postma *et al.*, 1991), while experimental studies on isolated reductants have shown that siderite and other Fe(II)-bearing minerals, such as detrital silicates, are also potentially important (Hofstetter *et al.*, 2003; Lee and Batchelor, 2003; Postma, 1990; Weber *et al.*, 2001). For example, (Böhlke and Denver, 1995) concluded that the oxidation of SOM, glauconite and pyrite were responsible for denitrification observed in a coastal plain aquifer.

Depending on the provenance, depositional environment and diagenetic history of aquifer sediments, several reductants may react concurrently upon oxidation (*Chapter 3*). In *Chapter 5* the molecular composition of SOM in aquifer sediments from two contrasting geological formations was characterized and it was concluded that the total amount of oxygen exposure controls the degree of SOM preservation. In the current study, aquifer sediments from a wide variety of geological formations are investigated. An integrated approach is used by characterizing the molecular composition of SOM and assessing the presence of other potentially reactive reductants in 0.01–20 My old sediments from various depositional settings. This approach helps to relate aquifer reduction capacity to the distribution and reactivity of sedimentary reductants. Knowledge of this relationship is required to assess the dominant reduction processes occurring in groundwater systems.



## **6.2 SITE DESCRIPTION**

### **6.2.1 Geohydrology**

The study area is located in the eastern part of The Netherlands near drinking water production site 't Klooster (Fig. 6.1). Thick unconsolidated sedimentary deposits of Pleistocene and Miocene origin form a complex of sandy layers, locally separated by clay layers to form interconnected aquifers. The hydrogeological base is formed by Miocene marine clays of the Breda Formation at 100–120 m below surface (Figs. 6.1 and 6.2). Within the aquifer system studied, the glauconitic Breda and Oosterhout Formations form the oldest deposits. These are of marine and near-shore origin. The continuous uplift of the hinterland in the East caused the coastal zone to gradually shift to the west. Towards the end of the Tertiary, the area was situated in the coastal zone with an influx of continental sands (Scheemda Formation). Fluvial sediments were deposited from the early Pleistocene onward. First, these fluvial deposits had a Baltic origin, but during the Middle Pleistocene Rhine–Meuse sediments (*e.g.*, the Urk Formation) became dominant. Glacial and fluvio-glacial sediments (Drente Formation) were deposited during the Saalian, when push moraines were formed and severe fluvio-glacial erosion occurred. Locally, the infill of deeply incised valleys (core 34-C104, Fig. 6.1) largely consists of eroded older strata. Fluvial sedimentation (Kreftenheye Formation) returned at the start of the Eemian interglacial. Additionally, local fluvio-aeolian sediments (Twente Formation) were deposited during the Weichselian periglacial period. Holocene aeolian deposits of the Kootwijk Formation are locally present (van den Berg *et al.*, 2000).

Groundwater levels are 2–6 m below surface (bs) and occur in the Twente and Kreftenheye deposits. Large-scale abstraction of phreatic groundwater ( $5 \text{ Mm}^3 \cdot \text{yr}^{-1}$ ) for drinking water production and intensified drainage have resulted in the disappearance of local seepage areas. At the site studied (Fig. 6.1), groundwater flow direction is NW (Uffink and Römken, 2001).

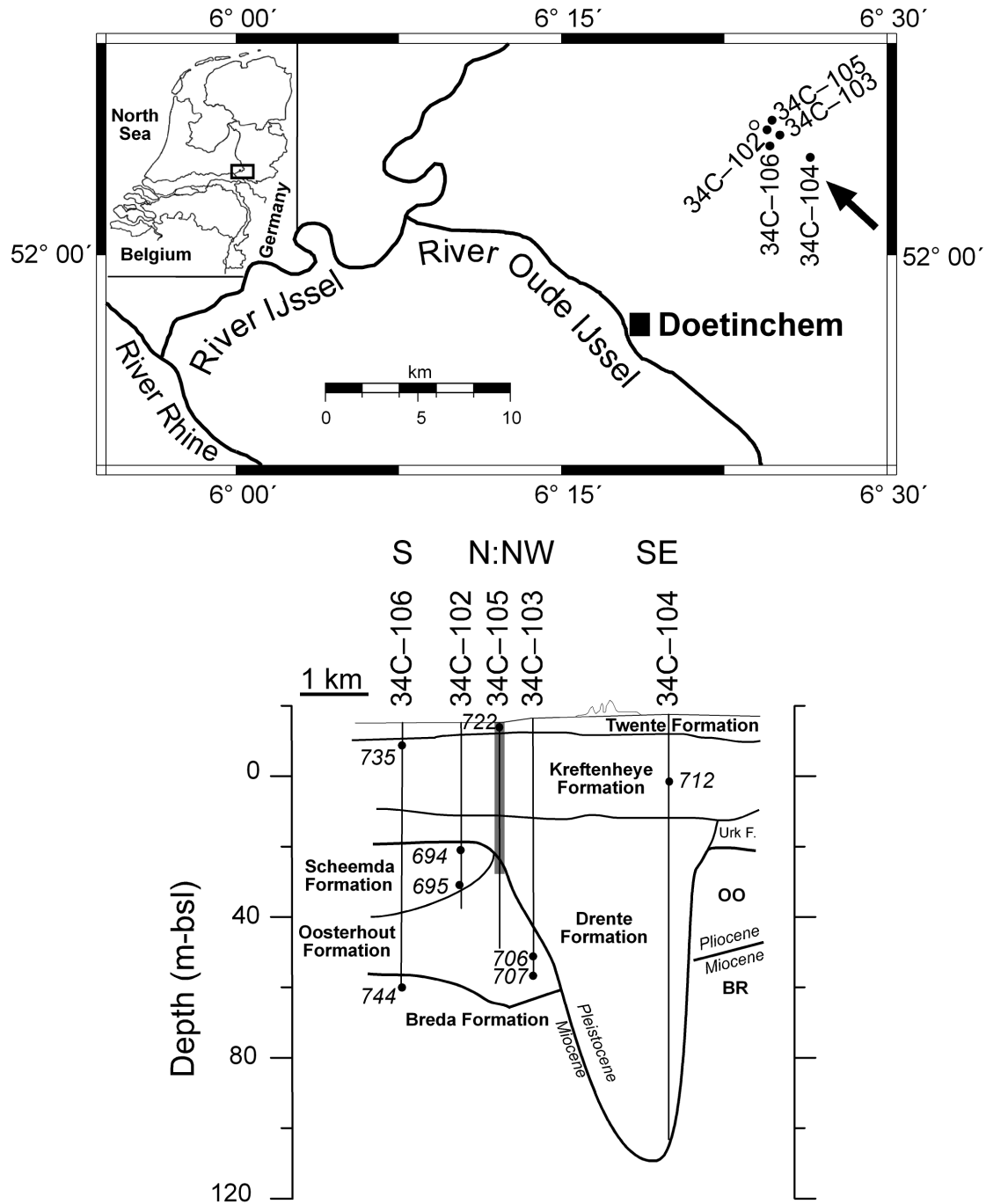


**Figure 6.1** Location of the study area near Doetinchem, The Netherlands, showing 1) the position of the cores used (filled circles), 2) location of the drinking water production site (open circle) 3) general groundwater flow direction (arrow). Profile shows the main geological formations within the cores studied. Depth is indicated in meters below sea level (m-bsl). Shaded area represents the depth range of samples that were selected for incubation experiments (Fig. 6.7). Numbers refer to the samples selected for Py-GC/MS analyses (Table 6.1).

AGE (Myr)	CHRONO STRATIGRAPH Y	LITHO STRATIGRAPHY
0.01	<b>HOLOCENE</b>	Kootwijk Formation
	<b>Quaternary</b>	
	<b>PLEISTOCENE</b>	
	Weichselian	722 Twente Formation
0.12	Eemian	712 735 Kreftenheye Formation
	Saalian	Drente Formation
0.60	Holsteinian	Urk Formation
	Elsterian	
	Cromerian	
	Bavelian	
1.15	Menapian	
	Waalian	
	Eburonian	
	Tiglian	
2.5	Pretiglian	
	<b>Late Tertiary</b>	
	<b>MIOCENE</b>	694, 695 Scheemda Formation
	<b>LIOCENE</b>	704, 706, 707 Oosterhout Formation
		744 Breda Formation
23		hiatus



**Figure 6.2** Late Tertiary and Quaternary chronostratigraphy and lithostratigraphic units for the area studied (simplified after van den Berg *et al.*, (2000)). Age indications after (Funnell, 1996; van den Berg *et al.*, 2000). Numbers refer to samples selected for Py-GC/MS analyses (Table 6.1).

## 6.2.2 Hydrochemistry

The groundwater chemistry of the area studied is well documented (Griffioen, 2001; van Beek and Vogelaar, 1998). Dissolved oxygen is depleted within the first two meters below surface, leaving the largest part of the sedimentary sequence presently under anoxic conditions. Locally, shallow groundwater is influenced by agricultural activities as illustrated by nitrate concentrations up to 200 mg/l at mini-screen well WP4 (core location: 34C-105, Fig. 6.1a). Denitrification takes place within the first 15 m below surface, while sulfate disappears in the depth interval between 30 and 55 m-bs. Methane is observed (Griffioen, 2001; van Beek and Vogelaar, 1998).

## 6.3 MATERIALS AND METHODS

### 6.3.1 Sediment Sampling

Sediment samples were selected from various cores around the drinking water production site 't Klooster (Fig. 6.1). Sediment cores were obtained in 40 cm long stainless steel tubing with a 65 mm inner diameter, using a hollow stem auger. Sediment samples collected were stored in glass bottles at 8°C until they were sieved into a 0–2000 µm fraction. The >2000 µm fraction (<5 wt.%) was discarded. Fractions were stove-dried (40°C) and sub-samples were taken for isotope analysis, sedimentary organic matter isolation and batch incubation experiments.

### 6.3.2 Sediment Analysis

#### 6.3.2.1 *SOM: Isolation and Molecular Characterization*

Samples were selected from the major geological formations within the aquifer system studied (Figs. 6.1 and 6.2). All selected samples were sandy, except one sample taken from a clay layer in the Kreftenheye Formation. To minimize the influence of reworked SOM, no samples were selected from the sediment-filled erosion valleys.

To concentrate the organic matter present, samples were treated with excess 10% HCl to remove carbonates and settled overnight, after which the samples were centrifuged at 2200 rpm for 7 minutes and the supernatant was decanted. Samples were then treated with excess 38% HF to dissolve the silicate mineral matrix, shaken at 250 rpm for two hours, after which the samples were centrifuged at 2200 rpm for 7 minutes and the supernatant was decanted. Then, the samples were washed three times with distilled water by centrifugation and decantation as described above. Subsequently, the HCl and HF procedure as described above was repeated. Finally, samples were treated with 30% HCl to remove any potential fluoride gels and were washed as described above until the samples were diluted to pH 7. Isolates were freeze-dried and weighed. The HCl/HF treatment removed 81–99 % of the mineral matrix. The dried isolates were stored in glass at 8 °C in the dark until analysis by pyrolysis-gas chromatography/mass spectrometry (Py-GC/MS).

Curie-point Py-GC/MS was used to characterize SOM at a molecular level. The organic matter isolates were pressed onto a ferromagnetic wire with a Curie temperature of 610°C. Py-GC/MS analyses were carried out using a Hewlett-Packard 5890 gas chromatograph (GC) equipped with a FOM-3LX unit for pyrolysis. The GC was interfaced to a VG Autospec Ultima mass spectrometer operated at 70 eV with a mass range of  $m/z$  50–800 and a cycle time of 1.7 s (resolution 1000). The GC, equipped with a cryogenic unit, was programmed from 0°C (5 min) to 300°C (10 min) at a rate of 3°C/min. Separation was achieved using a fused silica capillary column (25 m × 0.32 mm) coated with CP Sil-5CB (film thickness 0.4 µm). Helium was used as a carrier gas.

#### *6.3.2.2 Carbon and Oxygen Isotope Analysis*

Inorganic carbon was removed before analysis by shaking the sample for 24 hours in 1 M HCl. Stable carbon isotope analyses of bulk SOM ( $\delta^{13}\text{C}_{\text{org}}$ ) were obtained by on-line combustion of decalcified samples using a Fisons Instruments NA 1500 Elemental Analyser (EA) coupled via a ConFlo II interface to a Finningan MAT Delta Plus isotope ratio mass spectrometer (IRMS). Laboratory standards NBS-21 and NBS-22 were processed to check for systematic errors of  $\delta^{13}\text{C}_{\text{org}}$  analysis. Overall

analytical errors were better than  $\pm 0.1\text{‰}$  ( $2\sigma$ ). Anomalously heavy  $\delta^{13}\text{C}_{\text{org}}$ -values ( $> -10\text{‰}$ ) were recorded for some carbonate-rich samples. To remove recalcitrant carbonates, samples were re-exposed to acid for two weeks with dilute HCl (0.4 M) together with control samples. This additional acid treatment did not have a significant effect on the  $\delta^{13}\text{C}_{\text{org}}$  as indicated by the unaltered isotopic value of the control samples.

Oxygen and carbon isotopic ratios of carbonates ( $\delta^{18}\text{O}_{\text{carb}}$ ,  $\delta^{13}\text{C}_{\text{carb}}$ ) were measured on freeze-dried sediment samples. Samples were transferred to an automated carbonate preparation unit (IsoCarb). The samples were transferred into glass reaction tubes that were evacuated for 14 h. Subsequently, 100% phosphoric acid was added at  $25^{\circ}\text{C}$  under high vacuum for 6 hours. The  $\text{CO}_2$  released was cryogenically separated from other gases and isotope values were measured on an isotope ratio mass spectrometer (VG SIRA 24). Values are reported relative to the PeeDee Belemnite in standard  $\delta$  notation. Precision for  $\delta^{18}\text{O}$  and for  $\delta^{13}\text{C}$  measurements was better than  $0.5\text{‰}$ .

### 6.3.3 Incubation Experiments

Sediment samples with a dry weight of 34–41 gram were incubated with 50 ml of vitamin and trace elements solution (*Chapter 3*), under dark conditions for 7.5 days. The reaction chambers (100-ml bottle, Duran) were connected to the closed circuit of a respirometer (Micro-Oxymax, Columbus Instruments). Water-saturated gases were used to prevent evaporation in the reaction chambers. Oxygen ( $p_{\text{O}_2} = 10^{-0.68 \pm 0.002}$  atm) and carbon dioxide ( $p_{\text{CO}_2} = 10^{-3.51 \pm 0.11}$  atm) levels in the headspaces were kept at atmospheric conditions at  $25^{\circ}\text{C}$  ( $\pm 1^{\circ}\text{C}$ ). The  $\text{O}_2$  consumption and  $\text{CO}_2$  production were measured every 3 hours using an infrared sensor and an oxygen battery (fuel cell), respectively. The reaction chambers were shaken (100 rpm) to ensure a well-mixed chemical system and prevent gas transfer limitations.

Directly after incubation, pH was measured with a standard pH meter (Orion) and alkalinity was determined by acid titration. Dissolved cations and sulfate were analyzed using ICP-AES (Perkin-Elmer ICP-optima 3000). Speciation calculations

were performed using PHREEQC (Parkhurst and Appelo, 1999). The saturation index (SI) is defined as the logarithmic value of the ratio between the ion activity product

**Figure 6.1 Bulk characteristics of the sediment samples used for Py-GC/MS analysis**

Core	Sample Code	Formation	Depth (m-bs)	Depth (m-NAP)	TOC (wt.%)	Carbonate (wt.%)	Fe (wt.%)	S (wt.%)	Mn (wt.%)	$\delta^{18}\text{O}_{\text{carb}}$ (‰ PDB)	$\delta^{13}\text{C}_{\text{carb}}$ (‰ PDB)	$\delta^{13}\text{C}_{\text{org}}$ (‰ PDB)
4C-102	694	SC	39.2	-23.1	0.14	0.62	4.70	0.15	0.02	NA	NA	-24.9
4C-102	695	SC	49.2	-33.1	0.36	6.25	5.18	0.18	0.03	0.91	0.94	-25.8
4C-103	706	OO	68.2	-52.1	0.40	1.79	3.27	0.16	0.01	1.58	1.08	-25.0
4C-103	707	OO	74.2	-58.1	0.31	0.80	4.15	0.1	0.01	1.97	-0.15	-24.7
4C-104	712	KR	20.2	-2.7	0.76	6.74	2.25	0.1	0.07	-4.76	-0.74	-26.7
4C-105	722	TW	3.2	12.0	0.19	5.42	1.32	ND	0.03	-3.10	-7.96	-24.4
4C-106	735	KR	10.2	5.9	0.2	10.27	1.31	ND	0.04	-2.41	-7.30	-24.3
4C-106	744	BR	76.2	-60.1	0.24	0.73	3.85	0.16	0.01	2.42	1.98	-26.7

NA: not analysed

ND: not detected

TOC (Total Organic Carbon), Carbonate, Fe, Mn and S data from (van Beek and Vogelaar, 1998)

and the solubility constant for a given mineral.

## 6.4 RESULTS

First, the molecular composition and carbon isotope composition of SOM in aquifer sediments from various geological formations is presented. Then, the variation in and relationships between carbon and oxygen isotopic values of the carbonate phase are shown. Finally, the oxygen consumption and the relationship with carbon dioxide production during incubation of aquifer sediments from core 34C-105 are investigated.

### 6.4.1 Sediment Chemistry

#### 6.4.1.1 Molecular Composition of SOM

Curie point pyrolysis-GC/MS was used as a qualitative method to characterize the molecular composition of SOM in selected aquifer sediments (Table 6.1).

Evaporate/pyrolysate mixtures all revealed the presence of relatively abundant aromatic compounds, homologous series of *n*-alk-1-enes and *n*-alkanes and C<sub>16</sub> and C<sub>18</sub> fatty acids (24–25, Fig. 6.3). These compounds dominate the chromatograms of

the pyrolysates of the sandy Twente (722, Fig. 6.3) and Kreftenheye (735) samples. In contrast, phenolic and guaiacyl-lignin derived compounds with minor contributions from fatty acids (**24–25**) and branched hydrocarbons (*e.g.* **23**) dominate the evaporate/pyrolysate mixtures of the marine and coastal sands and the fluvial Kreftenheye clay sample (712).



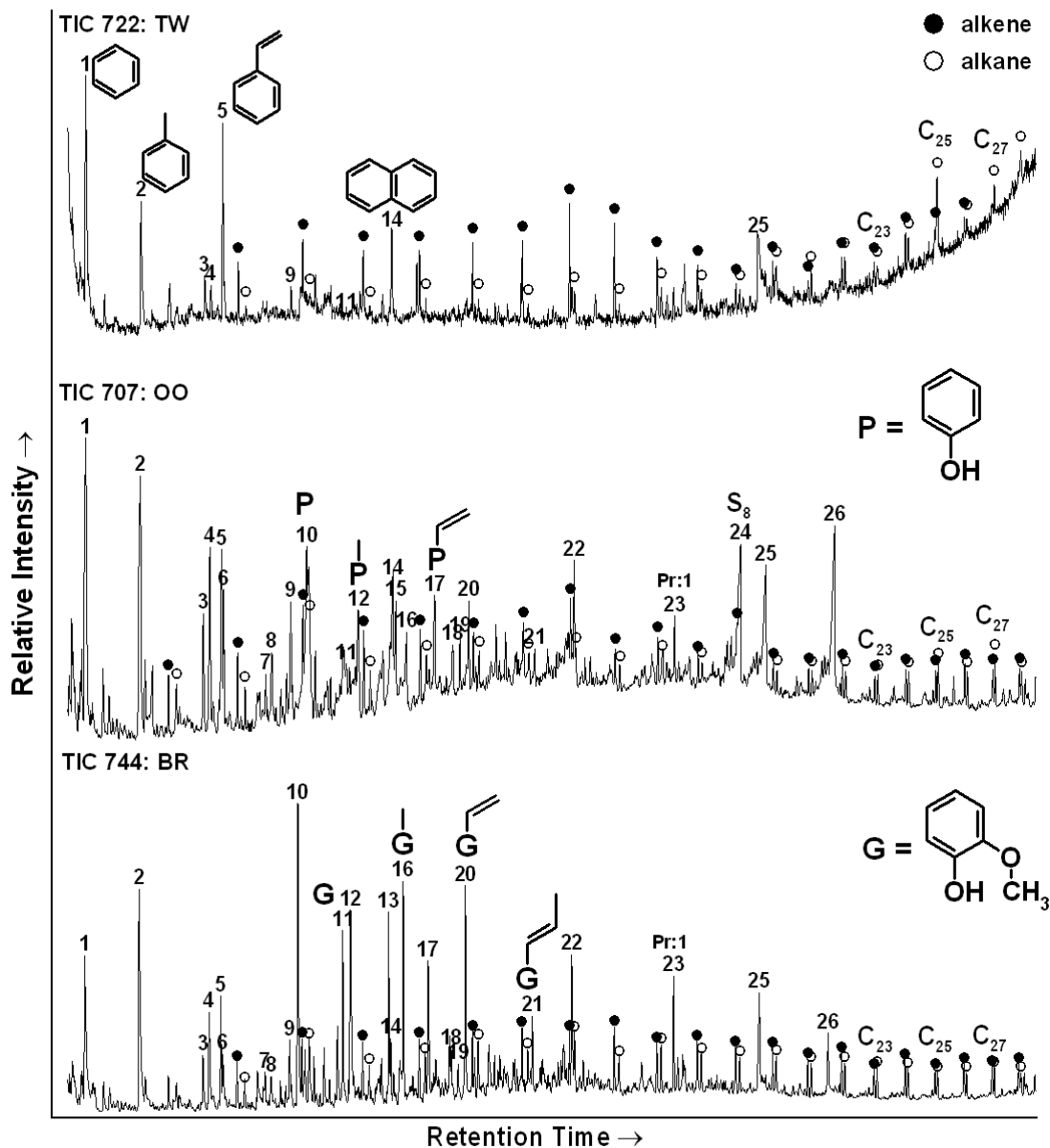


**Figure 6.3** Total ion current traces of the evaporate/pyrolysate mixtures of SOM samples from the Twente (722), Oosterhout (707) and Breda (744) Formation. Key: 1 Benzene, 2 Toluene, 3 C<sub>2</sub>-Alkylbenzene (AB), 4 C<sub>2</sub>-AB, 5 Styrene, 6 C<sub>2</sub>-AB, 7–9 C<sub>3</sub>-AB, 10 Phenol, 11 Guaiacol, 12 Methylphenol, 13 C<sub>4</sub>-AB, 14 Naphthalene, 15 C<sub>4</sub>-AB, 16 Methylguaiacol, 17 Vinylphenol, 18–19 Methylnaphthalene, 20 Vinylguaiacol, 21 *trans*-Isoeugenol, 22 3,5-di(*tert*-butyl)phenol (contaminant), 23 Prist-1-ene, 24 Elemental sulfur (S<sub>8</sub>), 25 C<sub>16</sub>-Fatty Acid, 26 C<sub>18</sub>-Fatty Acid, ○ = alkane, ● = alkene.

Alkane/alkene doublets form the dominant aliphatic contribution in all samples (Fig. 6.3). Alkenes dominate the alkane counterparts in the short-chain range (C<20). However, long-chain alkanes become more pronounced with increasing carbon number. Especially between C<sub>25</sub> and C<sub>29</sub>, the alkanes dominate their alkene counterparts. For these alkanes, a distinct odd-over-even predominance is observed, as illustrated by the mass chromatograms *m/z* 55+57 (Fig. 6.4).

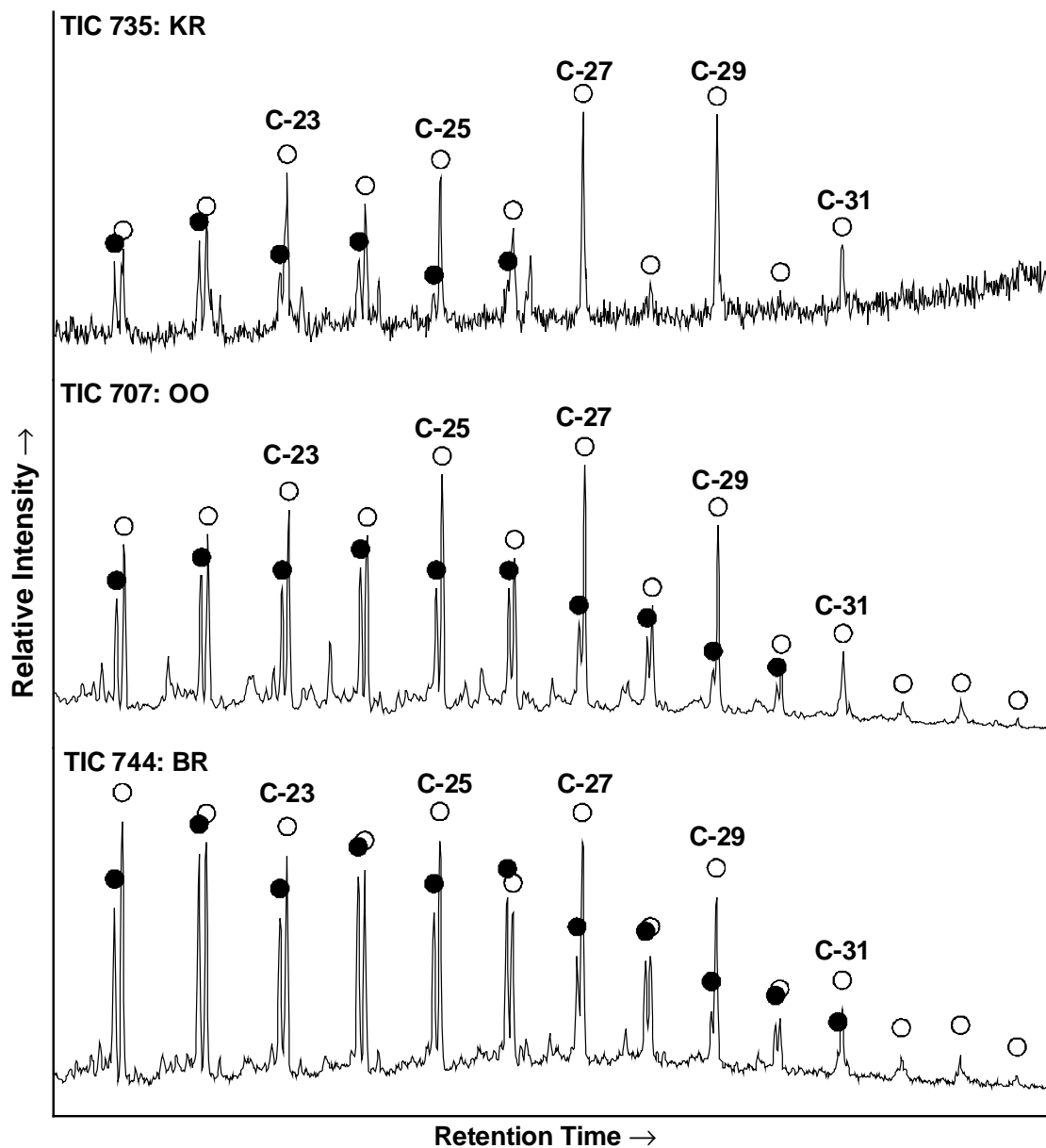


**Figure 6.4** Representative partial summed mass chromatograms for alkenes and alkanes ( $m/z$  55+57) of the evaporate/pyrolysate mixtures of SOM samples from the Twente (722), Oosterhout (707) and Breda (744) Formation. ○ = alkane, ● = alkene. Numbers above peaks indicate number of carbon atoms.

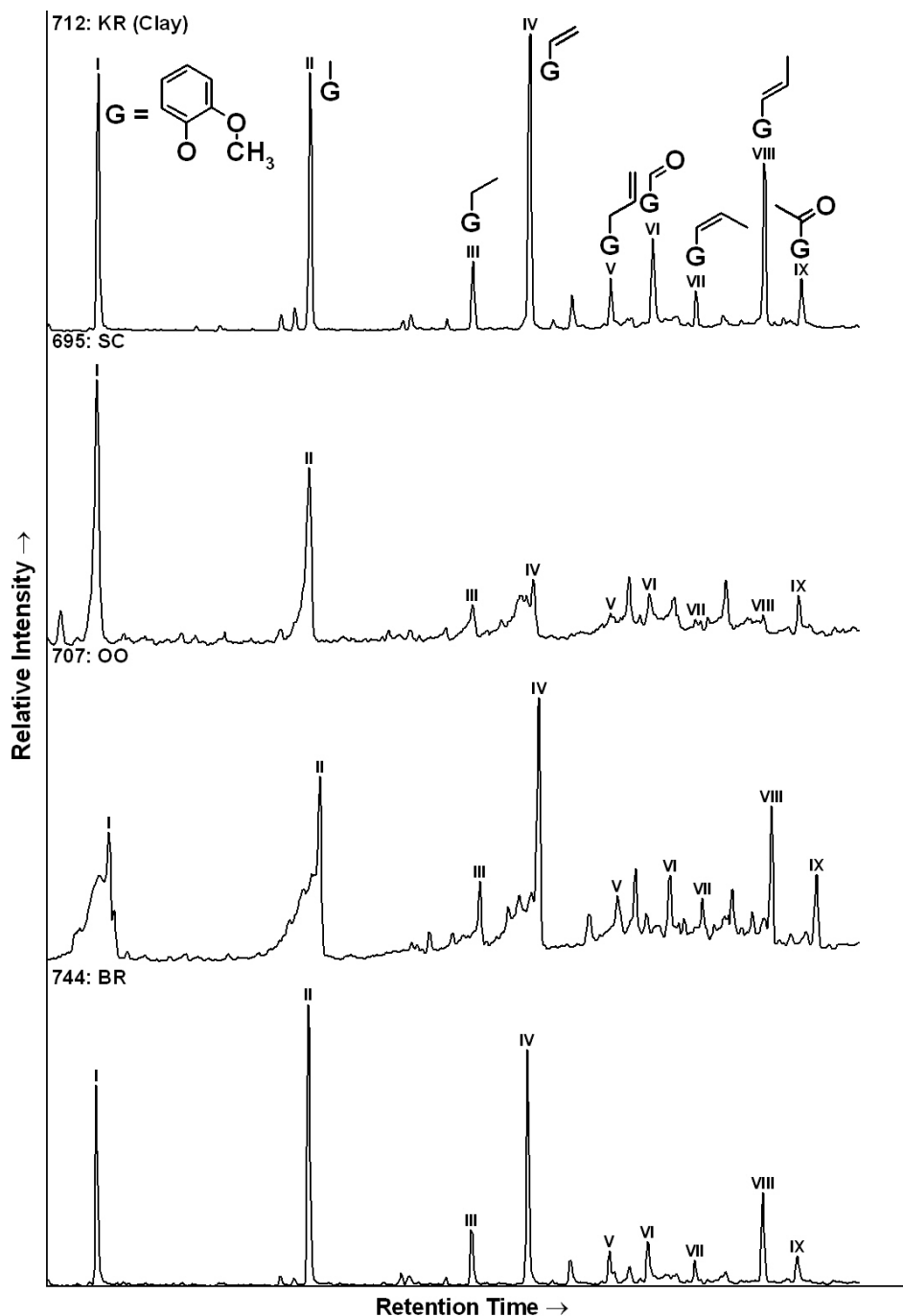


**Figure 6.5** Representative partial summed mass chromatograms for guaiacyl derivatives ( $m/z$  124+138+150+152+164+166) of the evaporate/pyrolysate mixtures of SOM from the Kreftenheye Clay (712), Schemda (695) Oosterhout (707) and Breda (744) samples. Roman numbers in bold refer to the following compounds: I 2-methoxyphenol (Guaiacol), II 4-methyl-2-methoxyphenol (Methylguaiacol), III 4-ethyl-2-methoxyphenol (Ethylguaiacol), IV 4-vinyl-2-methoxyphenol (Vinylguaiacol), V 4-(2-propenyl)-2-methoxyphenol (Eugenol), VI 4-Formyl-2-methoxyphenol (Vanillin), VII *cis*-4-(1-propenyl)-2-methoxyphenol (*cis*-Isoeugenol), VIII *trans*-4-(1-propenyl)-2-methoxyphenol (*trans*-Isoeugenol), IX 4-acetyl-2-methoxyphenol (Acetylguaiacol).

All samples reveal the presence of guaiacyl-derived lignin units with various degrees of side-chain degradation as illustrated by the mass chromatograms  $m/z$  124+138+150+152+164+166. In the pyrolysate/evaporate mixtures of the Kreftenheye sand (735) and Twente (722, Fig. 6.3) samples only a minor signal from guaiacol (**I**) was observed. All other samples showed guaiacyl components with various side chain lengths (Fig. 6.5) ranging from methylguaiacol (**II**) to the eugenol isomers (**V**, **VII**, **VIII**). Guaiacol was the dominant lignin derivative in the Scheemda samples, while 4-vinyl-2-methoxyphenol (**IV**) and the eugenol isomers were of equal importance in the Oosterhout and Breda samples. The guaiacyl side chains were remarkably well preserved in the Kreftenheye clay (712, Fig. 6.5) sample when compared with the Kreftenheye sand (735) sample. The oxidized lignin derivatives 4-formyl-2-methoxyphenol (**VI**) and 4-acetyl-2-methoxyphenol (**IX**) were observed in all samples except 722 and 735.

Parallel to the guaiacyl-derived lignin components, pentacyclic triterpenoid hydrocarbons of hopanoid origin showed sidechain degradation features, as illustrated by the mass chromatograms  $m/z$  191 (not shown). Hopanoid distributions range from  $C_{27}$  to  $C_{33}$ . No hopanoid-derived compounds were observed in the Twente (722) and Kreftenheye (735) samples.

#### 6.4.1.2 Organic Carbon and Carbonate Isotope Chemistry

The  $\delta^{13}C_{org}$ -values of 28 SOM samples ranged between  $-23$  and  $-27\text{‰}$  (average  $-25.1\text{‰} \pm 1.1$ ). No consistent variation over depth or with various geological formations was observed (Table 6.1).

All seven marine sediment samples (Oosterhout and Breda Formation) show  $\delta^{18}O_{carb}$  and  $\delta^{13}C_{carb}$  values close to the reference value of zero (Table 6.1, Fig. 6.6). Similarly, all six samples from the fluvio-glacial Drente Formation show only small ( $\pm 1.5\text{‰}$ ) excursions from the reference value. Three out of thirteen samples from the Kreftenheye Formation show strongly depleted  $\delta^{18}O_{carb}$  values ( $-6\text{‰}$ ) with  $\delta^{13}C_{carb}$  values depleted less than  $1\text{‰}$ . In addition, five samples from this formation and all three samples from the Twente Formation show strongly depleted  $\delta^{18}O_{carb}$  and  $\delta^{13}C_{carb}$

values down to  $-3\text{‰}$  and  $-8\text{‰}$ , respectively (Fig. 6.6). These strongly correlated dual depletions are locally present in sediment samples from the first 15 meters below surface and are associated with anomalously high carbonate contents of 5–20 wt.%.

### 6.4.2 Sediment Incubations

Aquifer sediments were selected from core 34C-105 (Fig. 6.1) for the incubation experiments (Table 6.2). Sediment samples were incubated for 7.5 days under aerobic conditions to determine the reduction activities of the aquifer sediments and to assess the dominantly reactive reductants (Fig. 6.7).

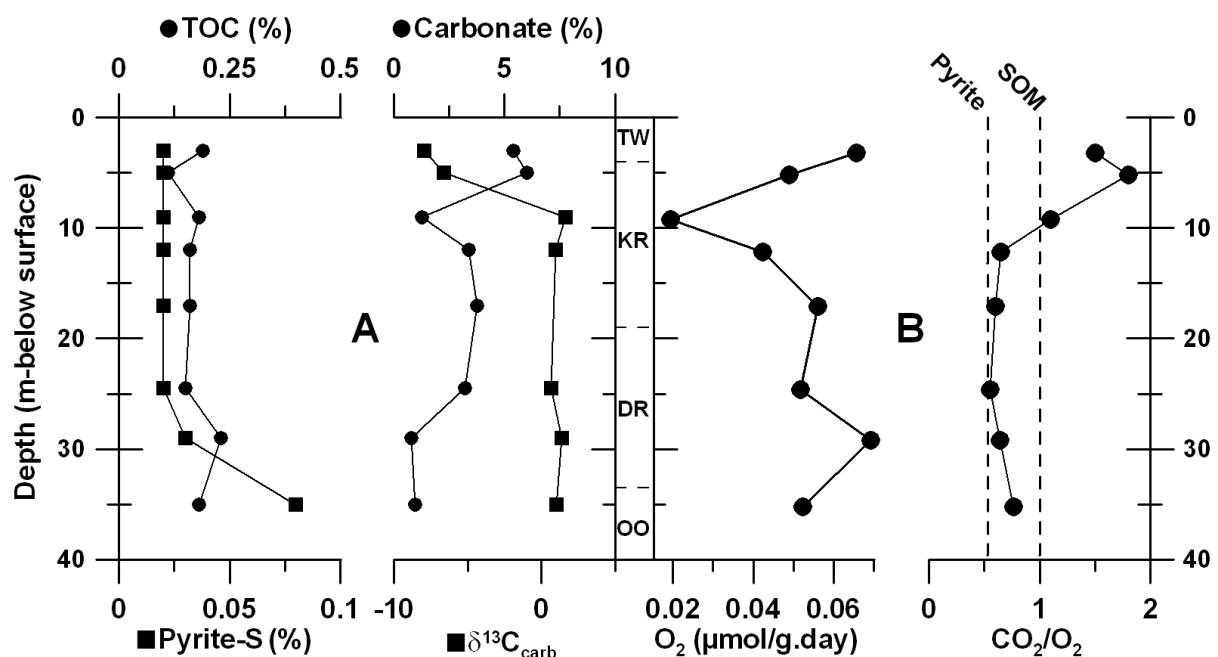


**Figure 6.6** Bulk chemistry (a) and incubation results (b) of sediments from core 34C-105 (Fig. 6.1). In (a) TOC, carbonate, and pyrite-S data from (van Beek and Vogelaar, 1998). In (b) vertical lines represent the molar  $\text{CO}_2/\text{O}_2$  ratios for the oxidation of pyrite (0.533) and SOM (1). Oxidation of ferrous carbonate yields a  $\text{CO}_2/\text{O}_2$  ratio of 4 (Chapter 3).

The first two shallow sediments showed high ( $>0.05 \mu\text{mol/g.day}$ ) oxygen consumption rates (Fig. 6.7b). The lowest rates ( $<0.02 \mu\text{mol/g.day}$ ) were observed for the Kreftenheye sample at 9 m below surface level. Highest rates (up to  $0.07 \mu\text{mol/g.day}$ ) were observed for the deeper Drente and Oosterhout sediments.

The ratios of  $\text{CO}_2$  production and  $\text{O}_2$  consumption were considerably larger than unity ( $>1.5$ ) for the two shallowest sediments (Fig. 6.7b) and were associated with high calcium concentrations in the supernatants at the end of the incubations

(Table 6.2). The  $\text{CO}_2/\text{O}_2$  ratio was near unity for the Kreftenheye sample at 9 m below surface level. For the incubation of the deeper sediments,  $\text{CO}_2/\text{O}_2$  ratios ranged from 0.55 to 1.0. Here, an equimolar increase of calcium and sulfate concentrations in the supernatants of the sediments was observed. Final pH values were slightly alkaline in all sediment incubation waters (Table 6.2). All final incubation waters were saturated ( $\text{SI}=0$ ) with respect to calcite and undersaturated ( $\text{SI}<-0.9$ ) with respect to gypsum (Table 6.2).

**Table 6.1** Chemical composition of the incubation waters and the ratio between  $\text{CO}_2$  produced and  $\text{O}_2$  consumed after 7.5 days of sediment incubation.

Sample Code	Depth (m-bs)	pH	Alkalinity (mmol/l)	Ca <sup>a</sup> (mmol/l)	S <sup>b</sup> (mmol/l)	SI Calcite	SI Gypsum	$\text{CO}_2/\text{O}_2$ (molar)
722	3.2	7.44	2.7	3.75	0.43	0.35	-1.69	1.51
723	5.2	7.43	2.6	3.20	0.34	0.27	-1.38	1.80
724	9.2	7.39	2	1.25	0.36	-0.24	-2.08	1.10
725	12.2	7.51	1.8	1.55	0.36	-0.08	-2.01	0.65
726	17.1	7.42	2.8	NA	NA			0.60
727	24.6	7.49	3	NA	NA			0.55
728	29.2	7.52	2.3	2.04	1.15	0.10	-1.47	0.64
729	35.2	7.41	2.4	3.96	2.95	0.20	-0.92	0.76

(a) initial calcium concentration: 1.1 mmol/l

(b) initial sulfur concentration: 0.21 mmol/l

NA: not analysed

## 6.5 DISCUSSION

### 6.5.1 SOM: Source and Preservation Controls

Both molecular and isotopic results point to a terrestrial source for the SOM present in the fluvial and coastal as well as in the marine formations. The observed range of  $\delta^{13}\text{C}_{\text{org}}$  isotopic values ( $\sim -25\text{‰}$ ) is characteristic for organic matter derived from higher land plants (Tyson, 1995). In addition, the observed long-chain alkanes (Figs. 6.3 and 6.4) with an odd-over-even predominance are typical for aliphatics derived from the cuticular waxes of higher plants (Eglinton and Hamilton, 1967). Also, the dominance of lignin-derived guaiacyl components and aromatics in the evaporate/pyrolysate mixtures (Figs. 6.3 and 6.4) reflect the contribution of plant debris (Saiz-Jimenez and De Leeuw, 1986). The terrestrial signature of SOM in the

aquifer sediments with a marine origin is in line with the predominance of terrestrial SOM in other aquifers (Routh *et al.*, 1999; Schulte, 1998).

The higher plant-derived SOM has been degraded at least to some extent in all samples analyzed, as indicated by the lack of more labile carbohydrate-based polymers (Tyson, 1995). However, as lignin is selectively preserved during the early stage of diagenesis (Hatcher *et al.*, 1989), the dominance of guaiacyl units with preserved side-chains in the marine Oosterhout and Breda sand samples (Figs. 6.3 and 6.5) and the fluvial Kreftenheye clay sample indicates an early stage of SOM degradation. In contrast, the high degree of lignin side-chain oxidation in the Scheemda sand samples (695, Fig. 6.5) and the near absence of guaiacol in the Twente (722, Fig. 6.3) and Kreftenheye sand samples reflect progressed SOM oxidation in these aquifer sediments.

Instead of a dominance by lignin-derived moieties, the samples with more degraded SOM exhibit a pronounced aliphatic signal derived from macromolecular structures (722, Fig. 6.3), as indicated by the distinct presence of alkanes with important alkene counterparts (Baas *et al.*, 1995; Mosle *et al.*, 1998; Van Smeerdijk and Boon, 1987). This is in line with the observation that macromolecularly-bound aliphatics are a relatively stable pool of SOM (Almendros *et al.*, 1996; Leinweber *et al.*, 1996). In addition to the dominance of the macromolecular aliphatic component, the odd predominance of long-chain *n*-alkanes is more pronounced in the Twente (722, Fig. 6.3) and Kreftenheye (735, Fig. 6.4) samples, illustrating the selective preservation of fossil leaf waxes (Logan *et al.*, 1995). Thus, the dominance of the aliphatic signal in these sediment samples reflects the most progressed degradation of SOM.

As SOM is the principal sorbent of organic contaminants (Pignatello, 1998), the molecular composition of SOM not only controls its degradability, it also affects the sorption capacity of aquifer sediments. The predominance of aliphatic components not only predicts orders of magnitude lower SOM degradability in the sediments with the most degraded SOM (*Chapter 5*), but also suggests a higher relative sorption capacity

for hydrophobic organic contaminants in these aquifer sediments (Johnson *et al.*, 2001; Salloum *et al.*, 2002; Weber Jr. *et al.*, 1998).

Several factors may be responsible for the observed differences in SOM preservation. Clearly, age is an influencing factor, since labile components are degraded preferentially over time. However, SOM from the oldest analyzed Breda Formation (Fig. 6.2) is relatively well preserved, while SOM from the youngest analyzed Twente and Kreftenheye Formations is more degraded. Therefore, the age difference of 20 My is not a dominant control on the degradation status of SOM in the aquifer sediments studied.

Alternatively, the degree of SOM preservation may reflect differences in oxidation prior to its deposition with the sediment. However, the lignin signal in the Kreftenheye clay sample (712, Fig. 6.5) is remarkably preserved, while lignin-derived components are insignificant in the sandy Kreftenheye (722, Fig. 6.3) and Twente (722) samples. This suggests that the lower degree of SOM preservation in the Kreftenheye sand (735) is not due to a source effect.

Therefore, the observed range in SOM preservation is most likely generated by differences in deposition and burial conditions, instead of by differences in age or source. Since the observed lignin degradation features are typical for aerobic oxidation (Dijkstra *et al.*, 1998; Dittmar and Lara, 2001; Kuder and Kruege, 1998), the duration that sediments are exposed to oxygen seems to be a controlling factor (Canfield, 1994; Hartnett *et al.*, 1998).

Various factors, such as the oxicity of bottom waters and sedimentation rate, have been linked to the oxygen exposure time (OET) of sediments in marine environments (Canfield, 1994; Gélinais *et al.*, 2001; Hartnett *et al.*, 1998). Gélinais *et al.* (2001) showed that high sedimentation rates caused shorter OETs for sediments deposited in coastal environments, which led to more preserved SOM when compared with deep-sea sediments, which are exposed to oxygen continuously.

The aquifer sediments studied originate from a wide range of depositional environments. The steady deposition of sediments in a shallow marine environment (Gélinais *et al.*, 2001; van den Berg *et al.*, 2000) probably resulted in limited OETs,



which led to the observed preservation of SOM in the Tertiary Oosterhout and Breda Formations (Figs. 6.3 and 6.5). Similarly, low energetic flow conditions, that enabled the deposition of Kreftenheye clay (Van Huissteden and Kasse, 2001), prevented extensive aerobic SOM degradation (Fig. 6.5). In contrast, the sandy sediments of the Kreftenheye Formation and Twente Formation were deposited in a dominantly braided river system and an ephemeral fluvio-aeolian system, respectively (Van Huissteden and Kasse, 2001; Van Huissteden *et al.*, 2000) These systems are characterized by repeated sediment remobilization and consequently frequent exposure to atmospheric oxygen. Therefore, the highly dynamic character of these depositional environments likely resulted in long OETs and allowed for extensive degradation of SOM in these sandy aquifer sediments.

### **6.5.2 Source of Isotopic variation of Sedimentary Carbonates**

The small excursions of less than 2‰ in  $\delta^{18}\text{O}_{\text{carb}}$  and  $\delta^{13}\text{C}_{\text{carb}}$  isotopic values in the Tertiary marine Oosterhout and Breda sediments indicate the syngenetic origin of their carbonate phase (Fig. 6.6). Syngenetic carbonate formation during the cold Saalian or Weichselian glacial periods is suggested by the strongly depleted  $\delta^{18}\text{O}$  and only slightly depleted  $\delta^{13}\text{C}$  values of the three Kreftenheye samples (Beets and Beets, 2003; Mayer and Schwark, 1999). However, the carbonate phase in other Kreftenheye samples have a marine isotopic signature. As for the Drente carbonate samples in particular, isotopic values plot close to zero with only a slight tendency towards more depleted  $\delta^{18}\text{O}_{\text{carb}}$ -values. Since these sediments (Fig. 6.2) were partly deposited under fluvio-glacial conditions (Saalian), more depleted  $\delta^{18}\text{O}$ -values would be expected for syngenetic carbonates. Therefore, the observed isotopic signature for these samples is at least in part caused by the presence of allogenic marine carbonates. These are likely derived from eroded marine sediments of the Oosterhout or Breda Formations (van den Berg *et al.*, 2000).

A diagenetic overprint is suggested by the strongly depleted  $\delta^{13}\text{C}_{\text{carb}}$ -values of the carbonate-enriched shallow Twente and Kreftenheye sediments (Fig. 6.6). Carbon isotope values of dissolved inorganic carbon (DIC) in present-day groundwater at the

site studied are strongly depleted and show an average  $\delta^{13}\text{C}$ -value of  $-11.9\text{‰}$  at depth ( $>10$  m-bs) (Van der Grift *et al.*, 2000), indicating that the oxidation of organic matter contributed to DIC (Mook, 1972; Saunders and Swann, 1992). A  $\delta^{13}\text{C}/\delta^{18}\text{O}$  end member for groundwater-derived carbonates (Fig. 6.7) is derived from the carbon isotope value for DIC and the average  $\delta^{18}\text{O}$ -value of  $-6.3\text{‰}$  for present-day precipitation (IAEA, 2000). Moreover, these depleted  $\delta^{13}\text{C}_{\text{carb}}$  and  $\delta^{18}\text{O}_{\text{carb}}$  values compare favorably with the range of those observed for carbonate precipitation in groundwater-fed lake sediments (Kallis *et al.*, 2000; Mayer and Schwark, 1999) and gyttja deposits (Hoek *et al.*, 1999).

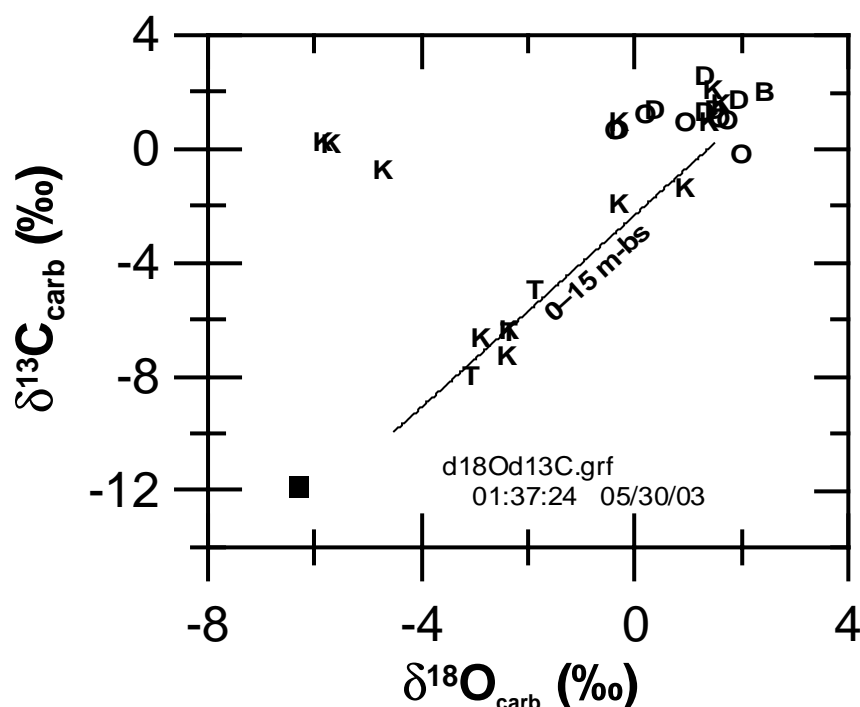
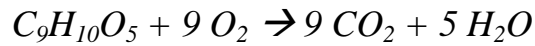


**Figure 6.7** Cross plot of carbonate isotopic values ( $\delta^{18}\text{O}_{\text{carb}}$  vs.  $\delta^{13}\text{C}_{\text{carb}}$ ) of the bulk carbonate phase present in the aquifer sediments studied. Codes correspond to samples from the following formations: T=Twente, K=Kreftenheye, D=Drente, O=Oosterhout and B= Breda Formation. Square depicts isotopic signature of dissolved inorganic carbon in present-day groundwater. Line represents the trend due to the diagenetic overprint of groundwater-driven carbonate precipitation.

### 6.5.3 Reactivity Distribution of Observed Reductants

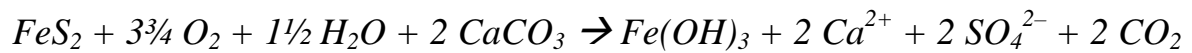
The final composition of the incubation waters together with the range of observed ratios of  $\text{CO}_2$  production to  $\text{O}_2$  consumption show that various reactive reductants are present in the sediment core studied. Not only do these reductants

oxidize concurrently, their relative importance varies with depth. During the incubation experiments (Table 6.2), SOM oxidation was dominant for the Kreftenheye sediment sample 724 as indicated by the CO<sub>2</sub>/O<sub>2</sub> ratio close to unity (Fig. 6.7b), according to:



Here, syringate (C<sub>9</sub>H<sub>10</sub>O<sub>5</sub>) is used as a labile model compound for lignin-derived components in SOM (*Chapter 3*, Chapelle and Bradley, 1996). The relatively unchanged calcium and sulfur concentrations in the final incubation water imply that iron sulfide oxidation was negligible in this sample (Table 6.2). Therefore, the low oxygen consumption rate of this sample illustrates the low reactivity of SOM in the Kreftenheye Formation, as suggested by its poor preservation.

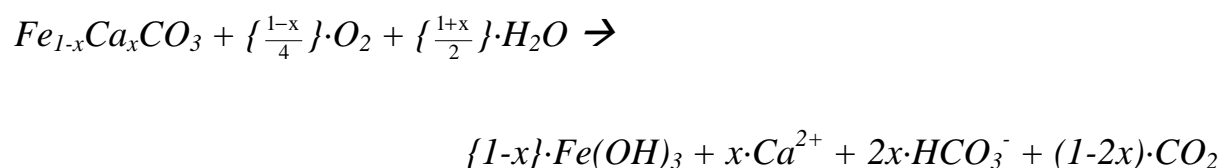
The incubated sediments from greater depth revealed the concurrent oxidation of SOM and iron sulfides, as indicated by the CO<sub>2</sub>/O<sub>2</sub> ratios lower than one and the equimolar increases of calcium and sulfur, according to:



While pyrite content increases below 25 m-bs (Fig. 6.7a), the increased CO<sub>2</sub>/O<sub>2</sub> ratios indicate a decrease in its relative importance of oxygen consumption. In other words, the increasing CO<sub>2</sub>/O<sub>2</sub> ratio suggests that SOM oxidation is more important due to the higher relative reactivity of SOM in the marine Oosterhout sediments. This interpretation is in line with the higher preservation and reactivity of SOM in sediments from the marine Oosterhout Formation when compared with SOM in sediments from the fluvio-glacial Drente Formation (*Chapter 5*). A more degraded status of SOM in the Drente sediments may have resulted from increased oxygen exposure during the reworking of marine sediments, as indicated by their carbonate isotope signatures (Fig. 6.6) suggest. Although speculative, the importance of pyrite oxidation during the incubations of Drente sediments (Fig. 6.6) suggests that the reworking of adjoining sediments from the Oosterhout and Scheemda Formation (Fig. 6.1) had a stronger impact on SOM than on pyrite reactivity. This suggestion is

supported by the observed predominance of pyrite oxidation and the lack of reactive organic matter in aquifer sediments of reworked origin (Postma *et al.*, 1991).

The CO<sub>2</sub>/O<sub>2</sub> ratios higher than 1 during the incubation of the two shallowest sediments and the elevated final calcium concentrations indicate the oxidation of ferrous iron bearing calcium carbonate under slightly alkaline conditions (Table 6.2), according to (McMillan and Schwertmann, 1998):



Oxidation of the siderite end member (FeCO<sub>3</sub>) yields a CO<sub>2</sub>/O<sub>2</sub> ratio of 4 (Chapter 3). Similarly, the aerobic oxidation of MnCO<sub>3</sub> results in a CO<sub>2</sub>/O<sub>2</sub> ratio of 2 and would thus also yield elevated CO<sub>2</sub>/O<sub>2</sub> ratios. While the presence of manganous carbonate cannot be excluded, its oxidation is not considered because of the two orders of magnitude lower total manganese contents in sediments as compared with iron (Table 6.1, van Beek and Vogelaar, (1998)). However, SOM oxidation must be held partly responsible for the total oxygen consumption, since the CO<sub>2</sub>/O<sub>2</sub> ratios for these samples are lower than expected for the sole oxidation of ferroan calcite (i.e. four). The slightly increased sulfur concentrations indicate only a minor contribution by the oxidation of iron sulfides.

The resistance to acid attack of part of the carbonate phase that interfered with the δ<sup>13</sup>C<sub>org</sub> determinations is further evidence for the presence of a diagenetic carbonates in the two shallowest sediments samples. The refractory nature of diagenetic Fe(II)-containing carbonates as compared with calcite is well known (Al-Aasm *et al.*, 1990; Jensen *et al.*, 2002; Moore *et al.*, 1992; Morin and Cherry, 1986). Finally, the depleted δ<sup>13</sup>C<sub>carb</sub>-values of these samples together with elevated carbonate contents (Fig. 6.7a) confirm a diagenetic origin (Saunders and Swann, 1992). Therefore, the diagenetic precipitation of a ferrous carbonate phase in these aquifer sediments likely occurred under past alkaline and iron-reducing conditions (Morin and Cherry, 1986). In contrast with the precipitation of ferrous carbonates in organic-rich strata (Aslan and Autin, 1996; Postma, 1982; Postma, 1983; Taylor, 1998), the

exfiltration of deep anoxic groundwater (Chae *et al.*, 2001; Hem and Lind, 1994; Hendry, 2002) may have provided these conditions in these sandy sediments. Since the Kreftenheye and Twente aquifer sediments contain highly degraded SOM (Figs. 6.3 and 6.5) and insignificant amounts of reduced sulfur (Table 6.1, Fig. 6.7a), the expected reduction potential of these sediments is generally low. However, the past diagenetic precipitation of a reactive ferroan calcite has locally resulted in a profound increase of the reduction capacity of the shallow Kreftenheye and Twente sediments in the area studied (Fig. 6.7b).

#### **6.5.4 Controls on the Reactivity of Sedimentary Reductants in Groundwater Systems**

The geochemical composition of sediments varies with provenance, depositional environment and paleohydrological conditions (Galloway and Hobday, 1983; Pettijohn, 1975). Consequently, when assessing the reduction capacity of aquifer sediments, the presence of a variety of sedimentary reductants has to be considered. In fact, field studies frequently reveal the oxidation of several sedimentary reductants (Böhlke and Denver, 1995; Pauwels *et al.*, 2001). Obviously, the importance of these reductants during sediment oxidation is determined by their relative abundance and reactivity. In the aquifer sediments studied, SOM, pyrite, and Fe(II)-bearing carbonates represent the most reactive phases (Fig. 6.7). In addition, glauconitic-Fe(II) may contribute to the reduction capacity of the Pliocene marine Breda sediments (van den Berg *et al.*, 2000; Weibel, 1998), as glauconite weathering presently affects groundwater chemistry in these deposits (Griffioen, 2001).

The overall reactivity of SOM critically depends on the chemical preservation of reactive organic compounds, since labile compounds are degraded preferentially over stable compounds. An order of magnitude difference in SOM reactivity was related to less pronounced side-chain oxidation of lignin-derived components in Oosterhout sediments as compared with Drente sediments (*Chapter 5*). Similarly, lignin side-chains are more preserved in SOM from the marine Oosterhout (707) and Breda (744) sediments than in SOM from the coastal Scheemda (695) sediments (Fig. 6.5), whereas lignin-derived components are depleted in the sandy Kreftenheye and

Twente (722, Fig. 6.3) sediments. Thus, the aquifer sediments studied show a wide range in SOM preservation that predicts degradation rates that differ in orders of magnitude. Therefore, the orders of magnitude range found for *in-situ* SOM oxidation rates in other sedimentary aquifer systems may reflect similar differences in molecular SOM preservation (Chapelle and Lovley, 1990; Jakobsen and Postma, 1994).

The relative preservation of SOM (Fig. 6.5 and *Chapter 5*) in the marine Oosterhout sediment coincides with increase of pyrite contents (Fig. 6.7a). The burial of degradable SOM and the supply of sulfate facilitated diagenetic pyrite formation in this marine sediment. Here, iron and sulfate reduction coupled to the oxidation of relatively preserved SOM resulted in the transfer of sediment reduction capacity from organic carbon to pyrite. Consequently, pyrite is an important reductant in the marine Oosterhout sediments (Fig. 6.7b). Under carbonate buffered conditions, the oxidation rate of pyrite is mainly controlled by the amount of reactive surface and impeded by the precipitation of iron hydroxide coatings. Therefore, the reactivity of pyrite decreases with progressive oxidation (Nicholson *et al.*, 1988; Nicholson *et al.*, 1990). While previous studies have shown that Fe(II)-bearing carbonates in aquifer sediments are potentially reactive towards oxygen and nitrate (*Chapter 3*, Weber *et al.*, 2001), the precipitation of iron hydroxide coatings may also decrease the reactivity of ferroan carbonates (*Chapter 3*), such as identified in the shallow sediments of the Kreftenheye and Twente Formations (Fig. 6.7).

The relative importance of reductants may change with progressive oxidation as SOM becomes more recalcitrant and reactive mineral reductants are oxidized. In the final stage of aquifer oxidation, when labile SOM components and reactive mineral pools have been oxidized, relatively stable Fe(II)-bearing detrital silicates may represent the main source of reducing activity (Hofstetter *et al.*, 2003; Postma, 1990). Under these conditions, the diffusion of labile organic compounds from adjoining strata rich in preserved SOM, such as clay aquitards (712, Table 6.1, Fig. 6.5) or peat layers, may significantly fuel oxidation processes in aquifers (Detmers *et al.*, 2001; McMahon, 2001; McMahon and Chapelle, 1991).

## **6.6 CONCLUSIONS**

Biomass derived from higher land plants is the dominant pool of SOM in the studied aquifer sediments of fluvial and marine origin. This terrestrial dominance is evidenced by 1) the bulk  $\delta^{13}\text{C}_{\text{org}}$ -values around  $-25\%$ , 2) the dominance of lignin-derived components and 3) the occurrence of long chain alkanes with an odd-over-even predominance.

Sedimentary organic matter is chemically best preserved in aquifer sediments from the Tertiary marine depositional environments, as illustrated by the dominance of lignin-derived components with preserved side-chains. In contrast, SOM in the Late Pleistocene fluvial sediments showed the strongest degradation, as demonstrated by insignificant amounts of remaining lignin-derived components and dominance of recalcitrant macromolecular aliphatic structures. The higher dynamics of fluvial depositional environments as compared with marine may have led to prolonged exposure to atmospheric oxygen and hence longer and more intense aerobic degradation of SOM.

Ferrous carbonates were recognized as reactive reductants, besides SOM and pyrite. The reactive ferroan carbonate phase that was locally observed in the shallow fluvial sediments, most probably originated from past carbonate precipitation during the exfiltration of Fe(II)-containing anoxic groundwater. This diagenetic overprint resulted in elevated reduction activities in the shallow part of the aquifer studied.

## **References**

- Al-Aasm I. S., Taylor B. E., and South B. (1990) Stable isotope analysis of multiple carbonate samples using selective acid extraction. *Chemical Geology* **80**, 119-125.
- Almendros G., Guadalix M. E., Gonzalez-Vila F. J., and Martin F. (1996) Preservation of aliphatic macromolecules in soil humins. *Organic Geochemistry* **24**(6-7), 651-659.
- Amirbahman A., Schonenberger R., Johnson C. A., and Sigg L. (1998) Aqueous- and solid-phase biogeochemistry of a calcareous aquifer system downgradient from a municipal solid waste landfill (Winterthur, Switzerland). *Environmental Science and Technology* **32**(13), 1933-1940.

Aslan A. and Autin W. J. (1996) Depositional and pedogenic influences on the environmental geology of Holocene Mississippi River floodplain deposits near Ferriday, Louisiana. *Engineering Geology* **45**, 417-432.

Baas M., Briggs D. E. G., van Heemst J. D. H., Kear A. J., and de Leeuw J. W. (1995) Selective preservation of chitin during the decay of shrimp. *Geochimica et Cosmochimica Acta* **59**(5), 945-951.

Barcelona M. J. and Holm R. T. (1991) Oxidation-reduction capacities of aquifer solids. *Environmental Science and Technology* **25**, 1565-1572.

Beets C. J. and Beets D. J. (2003) A high resolution stable isotope record of the penultimate deglaciation in lake sediments below the city of Amsterdam, The Netherlands. *Quaternary Science Reviews* **22**(2-4), 195-207.

Blowes D. (2002) Environmental chemistry - Tracking hexavalent Cr in groundwater. *Science* **295**(5562), 2024-2025.

Böhlke J. K. and Denver J. M. (1995) Combined use of groundwater dating, chemical, and isotopic analyses to resolve the history and fate of nitrate contamination in two agricultural watersheds, Atlantic coastal plain, Maryland. *Water Resources Research* **31**(9), 2319-2339.

Bradley P. M., Chapelle F. H., and Wilson J. T. (1998) Field and laboratory evidence for intrinsic biodegradation of vinyl chloride contamination in a Fe(III)-reducing aquifer. *Journal of Contaminant Hydrology* **31**, 111-127.

Bradley P. M., McMahon P. B., and Chapelle F. H. (1995) Effects of carbon and nitrate on denitrification in bottom sediments of an effluent-dominated river. *Water Resources Research* **31**(4), 1063-1068.

Canfield D. E. (1994) Factors influencing organic carbon preservation in marine sediments. *Chemical Geology* **114**, 315-329.

Chae G. T., Yun S. T., Kim S. R., and Hahn C. (2001) Hydrogeochemistry of seepage water collected within the Youngcheon diversion tunnel, Korea: source and evolution of SO<sub>4</sub>-rich groundwater in sedimentary terrain. *Hydrological Processes* **15**(9), 1565-1583.

Chapelle F. H. and Bradley P. M. (1996) Microbial acetogenesis as a source of organic acids in ancient Atlantic Coastal Plain sediments. *Geology* **24**, 925-928.

Chapelle F. H. and Lovley D. R. (1990) Rates of microbial metabolism in deep coastal plain aquifers. *Applied and Environmental Microbiology* **56**(6), 1865-1874.

Desimone L. A. and Howes B. L. (1996) Denitrification and nitrogen transport in a coastal aquifer receiving wastewater discharge. *Environmental Science and Technology* **30**(4), 1152-1162.

Detmers J., Schulte U., Strauss H., and Kuever J. (2001) Sulfate reduction at a lignite seam: Microbial abundance and activity. *Microbial Ecology* **42**(3), 238-247.

Dijkstra E. F., Boon J. J., and van Mourik J. M. (1998) Analytical pyrolysis of a soil profile under Scots pine. *European Journal of Soil Science* **49**, 295-304.

Dittmar T. and Lara R. J. (2001) Molecular evidence for lignin degradation in sulfate-reducing mangrove sediments (Amazônia, Brazil). *Geochimica et Cosmochimica Acta* **65**(9), 1417-1428.



- Eglinton G. and Hamilton R. J. (1967) Leaf epicuticular waxes. *Science* **156**(780), 1322-1335.
- Funnell B. M. (1996) Plio-Pleistocene palaeogeography of the Southern North Sea basin (3.75-0.60 Ma). *Quaternary Science Reviews* **15**(5-6), 391-405.
- Galloway W. E. and Hobday D. K. (1983) *Terrigenous Clastic Depositional Systems: Applications to Petroleum, Coal, and Uranium Exploration*. Springer-Verlag.
- Gélinas Y., Baldock J. A., and Hedges J. I. (2001) Organic carbon composition of marine sediments: Effect of oxygen exposure time on oil generation potential. *Science* **294**, 145-148.
- Griffioen J. (2001) Potassium adsorption ratios as an indicator for the fate of agricultural potassium in groundwater. *Journal of Hydrology* **254**(1-4), 244-254.
- Hartnett H. E., Keil R. G., Hedges J. I., and Devol A. H. (1998) Influence of oxygen exposure time on organic carbon preservation in continental margin sediments. *Nature* **391**, 572-574.
- Hatcher P. G., Wilson M. A., Vassallo A. M., and Lerch H. E., III. (1989) Studies of angiospermous wood in Australian brown coal by nuclear magnetic resonance and analytical pyrolysis: new insights into the early coalification process. *International Journal of Coal Geology* **13**(1-4), 99-126.
- Hem J. D. and Lind C. J. (1994) Chemistry of manganese precipitation in Pinal Creek, Arizona, USA: a laboratory study. *Geochimica et Cosmochimica Acta* **58**(6), 1601-13.
- Hendry J. P. (2002) Geochemical trends and palaeohydrological significance of shallow burial calcite and ankerite cements in Middle Jurassic strata on the East Midlands Shelf (onshore UK). *Sedimentary Geology* **151**(1-2), 149-176.
- Heron G. and Christensen T. H. (1995) Impact of Sediment-Bound Iron on Redox Buffering in a Landfill Leachate Polluted Aquifer (Vejen, Denmark). *Environmental Science and Technology* **29**(1), 187-192.
- Hill A. R., Devito K. J., Campagnolo S., and Sanmugas K. (2000) Subsurface denitrification in a forest riparian zone: Interactions between hydrology and supplies of nitrate and organic carbon. *Biogeochemistry* **51**, 193-223.
- Hoek W. Z., Bohncke S. J. P., Ganssen G. M., and Meijer T. (1999) Lateglacial environmental changes recorded in calcareous gyttja deposits at Gulickshof, southern Netherlands. *Boreas* **28**(3), 416-432.
- Hofstetter T. B., Schwarzenbach R. P., and Haderlein S. B. (2003) Reactivity of Fe(II) species associated with clay minerals. *Environmental Science & Technology* **37**(3), 519-528.
- IAEA. (2000) GNIP Database. The International Atomic Energy Agency.
- Jakobsen R. and Postma D. (1994) In situ rates of sulfate reduction in an aquifer (Rømø, Denmark) and implications for the reactivity of organic matter. *Geology* **22**, 1103-1106.
- Jakobsen R. and Postma D. (1999) Redox zoning, rates of sulfate reduction and interactions with Fe-reduction and methanogenesis in a shallow sandy aquifer, Rømø, Denmark. *Geochimica et Cosmochimica Acta* **63**(1), 137-151.

- Jensen D. L., Boddum J. K., Tjell J. C., and Christensen T. H. (2002) The solubility of rhodochrosite (MnCO<sub>3</sub>) and siderite (FeCO<sub>3</sub>) in anaerobic aquatic environments. *Applied Geochemistry* **17**(4), 503-511.
- Johnson M. D., Huang W. H., and Weber W. J. (2001) A distributed reactivity model for sorption by soils and sediments. 13. Simulated diagenesis of natural sediment organic matter and its impact on sorption/desorption equilibria. *Environmental Science & Technology* **35**(8), 1680-1687.
- Kallis P., Bleich K. E., and Stahr K. (2000) Micromorphological and geochemical characterization of Tertiary 'freshwater carbonates' locally preserved north of the edge of Miocen Molasse Basin (SW Germany). *Catena* **41**, 19-42.
- Kelly W. R. (1997) Heterogeneties in ground-water geochemistry in a sand aquifer beneath an irrigated field. *Journal of Hydrology* **198**, 154-176.
- Kuder T. and Kruge M. A. (1998) Preservation of biomolecules in sub-fossil plants from raised peat bogs — a potential paleoenvironmental proxy. *Organic Geochemistry* **29**(5-7), 1355-1368.
- Lee W. and Batchelor B. (2003) Reductive Capacity of Natural Reductants. *Environmental Science and Technology* **37**(3), 535-541.
- Leinweber P., Jordan E., and Schulten H. R. (1996) Molecular characterization of soil organic matter in Pleistocene moraines from the Bolivian Andes. *Geoderma* **72**(1-2), 133-148.
- Logan G. A., Smiley C. J., and Eglinton G. (1995) Preservation of fossil leaf waxes in association with their source tissues, Clarkia, northern Idaho, USA. *Geochimica et Cosmochimica Acta* **59**(4), 751-763.
- Lovley D. R., Chapelle F. H., and Phillips E. J. P. (1990) Fe(III)-Reducing Bacteria in Deeply Buried Sediments of the Atlantic Coastal-Plain. *Geology* **18**(10), 954-957.
- Magaritz M. and Luzier J. E. (1985) Water-rock interactions and seawater-freshwater mixing effects in the coastal dunes aquifer, Coos Bay, Oregon. *Geochimica et Cosmochimica Acta* **49**, 2515-2525.
- Mayer B. and Schwark L. (1999) A 15,000-year stable isotope record from sediments of Lake Steisslingen, Southwest Germany. *Chemical Geology* **161**, 315-337.
- McMahon P. B. (2001) Aquifer/aquitard interfaces: mixing zones that enhance biogeochemical reactions. *Hydrogeology Journal* **9**(1), 34-43.
- McMahon P. B. and Chapelle F. H. (1991) Microbial production of organic acids in aquitard sediments and its role in aquifer geochemistry. *Nature* **349**, 233-235.
- McMillan S. G. and Schwertmann U. (1998) Morphological and genetic relations between siderite, calcite and goethite in a Low Moor Peat from southern Germany. *European Journal of Soil Science* **49**, 283-293.
- Molenat J., Durand P., Gascuel-Oudoux C., Davy P., and Gruau G. (2002) Mechanisms of nitrate transfer from soil to stream in an agricultural watershed of French Brittany. *Water Air and Soil Pollution* **133**(1-4), 161-183.

- Mook W. G. (1972) Application of natural isotopes in ground water hydrology. *Geologie en Mijnbouw* **51**(1), 131-6.
- Moore S. E., Ferrell R. E., and Aharon P. (1992) Diagenetic Siderite and Other Ferroan Carbonates in a Modern Subsiding Marsh Sequence. *Journal of Sedimentary Petrology* **62**(3), 357-366.
- Morin K. A. and Cherry J. A. (1986) Trace amounts of siderite near a uranium-tailings impoundment, Elliot Lake, Ontario, Canada, and its implication in controlling contaminant migration in a sand aquifer. *Chemical Geology* **56**(1-2), 117-34.
- Morris J. T., Whiting G. J., and Chapelle F. H. (1988) Potential denitrification rates in deep sediments from the southeastern coastal plain. *Environmental Science and Technology* **22**(7), 832-836.
- Mosle B., Collinson M. E., Finch P., Stankiewicz B. A., Scott A. C., and Wilson R. (1998) Factors influencing the preservation of plant cuticles: a comparison of morphology and chemical composition of modern and fossil examples. *Organic Geochemistry* **29**(5-7), 1369-1380.
- Nicholson R. V., Gillham R. W., and Reardon E. J. (1988) Pyrite oxidation in carbonate-buffered solution: 1. Experimental kinetics. *Geochimica et Cosmochimica Acta* **52**, 1077-1085.
- Nicholson R. V., Gillham R. W., and Reardon E. J. (1990) Pyrite oxidation in carbonate-buffered solution: 2. Rate control by oxide coatings. *Geochimica et Cosmochimica Acta* **54**, 395-402.
- Parkhurst D. L. and Appelo C. A. J. (1999) User's guide to PHREEQC (Version 2). U.S. Geological Survey.
- Pauwels H., Lachassagne P., Bordenave P., Foucher J. C., and Martelat A. (2001) Temporal variability of nitrate concentrations in a schist aquifer and transfer to surface waters. *Applied Geochemistry* **16**, 583-596.
- Pedersen J. K., Bjerg P. L., and Christensen T. H. (1991) Correlation of nitrate profiles with groundwater and sediment characteristics in a shallow sandy aquifer. *Journal of Hydrology* **124**, 263-277.
- Pettijohn F. J. (1975) *Sedimentary Rocks*. Harper & Row.
- Pfenning K. S. and McMahon P. B. (1996) Effect of nitrate, organic carbon, and temperature on potential denitrification rates in nitrate-rich riverbed sediments. *Journal of Hydrology* **187**, 283-295.
- Pignatello J. J. (1998) Soil organic matter as a nanoporous sorbent of organic pollutants. *Advances in Colloid and Interface Science* **76-77**, 445-467.
- Postma D. (1982) Pyrite and siderite formation in brackish and freshwater swamp sediments. *American Journal of Science* **282**, 1151-1183.
- Postma D. (1983) Pyrite and siderite oxidation in swamp sediments. *Journal of Soil Science* **34**, 163-182.
- Postma D. (1990) Kinetics of nitrate reduction by detrital Fe(II)-silicates. *Geochimica et Cosmochimica Acta* **54**(3), 903-908.

- Postma D., Boesen C., Kristiansen H., and Larsen F. (1991) Nitrate reduction in an unconfined sandy aquifer: Water chemistry, reduction processes, and geochemical modeling. *Water Resources Research* **27**(8), 2027-2045.
- Puckett L. J. and Cowdery T. K. (2002) Transport and fate of nitrate in a glacial outwash aquifer in relation to ground water age, land use practices, and redox processes. *Journal of Environmental Quality* **31**(3), 782-796.
- Routh J., McDonald T. J., and Grossman E. L. (1999) Sedimentary organic matter sources and depositional environment in the Yegua formation (Brazos County, Texas). *Organic Geochemistry* **30**(11), 1437-1453.
- Saiz-Jimenez C. and De Leeuw J. W. (1986) Chemical characterization of soil organic matter fractions by analytical pyrolysis-gas chromatography-mass spectrometry. *Journal of Analytical and Applied Pyrolysis* **9**(2), 99-119.
- Salloum M. J., Chefetz B., and Hatcher P. G. (2002) Phenanthrene sorption by aliphatic-rich natural organic matter. *Environmental Science & Technology* **36**(9), 1953-1958.
- Saunders J. A. and Swann C. T. (1992) Nature and Origin of Authigenic Rhodochrosite and Siderite from the Paleozoic Aquifer, Northeast Mississippi, USA. *Applied Geochemistry* **7**(4), 375-387.
- Schulte U. (1998) Isotopengeochemische Untersuchungen zur Charakterisierung biologisch geteuerter Redoxprozesse in Aquiferen der Niederrheinischen Bucht, Ruhr-Universität Bochum.
- Smith R. L. and Duff J. H. (1988) Denitrification in a sand and gravel aquifer. *Applied and Environmental Microbiology* **54**(5), 1071-1078.
- Starr J. L., Sadeghi A. M., and Parkin T. B. (1996) A tracer test to determine the fate of nitrate in shallow groundwater. *Journal of Environmental quality* **25**, 917-923.
- Taylor K. G. (1998) Spatial and temporal variations in early diagenetic organic matter oxidation pathways in Lower Jurassic mudstones of eastern England. *Chemical Geology* **145**, 47-60.
- Tyson R. V. (1995) *Sedimentary Organic Matter*. Chapman & Hall.
- Uffink G. J. M. and Römkens P. F. A. M. (2001) Nitrate transport modeling in deep aquifers. Comparison between model results and data from the groundwater monitoring network, pp. 70. National Institute of Public Health and the Environment (RIVM).
- van Beek C. G. E. M. and Vogelaar A. J. (1998) Pompstation Hengelo 't Klooster—*Geohydrologische, geochemische en hydrochemische beschrijving*, pp. 84. KIWA N.V.
- van den Berg M. W., van Houten C. J., and den Otter C. (2000) Geologische Kaart van Nederland
- Blad Enschede West (34W) en Enschede Oost/Glanerbrug (34O/35). Nederlands Instituut voor Toegepaste Geowetenschappen TNO.
- Van der Grift B., Minnema B., and Griffioen J. (2000) Een geïntegreerd transportmodel voor grondwaterkwaliteit. Deelrapport 14. Test op freatische winning 't Klooster, Gelderland, pp. 27. NITG-TNO/KIWA.

- Van Huissteden J. K. and Kasse C. (2001) Detection of rapid climate change in Last Glacial fluvial successions in The Netherlands. *Global and Planetary Change* **28**, 319-339.
- Van Huissteden J. K., Vandenberghe J., Van der Hammen T., and Laan W. (2000) Fluvial and aeolian interaction under permafrost conditions: Weichselian Late Pleniglacial, Twente, eastern Netherlands. *CATENA* **40**(3), 307-321.
- Van Smeerdijk D. G. and Boon J. J. (1987) Characterisation of subfossil Sphagnum leaves, rootlets of ericaceae and their peat by pyrolysis-high-resolution gas chromatography-mass spectrometry. *Journal of Analytical and Applied Pyrolysis* **11**, 377-402.
- Weber Jr. W. J., Huang W., and Yu H. (1998) Hysteresis in the sorption and desorption of hydrophobic organic contaminants by soils and sediments; 2. Effects of soil organic matter heterogeneity. *Journal of Contaminant Hydrology* **31**(1-2), 149-165.
- Weber K. A., Picardal F. W., and Roden E. E. (2001) Microbially catalyzed nitrate-dependant oxidation of biogenic solid-phase Fe(II) compounds. *Environmental Science and Technology* **35**, 1644-1650.
- Weibel R. (1998) Diagenesis in oxidising and locally reducing conditions – an example from the Triassic Skagerrak Formation, Denmark. *Sedimentary Geology* **121**(3-4), 259-276.



# Synthesis

## 7.1 INTRODUCTION

Redox reactions have a strong impact on the overall biogeochemistry of groundwater systems. In particular, several common oxidizing groundwater contaminants (*e.g.* nitrate, chromate or chlorinated ethenes) are susceptible to reductive transformations. Aquifer sediments are the foremost source of the reduction capacity in groundwater systems (Barcelona and Holm, 1991a; Barcelona and Holm, 1991b). Therefore, the fate of these contaminants in aquifers strongly depends on the amounts and reactivity of sedimentary reductants present in the aquifer matrix.

Sedimentary reductants in aquifers mainly comprise organic compounds, ferrous iron, manganous and sulfide bearing minerals. To quantify the sum of their reducing capacity, Pedersen *et al.* (1991) oxidized aquifer sediments using an acid dichromate treatment. They introduced the term “total reduction capacity” (TRC) for the maximum amount of oxidant consumed by the aquifer sediments and used the change of TRC within a sediment profile to explain the disappearance of oxygen, nitrate and sulfate (Pedersen *et al.*, 1991). In the context of contaminated site remediation, others have studied aquifer sediments for their natural background TRC (Barcelona and Holm, 1991a; Barcelona and Holm, 1991b) and for increases of TRC due to the precipitation of ferrous iron bearing minerals in landfill leachates (Christensen *et al.*, 2000; Heron and Christensen, 1995). The use of dichromate oxidation under very acid conditions allows a rough estimate of the reductive capacity of aquifer sediments, but this aggressive abiotic method likely overestimates the microbially utilizable reduction capacity of aquifer sediments in field situations where weaker oxidants (such as O<sub>2</sub> and NO<sub>3</sub>) dominate (Barcelona and Holm, 1991a; Barcelona and Holm, 1991b; Pedersen *et al.*, 1991). Therefore, the extent to which the TRC of aquifer sediments will be available depends on the strength and specificity of the oxidant and the reactivity of the sedimentary reductants present (Barcelona and Holm, 1991a; Barcelona and Holm, 1991b).

## 7.2 REACTIVITY OF SEDIMENTARY REDUCTANTS

This study focuses on the reduction *reactivity* of sedimentary reductants in aquifers. The controls on the oxidation rates of sedimentary reductants in aquifer sediments were assessed during sediment incubation experiments. In particular, the reactivity and molecular composition of sedimentary organic matter (SOM) was investigated. The ability to identify the most reactive reductant(s) is important since changes in groundwater chemistry strongly depend on the type of reductant being oxidized. However, due to the general co-occurrence of several potentially reactive sedimentary reductants, the assessment of their separate reactivities could not be assessed by the sheer measurement of oxidant consumption during sediment exposure. In *Chapter 3*, a new experimental approach enabled the separation between the oxygen consumption due to SOM, pyrite and siderite oxidation based on differences in reaction stoichiometries. The continuous measurement of oxygen (O<sub>2</sub>) consumption and carbon dioxide (CO<sub>2</sub>) production allows the determination of the relative contribution of these sedimentary reductants during experimental exposure to atmospheric conditions, using the observed CO<sub>2</sub>/O<sub>2</sub> ratios and the chemical composition of the supernatants. While the reductants identified were frequently oxidized concurrently, their relative importance as well as the total rate of oxygen consumption of the aquifer sediments varied between the geological formations of different sedimentological origins (*Chapter 3 and 6*). This observed heterogeneity in reactivity indicates that reactive transport models not only require model layering in its physical properties of an aquifer but in its geochemical reactivity as well (Islam et al., 2001).

Ferrous iron turned out to be a dominant reductant in shallow aquifer sediments that were diagenetically enriched in ferroan carbonate (*Chapter 6*). While SOM and pyrite are long recognized as important sedimentary reductants in aquifers, the reduction potential of ferrous iron bearing carbonates has been largely overlooked in aquifers. This expectably coheres with the inability of current techniques to quantify this type of carbonates at the low contents expected in aquifer sediments. However ferroan carbonates are likely an important source of reducing capacity since



groundwaters are frequently supersaturated with respect to siderite ( $\text{FeCO}_3$ ) (Jensen et al., 2002; Magaritz and Luzier, 1985; Nicholson et al., 1983; Ptacek, 1998; Stuyfzand, 1989). In addition, the presence of ferroan, as well as manganous carbonates has been shown in both pristine (*Chapter 3*, (Fredrickson et al., 1998; Saunders and Swann, 1992) and contaminated aquifer sediments (Morin and Cherry, 1986; Tuccillo et al., 1999). While the need for a sensitive quantification method remains, the  $\text{CO}_2/\text{O}_2$  method can be used to assess whether ferroan carbonates are an important source of reducing activity.

To date, the reactivity of sedimentary reductants, has been mainly studied during the experimental oxidation of pure mineral phases such as Fe(II)-bearing silicates (Ernstsen et al., 1998; Hofstetter et al., 2003; Lee and Batchelor, 2003; Postma, 1990; Weber et al., 2001). The experiments on these potentially reactive minerals yielded useful information on the mechanisms and controls of the oxidation of their sedimentary counterparts, but did not allow the assessment of their actual importance during the oxidation of a given aquifer sediment. Moreover, the determined reactivity of these model reductants may not represent that of sedimentary reductants, as their reactivity varies with differences in their sediment history (*Chapter 3 and 6*). Therefore, the determination of important reductants in aquifer sediments can only be assessed within their sedimentary context.

As the geological history of aquifer sediments affects the types, amounts and characteristics of the reductants present, this sets an intrinsic limit to their reactivity and relative importance. However, changes in environmental conditions may affect the rate by which reductants are oxidized due to changes in microbial activity or the accessibility of the reductant. For example, pyrite oxidation was impeded by the precipitation of iron hydroxides on its surface at near neutral pHs (Nicholson et al., 1990). However, after the depletion of reactive carbonate buffer, pyrite oxidation was accelerated, probably by the dissolution of iron hydroxide coatings on the mineral surface around pH 4–5 (*Chapter 3*), a pH-range also known to favor microbial ferrous iron oxidation (Roychoudhury et al., 1998). These low pHs, however, inhibited the microbial oxidation of SOM (*Chapter 3*). The strong opposite effects of pH on the

reactivity of SOM and pyrite implies that the presence of sufficient reactive carbonates to buffer pH is a key factor that controls the extent of their oxidation.

In contrast with the instant microbial response during aerobic oxidation, slow microbial adaptation played a key role in reaching full denitrifying activity during sediment incubation experiments (*Chapter 4*). Moreover, observed nitrate reduction rates were two times lower those observed for oxygen reduction by the same aquifer sediments. While pyrite and SOM were both important reductants with respect to oxygen (*Chapter 3*), SOM was oxidized preferentially over pyrite during denitrification experiments (*Chapter 4*). Although preferential SOM oxidation has been observed during field experiments (Stuyfzand, 1998), other numerous other field studies have coupled the occurrence of denitrification to the oxidation of pyrite (Molenat et al., 2002; Moncaster et al., 2000; Pauwels et al., 2000; Postma et al., 1991). So far, results suggest that pH is an important control in the coupling of pyrite oxidation and nitrate reduction, but further experimental verification is needed to obtain detailed knowledge on the mechanism by which these processes are connected.

### **7.3 MOLECULAR COMPOSITION AND REACTIVITY OF SOM**

The factors that control the molecular composition, preservation and reactivity of SOM were assessed in aquifer sediments from geological formations with Pliocene to Holocene ages and with marine, fluvial, fluvio-glacial and aeolian depositional origins. The molecular characterization of SOM in aquifer sediments was complicated by the small amounts of organic compounds present as compared to surface soils. Therefore, the mineral phase of the aquifer sediments was dissolved using an HF/HCl procedure to concentrate SOM before pyrolysis-GC/MS analysis (*Chapter 5 and 6*). Regardless of depositional environment or age, SOM was primarily derived from higher land plants as indicated by the bulk stable carbon isotope values, the importance of lignin-derived components and the odd-over-even predominance for the C<sub>23</sub>–C<sub>27</sub> alkanes.

The absence of more labile compounds, such as cellulose, indicates that SOM had degraded to a considerable extent from its biomass precursor in all aquifer

sediments studied. A macromolecular aliphatic SOM component was present in all aquifer sediment studied, but was particularly pronounced in the fluvial and aeolian sediments (*Chapter 6*). In contrast, lignin-derived compounds were more dominant and more preserved in sediments from marine depositional environments than terrestrial aquifer sediments (*Chapter 5 and 6*). While lignin generally represents a recalcitrant compound compared to other original biopolymers in soils (Kogel-Knabner, 2002), the dominance of lignin in preserved SOM suggests that it represents one of the most degradable SOM component in the aquifer sediments studied. This is in line with the orders of magnitude lower reactivity of organic matter in aquifers than the rates in surface sediments from marine and limnic environments (Jakobsen and Postma, 1994; Jakobsen and Postma, 1999).

The reactivity of molecularly characterized SOM was determined in carbonaceous aquifer sediments of marine Miocene and fluvio-glacial Pleistocene origins (*Chapter 5*). The  $\text{CO}_2/\text{O}_2$  approach was used to verify that SOM was the most important reductant in these sediments during incubations. The reactivity towards oxygen of SOM in the Miocene sediments was almost an order of a magnitude higher than that of SOM in the Pleistocene sediment, demonstrating that sediment age did not significantly affect SOM reactivity. As the higher reactivity of SOM in the older marine sediments is in keeping with its more preserved status, this indicates that the molecular composition of SOM is the overall control on its oxidation rate (*Chapter 5*).

Molecular characteristics, such as the side-chain oxidation of lignin, indicates that the degradation status of SOM was mainly controlled by aerobic oxidation. Therefore, sediment oxygen exposure time (OET) is probably a key variable. Recently, OETs have been used to explain the observed differences in preservation and reactivity of SOM in marine surface sediments (Gélinas et al., 2001; Hartnett et al., 1998). In contrast with marine sediments, the higher dynamics of terrestrial depositional environments result in a more frequent exposure to subaerial conditions due to resuspension and reworking of sediments. The increased OET in these environments likely explains the more degraded nature of SOM in the aquifer

sediments of fluvial, aeolian and fluvio-glacial origins as compared to aquifer sediments of marine origin (*Chapter 5 and 6*).

## References

- Barcelona M. J. and Holm R. T. (1991a) Additions and Corrections: Oxidation-reduction capacities of aquifer solids. *Environmental Science and Technology* **26**(12), 2540.
- Barcelona M. J. and Holm R. T. (1991b) Oxidation-reduction capacities of aquifer solids. *Environmental Science and Technology* **25**, 1565-1572.
- Christensen T. H., Bjerg P. L., Banwart S. A., Jakobsen R., Heron G., and Albrechtsen H.-J. (2000) Characterization of redox conditions in groundwater contaminant plumes. *Journal of Contaminant Hydrology* **45**, 165-241.
- Ernstsen V., Gates W. P., and Stucki J. W. (1998) Microbial reduction of structural iron in clays - A renewable source of reduction capacity. *Journal of Environmental Quality* **27**(4), 761-766.
- Fredrickson J. K., Zachara J. M., Kennedy D. W., Dong H., Onstott T. C., Hinman N. W., and Li S. M. (1998) Biogenic iron mineralization accompanying the dissimilatory reduction of hydrous ferric oxide by a groundwater bacterium. *Geochimica et Cosmochimica Acta* **62**(19/20), 3239-3257.
- Gélinas Y., Baldock J. A., and Hedges J. I. (2001) Organic carbon composition of marine sediments: Effect of oxygen exposure time on oil generation potential. *Science* **294**, 145-148.
- Hartnett H. E., Keil R. G., Hedges J. I., and Devol A. H. (1998) Influence of oxygen exposure time on organic carbon preservation in continental margin sediments. *Nature* **391**, 572-574.
- Heron G. and Christensen T. H. (1995) Impact of Sediment-Bound Iron on Redox Buffering in a Landfill Leachate Polluted Aquifer (Vejen, Denmark). *Environmental Science and Technology* **29**(1), 187-192.
- Hofstetter T. B., Schwarzenbach R. P., and Haderlein S. B. (2003) Reactivity of Fe(II) species associated with clay minerals. *Environmental Science & Technology* **37**(3), 519-528.
- Islam J., Singhal N., and O'Sullivan M. (2001) Modeling biogeochemical processes in leachate-contaminated soils: a review. *Transport in Porous Media* **43**, 407-440.
- Jakobsen R. and Postma D. (1994) In situ rates of sulfate reduction in an aquifer (Rømø, Denmark) and implications for the reactivity of organic matter. *Geology* **22**, 1103-1106.
- Jakobsen R. and Postma D. (1999) Redox zoning, rates of sulfate reduction and interactions with Fe-reduction and methanogenesis in a shallow sandy aquifer, Rømø, Denmark. *Geochimica et Cosmochimica Acta* **63**(1), 137-151.
- Jensen D. L., Boddum J. K., Tjell J. C., and Christensen T. H. (2002) The solubility of rhodochrosite (MnCO<sub>3</sub>) and siderite (FeCO<sub>3</sub>) in anaerobic aquatic environments. *Applied Geochemistry* **17**(4), 503-511.

- Kogel-Knabner I. (2002) The macromolecular organic composition of plant and microbial residues as inputs to soil organic matter. *Soil Biology and Biochemistry* **34**(2), 139-162.
- Lee W. and Batchelor B. (2003) Reductive Capacity of Natural Reductants. *Environmental Science and Technology* **37**(3), 535-541.
- Magaritz M. and Luzier J. E. (1985) Water-rock interactions and seawater-freshwater mixing effects in the coastal dunes aquifer, Coos Bay, Oregon. *Geochimica et Cosmochimica Acta* **49**, 2515-2525.
- Molénat J., Durand P., Gascuel-Oudoux C., Davy P., and Gruau G. (2002) Mechanisms of nitrate transfer from soil to stream in an agricultural watershed of French Brittany. *Water Air and Soil Pollution* **133**(1-4), 161-183.
- Moncaster S. J., Botrell S. H., Tellam J. H., Lloyd J. W., and Konhauser K. O. (2000) Migration and attenuation of agrochemical pollutants: insights from isotopic analysis of groundwater sulphate. *Journal of Contaminant Hydrology* **43**, 147-163.
- Morin K. A. and Cherry J. A. (1986) Trace amounts of siderite near a uranium-tailings impoundment, Elliot Lake, Ontario, Canada, and its implication in controlling contaminant migration in a sand aquifer. *Chemical Geology* **56**(1-2), 117-134.
- Nicholson R. V., Cherry J. A., and Reardon E. J. (1983) Migration of contaminants in groundwater at a landfill: A case study 6. Hydrogeochemistry. *Journal of Hydrology* **63**(1-2), 131-176.
- Nicholson R. V., Gillham R. W., and Reardon E. J. (1990) Pyrite oxidation in carbonate-buffered solution: 2. Rate control by oxide coatings. *Geochimica et Cosmochimica Acta* **54**, 395-402.
- Pauwels H., Foucher J.-C., and Kloppmann W. (2000) Denitrification and mixing in a schist aquifer: influence on water chemistry and isotopes. *Chemical Geology* **168**, 307-324.
- Pedersen J. K., Bjerg P. L., and Christensen T. H. (1991) Correlation of nitrate profiles with groundwater and sediment characteristics in a shallow sandy aquifer. *Journal of Hydrology* **124**, 263-277.
- Postma D. (1990) Kinetics of nitrate reduction by detrital Fe(II)-silicates. *Geochimica et Cosmochimica Acta* **54**(3), 903-908.
- Postma D., Boesen C., Kristiansen H., and Larsen F. (1991) Nitrate reduction in an unconfined sandy aquifer: Water chemistry, reduction processes, and geochemical modeling. *Water Resources Research* **27**(8), 2027-2045.
- Ptacek C. J. (1998) Geochemistry of a septic-system plume in a coastal barrier bar, Point Pelee, Ontario, Canada. *Journal of Contaminant Hydrology* **33**(3-4), 293-312.
- Roychoudhury A. N., Viollier E., and Van Cappellen P. (1998) A plug flow-through reactor for studying biogeochemical reactions in undisturbed aquatic sediments. *Applied Geochemistry* **13**, 269-280.
- Saunders J. A. and Swann C. T. (1992) Nature and Origin of Authigenic Rhodochrosite and Siderite from the Paleozoic Aquifer, Northeast Mississippi, USA. *Applied Geochemistry* **7**(4), 375-387.

## Chapter 7

Stuyfzand P. J. (1989) Hydrology and water quality aspects of rhine bank groundwater in The Netherlands. *Journal of Hydrology* **106**(3-4), 341-363.

Stuyfzand P. J. (1998) Quality changes upon injection into anoxic aquifers in the Netherlands: Evaluation of 11 experiments. *Artificial Recharge of Groundwater*, 283-291.

Tuccillo M. E., Cozzarelli I. M., and Herman J. S. (1999) Iron reduction in the sediments of a hydrocarbon-contaminated aquifer. *Applied Geochemistry* **14**, 655-667.

Weber K. A., Picardal F. W., and Roden E. E. (2001) Microbially catalyzed nitrate-dependant oxidation of biogenic solid-phase Fe(II) compounds. *Environmental Science and Technology* **35**, 1644-1650.

# Samenvatting

## INTRODUCTIE

Reductie-oxidatie reacties hebben een sterke invloed op de algehele biogeochemie grondwatersystemen. Van bijzonder belang is dat verscheidene verontreinigende stoffen, zoals nitraat, chromaat en gechloreerde koolwaterstoffen door reductieprocessen van toxiciteit veranderen. Aangezien het grootste deel van de reductiecapaciteit van grondwatersystemen voor rekening komt van aquifersedimenten (Barcelona and Holm, 1991a; Barcelona and Holm, 1991b), is de mate waarin deze grondwatercontaminanten veranderen sterk afhankelijk van de reactiviteit van de sedimentaire reductoren die zich in de aquifermatrix bevinden.

Sedimentaire reductoren bestaan voornamelijk uit organische verbindingen en mineralen die gereduceerd ijzer, mangaan of sulfide bevatten. Om de totale reductiecapaciteit (TRC) van aquifers, behandelden Pedersen *et al.* (1991) aquifersedimenten met een zure dichromaat oplossing. De totale hoeveelheid verbruikt dichromaat is een maat voor het vermogen van de aanwezige sedimentaire reductoren om te reageren met oxidatoren. Aan de hand van veranderingen in de TRC met de diepte konden Pedersen *et al.* de verdwijning van zuurstof, nitraat en sulfaat in grondwater beschrijven. Anderen hebben dezelfde TRC-bepaling gebruikt om het natuurlijk reductie vermogen van aquifersedimenten te kwantificeren (Barcelona and Holm, 1991a; Barcelona and Holm, 1991b) en de vorming van gereduceerde mineralen in een verontreinigde aquifer te achterhalen (Christensen *et al.*, 2000; Heron and Christensen, 1995). Beide toepassingen zijn van groot belang bij het bepalen van de saneringsstrategie voor verontreinigde bodems. De TRC die bepaald wordt met de zure dichromaat behandeling is echter slechts een grove schatting van de werkelijke reductiecapaciteit van aquifersedimenten, omdat dichromaat veel aggresiever is dan de oxidatoren die gewoonlijk in grondwater gevonden worden. Hierdoor is het aanemelijk dat de beschikbare reductiecapaciteit, voor bijvoorbeeld zuurstof of nitraat

reducerende bacterieën, onderschat wordt (Barcelona and Holm, 1991a; Barcelona and Holm, 1991b; Pedersen et al., 1991). De mate waarin de TRC van aquifersedimenten gebruikt kan worden hangt dus af van de agressiviteit van de oxidator enerzijds en de reactiviteit van de sedimentaire reductoren anderzijds (Barcelona and Holm, 1991a; Barcelona and Holm, 1991b).

## **REACTIVITEIT VAN SEDIMENTAIRE REDUCTOREN**

Dit promotieonderzoek heeft zich vooral gericht op de reactiviteit van sedimentaire reductoren en in minder mate op de TRC. Doel van het onderzoek was om de factoren die van invloed zijn op de oxidatie snelheden van sedimentaire reductoren vast te stellen. Hiertoe werden er technieken ontwikkeld en toegepast die de reactiviteit van sedimentaire reductoren kunnen karakteriseren en helpen voorspellen. Incubatieexperimenten, waarbij aquifersedimenten werden blootgesteld aan zuurstof of nitraat, werden uitgevoerd om een koppeling te leggen tussen sedimentaire geochemie en reactiviteit. Middels pyrolyse GC/MS werd de variatie in moleculaire samenstelling van SOM in kaart gebracht en gerelateerd aan de geobserveerde afbreekbaarheid.

Doordat er in aquifersediment in het algemeen meerdere sedimentaire reductoren samen voorkomen konden de afzonderlijk reactiviteiten niet bepaald worden door tijdens sediment incubaties louter oxidatorconsumptie te meten. In *Hoofdstuk 3* wordt een nieuwe experimentele methode geïntroduceerd die het mogelijk maakt onderscheid te maken tussen de oxidatie van verschillende reductoren door zuurstof. Door tijdens de sedimentincubaties de zuurstofconsumptie ( $O_2$ ) en koolstofdioxideproductie ( $CO_2$ ) te meten kon de oxidatie van SOM, pyriet en sideriet van elkaar worden onderscheiden. Deze reductoren werden vaak parallel geoxideerd maar de totale zuurstof-consumptiesnelheid en het relatieve aandeel van elk daarin wisselde, afhankelijk van de geologische oorsprong van de sedimenten (*Hoofdstuk 3 en 6*). Deze variatie in de reductiereactiviteit geeft aan dat geochemische transport modellen voor aquifers gelaagdheid dienen aan te brengen in zowel de fysische als reactiviteitseigenschappen (Islam et al., 2001).



Gereduceerd ijzer in een diagenetisch gevormde carbonaatfase bleek een dominante bron voor reductiecapaciteit te zijn in ondiepe aquifersedimenten. Terwijl SOM en pyriet algemeen bekende reductoren in aquifers zijn, is de rol van ijzer(II)-houdende carbonaten als sedimentaire reductor tot nu toe onderbelicht gebleven. Dit houdt logischerwijs verband met het onvermogen van huidige meettechnieken om dit soort carbonaten met voldoende nauwkeurigheid te kwantificeren op de voor aquifersedimenten noodzakelijke lage meetniveaus. Echter, grondwater is dikwijls oververzadigd voor zowel sideriet ( $\text{FeCO}_3$ ) als rhodochrosiet ( $\text{MnCO}_3$ ) (Jensen et al., 2002; Magaritz and Luzier, 1985; Nicholson et al., 1983; Ptacek, 1998; Stuyfzand, 1989) en hun aanwezigheid is aangetoond in zowel natuurlijke (*Hoofdstuk 3*, Fredrickson et al., 1998; Saunders and Swann, 1992) als vervuilde aquifersedimenten (Morin and Cherry, 1986; Tuccillo et al., 1999). Hoewel de behoefte aan een techniek die voldoende gevoelig kan kwantificeren blijft, kan de  $\text{CO}_2/\text{O}_2$  methode gebruikt worden om te bepalen of ijzerhoudende carbonaten een belangrijke bron van reductie activiteit zijn.

Tot nu toe is de reactiviteit van sedimentaire reductoren vooral bestudeerd gedurende de oxidatie van pure mineraalfases, zoals Fe(II)-silicaten (Ernstsen et al., 1998; Hofstetter et al., 2003; Lee and Batchelor, 2003; Postma, 1990; Weber et al., 2001). Het gebruik van deze mogelijk reactieve mineralen bruikbare informatie verschaft over de mechanismen en factoren die een rol spelen bij hun oxidatie. Echter het blijft bij deze aanpak onduidelijk wat het belang is van de verschillende reductoren bij de oxidatie van een bepaald aquifersediment, aangezien die reactiviteit afhangt van variabele eigenschappen zoals, kristaliniteit, reactief mineraal oppervlak en coating daarop. Bovendien is de vastgestelde reactiviteit van deze modelreductoren wellicht niet representatief voor dat van sedimentaire reductoren, aangezien die reactiviteit afhangt van hun geologische voorgeschiedenis (*Hoofdstuk 3 en 6*). Daarom kunnen de bepaling het belang van verschillende sedimentaire reductoren en hun reactiviteit alleen worden uitgevoerd binnen een sedimentologisch kader.

Omdat het type, de hoeveelheid en eigenschappen van de aanwezige reductoren beïnvloed wordt door de geologische voorgeschiedenis van aquifersedimenten,

bepaald dit in grote mate hun reactiviteit en relatieve belangrijkheid. Wanneer echter de omgevingsfactoren veranderen (bijvoorbeeld pH of temperatuur) dan kan de reactiviteit van reductoren veranderen door effecten op de microbiële activiteit of veranderingen in de toegankelijkheid van de reductor (*Hoofdstuk 3*). De snelheid van pyriet oxidatie, bijvoorbeeld, neemt af naar mate er meer ijzerhydroxides neerslaan op het mineraal oppervlak (Nicholson et al., 1990). Echter toen tijdens incubatie expererimenten de kalkbuffer verbruikt was nam de snelheid weer toe, waarschijnlijk door het oplossen van de ijzerhydroxideneerslag bij een pH van 4–5. Dit is tevens het optimale pH-bereik voor de microbiële oxidatie van gereduceerd ijzer (Roychoudhury et al., 1998). Deze lage pHs echter hadden echter een remmende werking op de microbiële oxidatie van SOM. Veranderingen in pH hebben dus een tegengesteld effect op de reactiviteit van SOM en pyriet. Dit geeft aan dat het wel of niet aanwezig zijn van voldoende kalkbuffer de reductiecapaciteit voor beide reductoren bepaald.

In tegenstelling tot instantane microbiële respons tijdens de aerobe sediment incubaties, ontwikkelde de denitrificeerders zich pas volledige na meer dan een maand tijd (*Hoofdstuk 4*) Bovendien werd nitraat twee keer langzamer gereduceerd dan gemeten voor zuurstofreductie door de zelfde aquifersedimenten. Terwijl pyriet en SOM beide belangrijke reductoren waren voor zuurstof (*Hoofdstuk 3*) werd SOM preferent geoxideerd tijdens de denitrificatie experimenten. Alhoewel denitrificatie tijdens kunstmatige infiltratie experimenten ook voornamelijk gekoppeld was aan SOM oxidatie (Stuyfzand, 1998), hebben vele andere veldstudies het optreden van denitrificatie vooral gekoppeld aan de oxidatie van pyriet (Molénat et al., 2002; Moncaster et al., 2000; Pauwels et al., 2000; Postma et al., 1991). Studies tot dusver suggereren dat pH een belangrijke factor is die de koppeling tussen nitraatreductie en pyrietoxidatie bepaald (*Hoofdstuk 4*, Schippers and Jørgensen, 2002). Verdere experimentele studie is echter nodig om het reactiemechanisme te ontrafelen.

## **MOLECULAIRE SAMENSTELLING EN REACTIVITEIT VAN SOM**

In deze studie zijn de factoren die de moleculaire samenstelling en reactiviteit bepalen van sedimentair organisch materiaal (SOM) in aquifers beschouwd voor

sedimenten van Pliocene tot Holocene ouderdomen met mariene, fluviaatiele, fluvio-glaciale en eolische oorsprongen.

De moleculaire karakterisatie van SOM in aquifersedimenten wordt bemoeilijkt door de lage gehalten aan organische componenten vergeleken met bodems. Om SOM te concentreren werden daarom de minerale bestanddelen zoveel mogelijk opgelost middels een HF/HCl behandeling. Vervolgens werden de SOM bestanddelen geanalyseerd middels pyrolyse-GC/MS (*Hoofdstuk 5 en 6*). De stabiele koolstof isotoopwaarden voor SOM, de duidelijk aanwezige ligninecomponenten en de oneven–even verhoudingen voor de C<sub>23</sub>–C<sub>27</sub> alkanen gaven aan dat hogere landplanten de voornaamste bron voor SOM waren, ongeacht het afzettingsmilieu van de aquifersedimenten (*Hoofdstuk 5 en 6*). De afwezigheid van labielere componenten, zoals cellulose, gaf aan dat SOM reeds behoorlijk gedegradeerd was ten opzichte van het organische moedermateriaal. Een macromoleculaire component was aanwezig in alle bestudeerde aquifersedimenten maar was prominent aanwezig in de fluviaatiele en eolische sedimenten (*Hoofdstuk 6*). Daarentegen waren de lignine afgeleide fragmenten dominant en beter gepreserveerd in de mariene sedimenten dan in de terrestrische (*Hoofdstuk 5 en 6*). Alhoewel lignine in het algemeen, in vergelijking tot andere biopolymeren, als een moeilijk afbreekbaar wordt beschouwd, (Kogel-Knabner, 2002), suggereert de dominantie van lignine-afgeleide componenten in gepreserveerd SOM dat het een van de beter afbreekbare componenten is. Dit kan een verklaring zijn voor het feit dat de reactiviteit van SOM in aquifers ordes van grootte lager is dan in ondiepe mariene en lacustrine sedimenten (Jakobsen and Postma, 1994; Jakobsen and Postma, 1999).

Om na te gaan of de afbraaknelheden van SOM daadwerkelijk bepaald worden door de degradatiestatus van de organische verbindingen, werd de reactiviteit van SOM bepaald in carbonaathoudende mariene Mioocene en fluvio-glaciale Pleistocene sedimenten. (*Hoofdstuk 5*). Middels de CO<sub>2</sub>/O<sub>2</sub> methode werd geverifieerd dat SOM hoofdreductor was gedurende de incubatie van deze sedimenten. De reactiviteit van SOM in de Mioocene sedimenten was bijna een orde van grootte hoger dan in de Pleistocene sedimenten. De hogere reactiviteit van SOM in de oudere

mariene sedimenten is in overeenstemming met de betere preservatie van de moleculaire bestanddelen (*Hoofdstuk 5*).

Moleculaire karakteristieken, zoals de zijketen-oxidatie van lignine, duiden er op dat de degradatie van SOM vooral wordt bepaald door aerobe oxidatie. Daarom is de duur van sedimentblootstelling aan zuurstof waarschijnlijk cruciaal. Recentelijk, zijn die deze blootstellingstijden gebruikt om verschillen in SOM-preservatie en -reactiviteit in mariene oppervlaktesedimenten te bepalen (Gélinas et al., 2001; Hartnett et al., 1998). In tegenstelling tot mariene sedimenten, de hogere dynamiek van terrestrische afzettingmilieus resulteert in een frequentere blootstelling aan atmosferisch zuurstof door de resuspensie en het omwerken van sedimenten (*Hoofdstuk 6*). De langere blootstellingstijd aan zuurstof ten tijde van depositie verklaart waarschijnlijk de aanwezigheid van meer gedegraderd SOM in de aquifersedimenten van fluviaatiele, eolische en fluvio-glaciale origine in vergelijking tot de marine sedimenten (*Hoofdstuk 5 en 6*).

## **Referenties**

Zie pagina's 162-164.

## Curriculum vitae

Niels Hartog werd geboren op zaterdag 14 april 1974 te Zaandam. In 1992 behaalde hij zijn Gymnasium  $\beta$  diploma aan het Zaanlands Lyceum. Dat zelfde jaar begon hij aan zijn studie Fysische Geografie aan de Vrije Universiteit in Amsterdam. In 1996, deed hij bij de Rijks Geologische Dienst te Haarlem onderzoek naar de geochemische variatie binnen de sedimenten van de Kedichem Formatie. Na dit afstudeeronderzoek vertrok hij in 1997 naar de *New Mexico Institute of Mining and Technology* om daar een bijdrage te leveren aan het onderzoek naar de verzoutingsproblematiek binnen de overstromingsvlakte van de *Rio Grande*. Terug in Nederland, werkte hij korte tijd als bodemadviseur voor een milieuburo in Amsterdam, voordat hij begon als Assistent in Opleiding bij de projectgroep Geochemie van de Faculteit Aardwetenschappen aan de Universiteit Utrecht. Het promotieonderzoek werd uitgevoerd binnen het Interfacultair Centrum Hydrologie Utrecht (ICHU) en medegefinancierd door TNO-NITG. Het onderzoek leidde tot de in dit proefschrift uitgewerkte resultaten. Inmiddels werkt hij sinds augustus 2003 als post-doctoraal onderzoeker aan de Universiteit van Waterloo (Canada). Hier onderzoekt hij de geochemische en fysische processen die optreden tijdens de *in-situ* remediatie van aquifers vervuild met gechlloreerde koolwaterstoffen.













And evolving from the sea  
Would not be too much time for me  
To walk beside you in the sun

*(The Pixies-Sad Punk)*

